Universität Bremen

Zentrum für Humangenetik

Molekularzytogenetische und molekulargenetische Untersuchungen an Schilddrüsentumoren

Dissertation

zur Erlangung des Grades eines Doktors der Naturwissenschaften

– Dr. rer. nat. –

dem Promotionsausschuss Dr. rer. nat im Fachbereich Biologie / Chemie

der Universität Bremen

vorgelegt von

Norbert Drieschner

Bremen, im März 2012

(Datum des Kolloquiums: 23. Mai 2012)

1. Gutachter: Prof. Dr. Jörn Bullerdiek

2. Gutachter: PD Dr. Wolfgang Sendt

Erklärung

Hiermit erkläre ich, Norbert Drieschner, geboren am 26.05.1972, dass für das Verfassen der vorliegenden Dissertation mit dem Titel **„Molekularzytogenetische und molekulargenetische Untersuchungen an Schilddrüsentumoren“** folgende drei Aussagen zutreffen:

1. Ich habe die Arbeit ohne unerlaubte fremde Hilfe angefertigt.
2. Ich habe keine anderen als die von mir angegebenen Quellen und Hilfsmittel benutzt.
3. Ich habe die den benutzten Werken wörtlich oder inhaltlich entnommenen Stellen als solche kenntlich gemacht.

Bremen, im März 2012

_____

(Norbert Drieschner)

„Alles Wissen und alle Vermehrung unseres Wissens endet nicht mit einem Schlußpunkt, sondern mit Fragezeichen. Ein Plus an Wissen bedeutet ein Plus an Fragestellungen, und jede von ihnen wird immer wieder von neuen Fragestellungen abgelöst.“

- Hermann Hesse -

Inhaltsverzeichnis

Abkürzungsverzeichnis

AML	akute myeloische Leukämie
AP2	Poly (A) Adapter Primer
APO2L	APO2 Ligand
ATC	anaplastisches Schilddrüsenkarzinom (anaplastic thyroid carcinoma)
BAC	Bacterial Artificial Chromosome
BLAST	Basic Local Alignment Search Tool
bp	Basenpaare
C19MC	Chromosom 19 miRNA-Cluster
CAND1	Cullin-Associated and Neddylation-Dissociated 1
CC	Conventional Cytogenetics (konventionelle Zytogenetik)
cDNA	complementary DNA
CFA	Canines Chromosom (Canis familiaris)
CGH	Comparative Genomic Hybridization (komparative genomische Hybridisierung)
COG	Cluster of Orthologous Groups
DR5	Death Receptor 5
EDTA	Ethylendiamintetraacetat
EST	Expressed Sequence Tag
EVI1	Ecotropic Viral Integration Site 1
FFPE	formalin-fixiert und paraffin-eingebettet
FISH	Fluoreszenz *in situ* Hybridisierung
FTC	Follicular Thyroid Carcinoma (follikuläres Schilddrüsenkarzinom)
FV-PTC	Follicular Variant of Papillary Thyroid Carcinoma (follikuläre Variante des papillären Schilddrüsenkarzinomes)
HMGA1	High Mobility Group AT-Hook 1
HMGA2	High Mobility Group AT-Hook 2

HOPE	HEPES-glutamic acid Buffer Mediated Organic Solvent Protection Effect
I-FISH	Interphase-FISH
kb	Kilobasenpaare
Mb	Megabasenpaare
miRNA	microRNA
M-MLV	Moloney Murine Leukemia Virus
mRNA	messenger RNA
MTC	Medullar Thyroid Carcinoma (Medulläres Schilddrüsenkarzinom)
NCBI CDD	National Center for Biotechnology Information Conserved Domain Database
NIS	Solute Carrier Family 5 (Sodium Iodide Symporter), Member 5
ORF	Open Reading Frame
$p14^{Arf}$	Cyclin-Dependent Kinase Inhibitor 2A
PAC	P1-derived Artificial Chromosome
PAX8	Paired Box Gene 8
PPARγ	Peroxisome Proliferator-Activated Receptor-Gamma
PRKCE	Protein Kinase C Epsilon
PTC	Papillary Thyroid Carcinoma (papilläres Schilddrüsenkarzinom)
PUM1	Pumilio Homolog 1
PUM1-FUS-19q-I und PUM1-FUS-19q-II	PUM1-Fusionstranskripte
qRT-PCR	quantitative Real Time-PCR
R.T.	Raumtemperatur
RACE-PCR	Rapid Amplification of cDNA-ends with Polymerase Chain Reaction
RAD51L1	RAD51 homolog B (S. cerevisiae)
RAS	RAS-Onkogen Familie
RET	RET (rearranged during transfection) Proto-Oncogene
RET/PTC	RET-Fusionsgene unter Beteiligung verschiedener Partnergene in papillären Schilddrüsenkarzinomen

RITA	Rearranged In Thyroid Adenomas
RPCI-11	Humane BAC Library
RT	Reverse Transkriptase
SAGE	Serial Analysis of Gene Expression
SNP	Single Nukleotid Polymorphismus
STS	Sequence Tagged Sites
T2DM	Type 2 Diabetes Mellitus
TBPC19	Thyroid Breakpoint Cluster 19
TBPC2	Thyroid Breakpoint Cluster 2
THADA	Thyroid Adenoma Associated
THADA-FUS3p und 7p	THADA-Fusionstranskripte
TL1A	Tumor Necrosis Factor (ligand) Superfamily, Member 15
TNFR	Tumor Necrosis Factor Receptor Superfamily
TRAIL	TNF-related Apoptosis-Inducing Ligand
TSV40	Transformiert mit dem Simian-Virus 40 T-large Antigen
UTR	Untranslated Region (nicht-translatierte Region)
WRO	Zelllinie eines follikulären Schilddrüsenkarzinoms
ZNF331	Zinc Finger Protein 331

1 Einführung

1.1 Konventionelle und molekulare Tumorzytogenetik

Die konventionelle Zytogenetik (CC) hat wesentlich zum Nachweis spezifischer und nicht zufälliger, klonaler chromosomaler Veränderungen sowohl in malignen hämatologischen Neoplasien als auch in benignen und malignen soliden Tumoren beigetragen. Derzeit sind in der Literatur klonale zytogenetische Aberrationen, überwiegend chromosomale Rearrangierungen und insbesondere balancierte Translokationen, einschließlich diagnostisch relevanter bzw. pathognomonischer Veränderungen, in über 60.000 Fällen von humanen Neoplasien beschrieben (Mitelman, 2000; Mitelman *et al.*, 2007; Heim und Mitelman, 2009; Sandberg und Meloni-Ehrig, 2010; Mitelman *et al.*, 2011).

Der Nachweis solcher tumorzytogenetischen Aberrationen kann neben der CC auch mittels molekularzytogenetischer Methoden, wie z.B. der Fluoreszenz *in situ* Hybridisierung (FISH), der komparativen genomischen Hybridisierung (comparative genomic hybridization; CGH) oder der array-CGH, erfolgen (Tonnies, 2002; Sandberg und Meloni-Ehrig, 2010). Eine bedeutende Rolle nimmt dabei die FISH ein, die durch den Einsatz spezifischer DNA-Sonden auf Einzelzellebene die Detektion numerischer und struktureller Aberrationen, wie z.B. Rearrangierungen, Deletionen und Amplifikationen, ermöglicht (Werner *et al.*, 1997; Tonnies, 2002). Der Nachweis chromosomaler Aberrationen mittels FISH kann dabei im Gegensatz zur CC unabhängig von der mitotischen Aktivität der Zellen erfolgen, sodass sich entsprechende Veränderungen nicht nur an Metaphasechromosomen sondern mittels Interphase-FISH (I-FISH) auch an Zellkernen nachweisen lassen. Dies bedeutet weiterhin, dass eine Kultivierung der Tumorzellen nicht grundsätzlich Voraussetzung für die Detektion chromosomaler Veränderungen ist und somit auch zytologische Präparate (z.B. Touch- oder Ausstrichpräparate) oder formalin-fixierte, paraffin-eingebettete (FFPE) Gewebe verwendbar sind. Kleinere Populationen aberranter Zellen können daher identifiziert und der relative Anteil aberranter Zellen *in vivo* oder eine Korrelation spezifischer chromosomaler Aberrationen zu der Morphologie des Tumorgewebes bestimmt werden. Weiterhin zeichnet sich die FISH durch eine höhere Auflösung als die CC aus. So liegt die Nachweisgrenze der CC bei mehreren Megabasenpaaren (Mb), wohingegen mittels FISH Segmente von unter 10 Kilobasenpaaren (kb) detektierbar sind, wodurch auch der Nachweis von kryptischen Rearrangierungen oder Deletionen möglich ist (Korenberg *et al.*, 1995; Trask, 2002). Darüber

hinaus lassen sich (komplexe) strukturelle Aberrationen molekularzytogenetisch weiter charakterisieren, indem z.B. die betroffenen chromosomalen Regionen bzw. Abschnitte identifiziert, die Größe deletierter oder amplifizierter Regionen genauer bestimmt und – im Falle von chromosomalen Rearrangierungen – die beteiligten Bruchpunktregionen weiter eingegrenzt werden können, was letztlich die Identifizierung der involvierten Gene erleichtert (Gray und Pinkel, 1992; Trask, 2002).

In der vorliegenden Arbeit liegt der Schwerpunkt auf der Untersuchung benigner hyperplastischer und neoplastischer Veränderungen der Schilddrüse. Molekularzytogenetische wie auch molekulargenetische Analysen der häufigen zytogenetischen Subgruppen in diesen Läsionen sollen der weiteren Charakterisierung sowie dem besseren Verständnis hinsichtlich der Relevanz der zu untersuchenden Aberrationen mit Bezug auf ihre Entstehungsmechanismen sowie ihrem Einfluss auf die Tumorgenese dienen. Entsprechend erfolgten zudem an uterinen Leiomyomen – benignen mesenchymalen Tumoren des Uterus – molekularzytogenetische Untersuchungen.

1.2 Hyperplasien und Neoplasien der Schilddrüse

Zu den häufigsten Veränderungen der Schilddrüse zählen Hyperplasien der Follikelepithelzellen (Struma). Bei einer Struma handelt es sich um eine nichtneoplastische Vergrößerung der Schilddrüse bedingt durch eine hyperplastische Vermehrung der Follikelepithelzellen (Thyreozyten), bei der es zu einem unterschiedlichen Grad an Knotenbildung kommen kann (Sheu *et al.*, 2003; Perren *et al.*, 2008).

Die häufigsten in der Schilddrüse auftretenden Neoplasien sind Tumoren epithelialen Ursprungs, von denen wiederum die follikulären Adenome als benigne neoplastische Läsionen den größten Anteil einnehmen. Unter den malignen Tumoren der Schilddrüse werden entsprechend ihres Ursprungs die Schilddrüsenkarzinome ausgehend von den Follikelepithelzellen (bis zu 99% aller Schilddrüsenkarzinome) von den medullären C-Zell-Karzinomen (MTC; >1%) unterschieden. Erstere werden weiterhin unterteilt in differenzierte (papilläre Schilddrüsenkarzinome (PTC) und follikuläre Schilddrüsenkarzinome (FTC)) sowie undifferenzierte (anaplastische) Karzinome (ATC) (Schmid *et al.*, 2003; DeLellis *et al.*, 2004; Husmann und Berlin, 2010).

Hinsichtlich der Pathogenese der follikulären Schilddrüsentumoren wird von einem Multistep-Prozess ausgegangen, welcher von der Hyperplasie über das follikuläre Adenom hin zu einem follikulären Karzinom führt, wohingegen sich die papillären Karzinome unabhängig davon direkt aus den Thyreozyten entwickeln. Bei weiterer Dedifferenzierung bilden sich letztlich die anaplastischen Karzinome aus den follikulären bzw. papillären Karzinomen. Neben histologischen Charakteristika stützen u.a. auch genetische Faktoren diesen Prozess der Karzinogenese. So werden u.a. aktivierende *RAS*-Punktmutationen als frühes initiierendes Ereignis der Karzinogenese angesehen, da sich diese sowohl in den follikulären Adenomen als auch in den differenzierten Karzinomen nachweisen lassen. Als bedeutend für die Progression der differenzierten Karzinome gelten demgegenüber u.a. chromosomale Rearrangierungen, die unter Beteiligung des *Rearranged During Transfection* (*RET*)-Protoonkogens oder des *Peroxisome Proliferator-Activated Receptor-Gamma* (*PPARγ*)- und des *Paired Box Gene 8* (*PAX8*)-Gens zur Bildung von Fusionsgenen (*RET/PTC*, *PAX8/PPARγ*) führen, welche charakteristisch sind für PTC (*RET/PTC*) bzw. FTC (*PAX8/PPARγ*) (Fagin, 1992; Tallini, 2002; Williams, 2002; Delellis, 2006; Kondo *et al.*, 2006; Parameswaran *et al.*, 2010).

Frühe zytogenetische Untersuchungen sowohl an benignen als auch malignen Läsionen der Schilddrüse erfolgten in den 1960er Jahren mit dem Nachweis von Aneuploidien aber auch strukturellen chromosomalen Aberrationen (Socolow *et al.*, 1964; Atkin und Baker, 1965; Beierwaltes und al-Saadi, 1966). In einer Arbeit an 340 Hyperplasien sowie Adenomen der Schilddrüse von Belge *et al.* (1998) zeigten sich in ca. 20% der untersuchten Läsionen zytogenetische Veränderungen. Gemeinsam mit den Ergebnissen weiterer zytogenetischer Untersuchungen an benignen Schilddrüsenläsionen lassen sich demnach drei große zytogenetische Subgruppen klassifizieren (Bartnitzke *et al.*, 1989; Bondeson *et al.*, 1989; Teyssier *et al.*, 1990; van den Berg *et al.*, 1990; Antonini *et al.*, 1991; Belge *et al.*, 1992b; Dal Cin *et al.*, 1992; Roque *et al.*, 1992; Roque *et al.*, 1993b; Belge *et al.*, 1994; Belge *et al.*, 1995; Cigudosa *et al.*, 1995; Belge *et al.*, 1997; Bol *et al.*, 1999).

Die häufigste zytogenetische Subgruppe ist charakterisiert durch die Trisomie 7, die in ca. 30% der Hyperplasien und Adenome mit klonalen zytogenetischen Aberrationen auftritt (Belge *et al.*, 1998). Es konnte gezeigt werden, dass die Trisomie 7 entweder solitär auftritt oder gemeinsam mit weiteren Trisomien, darunter die Trisomien 12 und 17. Hierbei wird die Trisomie 7 als primäres Ereignis angesehen, gefolgt von einer Sequenz weiterer Trisomien,

die zu einer kontinuierlichen Zunahme der Chromosomenanzahl führen (Bondeson *et al.*, 1989; Teyssier und Ferre, 1989; van den Berg *et al.*, 1990; Gama *et al.*, 1991; Sozzi *et al.*, 1992; Antonini *et al.*, 1993; Roque *et al.*, 1993b; Belge *et al.*, 1994). Innerhalb dieser Gruppe besteht eine Korrelation zwischen der Chromosomenanzahl und der Histologie der benignen Läsionen, wobei Hyperplasien mit einer Trisomie 7 eine Chromosomenanzahl von 49 oder weniger aufweisen, Adenome i.d.R. hingegen mehr als 49 Chromosomen. Daher wird angenommen, dass das Auftreten sekundärer Trisomien neben der Trisomie 7 einhergeht mit histo-morphologischen Veränderungen von Hyperplasien hin zu Adenomen (Belge *et al.*, 1994; Belge *et al.*, 1998).

Mit einer Häufigkeit von ca. 20% bilden Translokationen unter Beteiligung der chromosomalen Region 19q13.4 die zweithäufigste zytogenetische Subgruppe sowie die häufigste strukturelle Veränderung innerhalb benigner Schilddrüsenläsionen mit klonalen chromosomalen Aberrationen (Belge *et al.*, 1998). Beschrieben sind zahlreiche Translokationen zwischen Chromosom 19q13.4 und variierenden Translokationspartnern (Bartnitzke *et al.*, 1989; Bondeson *et al.*, 1989; Teyssier und Ferre, 1989; Belge *et al.*, 1992b; Dal Cin *et al.*, 1992; Belge *et al.*, 1995). Dies weist darauf hin, dass strukturelle Aberrationen innerhalb der Region 19q13.4 für die Entwicklung follikulärer Adenome der Schilddrüse von Bedeutung sind (Dal Cin *et al.*, 1992). Molekularzytogenetische sowie molekulargenetische Analysen ermöglichten einerseits die Eingrenzung der Bruchpunkte innerhalb einer 400 kb-Bruchpunktregion, andererseits die Identifizierung des Kandidatengens *Rearranged In Thyroid Adenomas* (*RITA*) alias *Zinc Finger Protein 331* (*ZNF331*), welches nahe der Bruchpunktregion lokalisiert ist (Belge *et al.*, 1995; Belge *et al.*, 1997; Rippe *et al.*, 1999). Später konnten dann innerhalb der Bruchpunktregion die microRNA (miRNA)-Cluster Chromosom 19 miRNA-Cluster (C19MC) sowie miR-371-3 identifiziert (Suh *et al.*, 2004; Bentwich *et al.*, 2005) und ein kausaler Zusammenhang zwischen der Expression von miRNAs der genannten Cluster und der Rearrangierung der chromosomalen Region 19q13.4 in benignen Schilddrüsenläsionen beschrieben werden (Rippe *et al.*, 2010).

Als weitere strukturelle Veränderung stellen Translokationen unter Beteiligung der chromosomalen Region 2p21 in 10% der benignen Schilddrüsenläsionen mit klonalen chromosomalen Aberrationen die dritthäufigste zytogenetische Subgruppe dar (Belge *et al.*, 1998; Bol *et al.*, 1999). Dabei finden sich wie bei den 19q13.4-Rearrangierungen verschiedene Translokationen mit unterschiedlichen Translokationspartnern, so dass

entsprechend der Region 2p21 ebenfalls eine bedeutende Rolle in der Pathogenese benigner Schilddrüsenläsionen zuzukommen scheint (Bol *et al.*, 1999). Innerhalb dieser Gruppe konnten die Bruchpunkte in der chromosomalen Region 2p21 mittels molekularzytogenetischer Analysen auf eine Region von 450 kb eingegrenzt (Bol *et al.*, 2001) und mit dem *Thyroid Adenoma Associated* (*THADA*)-Gen das direkt von den Translokationen betroffene Gen identifiziert werden (Rippe *et al.*, 2003).

Hinsichtlich ihrer Relevanz für die Entstehung bzw. Entwicklung benigner Schilddrüsenläsionen sind quantitative Untersuchungen der drei zytogenetischen Subgruppen weiterhin von Bedeutung, insbesondere, da die bisherigen Daten sich überwiegend auf kultivierte Zellen aus Hyperplasien und Adenomen beziehen, seltener auf die Primärläsionen als solche. Des Weiteren ist die Identifizierung und Charakterisierung der direkt an den beiden häufigen strukturellen Aberrationen in benignen Läsionen der Schilddrüse beteiligten Gene Voraussetzung für das Verständnis der molekularen Pathogenese von Hyperplasien wie auch follikulären Adenomen der Schilddrüse. Beide Aspekte, Identifizierung und Charakterisierung von Kandidatengenen in 2p21 und 19q13.4, sowie eine Quantifizierung der drei zytogenetischen Subgruppen auf Basis molekularzytogenetischer Analysen sind ein wesentlicher Bestandteil dieser Arbeit.

Für die follikulären wie auch papillären Karzinome der Schilddrüse sind wie bei den Hyperplasien und Adenomen teilweise charakteristische zytogenetische Aberrationen in Form von chromosomalen Rearrangierungen beschrieben, wobei im Gegensatz zu den benignen Läsionen die involvierten Gene identifiziert und die aus den Rearrangierungen resultierenden Fusionsgene molekulargenetisch charakterisiert sind (Grieco *et al.*, 1990; Sozzi *et al.*, 1994; Kroll *et al.*, 2000).

So ist innerhalb der follikulären Schilddrüsenkarzinome die Translokation t(2;3)(q13;p25) als wiederholt auftretende zytogenetische Aberration beschrieben, wobei diese vereinzelt auch in follikulären Adenomen nachgewiesen werden konnte (Sozzi *et al.*, 1992; Roque *et al.*, 1993a; Roque *et al.*, 1993b; Kroll *et al.*, 2000). Die Translokation t(2;3)(q13;p25) resultiert dabei – unter Beteiligung des in 2q13 lokalisiertem Transkriptionsfaktors *PAX8* und des in 3p25 lokalisiertem *PPARγ* – in der Bildung des Fusionsgens *PAX8/PPARγ*, von dem Kroll *et al.* (2000) mutmaßen, dass es hinsichtlich der diagnostischen Differenzierung follikulärer Schilddrüsenkarzinome von follikulären Adenomen nützlich ist. Da allerdings der Nachweis des Fusionsgens später sowohl in follikulären Karzinomen als auch Adenomen erfolgte, wird

die Bedeutung von *PAX8/PPARγ* als diagnostischer Marker zur Differenzierung von follikulären Karzinomen und Adenomen diskutiert (Marques *et al.*, 2002). Aus diesem Grund widmet sich ein weiterer Teil dieser Arbeit sowohl der näheren Analyse der Bruchpunktregion in 3p25 als auch dem Nachweis des Fusionsgens *PAX8/PPARγ* in follikulären Neoplasien der Schilddrüse.

1.3 Genetik benigner mesenchymaler Tumoren am Beispiel der uterinen Leiomyome

Neben den benignen und malignen Läsionen der Schilddrüse gibt es weitere humane Tumoren, für die umfangreiche zytogenetische Untersuchungen vorliegen. So sind die uterinen Leiomyome innerhalb der Tumoren mesenchymalen Ursprungs zytogenetisch ebenfalls sehr gut untersucht und weisen in 20% - 50% klonale chromosomale Aberrationen auf (Nilbert und Heim, 1990; Kiechle-Schwarz *et al.*, 1991; Pandis *et al.*, 1991; Rein *et al.*, 1991; Meloni *et al.*, 1992). Wie bei den benignen Läsionen der Schilddrüse finden sich auch hier zytogenetische Subgruppen, unter denen die größte, in ca. 20% der Fälle mit klonalen Aberrationen, charakterisiert ist durch Rearrangierungen unter Beteiligung der chromosomalen Region 12q14~15, i.d.R. als Translokation seltener auch als parazentrische Inversion (Heim *et al.*, 1988; Schoenmakers *et al.*, 1995; Wanschura *et al.*, 1997). In 17% der Fälle mit aberrantem Karyotyp finden sich eine interstitielle Deletion del(7)(q22q32) bzw. Rearrangierungen unter Beteiligung der Region 7q22 (Rein *et al.*, 1991; Ozisik *et al.*, 1993; Sargent *et al.*, 1994) sowie, in weniger als 5%, Rearrangierungen der Region 6p21 (Nilbert und Heim, 1990; Kiechle-Schwarz *et al.*, 1991; Ozisik *et al.*, 1995).

Innerhalb der 12q14~15-Subgruppe ist die Translokation t(12;14)(q15;q23~24) die am häufigsten beobachtete strukturelle chromosomale Aberration (Heim *et al.*, 1988). Translokationen unter Beteiligung von 6p21 sind u.a. die t(1;6)(q23;p21), t(6;10)(p21;q22) und die t(6;14)(p21;q24) (Kiechle-Schwarz *et al.*, 1991; Ozisik *et al.*, 1995; Hennig *et al.*, 1996; Sandberg, 2005).

Die an 6p21- bzw. 12q14~15-Rearrangierungen beteiligten Gene sind die *High Mobility Group Protein*-Gene *High Mobility Group AT-Hook 1* (*HMGA1,* 6p21) (Kazmierczak *et al.*, 1996a; Kazmierczak *et al.*, 1998) und *High Mobility Group AT-Hook 2* (*HMGA2*, 12q14~15) (Ashar *et al.*, 1995; Fejzo *et al.*, 1995; Schoenmakers *et al.*, 1995). Entsprechende

chromosomale Rearrangierungen unter Beteiligung von *HMGA1* und *HMGA2* sind auch für andere benigne mesenchymale Tumoren, u.a. chondroide Hamartome der Lunge, beschrieben (Kazmierczak *et al.*, 1996c; Kazmierczak *et al.*, 1999). Die Expression von *HMGA1* und *HMGA2* ist i.d.R. auf embryonales Gewebe beschränkt und in differenzierten Zellen in adultem Gewebe reprimiert (Chiappetta *et al.*, 1996; Rogalla *et al.*, 1996; Hirning-Folz *et al.*, 1998). Bedingt durch die chromosomalen Rearrangierungen der Regionen 6p21 und 12q14~15 in benignen mesenchymalen Tumoren kommt es allerdings zu einer Re-Expression von *HMGA1* und *HMGA2* (Schoenberg Fejzo *et al.*, 1996; Sornberger *et al.*, 1999).

Aufgrund der Kartierung der Bruchpunkte in 6p21 (Kazmierczak *et al.*, 1996a; Kazmierczak *et al.*, 1998), 12q14~15 (Schoenberg Fejzo *et al.*, 1996) sowie 14q23~24 innerhalb des Kandidatengens *RAD51 homolog B* (*S. cerevisiae*) (*RAD51L1*) für die Translokation t(12;14)(q14~15;q23~24) (Schoenmakers *et al.*, 1999) lassen sich die entsprechenden Rearrangierungen molekularzytogenetisch mittels FISH nachweisen. Eine Etablierung geeigneter DNA-Sonden sowie deren Einsatz zum Nachweis der o.g. Rearrangierungen mittels FISH im Rahmen von Untersuchungen zur dysregulierten Expression von *HMGA1* und *HMGA2* in uterinen Leiomyomen ist ein weiterer Bestandteil dieser Arbeit. Des Weiteren sollte mittels FISH festgestellt werden, ob eine der Translokation t(12;14)(q14~15;q23~24) in uterinen Leiomyomen entsprechende Beteiligung von *RAD51L1* in chondroiden Harmatomen der Lunge mit der Translokation t(6;14)(p21;q24) vorliegt.

1.4 Zielsetzung

Der Nachweis wiederholt auftretender bzw. spezifischer Chromosomenaberrationen in humanen Tumoren mittels molekularzytogenetischer Methoden wie der FISH ermöglicht eine weitere quantitative Bestimmung der entsprechenden zytogenetischen Veränderungen und ist zudem Grundlage einer genaueren Charakterisierung der betroffenen chromosomalen Regionen einschließlich der involvierten Gene.

In der vorliegenden Arbeit liegt unter diesem Aspekt der Schwerpunkt auf der molekularzytogenetischen und molekulargenetischen Analyse der in follikulären Läsionen der Schilddrüse beschriebenen zytogenetischen Subgruppen. Insbesondere die nähere Charakterisierung der chromosomalen Bruchpunktregionen 2p21 und 19q13.4 und die Quantifizierung der drei häufigen zytogenetischen Subgruppen, wie auch der Nachweis der

Translokation t(2;3)(q13;p25) und die Charakterisierung der an dieser Translokation beteiligten Region 3p25 erfolgten mit dem Ziel, die durch diese Veränderungen bedingten molekularen Mechanismen in follikulären Läsionen der Schilddrüse sowie deren pathogenetische Relevanz besser zu verstehen.

Ein weiterer Teil dieser Arbeit beschäftigt sich mit dem molekularzytogenetischen Nachweis von häufig in benignen mesenchymalen Tumoren auftretenden strukturellen chromosomalen Aberrationen, insbesondere der Rearrangierungen der Gene *HMGA1* und *HMGA2*, um ergänzend zu molekulargenetischen Analysen zum Verständnis der Zusammenhänge dieser Veränderungen und deren funktioneller Bedeutung speziell in uterinen Leiomyomen beizutragen.

2 Material und Methoden

Nähere Angaben zu den Materialien und Methoden sind den angefügten Publikationen bzw. den dort aufgeführten Referenzen zu entnehmen. Darüber hinaus ergänzende Informationen sind im Folgenden aufgeführt.

2.1 Gewebematerial einschließlich Tumorgewebe und Zelllinien

Gewebe von benignen Schilddrüsenläsionen einschließlich Hyperplasien und follikulären Adenomen sowie malignen Schilddrüsentumoren wurden zur Verfügung gestellt vom Zentrum für Pathologie (Klinikum Bremen Mitte, Bremen) sowie der Klinik für Allgemein- und Viszeralchirurgie des Krankenhaus St. Joseph-Stift (Bremen). Proben von uterinen Leiomyomen stammen aus der Frauenklinik des Krankenhaus St. Joseph-Stift (Bremen) sowie der Abteilung für Geburtshilfe und Gynäkologie des DIAKO Ev. Diakonie Krankenhaus (Bremen).

Nicht-humane Proben stammen entweder aus der Klinik für Kleintiere der Tiermedizinischen Hochschule (Hannover) oder wurden kommerziell erworben.

Zelllinien wurden zur Verfügung gestellt von PD Dr. Gazanfer Belge (Zentrum für Humangenetik, Universität Bremen). Die Etablierung der Zelllinien aus benignen Schilddrüsenläsionen erfolgte durch eine Transfektion mit dem SV40-Plasmid (SV40 „early region“) (Kazmierczak *et al.*, 1990; Belge *et al.*, 1992a).

2.2 *In silico* Analyse

Sequenzanalysen einschließlich Design verwendeter DNA-Primer, Bearbeitung von Sequenzen und Sequenzhomologieanalysen erfolgten unter Verwendung der Lasergene Sequenzanalyse Software (DNAStar), Vector NTI (Invitrogen) sowie des Basic Local Alignment Search Tools (BLAST) (Altschul *et al.*, 1997) (http://blast.ncbi.nlm.nih.gov/Blast.cgi). Eine Bearbeitung von Sequenzierungsdaten erfolgte mit Chromas Lite (Technelysium Pty Ltd).

2.3 RNA-Isolierung und complementary DNA (cDNA)-Synthese

Gesamt-RNA aus kultivierten Zelllinien wurde gemäß den Herstellerangaben isoliert unter Verwendung des TRIzol Reagenz (Invitrogen – Life Technologies, Darmstadt).

Die cDNA-Synthese erfolgte entsprechend den Herstellerangaben mit der Moloney Murine Leukemia Virus (M-MLV) Reverse Transkriptase (RT) (Invitrogen – Life Technologies) unter Verwendung eines Poly (A)-Adapter Primers (AP2).

2.4 3‘-rapid amplification of cDNA-ends with polymerase chain reaction (RACE-PCR) und Southern Blot

Die 3‘-RACE-PCR wurde gemäß den Angaben des Advantage® cDNA PCR Kit (Clontech Laboratories, Mountain View, USA) durchgeführt. Hinsichtlich der Durchführung des Southern Blot sei auf das DIG Application Manual for Filter Hybridization (Roche Applied Science, Mannheim) bzw. die entsprechende Publikation verwiesen (Rippe *et al.*, 2003).

2.5 PCR

Die PCR wurde mit genspezifischen Primern unter Verwendung der Taq DNA Polymerase (Invitrogen – Life Technologies, Darmstadt) durchgeführt. Als Grundlage diente das Basic PCR Protocol (Invitrogen – Life Technologies, Darmstadt), wobei sowohl Annealing-Temperaturen als auch Inkubationszeiten und Zyklenzahl den jeweiligen Primern und Templates angepasst wurden.

Die Aufreinigung der PCR-Produkte erfolgte entweder mit dem QIAEX II Gel Extraction Kit bzw. dem QIAquick Gel Extraction Kit (QIAGEN, Hilden) oder dem QIAquick PCR Purification Kit (QIAGEN, Hilden).

2.6 Klone

Chromosom 19-spezifische P1-derived Artificial Chromosome (PAC)-Klone stammen aus einer humanen PAC-Library (Genome Systems) (Rippe *et al.*, 1999), Cosmid-Klone aus der LLNL Chromosome 19 Library LL19NC02 und LL19NC03 (Source Bioscience, Nottingham, UK) (Belge *et al.*, 1997; Rippe *et al.*, 1999) sowie Bacterial Artificial Chromosome (BAC)-Klone aus

der CalTech Human BAC library (Source Bioscience, Nottingham, UK). Weitere humane BAC-Klone wurden aus der Human BAC (RPCI-11) Library (imaGenes, Berlin, Deutschland) entnommen. Für die Auswahl von BAC-Klonen wurde der MapViewer (http://www.ncbi.nlm.nih.gov/projects/mapview/) bzw. der Human (Homo sapiens) Genome Browser (http://genome.ucsc.edu/cgi-bin/hgGateway) verwendet. Die Aufreinigung der Klone erfolgte mit dem QIAGEN Plasmid Midi Kit (QIAGEN, Hilden).

2.7 Fluoreszenz *in situ* Hybridisierung (FISH)

2.7.1 Anfertigung von Chromosomenpräparaten

Für die FISH wurden Chromosomenpräparate entweder aus Zelllinien oder Primärtumoren angefertigt. Die Arretierung der Zellen in der Metaphase erfolgte durch Zugabe von Colcemid (Biochrom, Berlin). Mittels einer Trypsin/Ethylendiamintetraacetat (EDTA)-Lösung (BD Biosciences, Heidelberg) wurden die Zellen in der Kulturflasche abgelöst und nach hypotoner Behandlung (Medium:bidest. H_2O – 1:7) abschließend mit einer Methanol:Eisessig (3:1)-Lösung fixiert und auf kalte und entfettete Objektträger getropft. Die Präparate wurden vor Einsatz in der FISH mindestens 2 Tage bei 37°C oder über Nacht bei ca. 60°C getrocknet.

2.7.2 GTG-Banding von Chromosomenpräparaten

Hinsichtlich der Identifizierung von Chromosomen nach der FISH wurde zuweilen eine GTG-Banding der Chromosomenpräparate durchgeführt. Diese erfolgte mit Modifikation nach Seabright (1971). So wurden die Präparate in einer niedrigkonzentrierten Trypsinlösung inkubiert und anschließend kurz in einer 1%igen Giemsalösung gefärbt. Nach Abwaschen überschüssiger Giemsalösung und Trocknung der Präparate bei Raumtemperatur (R.T.) wurden diese entweder mindestens 2 Tage bei 37°C oder über Nacht bei ca. 60°C getrocknet.

2.7.3 Anfertigung von Touch-Präparaten

Die Anfertigung von Touch-Präparaten wurde entsprechend eines modifizierten Protokolls von Xiao *et al.* (1995) durchgeführt. Dabei wurden kleinere Gewebeproben mit einem Durchmesser von bis zu 3mm auf sterile Objektträger mehrmals aufgepresst. Eine Fixierung der Präparate erfolgte für eine Stunde bei 4°C in 70% Ethanol. Eine langfristige Lagerung

erfolgte optional im Anschluss an eine aufsteigende Ethanolreihe in 96% Ethanol bei -20°C. Die Präparate wurden vor Einsatz in der FISH über Nacht bei R.T. getrocknet.

2.7.4 Markierung der Sonden-DNA

Der Einbau von Hapten- bzw. Fluoreszenz-konjugierten Nukleotiden erfolgte mittels Nick-Translation unter Verwendung des DIG- bzw. Biotin-Nick Translation Mix (Roche Applied Science, Mannheim) oder dem Nick Translation Kit (Abbott Molecular, Wiesbaden).

2.7.5 Zusammensetzung der Hybridisierungsmixe

Die Hybridisierungsmixe enthielten neben der markierten Sonden-DNA unmarkierte Competitor-DNA wie entweder humane Plazenta-DNA und Salmon Sperm DNA (SIGMA Aldrich, München) oder humane COT-DNA (Roche Applied Science, Mannheim) sowie weiterhin 50% Fomamid, 2xSSC sowie 10% Dextransulfat. Die Konzentration der markierten Sonden-DNA variierte in Abhängigkeit der Anzahl der enthaltenen Sonden sowie der Größe der Targetbereiche und ist den entsprechenden Publikationen zu entnehmen.

2.7.6 Kommerzielle Sonden

Kommerziell erhältliche Sonden wurden von Pan Path (Budel, Niederlande) bezogen.

2.7.7 Durchführung FISH an Chromosomen- und Touch-Präparaten

Die FISH wurde im wesentlichen nach einem von Kievits *et al*. (1990) modifizierten Protokoll durchgeführt. Die Modifikationen betreffen die Denaturierung der Sonden-DNA sowie der Präparate, die entweder separat oder co-denaturiert wurden, sowie die Posthybridisierungskonditionen, welche sowohl der jeweiligen Sonden-DNA als auch den Präparaten entsprechend angepasst wurden. Die jeweiligen Konditionen sind den Publikationen zu entnehmen.

2.7.8 Durchführung FISH an FFPE-Gewebeschnitten

Die FISH wurde an 4µm FFPE-Gewebeschnitten, welche auf Adhäsionsobjektträger (Gerhard Menzel GmbH, Braunschweig) aufgetragen waren, durchgeführt. Vor der FISH erfolgte eine Trocknung der Präparate entweder über Nacht bei 56°C oder für 3h bei 80°C. Die FISH erfolgte im wesentlichen nach einem Protokoll von Hopman und Ramaekers (2001) und wurde den Geweben entsprechend angepasst. Modifikationen betreffen dabei den Proteaseverdau der Gewebeschnitte hinsichtlich Inkubationszeit und verwendetem Enzym

sowie weiterhin die co-Denaturierungs- und Posthybridisierungskonditionen und sind den entsprechenden Publikationen zu entnehmen.

2.7.9 Durchführung FISH an HEPES-glutamic acid buffer mediated organic solvent protection effect (HOPE)-fixiertem, paraffin-eingebetteten Gewebeschnitten

5µm Schnitte HOPE-fixierter, paraffin-eingebetteter Gewebe wurden in Diethylether entparaffiniert und anschließend einem Proteaseverdau zum Abbau von Proteinen und Bindegewebe unterzogen. Die Inkubationszeit wurde den unterschiedlichen Geweben angepasst. Es folgte eine Postfixierung in einer 1%igen Formaldehyd/1xPBS-Lösung mit anschließender Dehydrierung und Trocknung der Präparate. Die weiteren Schritte wurden wie unter 2.7.7 angegeben durchgeführt.

2.7.10 Fluoreszenz-mikroskopische Auswertung der Präparate

Die Auswertung der Präparate sowie die Bilddokumentation erfolgte an einem geeigneten Fluoreszenzmikroskop (Zeiss, Göttingen) unter Verwendung entsprechender Analysesoftware wie MacProbe (Perceptive Scientific Instruments (PSI), Halladale, United Kingdom), AxioVision (Zeiss, Göttingen) oder FISHView (Applied Spectral Imaging (ASI), Migdal Haemek, Israel).

3 Ergebnisse

Molekularzytogenetische sowie molekulargenetische Untersuchungen spezifischer chromosomaler Aberrationen bei humanen Tumoren sind grundlegend für das Verständnis des Einflusses dieser Veränderungen hinsichtlich der Entstehung und Entwicklung der entsprechenden Tumoren. Der Fokus der vorliegenden Arbeit lag dabei auf der quantitativen Analyse der drei häufigsten zytogenetischen Subgruppen bei benignen follikulären Schilddrüsenläsionen (3.1) sowie der näheren Charakterisierung der beiden häufigsten strukturellen Veränderungen, Rearrangierungen der chromosomalen Region 2p21 (3.2) und 19q13.4 (3.3). Des Weiteren erfolgten molekulargenetische und molekularzytogenetische Untersuchungen des häufig bei follikulären Schilddrüsenkarzinomen nachgewiesenen und durch die Translokation t(2;3)(q13;p25) bedingten Fusionsgens *PAX8/PPARγ* in benignen und malignen Schilddrüsentumoren sowie der *PPARγ*-Bruchpunktregion in 3p25 in benignen follikulären Adenomen der Schilddrüse (3.4).

Ein weiter Aspekt dieser Arbeit waren die molekularzytogenetische Charakterisierung der an der Translokation t(6;14)(p21;q24) beteiligten Bruchpunktregion 14q24 in chondroiden Hamartomen der Lunge und molekularzytogenetische Untersuchungen in Ergänzung zu molekulargenetischen Analysen uteriner Leiomoyme mit Fokus auf den Genen *HMGA1* (6p21) und *HMGA2* (12q14~15) (3.5).

3.1 Quantitative Untersuchungen der drei häufigsten zytogenetischen Subgruppen bei benignen follikulären Schilddrüsenläsionen

I. Interphase fluorescence in situ hybridization analysis detects a much higher rate of thyroid tumors with clonal cytogenetic deviations of the main cytogenetic subgroups than conventional cytogenetics (Drieschner *et al.*, 2011)

Die Verteilung der drei häufigsten zytogenetischen Subgruppen in benignen Läsionen der Schilddrüse, Trisomie 7 und Rearrangierungen der chromosomalen Region 2p21 bzw. 19q13.4, basiert bisher im Wesentlichen auf konventionellen zytogenetischen Untersuchungen. Da es bedingt durch die Kultivierung der Zellen zur zytogenetischen Analyse zu einer *in vitro* Selektion gegenüber den Tumorzellen kommen kann und die Ergebnisse abhängig sind von der Quantität als auch Qualität der präparierten Metaphase-Chromosomen, kann die tatsächliche Verteilung zytogenetischer Subgruppen von der mittels

CC bestimmten abweichen. Daher wurde an 161 benignen Schilddrüsenläsionen von 117 Patienten sowohl eine I-FISH als auch CC durchgeführt. Die I-FISH erfolgte dabei an Touchpräparaten der Läsionen, die direkt vom Primärgewebe angefertigt wurden. Das Restgewebe wurde daraufhin für die CC kultiviert.

Insgesamt zeigte sich, dass die I-FISH eine deutlich höhere Erfolgsquote aufwies (in 160 von 161 Tumoren konnte ein Ergebnis erzielt werden) als die CC (132 von 161 Tumoren). Hinsichtlich klonaler chromosomaler Aberrationen waren nach CC 16 von 132 Tumoren positiv, wohingegen mit der I-FISH 41 von 160 Tumoren entsprechende Aberrationen aufwiesen. Unter den 116 Tumoren, die nach CC unauffällig waren, fanden sich 14, die nach I-FISH klonale chromosomale Aberrationen aufwiesen.

Mit Bezug auf die zytogenetischen Subgruppen waren nach CC drei Fälle positiv hinsichtlich der Trisomie 7 (18,8% der Fälle mit klonalen chromosomalen Aberrationen), wohingegen mittels I-FISH insgesamt 23 Fälle der Gruppe mit Trisomie 7 zugeordnet werden konnten (56,1% der Fälle mit klonalen chromosomalen Aberrationen).

19q13.4-Rerrangierungen fanden sich in fünf Fällen nach CC sowie in acht Fällen nach I-FISH. In vier der fünf Tumoren, die nach CC positiv hinsichtlich einer 19q13.4-Rearrangierung waren, konnte die Rearrangierung auch mittels I-FISH nachgewiesen werden. Für den fünften Tumor zeigte eine Metaphase-FISH, dass hier die Bruchpunkte nicht innerhalb des Bruchpunktclusters in 19q13.4 lokalisiert sind. Die drei Fälle, die ausschließlich nach I-FISH positiv auf eine 19q13.4-Rearrangierung waren, zeigten nach CC keine Aberration (2 Fälle) oder lediglich eine Deletion des langen Arms von Chromosom 6.

In nur einem Fall fand sich nach CC eine Deletion des kurzen Arms von Chromosom 2 einschließlich der Region 2p21. Mittels I-FISH ließen sich strukturelle Aberrationen unter Beteiligung der Region 2p21 in insgesamt sechs Tumoren nachweisen.

Aberrationen, die ausschließlich mittels CC nachweisbar waren, fanden sich in fünf Fällen. Alle Aberrationen waren in diesen Fällen über I-FISH nicht nachweisbar, da diese mit den verwendeten FISH-Sonden nicht erfasst werden konnten.

Eine statistische Analyse der Fälle, für die ein Ergebnis nach CC vorlag und die positiv hinsichtlich chromosomaler Aberrationen nach I-FISH waren, zeigte einen signifikanten Unterschied mit Bezug auf die Häufigkeit positiver Interphase-Kerne zwischen den Fällen, für die die CC die entsprechende Aberration zeigen konnte und solchen Fällen, die nach I-FISH

positiv, nach CC hingegen unauffällig waren. So war der Anteil positiver Kerne in den Fällen, in denen beide Methoden die Aberration erfassten, höher im Vergleich zu den Fällen, unter denen nur die I-FISH eine Aberration nachweisen konnte.

Insgesamt scheint somit der Anteil von benignen Schilddrüsenläsionen, die den drei häufigen zytogenetischen Subgruppen zugeordnet werden können, höher zu sein als bisher angenommen. Zudem erwies sich die I-FISH als deutlich sensitivere Methode zum Nachweis der drei zytogenetischen Subgruppen bei benignen Schilddrüsenläsionen.

I

Interphase fluorescence in situ hybridization analysis detects a much higher rate of thyroid tumors with clonal cytogenetic deviations of the main cytogenetic subgroups than conventional cytogenetics

Norbert Drieschner, Volkhard Rippe, Anne Laabs, Lea Dittberner, Rolf Nimzyk, Klaus Junker, Birgit Rommel, Yvonne Kiefer, Gazanfer Belge, Jörn Bullerdiek, Wolfgang Sendt

(Cancer Genetics 204(7): 366-374)

Eigenanteil:

- Planung und Durchführung der molekularzytogenetischen Untersuchungen.
- Auswertung der zytogenetischen und molekularzytogenetischen Daten.
- Verfassen des Artikels gemeinsam mit Jörn Bullerdiek.

ELSEVIER

Cancer Genetics 204 (2011) 366–374

Cancer Genetics

Interphase fluorescence in situ hybridization analysis detects a much higher rate of thyroid tumors with clonal cytogenetic deviations of the main cytogenetic subgroups than conventional cytogenetics

Norbert Drieschner [a], Volkhard Rippe [a], Anne Laabs [a], Lea Dittberner [a], Rolf Nimzyk [a], Klaus Junker [b], Birgit Rommel [a], Yvonne Kiefer [a], Gazanfer Belge [a], Jörn Bullerdiek [a,c,*], Wolfgang Sendt [d]

[a] *Center for Human Genetics, University of Bremen, Germany;* [b] *Department of Pathology, Hospital Bremen-Mitte, Bremen, Germany;* [c] *Small Animal Clinic, University of Veterinary Medicine, Hanover, Germany;* [d] *Department of General and Visceral Surgery of the St. Joseph Stift, Bremen, Germany*

In benign thyroid lesions, three main cytogenetic subgroups, characterized by trisomy 7 or structural aberrations involving either chromosomal region 19q13.4 or 2p21, can be distinguished by conventional cytogenetics (CC). As a rule, these aberrations seem to be mutually exclusive. Interphase fluorescence in situ hybridization (I-FISH) analysis on benign as well as malignant thyroid neoplasias has been performed in the past, but rarely in combination with CC. In the present paper, we have analyzed 161 benign thyroid lesions both with CC and I-FISH on touch preparations by using a multi-target, triple-color FISH assay as well as dual-color break-apart probes for detection of the main cytogenetic subgroups. Within the samples, I-FISH detected tumors belonging to either of the subgroups more frequently than CC (23 vs. 11.4%), either due to small subpopulations of aberrant cells or to cryptic chromosomal rearrangements (three cases). Thus, I-FISH seems to be more sensitive than CC, particularly in the detection of subpopulations of cells harboring cytogenetic aberrations that may be overlooked by CC. In summary, I-FISH on touch preparations of benign thyroid lesions seems to be a favorable method for cytogenetic subtyping of thyroid lesions.

Keywords Thyroid, benign thyroid lesions, cytogenetic subgroups, interphase FISH, conventional cytogenetic

Conventional cytogenetics (CC) of benign thyroid lesions has revealed recurrent identical cytogenetic subgroups both in thyroid hyperplasias and follicular thyroid adenomas (1–8). The main cytogenetic subgroups are, in order of frequency, trisomy 7 alone or with trisomies involving additional chromosomes (9,10) and structural aberrations either of the chromosomal bands 19q13.4 (4,10) or 2p21 (5,11). These three subgroups account for approximately one half of all clonal chromosomal changes found by CC in benign thyroid lesions (10,11).

However, the accuracy of CC depends on the availability and quality of metaphase chromosomes and may be influenced by in vitro selection against tumor cells. To circumvent these limitations in the detection of cases with recurrent chromosomal aberrations, interphase fluorescence in situ hybridization (I-FISH) on cytologic preparations or formalin-fixed, paraffin-embedded tissue sections (FFPEs; 12,13) offers an alternative approach.

As for benign and malignant thyroid lesions, I-FISH analyses were performed previously for the detection of

Received August 17, 2010; received in revised form March 22, 2011; accepted March 31, 2011.

* Corresponding author.
E-mail address: bullerdiek@uni-bremen.de

2210-7762/$ - see front matter © 2011 Elsevier Inc. All rights reserved.
doi:10.1016/j.cancergen.2011.03.008

either numeric chromosomal aberrations such as trisomy 7, trisomy 10, or trisomy 12 (14–17), or for structural aberrations involving *RET* rearrangements (18,19) or *PPARγ* rearrangements (20). Most of these analyses, however, were based on archival material, such as FFPE samples and, thus, CC has not been performed in parallel. Moreover, in benign lesions, I-FISH and CC have been performed only with respect to numerical aberrations of chromosomes 7 and 12 (16). To our knowledge, no such study so far has examined benign thyroid lesions for the detection of all main cytogenetic subgroups.

Using a multi-target FISH probe set, including a centromeric probe for chromosome 7, as well as dual-color break-apart probes for the detection of 19q13.4 (TBPC19; thyroid breakpoint cluster 19q13) and 2p21 (TBPC2; thyroid breakpoint cluster 2p21) rearrangements, we have performed I-FISH on touch preparations of 161 benign thyroid lesions. CC was done in parallel, thus allowing for the comparison of cytogenetic data with the results obtained by I-FISH.

Material and methods

Samples

A total of 161 benign thyroid lesions from 117 patients were used for CC and FISH analysis. All samples were obtained from patients undergoing thyroid resection in the Department of General and Visceral Surgery of the St. Joseph Stift (Bremen, Germany) during a 12-month time period. Histopathology examination was done in the Department of Pathology, Hospital Bremen-Mitte (Bremen, Germany). One piece of each tumor was stored in Hank's solution for cell culture. The use of human thyroid tumors for this study was approved by the local medical ethics committee and followed the guidelines of the declaration of Helsinki. Only samples that were initially taken for diagnostic purposes were secondarily used for the present study. Because the samples were de-identified and were considered as samples normally discarded, the committee felt that there was no specific patient consent necessary.

Touch preparations

For each lesion, part of the tissue sample (about 3 mm in diameter) was used for touch preparations, which were obtained by pressing fresh or previously frozen tissue samples several times on the surface of a clean, sterilized slide. The slides were then immediately placed in 70% ethanol and incubated for 1 hour at 4°C (21). For long-term storage, the touch preparations were dehydrated in an ascending ethanol series (70, 80, 96%; 2 minutes each) and stored in 96% ethanol at -20°C before use. Before FISH, the slides were air-dried overnight at room temperature.

Cell preparations and conventional cytogenetics

Cell culture of the thyroid lesions was performed as described previously (10). Briefly, the samples were mechanically reduced to small pieces and enzymatically digested by use of collagenase (Serva, Heidelberg, Germany). For in vitro cell culture, the suspension was then resuspended in culture medium and transferred into 25-cm^2 culture flasks. Medium was changed after 2 days of incubation, at least twice a week. Chromosome preparations and CC, respectively, were performed using routine methods (22). If available, at least 10 metaphases per case were karyotyped.

FISH analysis

I-FISH analysis was performed on touch preparations of thyroid lesions. For detection of common chromosomal aberrations in benign thyroid lesions (i.e., 2p21 rearrangements, 19q13.4 rearrangements, or trisomy 7), a multi-target, triple-color FISH assay (PanPath, Budel, The Netherlands) was used. The triple-color FISH assay contains break-apart probes located within 2p21 flanking the *THADA* gene (red fluorescent probes labeled with AlexaFluor 555) and within 19q13.4, flanking the common breakpoint-cluster (green fluorescent probes labelled with AlexaFluor 488), as well as a centromere 7–specific alpha-satellite probe (aqua fluorescent probe labelled with 7-diethylaminocoumarin-3-carboxylic acid (DEAC)). Ten microliters of the triple-color FISH assay was used per slide. Co-denaturation was performed on a Mastercycler gradient (Eppendorf, Hamburg, Germany) for 3 minutes at 80°C followed by O/N hybridization in a humidified chamber at 37°C. Post-hybridization was performed at 61°C for 5 minutes in 0.1× standard saline citrate. Interphase nuclei were counterstained with 4′,6′-diamidino-2′-phenylindol-dihydrochloride (DAPI; 0.75 μg/ml). Slides were examined with an Axioskop 2 plus fluorescence microscope (Zeiss, Göttingen, Germany). Images were captured with an AxioCam MRm digital camera and edited with AxioVision (Zeiss, Göttingen, Germany). A total of 200 non-overlapping nuclei were scored from each case. For each probe, cut-off values were calculated. The cut-off values were defined as the mean plus three standard deviations (M+3SD) of the number of nuclei with abnormal signal patterns in control specimens (23). Touch preparations of four previously frozen normal thyroid tissue samples were used as controls. FISH was performed twice for each control specimen. To calculate the cut-off values, the signal patterns of 200 non-overlapping nuclei of the control specimen were determined independently by three different observers. A normal nucleus is characterized by two signals for each probe (two red, two green, and two aqua signals; 2R2G2A; Figure 1A). Trisomy 7 is indicated by three aqua signals (e.g., 2R2G3A). Three red or green signals indicate either a rearrangement or a trisomy of chromosomal region 2p21 (3R2G2A) or of chromosomal region 19q13.4 (2R3G2A). The detailed classifications of aberrations, depending on the signal pattern, are shown in Table 1. To further discriminate between rearrangements or trisomy of chromosomal regions 2p21 or 19q13.4, a subsequent FISH was performed with dual-color break-apart probes (PanPath, Budel, The Netherlands) of the respective region (i.e., TBPC19 or TBPC2) on touch preparations of cases that either showed three signals for chromosomal region 19q13.4 or 2p21. The two-color break-apart probes correspond to the 2p21 or 19q13.4 break-apart probes of the triple-color FISH assay. FISH was performed as described above. Three fusion signals (3F) indicate a trisomy, whereas one fusion signal along with a single green and a single red signal (1R1G1F)

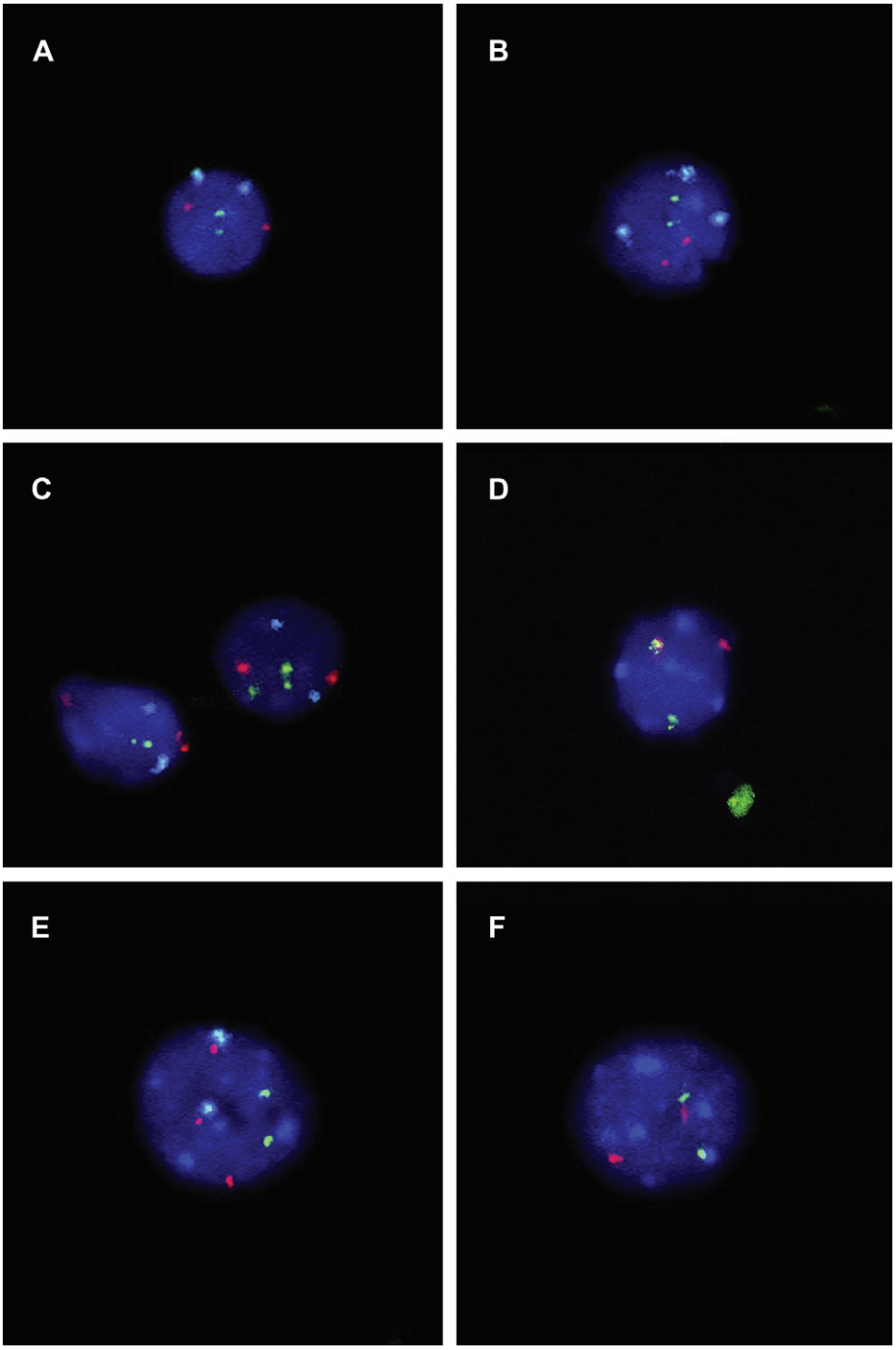

Figure 1 Interphase FISH (I-FISH) on touch preparations of benign thyroid lesions. (A) I-FISH with the multi-target, triple-color FISH assay shows a normal signal pattern (2R2G2A) in case 88-1. (B) I-FISH reveals a trisomy 7 (2R2G3A) in case 55 by use of the multi-target, triple-color FISH assay. (C) A 19q13.4 rearrangement or a trisomy 19 is indicated by three green signals (2R3G2A) of the thyroid breakpoint cluster 19q13 (TBPC19) probe after I-FISH with the multi-target, triple-color FISH assay on case 96. (D) On the same case the signal pattern 1R1G1F after I-FISH with the dual-color break-apart probe TBPC19 confirms a 19q13.4 rearrangement. (E) I-FISH on case 45 with the multi-target, triple-color FISH assay shows the signal pattern 3R2G2A, indicating either a 2p21 rearrangement or a trisomy 2. (F) Subsequent I-FISH on case 45 with the dual-color break-apart probe (TBPC2) confirms a 2p21 rearrangement indicated by the signal pattern 1R1G1F.

Table 1 Classification of different signal patterns after FISH on interphase nuclei by use of the multi-target, triple-color FISH assay

Description of signal number/nucleus	Signal pattern (multi−target, triple-color FISH assay)[a]	Corresponding aberration
Two signals for each locus	2R2G2A	Normal
One signal for 2p21 (or 19q13.4)	1R2G2A (or 2R1G2A)	(Partial) deletion of 2p21/*THADA* (or 19q13.4) or monosomy 2 (or 19)
One signal for centromere 7	2R2G1A	Monosomy 7
≥4 signals for at least one locus	4R2G2A, 2R4G2A, 2R2G4A etc.	Polysomy of the corresponding chromosome(s)
≥3 signals for centromere 7 (and ≥3 signals for 2p21 or 19q13.4), ≥3 signals for each locus	2G2R3A (3R2G3A, 2R3G3A etc.), ≥3R3G3A	Tri-/polysomy 7 (with additional Tri-/polysomy)[b]
3 signals for 2p21 (or 19q13.4)	3R2G2A (2R3G2A)	Trisomy 2 (or 19) or rearrangement of 2p21/*THADA* (or 19q13.4)[b]

[a] Fluorescence colors of the triple-color FISH probe are red (R; AlexaFluor555; 2p21/*THADA*), green (G; AlexaFluor488; 19q13.4), and aqua (A; DEAC; centromere 7); not all possible signal patterns are shown.
[b] For discrimination between trisomy or rearrangement subsequent FISH with two-color, break-apart probes for the corresponding locus is recommended.

indicate a rearrangement of the corresponding chromosomal region. Depending on the availability and quality of metaphase chromosomes on cases with rearrangements, metaphase FISH was performed as described above after GTG banding of the same metaphase spreads to determine the involved translocation partners.

Statistical analysis

Statistics were performed by a Wilcoxon rank sum test (using continuity correction) to compare differences between cases positive for chromosomal aberrations after I-FISH with and without the corresponding chromosomal aberrations as found by CC. $P < 0.05$ was considered significant.

Results

Overview of I-FISH and CC analyses on benign thyroid lesions

CC was successful on 132/161 cases (82.0%). For the remaining 29 cases (18.0%), chromosome analysis was not possible due to failure during in vitro cultivation, poor chromosome morphology, or less than 10 metaphases available for analysis (Supplementary Table 1). A total of 16 cases were characterized by clonal chromosomal abnormalities including numerical ($n = 3$), structural ($n = 11$), and both numerical and structural aberrations ($n = 2$; cases 10-1 and 11-1). Thus, 116/132 cases (87.9%) were classified as non-aberrant.

I-FISH was successful on touch preparations in 160/161 cases (99.4%; Table 2, Supplementary Table 1). In three cases (nos. 2, 3-2, and 4), I-FISH was successful only with the dual-color break-apart probes specific for 2p21 rearrangements (TBPC2) and 19q13.4 rearrangements (TBPC19). In one case (no. 18-2), signals were too weak for evaluation after I-FISH with the triple-color FISH assay, and due to a limited number of slides, no further I-FISH with the dual-color break-apart probes was possible. A total of 119 cases (74.4%) did not show chromosomal aberrations (Figure 1A), whereas 41 cases (25.6%) revealed chromosomal aberrations, as detected by I-FISH. Of the latter cases, CC confirmed the results of I-FISH in nine cases (case nos. 2, 10-1, 27, 60, 62-2, 70, 72, 84, and 111; Table 2). Of 116 cases with normal karyotypes, 14 samples were positive for aberrations, as shown by I-FISH (Table 2). It is noteworthy that I-FISH did not fail to detect aberrations of one of the three subtypes detected by CC in any of the cases.

Trisomy 7

CC detected three cases (case nos. 62-2, 72, and 84) belonging to the trisomy 7 cytogenetic subgroup (2.3% of all 132 cases with successful CC and 18.8% of cases with clonal chromosomal abnormalities).

I-FISH on 160 touch preparations of benign thyroid lesions revealed that trisomy or polysomy 7 alone or with additional gains of 2p21 or 19q13.4, respectively, most likely reflecting trisomies/polysomies, was the most frequent aberration (Figure 1B; $n = 23$; 14.4% of 160 cases with successful I-FISH and 56.1% of 41 cases positive for chromosomal aberrations, respectively).

19q13.4 rearrangements

Of the 11 cases with structural aberrations, CC detected chromosome 19 rearrangements in five cases (nos. 2, 17-2, 27, 60, and 111; 3.8% of all 132 cases with successful CC and 31.3% of cases with clonal chromosomal abnormalities). In contrast, 19q13.4 rearrangements were detectable by I-FISH in eight cases (Figure 1, C and D; 5% of 160 cases with successful I-FISH and 19.5% of 41 cases positive for chromosomal aberrations). For one case (no. 62-1), I-FISH showed three signals for chromosomal region 19q13.4 (signal pattern 2R3G2A). Due to a small sample size, it was not possible to further discriminate between trisomy 19 and rearrangement of 19q13.4 by subsequent I-FISH with the dual-color break-apart probe TBPC19.

In four of five cases with chromosome 19 rearrangements as described by CC, 19q13.4 rearrangements were detected previously by I-FISH. For the fifth case (no. 17-2), it was

Table 2 Results of conventional cytogenetic (CC) and FISH analysis of 161 benign thyroid lesions, including I-FISH on touch preparations of all cases. Cases in which CC was not performed or I-FISH did not reveal any data are shown in Supplementary Table 1; cases with normal karyotype and nonaberrant I-FISH results are not shown.

		Conventional cytogenetic	Interphase FISH results			
Case no.	Histopathology	Karyotype	2p21	19q13.4	Cen7	trisomy 7 with additional tri-/polysomies (≥3signals for each probe)
2	FA	46,XY,t(2;4;14;19)(p?13;q?31;q11.2;q13)		r [87%]	–*	
3–1	FA	46,XY				tr7 [15.5% (2p21) – 18% (Cen7)]†
8–2	NA	46,XX			tr [26%] / p [72%]	
10–1	FA	46∼88,XX,t(3;10)(q2?4;q2?4)[4],der(12)[2],+mar[4][cp9]/46,XX[2]				tr7 [8% (Cen7) – 8.5% (2p21, 19q13.4)]
10–2	FA	46,XX,del(6)(q21∼q22)		r [88%]		
12	FA	46,XY				tr7 [7% (2p21, Cen7) – 8.5% (19q13.4)]
17–2	NG	46,XX,t(3;19)(p2?1;?p13)[9]/46,XX[2]		r/tr [95%]‡		
17–3	FA	46,XX	tr [7.5%]			
21–1	NG	46,XX			tr [8.5%]	
27	NG	46,XX,t(1;19)(q32;q13)[8]/46,XX[24]		r [12.5%]		
30	FA	46,XY		r [24%]		
38	NG	46,XX	d [11.5%]			
57	NG	46,XX				tr7 [17.5% (19q13.4) – 42.5% (Cen7)]
60	FA	46,XY,t(19;20)(q13;p11.2)		r [64%]		
62–1	FA	46,XX		r/tr [6.5%]‡		
62–2	FA	53,XX,+5,+7,+8,+12,+16,+17,+20[6]/46,XX[15]			tr [52%]	
66	NG	46,XY	p [8.5%]		p [9%]	
67–1	NG	46,XY	p [5.5%]		p [4%]	
70	FA	46,XY,del(2)(p?21)	d [88%]			
72	FA	55∼57,XX,+3,+4,+5,+7,+8,+9,+12,+17,+21[cp12]/46,XY[6]			tr [50.5%]	
73	FA	46,XY			tr [12%] / p [60%]	
84	FA	71∼73,XXXX,-2,+4,+7,-8,+17[cp3]				tr7 [5% (2p21) – 100% (Cen7)]
92–2	NG	46,XX	p [9%]		p [6%]	
96	FA	46,XX		r [73%]		
111	NG	46,XX,9qh+,t(15;19)(q22;q?13.4)		r [97%]		

Abbreviations: NG, nodular goiter including uninodular and multinodular goiter; FA, follicular adenoma; NA, detailed histopathology data of the benign lesions were not available; tr, trisomy; p, polysomy; r, rearrangement; m, monosomy; d, deletion; tr7, trisomy 7 with additional tri-/polysomies; [n%], relative amount of positive nuclei.

* For case 2 FISH could only be done with dual-color, break-apart probes for 2p21-rearrangements (TBPC2) and 19q13.4-rearrangements (TBPC19).

† In case of trisomy 7 with additional tri-/polysomies only the lowest and highest proportion of nuclei with gain of signals is denoted.

‡ For case 17-2 and 62-1 FISH could only be done with multi-target, triple-color FISH assay; thus a discrimination between a trisomy 19 and 19q13.4-rearrangement was not possible by I-FISH; for case 17-2 a partial trisomy 19 was shown by metaphase FISH (Supplementary Table 2).

possible to demonstrate by metaphase FISH that the rearrangement of chromosome 19 did not affect the thyroid breakpoint cluster region on chromosome 19q13.4 (see below). Another case (no. 10-2) was positive for a 19q13.4 rearrangement by I-FISH, whereas after CC, only an interstitial deletion of the long arm of chromosome 6 was detected. Furthermore, two cases (nos. 30 and 96) without apparent cytogenetic aberration were also positive for a 19q13.4 rearrangement, as shown by I-FISH (Figure 1, C and D).

If possible, FISH on metaphases was performed in cases with rearrangements detected by I-FISH on touch preparations to identify the chromosomes involved. In six of eight cases with 19q13.4 rearrangements, as detected by I-FISH, metaphase FISH was possible (case nos. 2, 10-2, 27, 60, 96, and 111; Supplementary Table 2). The 19q13.4 rearrangements have been confirmed in all cases analysed. As an example, Figure 2 A–C shows a metaphase FISH on case 111 with a t(15;19)(q22;q?13.4), confirming that the breakpoint on chromosome 19q is located within sub-band 13.4. In two additional cases (nos. 10-2 and 96), CC also revealed karyotypes without apparent 19q13.4 rearrangements. In both cases, metaphase FISH was positive for a 19q13.4 rearrangement, indicating translocations of 19q13.4 (Figure 3). For case 17-2 showing either a trisomy 19 or a 19q13.4 rearrangement after I-FISH, but a t(3;19)(p?21;?p13) after CC, FISH on metaphases was also performed (Supplementary

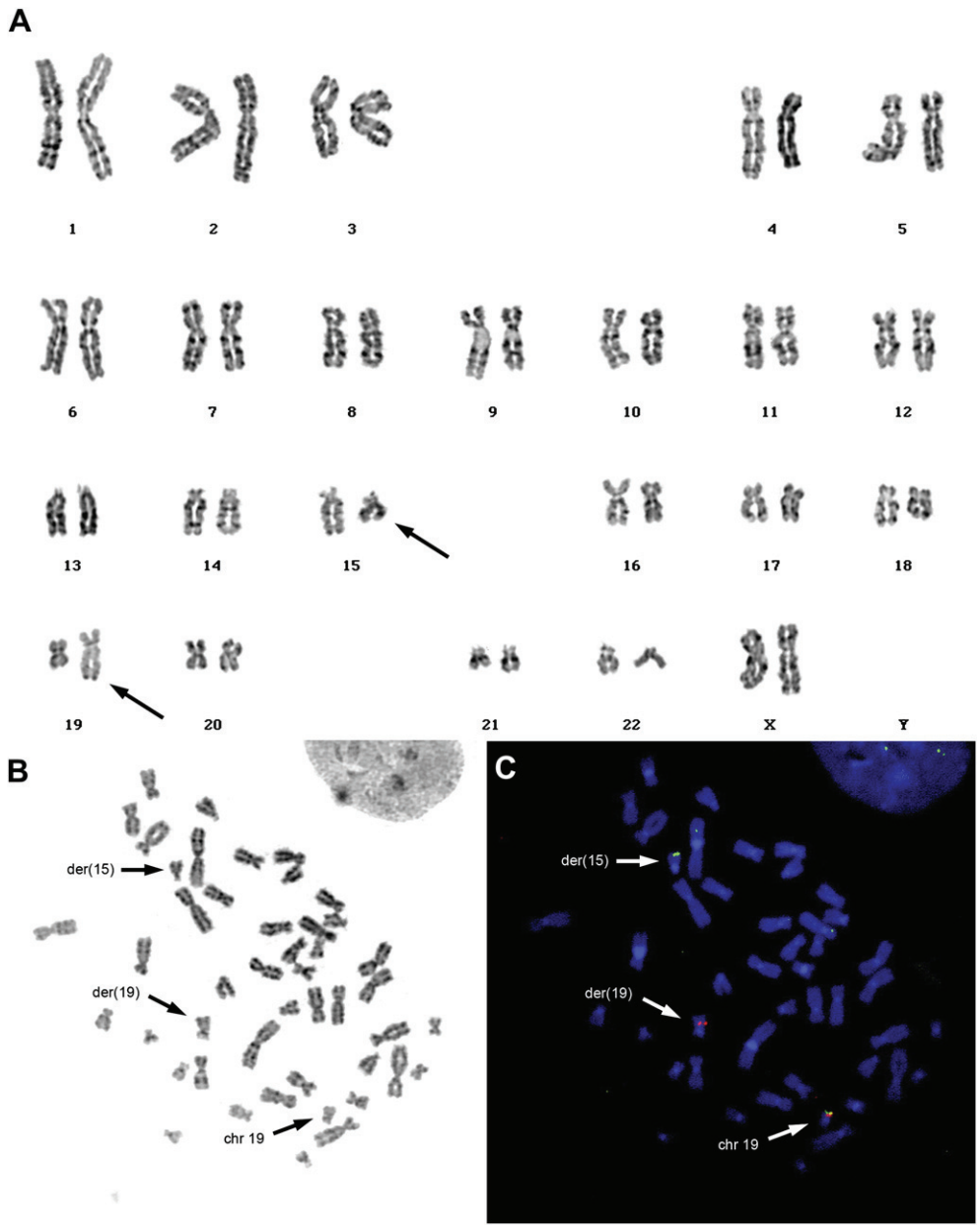

Figure 2 (A) Representative G-banded karyotype of case 111 showing the balanced t(15;19)(q22;q?13.4) (arrows). (B) G-Banded metaphase of case 111. Arrows indicate the derivative chromosomes as well as the normal chromosome 19. (C) The same metaphase after FISH with the dual-color break-apart probe TBPC19 of case 111 with a t(15;19)(q22;q?13.4) confirming that the breakpoint is located within 19q13.4. Arrows indicate the derivative chromosomes as well as the normal chromosome 19.

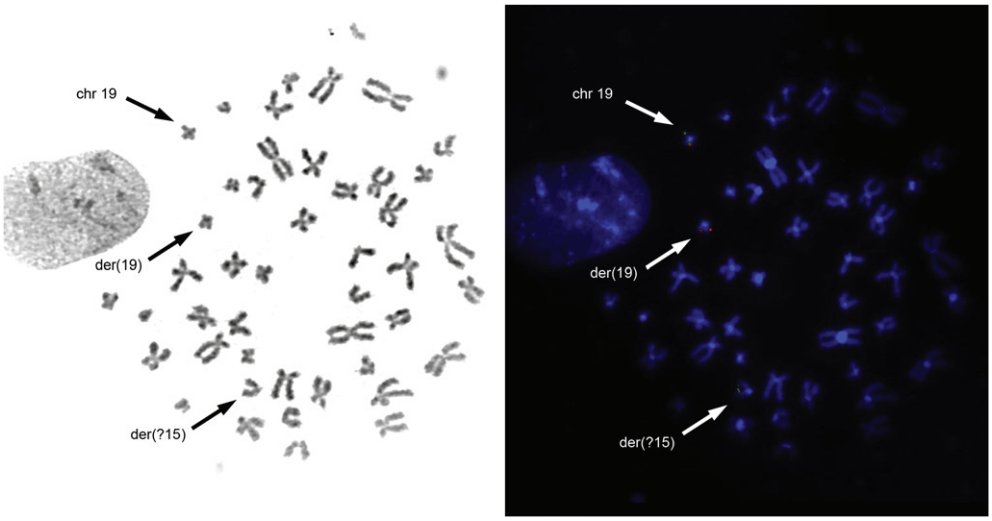

Figure 3 Metaphase FISH with the dual-color break-apart probe TBPC19 on case 96 showing a cryptic translocation t(?15;19)(q?;q13.4). The derivative chromosomes as well as the normal chromosome 19 are indicated by the arrows. Conventional cytogenetic analysis in this case revealed a 46,XX karyotype.

Table 2). Here, the FISH showed a partial trisomy of chromosome 19 with signals on the normal chromosome 19, the derivative chromosome 19, and a derivative chromosome (not shown). Accordingly, in this case, the breakpoint mapped to the short arm of chromosome 19. For the remaining cases (2, 27, and 60), metaphase FISH confirmed the 19q13.4 rearrangements as detected by I-FISH and CC.

2p21 rearrangements

In only one case (no. 70), a deletion of the short arm of chromosome 2 was detected by CC (46,XX,del(2)(p?21)). In contrast, structural aberrations involving chromosomal region 2p21 and *THADA*, respectively, were found by I-FISH in six cases (nos. 29, 38, 43, 45, 48-1, and 70); i.e., deletions in four cases (2.5% of 160 cases with successful I-FISH and 9.8% of 41 cases positive for chromosomal aberrations, respectively) and rearrangements (Figure 1, E and F) in two cases (1.3 and 4.9%, respectively). Metaphase FISH in these cases was not performed due to lack of metaphase chromosomes (case nos. 29, 43, 45, and 48-1) or an insufficient volume of cell suspension (case nos. 38 and 70).

General findings

Five samples (case nos. 3-2, 11-1, 74, 81, and 105) revealed clonal cytogenetic aberrations that were previously not detectable by I-FISH (Supplementary Table 2). Of these, three cases showed chromosome 2 aberrations, including t(2;7;12)(q?11.2;q?36;p11.2) (case 3-2), t(2;3)(q12∼14;p24∼25) (case 81), and del(2)(p?23) (case 105). In these cases, the aberrations apparently did not affect the chromosomal regions where the FISH probes used in this study are localized.

Statistical analysis

Comparing the proportion of positive interphase nuclei (as detected by I-FISH) in cases analyzed by conventional cytogenetics and positive for chromosomal aberrations, as detected by I-FISH, reveals a significant difference between the frequency of positive nuclei in 9 cases with and 12 cases without the corresponding aberration confirmed by CC (medians, 64 and 9%, respectively; $P = 0.009372$). This excludes case 96 because the metaphase FISH shows a cryptic 19q13.4 rearrangement and case 30 because metaphase FISH was not performed (i.e., a cryptic 19q13.4 rearrangement might be present). In cases with more than one chromosomal aberration, only the value (percentage of nuclei) for the most frequent aberration was used for statistical analysis. The distribution of the frequency of positive nuclei in cases with and without the corresponding chromosomal aberration confirmed by CC is visualized by a box plot (Figure 4).

Discussion

Benign thyroid lesions are characterized by recurrent chromosomal changes, including trisomy 7 and structural aberrations involving either 19q13.4 or 2p21 that had been detected by CC (4,5,9–11). For the 2p21 and the 19q13.4 rearrangements, we had been able to characterize the breakpoint regions (5,24,25) as well as the genes involved; i.e., the thyroid adenoma associated gene (*THADA*) in 2p21 (25) and, recently, the two microRNA gene clusters C19MC and miR-371-3 in 19q13.4 (26). Of the three main cytogenetic subgroups, however, only the frequency of trisomy 7 was analyzed previously by I-FISH in a study based predominantly on archival material (14–17). In the present study, we analyzed 161 benign thyroid lesions by CC as well as by I-FISH on touch preparations for the presence of the three main cytogenetic subgroups. To the best of our knowledge, this is the first study analyzing a large group of

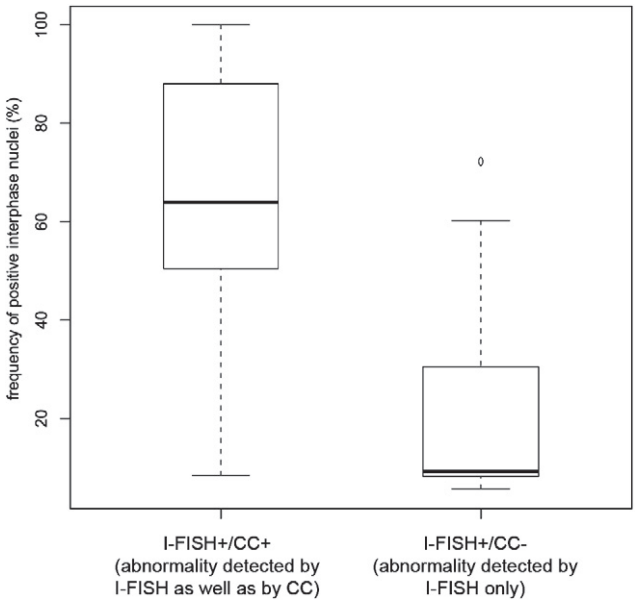

Figure 4 Box plot comparing the frequency of interphase nuclei positive for chromosomal aberrations detectable by I-FISH in cases with (I-FISH+/CC+; $n=9$) and without the corresponding chromosomal aberration as found by CC analysis (I-FISH+/CC-; $n=12$). Outlier is displayed as a circle.

benign thyroid lesions by CC as well as by a cytologic FISH approach using probes allowing the detection of the three most common types of cytogenetic deviations in benign thyroid tumors. In general, the study revealed that CC underestimates the frequency of cytogenetic changes in benign thyroid lesions. Overall, I-FISH had a higher success rate and detected a higher proportion of chromosomal abnormalities than CC. The frequency of trisomy 7, as found by I-FISH (56.1%) in the present study, is in accordance with previously reported data in which the proportion of benign thyroid lesions with gain of chromosome 7, as observed by FISH on interphase nuclei, ranges between 23.3 and 63.3% (14–16). In contrast, however, the proportion of trisomy 7, as found by CC (18.8%), is not as large as observed previously by conventional cytogenetics in which the proportion ranges between 20 (16) and 28.4% (10). With respect to rearrangements of 19q13.4, the observed frequencies of positive cases as detected by I-FISH (19.5%) and CC (31.3%) are slightly higher than that seen in previous cytogenetic studies (10). For 2p21 structural aberrations, 14.7% of cases with chromosomal aberrations were positive after I-FISH, whereas by CC, only one case was positive for a deletion of the chromosomal region 2p21. Structural aberrations involving 2p21 account for approximately 10% of clonal aberrations, as described previously by CC (10,11), and, therefore, are less frequently detected than with the I-FISH analysis presented here. These discrepancies between FISH and CC may be explained by methodologic limitations of CC due to availability and quality of metaphase chromosomes and due to that fact that small clones detectable by FISH may be overlooked by CC, as suggested by Criado et al. (15). By statistical analysis, the frequency of positive interphase nuclei between cases with and without the corresponding chromosomal aberrations as found by CC was significantly different ($P = 0.009372$). Furthermore, cryptic rearrangements of the chromosomal region 19q13.4 were identified in three cases. In our previous study aimed at the detection of hidden 19q13 rearrangements by FISH analysis with a 19q subtelomeric probe, no cryptic 19q13 rearrangements were found in all 38 cases analyzed (27). We presume that the lack of hidden 19q13 rearrangements in that study is due to the small number of cases analyzed, presuming that the three cases positive for cryptic 19q13.4 rearrangements out of 132 analyzed by CC in the present study better reflect the real frequency of such clonal aberrations.

In conclusion, the present findings, e.g. the results of I-FISH on touch-preparations, confirm the order of the three main cytogenetic subgroups in benign thyroid lesions (i.e., the trisomy 7 group as the most common cytogenetic subgroup, followed by 19q13.4 rearrangements and 2p21 rearrangements). Furthermore, not only the trisomy 7 group, but also structural aberrations involving either 19q13.4 or 2p21 occur more frequently in benign thyroid lesions than described previously by CC. I-FISH analysis on touch preparations of benign thyroid lesions have a higher success rate and are more sensitive in comparison to CC. Thus, I-FISH on touch preparations seems to be a fast and accurate method for analysis of benign thyroid lesions with respect to current chromosomal aberrations and can be applied to cytologic samples as well. The advantage of I-FISH is its ability to detect cryptic rearrangements as well as small cell populations with chromosomal aberrations that may escape CC analysis. Particularly in benign thyroid nodules of polyclonal origin (28), subpopulations of cells with chromosomal aberrations may be detectable by I-FISH, whereas these cells may be overlooked by CC (15).

Acknowledgments

We thank Tais Sommerfeld, Merle Skischus, Sabrina Dorschner, Alexander Pajung, Manuela Grund, Aneta Bogaczewicz, Beverly vom Bruch, and Henrieke Förster for their technical assistance with fluorescence in situ hybridization (T.S., M.S., S.D., A.P.) and cell culture (M.G., A.B., B.v.B., H.F.). We also thank Peter Hanisch (Department of Pathology, Hospital Bremen-Mitte) for his support in cytologic as well as histologic analyses.

Supplementary data

Supplementary data associated with this article can be found online at 10.1016/j.cancergen.2011.03.008.

References

1. Roque L, Castedo S, Gomes P, Soares P, Clode A, Soares J. Cytogenetic findings in 18 follicular thyroid adenomas. Cancer Genet Cytogenet 1993;67:1–6.
2. Sozzi G, Miozzo M, Cariani TC, Bongarzone I, Pilotti S, Pierotti MA, Della Porta G. A t(2;3)(q12-13;p24-25) in follicular thyroid adenomas. Cancer Genet Cytogenet 1992;64:38–41.
3. Antonini P, Venuat AM, Linares G, Caillou B, Schlumberger M, Travagli JP, Berger R, Parmentier C. Cytogenetic abnormalities in thyroid adenomas. Cancer Genet Cytogenet 1991;52: 157–164.

4. Belge G, Thode B, Bullerdiek J, Bartnitzke S. Aberrations of chromosome 19. Do they characterize a subtype of benign thyroid adenomas? Cancer Genet Cytogenet 1992;60:23–26.
5. Bol S, Belge G, Rippe V, Bullerdiek J. Molecular cytogenetic investigations define a subgroup of thyroid adenomas with 2p21 breakpoints clustered to a region of less than 450 kb. Cytogenet Cell Genet 2001;95:189–191.
6. Bondeson L, Bengtsson A, Bondeson AG, Dahlenfors R, Grimelius L, Wedell B, Mark J. Chromosome studies in thyroid neoplasia. Cancer 1989;64:680–685.
7. Roque L, Clode A, Belge G, Pinto A, Bartnitzke S, Santos JR, Thode B, Bullerdiek J, Castedo S, Soares J. Follicular thyroid carcinoma: chromosome analysis of 19 cases. Genes Chromosomes Cancer 1998;21:250–255.
8. van den Berg E, Oosterhuis JW, de Jong B, Buist J, Vos A, Dam A, Vermeij B. Cytogenetics of thyroid follicular adenomas. Cancer Genet Cytogenet 1990;44:217–222.
9. Belge G, Thode B, Rippe V, Bartnitzke S, Bullerdiek J. A characteristic sequence of trisomies starting with trisomy 7 in benign thyroid tumors. Hum Genet 1994;94:198–202.
10. Belge G, Roque L, Soares J, Bruckmann S, Thode B, Fonseca E, Clode A, Bartnitzke S, Castedo S, Bullerdiek J. Cytogenetic investigations of 340 thyroid hyperplasias and adenomas revealing correlations between cytogenetic findings and histology. Cancer Genet Cytogenet 1998;101:42–48.
11. Bol S, Belge G, Thode B, Bartnitzke S, Bullerdiek J. Structural abnormalities of chromosome 2 in benign thyroid tumors. Three new cases and review of the literature. Cancer Genet Cytogenet 1999;114:75–77.
12. Werner M, Wilkens L, Aubele M, Nolte M, Zitzelsberger H, Komminoth P. Interphase cytogenetics in pathology: principles, methods, and applications of fluorescence in situ hybridization (FISH). Histochem Cell Biol 1997;108:381–390.
13. Wolfe KQ, Herrington CS. Interphase cytogenetics and pathology: a tool for diagnosis and research. J Pathol 1997;181: 359–361.
14. Barril N, Carvalho-Sales AB, Tajara EH. Detection of numerical chromosome anomalies in interphase cells of benign and malignant thyroid lesions using fluorescence in situ hybridization. Cancer Genet Cytogenet 2000;117:50–56.
15. Criado B, Barros A, Suijkerbuijk RF, Weghuis DO, Seruca R, Fonseca E, Castedo S. Detection of numerical alterations for chromosomes 7 and 12 in benign thyroid lesions by in situ hybridization. Histological implications. Am J Pathol 1995;147: 136–144.
16. Roque L, Serpa A, Clode A, Castedo S, Soares J. Significance of trisomy 7 and 12 in thyroid lesions with follicular differentiation: a cytogenetic and in situ hybridization study. Lab Invest 1999;79:369–378.
17. Taruscio D, Carcangiu ML, Ried T, Ward DC. Numerical chromosomal aberrations in thyroid tumors detected by double fluorescence in situ hybridization. Genes Chromosomes Cancer 1994;9:180–185.
18. Chen F, Clark DP, Hawkins AL, Morsberger LA, Griffin CA. A break-apart fluorescence in situ hybridization assay for detecting RET translocations in papillary thyroid carcinoma. Cancer Genet Cytogenet 2007;178:128–134.
19. Cinti R, Yin L, Ilc K, Berger N, Basolo F, Cuccato S, Giannini R, Torre G, Miccoli P, Amati P, Romeo G, Corvi R. RET rearrangements in papillary thyroid carcinomas and adenomas detected by interphase FISH. Cytogenet Cell Genet 2000;88:56–61.
20. Dwight T, Thoppe SR, Foukakis T, Lui WO, Wallin G, Hoog A, Frisk T, Larsson C, Zedenius J. Involvement of the PAX8/peroxisome proliferator-activated receptor gamma rearrangement in follicular thyroid tumors. J Clin Endocrinol Metab 2003;88: 4440–4445.
21. Xiao S, Renshaw A, Cibas ES, Hudson TJ, Fletcher JA. Novel fluorescence in situ hybridization approaches in solid tumors. Characterization of frozen specimens, touch preparations, and cytological preparations. Am J Pathol 1995;147:896–904.
22. Bullerdiek J, Boschen C, Bartnitzke S. Aberrations of chromosome 8 in mixed salivary gland tumors–cytogenetic findings on seven cases. Cancer Genet Cytogenet 1987;24:205–212.
23. Castagne C, Muhlematter D, Beyer V, Parlier V, van Melle G, Jotterand M. Determination of cutoff values to detect small aneuploid clones by interphase fluorescence in situ hybridization: the Poisson model is a more appropriate approach. Should single-cell trisomy 8 be considered a clonal defect? Cancer Genet Cytogenet 2003;147:99–109.
24. Belge G, Rippe V, Meiboom M, Drieschner N, Garcia E, Bullerdiek J. Delineation of a 150-kb breakpoint cluster in benign thyroid tumors with 19q13.4 aberrations. Cytogenet Cell Genet 2001;93:48–51.
25. Rippe V, Drieschner N, Meiboom M, Escobar HM, Bonk U, Belge G, Bullerdiek J. Identification of a gene rearranged by 2p21 aberrations in thyroid adenomas. Oncogene 2003;22:6111–6114.
26. Rippe V, Dittberner L, Lorenz VN, Drieschner N, Nimzyk R, Sendt W, Junker K, Belge G, Bullerdiek J. The two stem cell microRNA gene clusters C19MC and miR-371-3 are activated by specific chromosomal rearrangements in a subgroup of thyroid adenomas. PLoS ONE 2010;5:e9485.
27. Meiboom M, Belge G, Bol S, El-Aouni C, Schoenmakers EF, Bullerdiek J. Does conventional cytogenetics detect the real frequency of 19q13 aberrations in benign thyroid lesions? A survey of 38 cases. Cancer Genet Cytogenet 2003;146:70–72.
28. Studer H, Derwahl M. Mechanisms of nonneoplastic endocrine hyperplasia–a changing concept: a review focused on the thyroid gland. Endocr Rev 1995;16:411–426.

3.2 Molekulargenetische Charakterisierung der 2p21-Bruchpunktregion bei benignen follikulären Läsionen der Schilddrüse

II. Identification of a gene rearranged by 2p21 aberrations in thyroid adenomas (Rippe *et al.*, 2003)

Nachdem die Bruchpunkte in 2p21 mittels molekularzytogenetischer Untersuchungen an vier Zelllinien bzw. Primärtumoren auf eine Region von maximal 450 kb eingegrenzt wurden (Bol *et al.*, 2001), ließen sich unter Verwendung der Sequenzdaten der im Bruchpunktbereich lokalisierten BAC-Klone RP11-339H12, RP11-1069E24, RP11-183F15 und RP11-204D19 mehrere humane Expressed Sequence Tags (EST) nachweisen, die auf ein bis dahin nicht charakterisiertes Gen innerhalb der Bruchpunktregion hindeuteten. Mittels weiterführender *in silico*-Analysen sowie RT-PCR-Untersuchungen konnte die genomische Struktur eines Gens identifiziert werden, welches als *THADA* bezeichnet wurde. *THADA* weist genomisch eine Größe von ca. 365 kb auf, umfasst insgesamt 38 Exons und ist innerhalb der chromosomalen Bande 2p21 vom Centromer (5‘-Untranslated Region (UTR)) in Richtung Telomer (3‘-UTR) orientiert, wobei mehr als die Hälfte des Gens innerhalb des 2p21-Bruchpunktbereiches lokalisiert ist. Identifiziert wurden zwei Spleißvarianten mit einer Transkriptlänge von 6090 bp (*THADA*) bzw. 5.868 bp (*THADA-A2*). Der Open Reading Frame (ORF) von *THADA* weist eine Größe von 5.862 bp auf und kodiert für ein 1953 Aminosäuren langes Protein. Hinsichtlich der Funktion von THADA fanden sich Hinweise auf eine Apoptose-Beteiligung, da sich in einem GenBank-Eintrag für ein *THADA* entsprechendes cDNA-Fragment („death receptor interacting protein mRNA“) der Verweis auf eine Interaktion mit dem Death Receptor 5 (DR5) fand.

In silico-Analysen unter Verwendung der Serial Analysis of Gene Expression (SAGE)- und EST-Datenbank deuten auf eine nahezu ubiquitäre Expression von *THADA* hin. Entsprechend ließ sich in einem Northern Blot eine Expression eines 6.2 kb großem Transkriptes an verschiedenen Normalgeweben nachweisen.

Mittels 3‘-RACE-PCR an den Zelllinien S325/TSV40 und S533/TSV40 mit den Translokationen t(2;20;3)(p21;p11.2,p25) (S325/TSV40) und t(2;7)(p21;p15) (S533/TSV40) war es möglich, jeweils Fusionstranskripte (*THADA-FUS3p und THADA-FUS7p*) nachzuweisen, in denen die Exons 29 – 38 von *THADA* trunkiert sind und die neben den Exons 1 – 28 kurze, nicht-kodierende Sequenzen aus den chromosomalen Bruchpunktregionen der jeweiligen

Translokationspartner enthalten. Die beteiligten Sequenzen aus den chromosomalen Regionen 3p25 (S325/TSV40) und 7p15 (S533/TSV40) konnten keinem bis dahin bekannten Gen zugeordnet werden. In beiden Fusionstranskripten endet der ORF kurz nach Exon 28 von *THADA*, weshalb davon ausgegangen wird, dass eher der Verlust der 3‘-Region mit Exon 29 – 38 von *THADA* als die Fusion mit nur zum Teil kodierenden Sequenzen von entscheidender Bedeutung in benignen Schilddrüsenläsionen mit 2p21-Rearrangierungen ist.

II

Identification of a gene rearranged by 2p21 aberrations in thyroid adenomas

Volkhard Rippe, Norbert Drieschner, Maren Meiboom, Hugo Murua Escobar, Ulrich Bonk, Gazanfer Belge, Jörn Bullerdiek

(Oncogene 22(38): 6111-6114)

Eigenanteil:

- Durchführung der molekularzytogenetischen und PCR-Analysen.
- Identifizierung und Beschreibung der molekulargenetischen Struktur von *THADA* und *THADA*-Fusionstranskripten einschließlich Spleißvarianten.

Oncogene (2003) 22, 6111–6114

www.nature.com/onc

Identification of a gene rearranged by 2p21 aberrations in thyroid adenomas

Volkhard Rippe[1], Norbert Drieschner[1], Maren Meiboom[1], Hugo Murua Escobar[1], Ulrich Bonk[2], Gazanfer Belge[1] and Jörn Bullerdiek*[,1]

[1]*Center for Human Genetics, University of Bremen, Leobener Str. ZHG, D-28359 Bremen, Germany;* [2]*Institute of Pathology, Central Hospital Bremen-Nord, Bremen, Germany*

Thyroid adenomas belong to the cytogenetically best investigated human epithelial tumors. Cytogenetic studies of about 450 benign lesions allow one to distinguish between different cytogenetic subgroups. Two chromosomal regions, that is, 19q13 and 2p21, are frequently rearranged in these tumors. Although 2p21 aberrations only account for about 10% of the benign thyroid tumors with clonal cytogenetic deviations, 2p21 rearrangements belong to the most common cytogenetic rearrangements in epithelial tumors due to the high frequency of these benign lesions. The 2p21 breakpoint region recently has been delineated to a region of 450 kbp, but the gene affected by the cytogenetic rearrangements still has escaped detection. Positional cloning and 3′ RACE–PCR allowed us to clone that gene which we will refer to as thyroid adenoma associated (*THADA*) gene. In cells from two thyroid adenomas characterized by translocations t(2;20;3)(p21;q11.2;p25) and t(2;7)(p21;p15), respectively, we performed 3′-RACE–PCRs and found two fusions of *THADA* with a sequence derived from chromosome band 3p25 or with a sequence derived from chromosome band 7p15. The *THADA* gene spans roughly 365 kbp and, based on preliminary results, encodes a death receptor-interacting protein.
Oncogene (2003) **22,** 6111–6114. doi:10.1038/sj.onc.1206867

Keywords: 2p21 aberrations; thyroid adenomas; THADA; fusion gene

Introduction

Adenomas of the thyroid are rare examples of epithelial tumors frequently displaying specific chromosomal translocations. There are two chromosomal bands most frequently rearranged by these translocations, that is, 19q13 (Bartnitzke *et al*., 1989; Bondeson *et al*., 1989; Dal Cin *et al*., 1992; Belge *et al*., 1998) and 2p21 (Teyssier *et al*., 1990; Belge *et al*., 1998; Bol *et al*., 1999). Both types of translocations apparently do not co-occur in thyroid tumors, thus indicating two independent cytogenetic subgroups. As for the translocation partners there is also no apparent overlap and in both groups other chromosomal regions involved in the translocations remarkably vary. Nevertheless, there are preferred translocation partners that are more often involved than others, as for example chromosomal band 5q13 in cases with 19q13 translocations and band 7p15 in cases with 2p21 translocations. Whereas the breakpoint region of chromosome 19 has been characterized molecularly in detail and candidate genes have been found (Rippe *et al*., 1999; Belge *et al*., 2001), for the 2p21 region only a rough mapping of the breakpoint has been obtained with no candidate genes identified so far (Bol *et al*., 2001). Herein, we describe the identification of the target gene of the 2p21 aberrations which we have tentatively referred to as thyroid adenoma-associated gene (*THADA*). The identification of genes affected by these aberrations and the elucidation of their mechanisms of action certainly will lead to better insights into the pathogenesis of these frequent diseases.

*Correspondence: J Bullerdiek; E-mail: bullerdiek@uni-bremen.de
Received 24 January 2003; revised 11 June 2003; accepted 13 June 2003

Results

In the thyroid adenoma cell line S325/TSV40 characterized by a translocation t(2;20;3)(p21;q11.2;p25), we found a single chromosome 2 BAC clone, 1069E24, that hybridized to both the der(2) and the der(20) chromosome and thus contained the altered 2p21 gene locus (Bol *et al*., 2001) (Figure 1). Database search based on clone 1069E24 and the flanking BACs 339H12, 183F15, and 204D19 identified numerous anonymous human ESTs (BLAST analysis, version 2.2.6; Altschul *et al*., 1997). Alignment and RT–PCR analyses point to a novel gene that we referred to as *THADA* (Figure 2). *THADA* cDNA contains 38 exons with at least one alternative splice variant (Figure 3). As for its possible function, *THADA* corresponds to the *death receptor-interacting protein* mRNA encoding a protein that in two-hybrid experiments was found to be a ligand of death receptor DR5 (Puduvalli VK and Ridgway L, GenBank accession reference note). The hypothetical 1954 amino acids (predicted molecular weight: 220 kDa) have no apparent homology to other human proteins as retrieved from public databases. Nevertheless, there are homologies to undefined ESTs in other organisms, as for example the mouse.

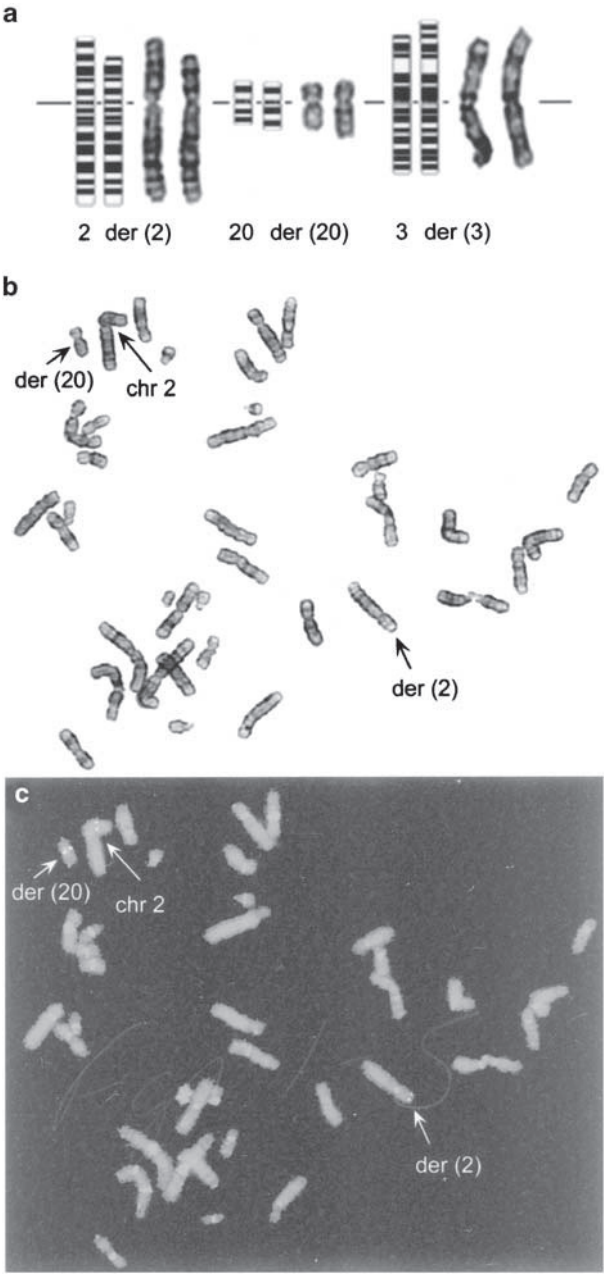

Figure 1 Molecular cytogenetic investigations of the thyroid adenoma cell line S325/TSV40 with a translocation t(2;20;3)(p21;q11.2;p25). (**a**) Partial G-banded karyotype and schematic representation of the chromosomal aberrations showing normal (left) and derivative (right) chromosomes 2, 20, and 3, respectively. (**b**) Part of a metaphase of the cell line S325/TSV40 with t(2;20;3)(p21;q11.2;p25) after G-banding; the chromosomes 2, der(2), and der(20) are marked (arrows). (**c**) The same metaphase after FISH with BAC 1069E24; the hybridization signals are located on chromosomes 2, der(2), and der(20) (arrows)

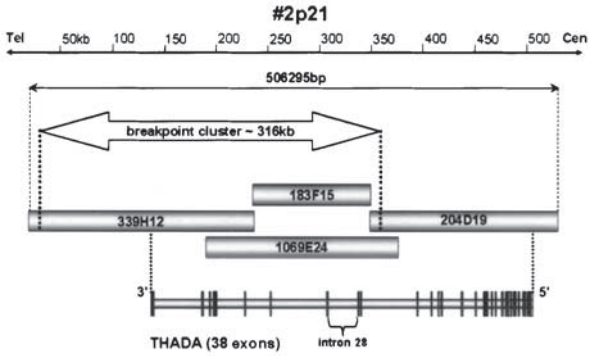

Figure 2 Genomic organization of the breakpoint cluster region in thyroid lesions with aberrations of chromosomal band 2p21 and *THADA*. The BAC clones spanning the breakpoint region are represented as gray bars. The genomic structure of *THADA* is shown below. The breakpoints of the cell lines S325/TSV40 and S533/TSV40 are located in the intron 28 of *THADA*

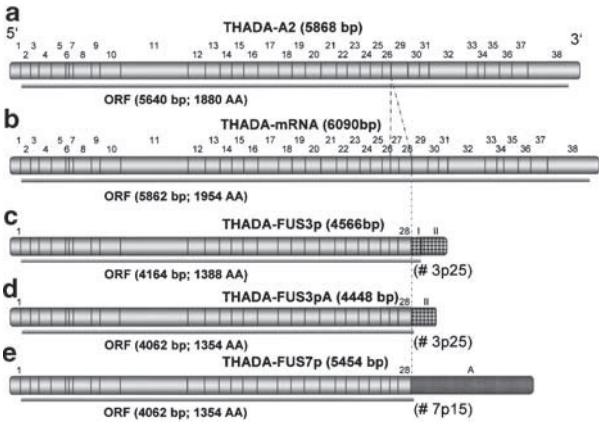

Figure 3 mRNA organization of *THADA, THADA-FUS3p*, and *THADA-FUS7p*. (**a**) Splice variant of *THADA* (*THADA-A2*) lacking exons 27 and 28. (**b**) mRNA structure of *THADA* consisting of 38 exons. (**c**) mRNA structure of *THADA-FUS3p*. *THADA* stops after exon 28 followed by two 'exons' of the fusion part from chromosome region 3p25 (exons I and II). 3p25 fusion sequences are marked by checked pattern. (**d**) mRNA structure of *THADA-FUS3pA*. After exon 28, only 'exon' II of *FUS3p* is fused to *THADA*. (**e**) mRNA structure of *THADA-FUS7p*. The fusion part from chromosome region 7p15 (exon A) is fused to *THADA* downstream of exon 28 (marked by dot pattern). Under each mRNA, the potential ORF is shown as thin gray bar

The gene is widely expressed as revealed by *in silico* analyses using serial analysis of gene expression (SAGE) and EST-library database.

EST data show a high expression in adult normal placenta and SAGE data point to a strong expression in breast cancer cell line MCF7 and normal breast epithelium. A multiple Northern blot was probed with an 820 bp fragment from the ORF allowing us to detect a 6.2 kbp signal in all tissues investigated (Figure 4).

To identify possible *THADA* fusion partners, we used exon 18 and 28 oligonucleotide primers to perform 3′-RACE–PCR in cell lines S325/TSV40 and S533/TSV40. Amplification products were cloned and sequenced leading to the identification of clones in which the sequence diverged from *THADA* after exon 28. A database search revealed that the sequence fused to *THADA* in S325/TSV40 (*FUS3p*) maps to

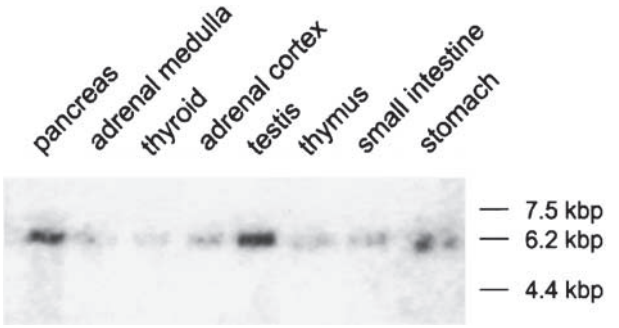

Figure 4 Expression studies of *THADA*. Hybridization of part of the cDNA of *THADA* (exons 25–32) on a commercially available poly(A)+ RNA Northern blot revealed a transcript of about 6.2 kbp of varying intensity in all tissues. A strong expression of *THADA* is seen in pancreas and testis, thyroid tissue shows a weak expression of *THADA*

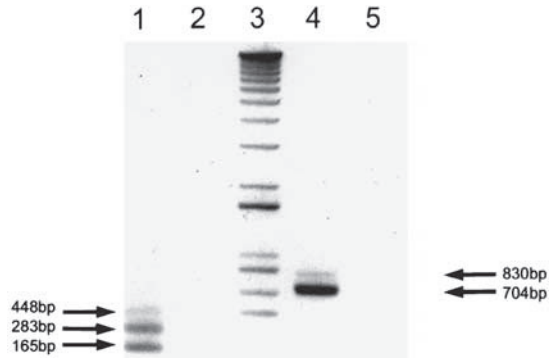

Figure 5 RT–PCR detection of *THADA* fusion genes in the cell lines S325/TSV40 and S533/TSV40. Primers are located within exon 28 of *THADA* and the novel sequences derived from the corresponding translocation partners of chromosome 2. In lane 1, three amplification products of the cell line S325T/SV40 representing the three splice variants (165, 283 and 448 bp) of *THADA-FUS3p* were seen. In S533T/SV40, the fusion transcripts *THADA-FUS7p* were detected as 704 and 830 bp PCR products, as shown in lane 4. Both RT–PCRs confirmed the existence of *THADA-FUS3p* and *THADA-FUS7p*. In lanes 2 and 5, RT–PCR analyses with the same primers used on the cell lines were performed on normal thyroid with no detectable products. DNA molecular weight marker 1 kb-plus ladder (Invitrogen, Karlsruhe, Germany) is seen in lane 3

chromosomal band 3p25, BAC 167M22 and in S533/TSV40 (*FUS7p*) to chromosomal band 7p15, BAC 379L16 (Figure 3). By database search we have not been able to correlate these sequences to any described gene structures.

In order to confirm the fusions in both cell lines, RT–PCR analyses were performed. Amplification products corresponding to those found by RACE–PCR were obtained for both cell lines, thus confirming the *THADA-FUS3p* and *THADA-FUS7p* fusions (Figure 5). In both cell lines, *THADA* stops after exon 28 followed by the fused sequences from either of the translocation partners.

Discussion

Chromosome 2p21 aberrations characterize the second most frequent structural chromosomal rearrangements in benign adenomas of the thyroid (Belge *et al*., 1998; Bol *et al*., 1999). From the results presented herein, there is little doubt that *THADA* is indeed the target gene of those translocations. In the translocations observed in both cell lines, the identical part of *THADA* becomes fused to ectopic sequences both mapping to the breakpoints of the translocation partners. Since no similarity of the ectopic sequences with known genes became apparent, it seems tempting to speculate that the truncation of the gene and the protein rather than its fusion to particular coding sequences is the critical event. As for the function of the THADA protein, there is so far only one unpublished report based on two-hybrid experiments indicating the involvement of THADA in death receptor pathway (Puduvalli VK and Ridgway L, GenBank accession reference note). We hypothesize that the truncation of the gene, and the loss of the 3′ part of *THADA* leads to an alterated apoptosis induction. This may cause an increased proliferation in benign thyroid tumors with chromosome 2p21 alterations. Previous studies revealed that truncation of genes could be an important event in human tumor development. For example, truncation of the 3′ part of the high-mobility group gene *HMGA2* could be relevant for the etiology of human sarcomas (Berner *et al*., 1997) or causes malignant transformation of NIH3T3 cells (Fedele *et al*., 1998). Apparently, further elucidation of the function of the THADA protein will be helpful to get insights into the molecular pathogenesis of benign adenomas of the thyroid and possibly also into benign proliferation in general.

Materials and methods

FISH analysis

For chromosome analyses and FISH studies, materials of the cell lines S325/TSV40 and S533/TSV40, derived from a thyroid adenoma, were used. The cell lines were obtained by transfection with a construct containing the SV40 large T antigen, as reported previously (Belge *et al*., 1992). Cell culture of the cell lines and chromosome analyses were performed as previously described for pleomorphic adenomas of the parotid gland (Bullerdiek *et al*., 1987). The BAC clones were obtained from the RP-11-Library (RZPD, Heidelberg, Germany). DNA of BAC clones was isolated using the QIAGEN Plasmid Midi Kit (QIAGEN, Hilden, Germany). FISH analyses were performed after GTG banding of the same metaphase spreads. Treatment of metaphases and subsequent FISH experiments were performed using the protocol of Kievits *et al*. (1990). For FISH studies, BAC DNA was labeled either with dig-11-dUTP or biotin-16-dUTP by nick translation (Roche Diagnostics, Mannheim, Germany). For two-color FISH experiments, the labeled BAC DNA was pooled (concentration: 4 ng/μl). For one-color FISH, 4 ng/μl of each BAC clone was used. Detection was performed with anti-dig-fluorescein fab-fragments (Roche Diagnostics, Mannheim, Germany) and Cy3-conjugated streptavidin (Jackson Immuno Research, West

Grove, PA, USA). Chromosomes were counterstained with DAPI (0.025 μg/ml). For each cell line, at least 10 metaphases were examined. Slides were analysed on a Zeiss Axiophot fluorescence microscope using an FITC, Cy3, and DAPI filter set. Metaphases were recorded with the Power Gene Karyotyping System (Applied Imaging, Newcastle, UK).

PCR analyses

Total RNA was isolated from cells of S325/TSV40 and S533/TSV40 using TRIzol reagent (Invitrogen, Karlsruhe, Germany). Total RNA (5 μg) was reverse transcribed into first-strand cDNA by M-MLV Reverse Transcriptase (Invitrogen, Karlsruhe, Germany). For 3′-RACE–PCR, a gradient thermocycler (Biometra, Göttingen, Germany) was used. Amplifications were carried out in a final volume of 50 μl containing 1.5 μl template cDNA, 1 × AdvanTaqPlus buffer, 0.2 μM of each primer, 200 μM dNTP mix, and 1 μl 50 × AdvanTaq cDNA Polymerase Mix. Primer sequences used for 3′-RACE were: 5′-GCTTCAGGCAGCAGCAGCATTTCCA-3′ (exon 18) and 5′-AGACTCTACGCTTCCCCGATGGATGGT-3′ (exon 28). The PCR reaction was performed according to the Advantage cDNA PCR Kit manual (Clontech, Palo Alto, CA, USA). After an initial denaturation at 94°C for 5 min, 35 cycles were performed. Each cycle consisted of denaturation (94°C) for 30 s and a combined annealing/extension step for 6 min at 68°C. 3′-RACE was completed with a final extension for 6 min at 68°C. RACE products were separated on a 1.2% agarose gel and transferred onto nylon membrane Hybond-N + (Amersham Pharmacia Biotech, Little Chalfont, England) in 20 × SSC followed by UV crosslinking. Probe DNA (201 bp) was labeled with dig-11-dUTPs in a PCR reaction on a cDNA clone containing a *THADA*-sequence using primers 5′-GCTTCAGGCAGCAGCATTTCCA-3′ and 5′-ATTGGGATGAGGCCTTCAGGGGATGA-3′. Labeling, hybridization, and detection were performed according to the manufacturer's protocol (Roche Diagnostics, Mannheim, Germany). RT–PCR detection of the fusion genes was performed with primers 5′-AGACTCTACGCTTCCCCGATGGATGGT-3′ 5′-TCCAGGGAAATTCACTGCTTTGGGAGCCA-3′ (*THADA-FUS3p*) and 5′-AGACTCTACGCTTCCCCGATGGATGGT-3′ 5′-GGTAGCGGGAGCAATCACAAAACTGTAA-3′ (*THADA-FUS7p*).

Amplifications were carried out in a final volume of 50 μl containing 0.5 μl template cDNA, 0.05 U/μl *Taq* DNA Polymerase recombinant (Invitrogen, Karlsruhe, Germany), 0.2 μM of each primer, 200 μM dNTP mix, and 1 × PCR R × N Puffer (Invitrogen, Karlsruhe, Germany). After an initial denaturation at 94°C for 3 min, 35 cycles were performed. Each cycle consisted of denaturation (94°C) for 45 s, annealing for 45 s (58°C, *THADA-FUS3p*; 60°C, *THADA-FUS7p*), and extension for 1 min at 72°C.

Northern blot hybridization

Expression patterns of *THADA* were studied using a commercially available Northern blot membrane (Human Endocrine System MTN Blot, Clontech, Palo Alto, CA, USA). A partial cDNA clone of *THADA* was labeled with ^{32}P by random primer extension (Feinberg and Vogelstein, 1983) and used as molecular probe. The probe was amplified by PCR using primers 5′-AGAGTAAATCCAAACGTGAACCAGAGAATGAGT-3′ and 5′-ATTGGGATGAGGCCTTCAGGGGATGA-3′. Hybridization was carried out as described (Rippe *et al*., 1999), with 30 min prehybridization and hybridization for 1 h at 68°C. The membranes were washed four times for 10 min at room temperature in 2 × SSC/0.05% SDS, and twice for 20 min at 50°C in 0.1 × SSC/0.1% SDS. Signals were visualized by using a STORM phosphorimager 860 (Amersham Pharmacia Biotech, Little Chalfont, England).

The GenBank Accession numbers are: *THADA*, AY149629; *THADA-FUS3p*, AY149630; *THADA-FUS3pA*, AY149631; *THADA-FUS7p*, AY149632; *THADA-A2*, AY149633; death receptor-interacting protein mRNA, AF323176; BAC clones from RPC-11: 1069E24, AQ694385, AQ703756; 339H12, AC010883; 183F15, AC092838; 204D19, AC092615; 167M22, AC093174; 379L16, AC079780.

Acknowledgements
We thank Jessica Hommes for technical assistance.

References

Altschul SF, Madden TL, Schaffer AA, Zhang J, Zhang Z, Miller W and Lipman DJ. (1997). *Nucleic Acids Res.,* **25,** 3389–3402.

Bartnitzke S, Herrmann ME, Lobeck H, Zuschneid W, Neuhaus P and Bullerdiek J. (1989). *Cancer Genet. Cytogenet.,* **39,** 65–68.

Belge G, Kazmierczak B, Meyer-Bolte K, Bartnitzke S and Bullerdiek J. (1992). *Cell. Biol. Int. Rep.,* **16,** 339–347.

Belge G, Rippe V, Meiboom M, Drieschner N, Garcia E and Bullerdiek J. (2001). *Cytogenet. Cell Genet.,* **93,** 48–51.

Belge G, Roque L, Soares J, Bruckmann S, Thode B, Fonseca E, Clode A, Bartnitzke S, Castedo S and Bullerdiek J. (1998). *Cancer Genet. Cytogenet.,* **101,** 42–48.

Berner JM, Meza-Zepeda LA, Kools PF, Forus A, Schoenmakers EF, Van de Ven WJ, Fodstad O and Myklebost O. (1997). *Oncogene,* **14,** 2935–2941.

Bol S, Belge G, Rippe V and Bullerdiek J. (2001). *Cytogenet. Cell Genet.,* **95,** 189–191.

Bol S, Belge G, Thode B, Bartnitzke S and Bullerdiek J. (1999). *Cancer Genet. Cytogenet.,* **114,** 75–77.

Bondeson L, Bengtsson A, Bondeson AG, Dahlenfors R, Grimelius L, Wedell B and Mark J. (1989). *Cancer,* **64,** 680–685.

Bullerdiek J, Böschen C and Bartnitzke S. (1987). *Cancer Genet. Cytogenet.,* **24,** 205–212.

Dal Cin P, Sneyers W, Aly MS, Segers A, Ostijn F, Van Damme B and Van den Berghe H. (1992). *Cancer Genet. Cytogenet.,* **60,** 99–101.

Fedele M, Berlingieri MT, Scala S, Chiariotti L, Viglietto G, Rippel V, Bullerdiek J, Santoro M and Fusco A. (1998). *Oncogene,* **17,** 413–418.

Feinberg AP and Vogelstein B. (1983). *Anal. Biochem.,* **132,** 6–13.

Kievits T, Dauwerse JG, Wiegant J, Devilee P, Breuning MH, Cornelisse CJ, Van Ommen GJ and Pearson PL. (1990). *Cytogenet. Cell Genet.,* **53,** 134–136.

Rippe V, Belge G, Meiboom M, Kazmierczak B, Fusco A and Bullerdiek J. (1999). *Genes Chromosomes Cancer,* **26,** 229–236.

Teyssier JR, Liautaud-Roger F, Ferre D, Patey M and Dufer J. (1990). *Cancer Genet. Cytogenet.,* **50,** 249–263.

III. A domain of the thyroid adenoma associated gene (*THADA*) conserved in vertebrates becomes destroyed by chromosomal rearrangements observed in thyroid adenomas (Drieschner *et al.*, 2007)

Um nähere Informationen hinsichtlich der Funktion von THADA sowie über die in den Fusionsgenen bei benignen Läsionen der Schilddrüse mit 2p21-Rearrangierungen trunkierten Sequenzen zu gewinnen, wurde die Struktur der homologen *THADA*-Gene der Organismen *Canis familiaris* (Haushund), *Gallus gallus* (Haushuhn), *Mus musculus* (Hausmaus) sowie *Chlorocebus aethiops* (Grüne Meerkatze) charakterisiert. Hierzu wurde mittels *in silico*-Analyse sowohl die messenger RNA (mRNA)- als auch die genomische Sequenz von *THADA* der genannten Organismen mit Ausnahme von *Chlorocebus aethiops* ermittelt. Anhand dieser Sequenzen erfolgte für spätere RT-PCR Analysen die Erstellung geeigneter PCR-Primer. Für *Chlorocebus aethiops* wurden für entsprechende Analysen humane PCR-Primer verwendet. Zudem wurde an der Nieren-Zelllinie CV1 eine molekularzytogenetische Analyse mit den humanen BAC-Klonen RP11-1069E24 und RP11-183F15 durchgeführt, über die die genomische Lokalisation von *THADA* auf dem Chromosom 14 von *Chlorocebus aethiops* bestimmt werden konnte. Die mittels RT-PCR und Sequenzierung der entsprechenden PCR-Produkte erstellten homologen mRNA-Sequenzen umfassten jeweils den kompletten ORF. Im Vergleich zum Menschen (*Homo sapiens*) (365.186 bp) ist die genomische Länge von *THADA* bei *Canis familiaris* (326.318 bp), *Gallus gallus* (152.400 bp) sowie *Mus musculus* (274.170 bp) z.T. deutlich kürzer. Die Länge der sequenzierten mRNA einschließlich *Homo sapiens* liegt zwischen 5.899 bp (*Chlorocebus aethiops*) und 6.501 bp (*Gallus gallus*). Weiterhin wurde bei allen Organismen das ATG Start-Codon ermittelt und somit der jeweilige ORF, wobei die Länge des ORF mit 5.793 bp (*Gallus gallus*) bis 5.862 bp (*Chlorecebus aethiops* und *Homo sapiens*) nur eine geringe Abweichung unter den untersuchten Organismen aufweist. Entsprechendes gilt für die Länge der jeweiligen Proteinsequenzen.

Ein Vergleich sowohl der *THADA*-mRNA- als auch der THADA-Proteinsequenzen von allen Organismen mit Bezug zu den entsprechenden humanen Sequenzen ergab für *Chlorocebus aethiops* die höchste Übereinstimmung (97,1% für den ORF und 95,9% für die Proteinsequenz), während die Übereinstimmung bei *Gallus gallus* nur 64,7% (ORF) und 57,2% (Protein) betrug. Insgesamt entsprechen die relativen Übereinstimmungen des ORF

und der Proteinsequenz den bekannten phylogenetischen Beziehungen der untersuchten Organismen untereinander.

Hinsichtlich konservierter Bereiche innerhalb der THADA-Proteinsequenzen von allen analysierten Organismen zeigte ein multiples Sequenzalignment die höchste Übereinstimmung mit 70,4% identischer Aminosäuren innerhalb der Region von Aminosäure 1033 – 1415 des humanen THADA-Proteins. Berücksichtigt man konservierte Aminosäureaustausche so liegt die relative Übereinstimmung sogar bei 78,6% für den genannten Bereich. Für die gesamte Proteinsequenz liegt der Anteil identischer Aminosäuren bei allen Organismen bei 48,6% bzw. 60,9% unter Berücksichtigung konservierter Aminosäureaustausche.

Unter Anwendung des InterProScan Tools sowie der National Center for Biotechnology Information Conserved Domain Database (NCBI CDD) konnte mit Hilfe der NCBI CDD die Domäne COG5543 (COG = Cluster of orthologous groups) nachgewiesen werden, für die bisher keine funktionellen Eigenschaften bekannt sind. Mit einer Länge von 1400 Aminosäuren liegt die Domäne COG5543 innerhalb der oben genannten konservierten Region bei allen THADA-Proteinen. Mittels des InterproScan Tools fanden sich weiterhin Übereinstimmungen zur ARM Repeat Superfamilie (SSF48371), die an Protein-Protein Interaktionen beteiligt sind. Desweiteren ließen sich Proteinhomologien zu Cullin-Associated and Neddylation-Dissociated 1 (CAND1) sowie verschiedenen importin Proteinen ableiten, die alle ARM Repeat-ähnliche Strukturen aufweisen.

III

A domain of the thyroid adenoma associated gene (*THADA*) conserved in vertebrates becomes destroyed by chromosomal rearrangements observed in thyroid adenomas

Norbert Drieschner, Svenja Kerschling, Jan T. Soller, Volkhard Rippe, Gazanfer Belge, Jörn Bullerdiek, Rolf Nimzyk

(Gene 403(1-2): 110-117)

Eigenanteil:

- Planung und Durchführung der molekularzytogenetischen und molekulargenetischen Untersuchungen.
- Auswertung der molekular-zytogenetischen Untersuchungen.
- Verfassen des Artikels gemeinsam mit Rolf Nimzyk.

Available online at www.sciencedirect.com
ScienceDirect
Gene 403 (2007) 110–117
GENE
www.elsevier.com/locate/gene

A domain of the thyroid adenoma associated gene (*THADA*) conserved in vertebrates becomes destroyed by chromosomal rearrangements observed in thyroid adenomas

Norbert Drieschner [a], Svenja Kerschling [a], Jan T. Soller [a,b], Volkhard Rippe [a], Gazanfer Belge [a], Jörn Bullerdiek [a,*], Rolf Nimzyk [a]

[a] *Center for Human Genetics, University of Bremen, Leobenerstr./ZHG, D-28359 Bremen, Germany*
[b] *Small Animal Clinic, University of Veterinary Medicine, Bischofsholer Damm 15, D-30173 Hanover, Germany*

Received 16 May 2007; received in revised form 25 June 2007; accepted 25 June 2007
Available online 7 August 2007
Received by A. Bernardi

Abstract

THADA, mapping to chromosomal band 2p21 is target gene of specific chromosomal rearrangements observed in thyroid benign tumors. Thus, it is one of the most common gene targets in chromosomal rearrangements in benign epithelial tumors. Nevertheless, nothing is known about the function of its protein. Therefore, we have analyzed the genetic structure of *THADA* homologous genes in selected vertebrates (*Canis familiaris*, *Chlorocebus aethiops*, *Gallus gallus*, and *Mus musculus*), which are not characterized up to now. The coding sequences of the mRNA of these species have been sequenced and analyzed revealing similarities to ARM repeat structures which indicates an involvement in protein–protein interactions. Using multiple alignments we identified the most conserved part of the protein (aa 1033–1415 *Homo sapiens*) with an identity of 70.5% between the most different organisms implying a putative important functional domain. The truncations observed in human thyroid adenomas disrupt this conserved domain of the protein indicating a loss of function of THADA contributing to the development of the follicular neoplasias of the thyroid.

Keywords: THADA; ARM repeat; Chromosomal rearrangement; Adenoma; Thyroid; Conserved domain

1. Introduction

The thyroid adenoma associated gene (*THADA*) first has been described as the target gene of chromosomal 2p21 rearrangements in benign thyroid lesions (Rippe et al., 2003). For benign thyroid lesions including hyperplasias and follicular thyroid adenomas 2p21 rearrangements are beneath rearrangements of chromosomal region 19q13.4 and trisomy 7 the third frequent cytogenetic subgroup (Bondeson et al., 1989; Teyssier et al., 1990; Dal Cin et al., 1992; Belge et al., 1994, 1998; Bol et al., 1999). 3′-RACE analysis on two cell lines derived from benign thyroid lesions with 2p21-translocations revealed fusion genes involving *THADA* (*THADA-FUS3p* and *THADA-FUS7p*). The breakpoints of chromosomal band 2p21 in these cell lines are located within intron 28 of *THADA*. In both fusion genes *THADA* ends after exon 28 followed by ectopic non-coding sequences derived from the translocation partners (Rippe et al.,

Abbreviations: aa, amino acid(s); A, adenosine; BLAST, basic local alignment search tool; bp, base pair(s); CDD, conserved domain database; cDNA, DNA complementary to RNA; CDS, coding sequence(s); COG, cluster of orthologous groups of proteins; CV1, cell line deriving from fibroblasts of *Chlorocebus aethiops*; dNTP(s), deoxyribonucleoside triphosphate(s); EBI, European bioinformatics institute; FISH, fluorescence in situ hybridization; G, guanine; kb, kilo base(s); HMM, hidden Markov model; Mb, mega base(s); M-MLV, Moloney murine leukaemia virus; mRNA, messenger ribonucleic acid; NCBI, National Center for Biotechnology Information; NIH3T3, cell line deriving from embryonic fibroblasts of *Mus musculus*; PPARγ, Peroxisome proliferator-activated gene gamma; Probcons, Probabilistic Consistency-based Multiple Alignment of Amino Acid Sequences; RNA, ribonucleic acid; SCOP, Structural classification of proteins; T, thymidine; *THADA*, Thyroid adenoma associated gene; THADA-FUS3p, Thyroid adenoma associated fusion gene 3p; *THADA-FUS7p*, Thyroid adenoma associated fusion gene 7p; UTR, untranslated region(s).

* Corresponding author. Tel./fax: +49 421 218 4239.
E-mail address: bullerd@uni-bremen.de (J. Bullerdiek).

0378-1119/$ - see front matter © 2007 Elsevier B.V. All rights reserved.
doi:10.1016/j.gene.2007.06.029

2003). In *THADA-FUS3p* the ectopic sequences are derived from an intronic region of the *peroxisome proliferator-activated gene gamma* (*PPARγ*). A functional *THADA/PPARγ* fusion was excluded because the fused sequences were in reverse orientation to the genomic *PPARγ* orientation (Drieschner et al., 2006). It was thus concluded that the truncation of the gene rather than its fusion to coding sequences is the critical event in benign thyroid tumors with *THADA* rearrangements (Rippe et al., 2003; Drieschner et al., 2006).

As for the possible function of THADA there is only one databank entry indicating that THADA is involved in the death receptor pathway (Puduvalli VK and Ridgeway L, Gene Bank reference note). Accordingly, the truncation of THADA and its loss of the C-terminus may lead to an altered apoptosis induction facilitating the development and/or the proliferation of benign thyroid lesions (Rippe et al., 2003).

THADA has a genomic size of about 365 kb. So far, two transcript variants (GeneBank accession nos. NM_022065 and NM_198554) have been described. The cDNA of transcript variant 1 (NM_022065) contains 38 exons with a size of 6090 bp. Transcript variant 2 comprises 36 exons with a size of 5900 bp (GeneBank accession no. NM_198554). To date for other species (e.g. *Pan troglodytes*, *Mus musculus*, and *Rattus norvegicus*) only predicted cDNA and/or mRNA sequences are accessible from databases.

The ORF of transcript variant 1 of human *THADA* has a length of 5862 bp hypothetically coding for 1953 amino acids. There is so far no homology to other human proteins or domains described and only one uncharacterized conserved domain COG5543 (Cluster of Orthologous Groups NCBI (Tatusov et al., 2003)) has been found in databases.

In this work, the *THADA* cDNA sequences of four different species (*Canis familiaris*, *Chlorocebus aethiops*, *Gallus gallus*, and *M. musculus*) have been analyzed and the genomic structures of *THADA* have been described. Based on these results the mRNA sequences as well as the protein sequences of the different species were compared in order to identify similar regions and possible conserved domains.

2. Materials and methods

2.1. Tissue samples and cell lines

For RNA isolation fresh-frozen tissue samples of liver and myocardium (*G. gallus*) and of the testis (*C. familiaris*) were used. The tissue samples were obtained commercially (*G. gallus*) and from the Small Animal Clinic (University of Veterinary Medicine, Hanover, Germany) (*C. familiaris*), respectively. For *C. aethiops* a cell line (CV1) derived from fibroblasts of the kidney and for *M. musculus* a cell line (NIH3T3) derived from embryonic fibroblasts were used for RNA isolation.

2.2. Fluorescence in situ hybridization (FISH)

For analysis of chromosomal localisation of *THADA* in *C. aethiops* fluorescence in situ hybridization on the cell line CV1 was performed. Cell culture of the cell line and karyotyping of Giemsa-banded metaphases were performed as previously described for pleomorphic adenomas of the parotid gland (Bullerdiek et al., 1987). For FISH analyses human BAC clones (RP11-1069E24 (GeneBank accession nos. AQ694385 and AQ703756) and RP11-183F15 (GeneBank accession no. AC092838)) (RZPD, Heidelberg, Germany) located within human *THADA* were used. FISH analyses were performed after GTG banding of the same metaphase spreads. Treatment of metaphases and subsequent FISH experiments were performed as described previously (Kievits et al., 1990). For FISH studies, BAC DNA was labeled with dig-11-dUTP by nick translation (Roche Diagnostics, Mannheim, Germany). For FISH experiments the labeled BAC DNA was pooled (concentration: 3 ng/μl). Post-hybridization was performed at 42 °C in 0.1× SSC for 5 min. Detection was performed with anti-dig-fluorescein fab-fragments (Roche Diagnostics, Mannheim, Germany). Chromosomes were counterstained with DAPI (0.025 mg/ml). For the cell line CV1, 10 metaphases were examined. Slides were analyzed on a Zeiss Axiophot fluorescence microscope using an FITC and DAPI filter set. Metaphases were recorded with the Power Gene Karyotyping System (Applied Imaging, Newcastle, UK).

2.3. RNA isolation and cDNA synthesis

The RNeasy Mini Kit (QIAGEN, Hilden, Germany) was used for the extraction and purification of total RNA from the fresh–frozen tissue samples (*G. gallus* and *C. familiaris*). Prior to the RNA isolation the tissue samples were homogenized with a tissue lyser (QIAGEN, Hilden, Germany). Total RNA was isolated from the cell lines (CV1 and NIH3T3) using the Trizol reagent (Invitrogen, Karlsruhe, Germany).

cDNA synthesis was performed with 5 μg total RNA using the M-MLV reverse transcriptase (Invitrogen, Karlsruhe, Germany).

2.4. Oligonucleotides and RT-PCR

Primers were designed using Lasergene primer select (DNAStar) and Vector NTI (Invitrogen). Up to nine PCR primer pairs were selected covering the whole CDS of the predicted *THADA* cDNA sequence of each organism. The fragment lengths of the primer pairs varied between 200 bp and 1800 bp. RT-PCR was performed with the Taq-DNA Polymerase (Invitrogen, Karlsruhe, Germany). Optimal annealing temperatures were detected by gradient RT-PCR (55 °C–65 °C) with a Mastercycler Gradient (Eppendorf, Hamburg, Germany) for each primer pair and organism. 1 μl of cDNA was used as template in a total reaction volume of 50 μl containing 0.2 mM of each primer, the reaction buffer supplied by manufacturer (Invitrogen, Karlsruhe, Germany), 0.2 mM dNTPs, 1.5 mM $MgCl_2$, and 2.5 U Taq DNA polymerase (Invitrogen, Karlsruhe, Germany). After 3 min initial denaturation at 95 °C 35 cycles of 60 s at 95 °C, 90 s at optimized annealing temperature (55 °C–65 °C) and 60 s at 72 °C followed by a final extension at 72 °C for 10 min. were performed in a Mastercylcer Gradient (Eppendorf, Hamburg, Germany).

2.5. Purification and determination of yield of RT-PCR products

RT-PCR fragments were isolated and purified with the Gel Extraction Kit (QIAGEN, Hilden, Germany). Quantification of the purified DNA was done by dot blot. A dilution series of the purified DNA was dotted on an agarose gel (1%) and stained with ethidiumbromide. The concentration was estimated by comparing the intensities of the dots of the purified DNA and a standardized dilution series of the 1 kb Plus DNA ladder (Invitrogen, Karlsruhe, Germany).

2.6. Determination of gene sequences

The sequence analysis of the mRNA and chromosomal assignment of the human *THADA* gene have been described previously (Rippe et al., 2003). According to the human *THADA* gene sequence the genomic structures of the homolog *THADA* genes in the examined organisms have been predicted aligning the human *THADA* sequence (GeneBank accession nos. NM_022065 and NP_071348) with the available genomic sequences (*C. familiaris*, *G. gallus*, and *M. musculus*). For this purpose Spidey (Lander et al., 2001), BLAST (Altschul et al., 1997), and Perl (www.perl.org) with Bioperl Modules (Stajich et al., 2002) have been used for sequence assembly and identification of splicing sites. If no similarities were detectable or splice sites have been missed manual corrections have been done. For all species described mRNA sequences have been included in the analyses.

20 ng/100 bp of purified DNA was used for DNA sequencing (MWG Biotech, Ebersberg, Germany). Each PCR fragment was sequenced in both directions using the corresponding PCR-primers. The sequencing chromatograms were corrected manually using the ChomasLite software (http://www.technelysium.com.au/). Clustering of the sequences has been done with the help of the Vector NTI Software ContigExpress (Vector NTI, Invitrogen).

2.7. Bioinformatics

The genomic organisation of the different *THADA* genes were determined by aligning the cDNA sequences with the available genomic sequences using Spidey with the option to use large intron sizes (Lander et al., 2001). Comparative interspecies sequence alignments were performed by the European Bioinformatics Institute (EBI) online tool, clustalw (http://www.ebi.ac.uk/clustalw/) (Higgins, 1994), PROBCONS (http://probcons.stanford.edu/), and AlignX (Vector NTI, Invitrogen). Protein pattern, profiles, and motives have been searched using the EBI tool InterProScan an integrated documentation resource for protein families, domains, and sites (http://www.ebi.ac.uk/) and HHpred using Homology detection by Hidden Markov Model — Hidden Markov Model comparison (http://toolkit.tuebingen.mpg.de/).

3. Results

3.1. Gene prediction and primer design

For primer design the *THADA* genes or *THADA* homologous sequences, respectively, of the analyzed organisms (*C. familiaris*, *C. aethiops*, *G. gallus*, and *M. musculus*) have been determined with bioinformatic tools. The human *THADA* mRNA and amino acid sequences (GeneBank accession nos. NM_022065, NP_071348) were split into sequences corresponding to single exons of the human gene. The conserved sequences AG and GT indicating the splice sites have been added to the nucleotide sequences. For alignments with the mouse, dog, and chicken genomic sequences in which the *THADA* genes have been detected (GenBank accession nos. NT_039649, NW_876251, NW_001471679) bl2seq blastn and tblastn programs have been used (Tatusova and Madden, 1999)). Perl and Bioperl Modules (Stajich et al., 2002) in combination with the program BLAST (Altschul et al., 1997) and Spidey have been used for sequence assembly and identification of splicing sites. The predicted sequences which were nearly identical to the later determined sequences (data not shown) served as template for the primer design. For the analysis of the African green monkey human *THADA* specific primers have been used. The primer pairs were constructed spanning 200 to 1800 bp and the produced PCR products were overlapping for optimal sequencing and contig building.

3.2. Genomic organisation of the THADA homologous genes from C. familiaris, C. aethiops, G. gallus, and M. musculus

The predicted mRNA sequences from *C. familiaris*, *G. gallus*, and *M. musculus* have been used for primer design. Therefore, the lengths of the deduced mRNA sequences and the

Table 1
Genomic, mRNA and protein sequence organisation of the THADA genes from *Canis familiaris*, *Chlorocebus aethiops*, *Gallus gallus*, *Homo sapiens* and *Mus musculus*

	Homo sapiens	*Mus musculus*	*Canis familiaris*	*Chlorocebus aethiops* [a]	*Gallus gallus*
Chromosome	2	17	10	14	3
Genomic length	365186 bp	274170 bp	326318 bp	–	152400 bp [b]
Number of exons	38	38	38	–	38
Sequenced mRNA	6.090 bp	5.914 bp	5.976 bp	5.899 bp	6.501 bp
Open reading frame	5.862 bp	5.817 bp	5.847 bp	5.862 bp	5.793 bp
Protein length	1.954 aa	1.939 aa	1.949 aa	1.954 aa	1.931 aa

[a] Genomic sequences of *Chlorocebus aethiops* not available.
[b] The genomic contig (GeneBank accession no. NW_001471679) of *Gallus gallus* chromosome 3 contains parts in this region which are not fully determined. This result should be treated as preliminary.

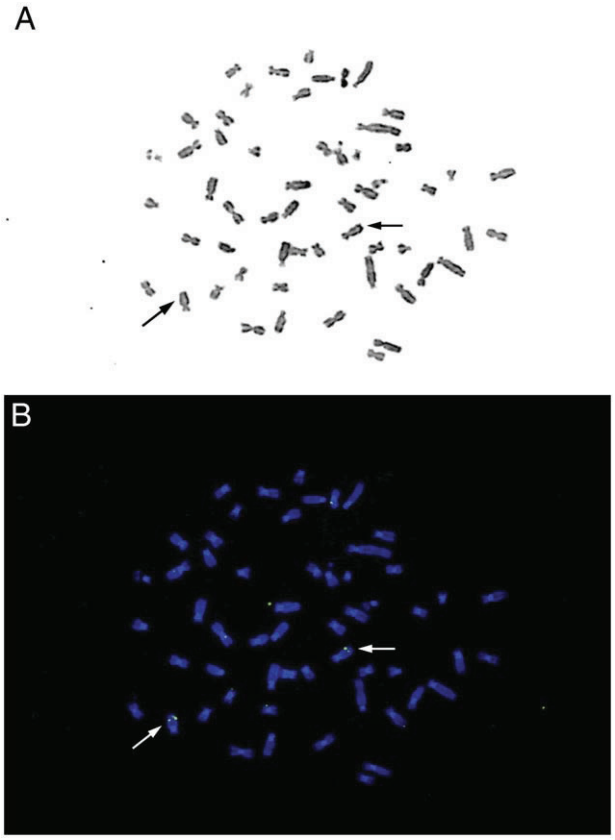

Fig. 1. Chromosomal localisation of *THADA* in *Chlorocebus aethiops*. A metaphase of the cell line CV1 after GTG banding (A) and the same metaphase after FISH with human *THADA* BAC clones (B). Arrows indicating signals on the long arms of both chromosomes 14 of *Chlorocebus aethiops*.

corresponding genomic regions depend on this design. Parts of the 5′ and 3′ untranslated regions have not been determined. Nevertheless, in all cases the predicted coding regions have been sequenced including ATG translational initiation codons and stop codons. The mRNA sequences of the analyzed organisms (Table 1) were submitted to GenBank (Benson et al., 2006) under accession numbers EF222204 (*C. familiaris*), EF222205 (*C. aethiops*), F222206 (*G. gallus*), and EF222207 (*M. musculus*). The genomic size of *THADA* in human is 365.186 bp. The *THADA* homologous sequences of the organisms analyzed herein are spanning shorter genomic regions compared to the human *THADA* gene (Table 1). For *C. aethiops* no genomic sequences of the corresponding region are available. Fluorescence in situ hybridization (FISH) analysis with human BAC clones containing *THADA* confirms the localisation on the long arm of *C. aethiops* chromosome 14 (Fig. 1).

3.3. Identification and characterization of the open reading frame

All deduced mRNA sequences of *THADA* from *C. familiaris*, *C. aethiops*, *G. gallus*, and *M. musculus* are containing only one reasonable open reading frame (Table 1). To determine the position of the start codon a sequence analysis of a 100 bp region containing the putative start codon has been performed by multiple alignments of the *C. familiaris*, *G. gallus*, *Homo sapiens*, and *M. musculus* mRNAs. The overall nucleotide similarity calculated by an AlignX (Invitrogen) multiple alignment is 13.7% upstream the predicted start codon and 58.8% within the first 50 bp of the coding region indicating the translation start at this ATG. Furthermore a Kozak sequence is strongly indicating the translation start. The most important positions at position −3 (A) and position +4 (G) (Kozak, 2002) with respect to the predicted translation initiation codon ATG were found to be conserved in all analyzed organisms.

The physical properties of the deduced proteins resemble the human THADA. The lengths of the proteins range between 1930 aa (*G. gallus*) and 1953 aa (*C. aethiops*) which is the same as in humans (Table 1). Thus, the molecular weight is between 216,601 Da (*G. gallus*) and 219,595 Da (*Homo sapiens*), respectively.

3.4. Sequence comparison

Using PROBCONS (Do et al., 2005) for the alignment and AlignX (Vector NTI, Invitrogen) for calculation of the similarity the determined mRNA and protein sequences have been aligned and the similarity has been calculated. The similarities between the human THADA and the THADA proteins of the other organisms correspond to the evolutionary relationship between these organisms. The African green monkey as the nearest relative has the highest similarity to the human (97.1% nucleotide similarity of the coding region and 95.9% amino acid similarity). The chicken as the only non-mammalian organism has the lowest similarity, i.e. 64.7% nucleotide similarity of the coding region and 64.9% amino acid similarity (Table 2).

3.5. Identification of conserved domains

The predicted THADA protein sequences from *C. familiaris*, *C. aethiops*, *G. gallus*, *M. musculus*, and the human sequence have been aligned with PROBCONS (Do et al., 2005) in a multiple sequence alignment. For visualisation of the similarity and identification of conserved regions a similarity plot has been calculated (AlignX similarity plot) (Fig. 2). The region with the highest similarity is found from position 1043–1425 in the

Table 2
Similarity comparison of the open reading frame and deduced protein sequences from *Canis familiaris*, *Chlorocebus aethiops, Gallus gallus,* and *Mus musculus* (GeneBank accession nos. ABQ10598, ABQ10599, ABQ10600, and ABQ10601) to the human mRNA transcript of THADA (GeneBank accession no. NM_022065) and the human THADA protein (GeneBank accession no. NP_071348)

Organism	Similarity to THADA *Homo sapiens*	
	ORF/CDS (%)	Protein (%)
Chlorocebus aethiops	97.1	95.9
Canis familiaris	86.7	83.1
Mus musculus	81.1	78.2
Gallus gallus	64.7	57.2

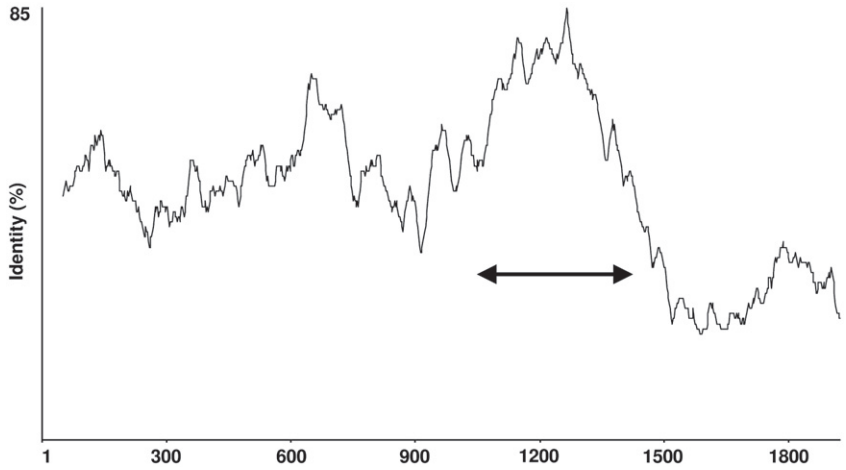

Fig. 2. Similarity plot of the THADA protein from *Canis familiaris*, *Chlorocebus aethiops*, *Gallus gallus*, *Homo sapiens*, and *Mus musculus*. For the sake of visualisation clarity only identical positions in all organisms are included. A window size of 100 aa has been used, therefore the first and last positions are not shown. The most conserved part, position 1043–1425, is marked by an arrow.

multiple alignment corresponding to region 1033–1415 in humans with an identity calculation of 70.4% and the similarity including conserved amino acid changes being 78.6%. The overall similarity of the THADA proteins is calculated to 48.6% identical amino acids and including conserved amino acid changes to 60.9%. Another shorter segment (position 586–705 in humans) is highly similar, 72.5% identity and 78.3% similarity including conserved amino acid substitutions. The lowest similarity is seen in the carboxy terminal part of the protein from position 1491 to 1953 in humans with 27.5% identical positions and 41.9% if conserved substitutions are included.

3.6. Domain and motif assignment

The deduced THADA protein sequences were compared with different domain and motif databases by the help of EBI InterProScan tool and NCBI Conserved Domain Database (CDD) to gather more information regarding the function of THADA. The conserved domain search of the NCBI CDD yields one domain with the identifier COG5543 (COG = Clusters of orthologous groups of proteins). The COG5543 is a cluster of 3 hypothetical proteins from different fungi (GeneBank accession nos. NP_588532, NP_597091, Q03496)

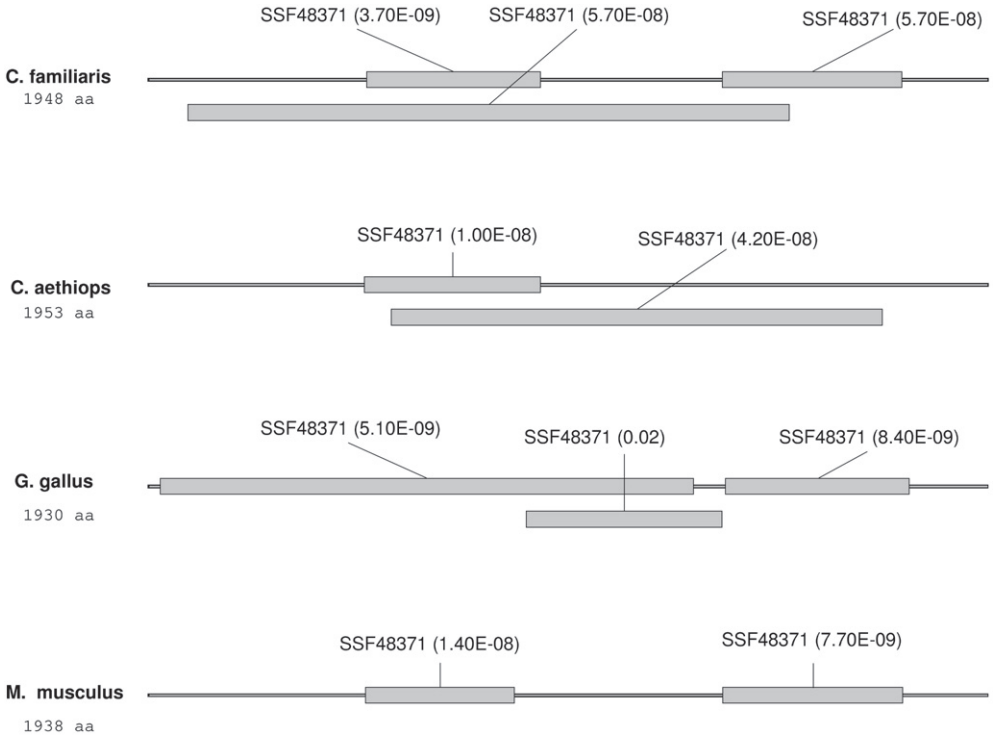

Fig. 3. Similarities to the superfamily of ARM repeat structures (SSF48371) detected in the THADA protein from *Canis familiaris*, *Chlorocebus aethiops*, *Gallus gallus* and *Mus musculus*.

without functional assignment. This conserved multi domain cluster COG5543 has a length of 1400 aa. The alignment to the conserved cluster is localised in the most conserved region of the protein (see Identification of conserved domains) from approx. aa 1025 to aa 1425 in the different THADA proteins with an expect value around 2e−40. In mouse and chicken another part of the THADA protein shows similarities to this cluster with a lower significance (mouse THADA pos 394–902, e-value 0.00002 and chicken THADA position 396–837, e-value 0.00009).

The InterProScan reveals in the THADA proteins from all analyzed organisms significant assignments to the superfamily ARM repeat (SSF48371) of the Superfamily database of profile Hidden Markov Models (HMMs) (Gough et al., 2001) (Fig. 3). The Superfamily database is based of the SCOP (Structural Classification of Proteins) database which provides a description of structural and evolutionary relationships of proteins with known structure (Murzin et al., 1995). The ARM repeat superfamily summarizes different right-handed superhelices of helices like Armadillo repeat, HEAT repeat, and clathrin associated domains. Similarities with low significance (e-value from 17 to 0.055) to HEAT domains have been found repeatedly, from 5 in the human, dog, and green monkey to 8 in the chicken THADA using the Pfam database (Finn et al., 2006) (data not shown).

The HHpred server of the Max Planck Institute for Developmental Biology for remote protein homology detection and structure prediction has been used for aligning the previously described PROBSCON multiple alignment of THADA from *C. familiaris*, *C. aethiops*, *G. gallus*, *Homo sapiens*, and *M. musculus* with Hidden Markov Models from different databases of protein domains like InterPro, SCOP, Superfamily and COG. The HHpred software is an implementation of pair wise comparisons of profile Hidden Markov Models (HMM) (Soding et al., 2005). The HMM of the COG5543 cluster found with a PSI-BLAST in the CDD Database "aligns" using the HHpred software with an e-value of 0 to the HMM of the THADA multiple alignment (position 394–1749). If the Superfamily database was used in the HHpred scan different models of the superfamily ARM repeat SSF48371 aligning with lower significance (e-values 16–8600) to the multiple alignment of THADA (position 35–1756). Using HMMs calculated by HHpred from entries of the Protein Data Bank (PDB) (Berman et al., 2000) and the SCOP database the best matches to THADA are CAND1 (e-value 0.00025) and different importin proteins (e-value 0.11–10). CAND1 and importins are proteins containing ARM repeat related structures.

4. Discussion

The human *THADA* gene is the target gene of rearrangements involving chromosomal region 2p21 in thyroid neoplasias (Rippe et al., 2003). These rearrangements constitute one of the most frequent specific chromosomal rearrangements in human epithelial tumors at all and lead to fusion genes in which the 3′ part of *THADA* is truncated. Up to now there is no further information regarding the function of the protein and the possible molecular background of the cell transformation resulting from that chromosomal rearrangement (Rippe et al., 2003). Hypothetically the truncated form of the protein may lead to an altered apoptosis induction due to the possible involvement in the death receptor pathway (Rippe et al., 2003). In the present study the orthologeous *THADA* mRNA sequences of the vertebrates *C. familiaris*, *C. aethiops*, *G. gallus*, and *M. musculus* have been determined and characterized to gather more information regarding the function of the *THADA* gene and its role in the development of human thyroid neoplasias.

The size of the mRNA, the protein size, and the genomic organisation of *THADA* is conserved among humans and the other species analyzed. Furthermore the genomic organisation of *THADA* in all analyzed organisms is very similar to the genomic organisation of the *THADA* gene in humans. All homologous *THADA* genes have the same number of 38 exons corresponding to the genomic organisation of the human *THADA* gene (Table 1). The start codons are localised always in the second exon and the stop codon in the last exon. With the exception of exons 1, 2, and 38 containing the 5′ and 3′ untranslated regions all exons have a very similar size and 23 exons are even identical in length. All exon/intron boundaries are conforming to the AG/GT rule for acceptor and donor of splicing sites (Madhani and Guthrie, 1994). Thus, the different genomic sizes of *THADA* in the analyzed organisms are due to distinct length of the intronic sequences. The chromosomal expansion of the genes (*Homo sapiens* 365186 bp, *C. familiaris* 326318 bp, *M. musculus* 274,170 bp, and *G. gallus* approx. 152,400 bp) corresponds roughly – with the exception of mouse and dog, which differ in length only slightly – to the total length of the genome of the analyzed organisms (3000 Mb in humans, 2400 Mb in the dog, 2500 Mb in the mouse, and 1200 Mb in the chicken; estimated genome lengths according to NCBI genome database). This observation is in accordance to the general findings by (Deutsch and Long, 1999) that the lengths of the introns correspond with the size of the whole genome.

Neither the structures nor the sequences of the deduced proteins of THADA were confirmed with biochemical techniques. This study was aimed at the characterization of the coding region and the determination of the start codon for further expression studies. The longest putative open reading frames have been predicted as coding regions. Similarity in length (>1930 aa in all analyzed organisms) and sequence make this assumption highly reasonable. The first ATG translational initiation codon of the open reading frame is seen as start codon. The analysis of the region surrounding the predicted start position revealed a high similarity of the sequence beginning with the position −3 (A) in all organisms whereas the 5′ untranslated region is showing less similarity. This is in concordance with the observation that sequences of 5′-UTRs as well as 3′-UTRs are less conserved compared to coding regions (Pesole et al., 2000). Furthermore, the positions at −3 (A) and +4 (G) to the predicted ATG translation initiation codon meet the criteria for a Kozak sequence (Kozak, 2002). Thus, it is highly probable that this ATG codon is the initial start codon for protein synthesis.

The protein size of all analyzed organisms lies in between 1931 aa (*G. gallus*) and 1954 aa (*C. aethiops* and *Homo sapiens*). Interestingly only 5% (513) of 24,264 annotated human proteins (NCBI RefSeq database; (Pruitt et al., 2005)) exceed the human THADA size.

The multiple alignment of the THADA protein sequences serves to identify conserved domains in THADA. In the region from approximately 1033–1415 aa in human THADA the sequence similarity in the PROBCONS multiple alignment shows the highest regional similarity with an identity calculation of 70.5% and including conserved amino acid substitutions of 78.6%. Furthermore, there are two parts within this region with a size of 21 aa and 23 aa that are identical in all species analyzed. In the same region similarities to the uncharacterized conserved domain COG5543 of the NCBI Conserved Domain Database have been detected. This conserved part of the protein could be a functional important region of THADA as conserved domains correspond in most cases to functional regions (Bornberg-Bauer et al., 2005).

Interestingly, the truncation at the position 1352 of THADA observed in the previously described fusion genes in human benign thyroid lesions (Rippe et al., 2003) is located in the middle of the conserved part of THADA. Thus, it seems that this part harbours a domain with important function and in thyroid adenomas this function is destroyed. Also, it cannot be excluded that the c-terminal part of THADA beginning with position 1491 in humans showing the lowest similarity of 27.5% identity could have structural important functions and maybe the truncation results in an overall rearrangement of the protein.

The similarities to the superfamily domain ARM repeat (SSF48371) a domain of the Superfamily database (Gough et al., 2001) and the HHpred alignments (Soding et al., 2005), which are used for more remote homology detection, are helpful to gather more information regarding the function of THADA. The Superfamily database is based of the SCOP (Structural Classification of Proteins) database and superfamilies are families of proteins, that have low sequence identities but whose structures and, in many cases, functional features suggest that they have a common evolutionary origin (Murzin et al., 1995). The superfamily ARM repeat summarizes repeated domains like Armadillo repeats and HEAT repeats which contain tandem copies of a degenerate protein sequence motif that forms right-handed superhelices of helices. This repeated structure creates a surface for protein–protein interaction (Coates, 2003). The HEAT domains are detected repeatedly with low significance in the human THADA and as well as in the predicted THADA homologous proteins herein analyzed. The ARM repeats like the here mentioned Armadillo repeat and HEAT repeat are difficult to detect because of low constraints of sequence conservation (Andrade et al., 2001). Armadillo repeats were found among others in plakoglobin, β-cathenin, the nuclear import factor α-importin, and the tumor suppressor adenomatous polyposis coli (Andrade et al., 2001). HEAT domains are present in importins β1, β2, and proteins related to the clathrin-associated adaptor complex. Members of these proteins are also detected in the HHpred scan. The best alignment is to CAND1/TIP120 cullin-associated neddylation-dissociated protein 1. This protein is binding to cullin-RING-ligases, which regulate diverse cellular functions such as cell cycle progression and cytokine signalling by ubiquitinating key regulatory proteins (Min et al., 2005). With lower significance similarities to importins which are involved in the protein transport through nuclear pore complexes are found. All proteins with similarities to THADA share the ARM repeats which are involved in protein–protein interactions. The Gene Ontology (Ashburner et al., 2000) term "protein binding (GO:0005515)" commonly refer to different protein binding activities like, among others, the death receptor activities.

With these new findings, similarities to protein–protein binding proteins with receptor activities and the possible structure with ARM repeats, the conserved and expressed in *Homo sapiens*, *C. familiaris*, *C. aethiops*, *G. gallus*, and *M. musculus* THADA appears to be involved in protein binding activity as e.g. found in proteins belonging to the death receptor pathway. This, indicating a function as receptor with protein–protein interaction, corroborates our theory of THADA involvement in the death receptor pathway. In thyroid adenomas with 2p21 rearrangements (Rippe et al., 2003) the truncation results in a disruption of the most conserved part of the protein which seems to be a functional important domain.

References

Altschul, S.F., Madden, T.L., Schaffer, A.A., Zhang, J., Zhang, Z., Miller, W., Lipman, D.J., 1997. Gapped BLAST and PSI-BLAST: a new generation of protein database search programs. Nucleic Acids Res. 25, 3389–3402.

Andrade, M.A., Perez-Iratxeta, C., Ponting, C.P., 2001. Protein repeats: structures, functions, and evolution. J. Struct. Biol. 134, 117–131.

Ashburner, M., et al., 2000. Gene ontology: tool for the unification of biology. The gene ontology consortium. Nat. Genet. 25, 25–29.

Belge, G., Thode, B., Rippe, V., Bartnitzke, S., Bullerdiek, J., 1994. A characteristic sequence of trisomies starting with trisomy 7 in benign thyroid tumors. Hum. Genet. 94, 198–202.

Belge, G., Roque, L., Soares, J., Bruckmann, S., Thode, B., Fonseca, E., Clode, A., Bartnitzke, S., Castedo, S., Bullerdiek, J., 1998. Cytogenetic investigations of 340 thyroid hyperplasias and adenomas revealing correlations between cytogenetic findings and histology. Cancer Genet. Cytogenet. 101, 42–48.

Benson, D.A., Karsch-Mizrachi, I., Lipman, D.J., Ostell, J., Wheeler, D.L., 2006. GenBank. Nucleic Acids Res. 34, D16–D20.

Berman, H.M., Westbrook, J., Feng, Z., Gilliland, G., Bhat, T.N., Weissig, H., Shindyalov, I.N., Bourne, P.E., 2000. The protein data bank. Nucleic Acids Res. 28, 235–242.

Bol, S., Belge, G., Thode, B., Bartnitzke, S., Bullerdiek, J., 1999. Structural abnormalities of chromosome 2 in benign thyroid tumors. Three new cases and review of the literature. Cancer Genet. Cytogenet. 114, 75–77.

Bondeson, L., Bengtsson, A., Bondeson, A.G., Dahlenfors, R., Grimelius, L., Wedell, B., Mark, J., 1989. Chromosome studies in thyroid neoplasia. Cancer 64, 680–685.

Bornberg-Bauer, E., Beaussart, F., Kummerfeld, S.K., Teichmann, S.A., Weiner 3rd, J., 2005. The evolution of domain arrangements in proteins and interaction networks. Cell. Mol. Life Sci. 62, 435–445.

Bullerdiek, J., Boschen, C., Bartnitzke, S., 1987. Aberrations of chromosome 8 in mixed salivary gland tumors—cytogenetic findings on seven cases. Cancer Genet. Cytogenet. 24, 205–212.

Coates, J.C., 2003. Armadillo repeat proteins: beyond the animal kingdom. Trends Cell Biol. 13, 463–471.

Dal Cin, P., Sneyers, W., Aly, M.S., Segers, A., Ostijn, F., Van Damme, B., Van Den Berghe, H., 1992. Involvement of 19q13 in follicular thyroid adenoma. Cancer Genet. Cytogenet. 60, 99–101.

Deutsch, M., Long, M., 1999. Intron–exon structures of eukaryotic model organisms. Nucleic Acids Res. 27, 3219–3228.

Do, C.B., Mahabhashyam, M.S., Brudno, M., Batzoglou, S., 2005. ProbCons: probabilistic consistency-based multiple sequence alignment. Genome Res. 15, 330–340.

Drieschner, N., Belge, G., Rippe, V., Meiboom, M., Loeschke, S., Bullerdiek, J., 2006. Evidence for a 3p25 breakpoint hot spot region in thyroid tumors of follicular origin. Thyroid 16, 1091–1096.

Finn, R.D., Mistry, J., Schuster-Bockler, B., Griffiths-Jones, S., Hollich, V., Lassmann, T., Moxon, S., Marshall, M., Khanna, A., Durbin, R., Eddy, S.R., Sonnhammer, E.L., Bateman, A., 2006. Pfam: clans, web tools and services. Nucleic Acids Res. 34, D247–D251.

Gough, J., Karplus, K., Hughey, R., Chothia, C., 2001. Assignment of homology to genome sequences using a library of hidden Markov models that represent all proteins of known structure. J. Mol. Biol. 313, 903–919.

Higgins, D.G., 1994. CLUSTAL V: multiple alignment of DNA and protein sequences. Methods Mol. Biol. 25, 307–318.

Kievits, T., Dauwerse, J.G., Wiegant, J., Devilee, P., Breuning, M.H., Cornelisse, C.J., van Ommen, G.J., Pearson, P.L., 1990. Rapid subchromosomal localization of cosmids by nonradioactive in situ hybridization. Cytogenet. Cell Genet. 53, 134–136.

Kozak, M., 2002. Pushing the limits of the scanning mechanism for initiation of translation. Gene 299, 1–34.

Lander, E.S., et al., 2001. Initial sequencing and analysis of the human genome. Nature 409, 860–921.

Madhani, H.D., Guthrie, C., 1994. Dynamic RNA–RNA interactions in the spliceosome. Annu. Rev. Genet. 28, 1–26.

Min, K.W., Kwon, M.J., Park, H.S., Park, Y., Yoon, S.K., Yoon, J.B., 2005. CAND1 enhances deneddylation of CUL1 by COP9 signalosome. Biochem. Biophys. Res. Commun. 334, 867–874.

Murzin, A.G., Brenner, S.E., Hubbard, T., Chothia, C., 1995. SCOP: a structural classification of proteins database for the investigation of sequences and structures. J. Mol. Biol. 247, 536–540.

Pesole, G., Grillo, G., Larizza, A., Liuni, S., 2000. The untranslated regions of eukaryotic mRNAs: structure, function, evolution and bioinformatic tools for their analysis. Brief. Bioinform. 1, 236–249.

Pruitt, K.D., Tatusova, T., Maglott, D.R., 2005. NCBI Reference Sequence (RefSeq): a curated non-redundant sequence database of genomes, transcripts and proteins. Nucleic Acids Res. 33, D501–D504.

Rippe, V., Drieschner, N., Meiboom, M., Escobar, H.M., Bonk, U., Belge, G., Bullerdiek, J., 2003. Identification of a gene rearranged by 2p21 aberrations in thyroid adenomas. Oncogene 22, 6111–6114.

Soding, J., Biegert, A., Lupas, A.N., 2005. The HHpred interactive server for protein homology detection and structure prediction. Nucleic Acids Res. 33, W244–W248.

Stajich, J.E., et al., 2002. The Bioperl toolkit: Perl modules for the life sciences. Genome Res. 12, 1611–1618.

Tatusov, R.L., et al., 2003. The COG database: an updated version includes eukaryotes. BMC Bioinformatics 4, 41.

Tatusova, T.A., Madden, T.L., 1999. BLAST 2 Sequences, a new tool for comparing protein and nucleotide sequences. FEMS Microbiol Lett 174, 247–250.

Teyssier, J.R., Liautaud-Roger, F., Ferre, D., Patey, M., Dufer, J., 1990. Chromosomal changes in thyroid tumors. Relation with DNA content, karyotypic features, and clinical data. Cancer Genet. Cytogenet. 50, 249–263.

IV. Chromosomal assignment of canine *THADA* gene to CFA 10q25 (Soller *et al.*, 2008)

Um Informationen hinsichtlich der Beteiligung von THADA an caninen Tumoren der Schilddrüse zu erhalten, wurde die chromosomale Lokalisation des caninen *THADA*-Gens ermittelt. Hierzu erfolgte die Identifizierung eines caninen BAC-Klons mittels Screening einer *Canis familiaris* DogBAC Library mit *THADA*-spezifischen PCR-Primern. Die entsprechende PCR wurde zuvor an caniner genomischer DNA aus peripherem Blut etabliert. Der so identifizierte BAC-Klon (DogBAC Library ID S011P24K05RE) wurde nach Verifizierung mit einer semi-nested PCR für eine FISH-Kartierung an Metaphasechromosomen, die aus caninem Gesamtblut präpariert wurden, verwendet. Die FISH ergab dabei die Lokalisation des caninen *THADA* auf dem Chromosom (CFA) 10q25 des Hundes. Die Region 10q25 des Hundes entspricht der Region p21 des humanen Chromosoms 2. Ein Vergleich zu zytogenetischen Veränderungen, die zuvor für canine Adenome der Schilddrüse beschrieben worden sind, zeigte, dass die Region CFA 10q25 nicht in diesen Tumoren beteiligt ist, wobei allerdings bisher nur wenige Schilddrüsenadenome des Hundes zytogenetisch charakterisiert sind.

IV

Chromosomal assignment of canine *THADA* gene to CFA 10q25

Jan T. Soller, Claudia Beuing, Hugo Murua Escobar, Susanne Winkler, Nicola Reimann-Berg, Norbert Drieschner, Gaudenz Dolf, Claude Schelling, Ingo Nolte, Jörn Bullerdiek

(Molecular Cytogenetics 1(1): 11)

Eigenanteil:

- Durchführung der molekularzytogenetischen Untersuchungen.

Molecular Cytogenetics

BioMed Central

Short report

Open Access

Chromosomal assignment of canine *THADA* gene to CFA 10q25

Jan T Soller[†1,2], Claudia Beuing[†2], Hugo Murua Escobar*[1,2], Susanne Winkler[1], Nicola Reimann-Berg[1], Norbert Drieschner[1], Gaudenz Dolf[3], Claude Schelling[4], Ingo Nolte[2] and Jörn Bullerdiek[1,2]

Address: [1]Centre for Human Genetics, University of Bremen, Leobener Straße ZHG, 28359 Bremen, Germany, [2]Small Animal Clinic and Research Cluster of Excellence "REBIRTH", University of Veterinary Medicine Hanover, Bischofsholer Damm 15, 30173 Hannover, Germany, [3]Institute of Genetics, Vetsuisse Faculty, University of Berne, Bremgartenstrasse 109a, PO Box 8466, 3001 Bern, Switzerland and [4]Department of Animal Science, Swiss Federal Institute of Technology Zurich, Vetsuisse-Faculty Zurich, University of Zurich, Winterthurerstrasse 204, 8057 Zürich, Switzerland

Email: Jan T Soller - soller@uni-bremen.de; Claudia Beuing - claudia.beuing@tiho-hannover.de; Hugo Murua Escobar* - escobar@uni-bremen.de; Susanne Winkler - winklers@uni-bremen.de; Nicola Reimann-Berg - nicola.reimann-berg@uni-bremen.de; Norbert Drieschner - norbert.drieschner@uni-bremen.de; Gaudenz Dolf - dolf.gaudenz@itz.unibe.ch; Claude Schelling - claude.schelling@inw.agrl.ethz.ch; Ingo Nolte - inolte@klt.tiho-hannover.de; Jörn Bullerdiek - bullerd@uni-bremen.de

* Corresponding author †Equal contributors

Published: 3 June 2008

Molecular Cytogenetics 2008, **1**:11 doi:10.1186/1755-8166-1-11

Received: 13 March 2008
Accepted: 3 June 2008

This article is available from: http://www.molecularcytogenetics.org/content/1/1/11

Abstract

Background: Chromosomal translocations affecting the chromosome 2p21 cluster in a 450 kb breakpoint region are frequently observed in human benign thyroid adenomas. *THADA* (thyroid adenoma associated) was identified as the affected gene within this breakpoint region. In contrast to man tumours of the thyroid gland of dogs (*Canis lupus familiaris*) constitute mainly as follicular cell carcinomas, with malignant thyroid tumours being more frequent than benign thyroid adenomas. In order to elucidate if the *THADA* gene is also a target of chromosomal rearrangements in thyroid adenomas of the dog we have physically mapped the canine *THADA* gene to canine chromosome 10.

A PCR was established to screen a canine genome library for a BAC clone containing the gene sequence of canine *THADA*. Further PCR reactions were done using the identified BAC clone as a template in order to verify the corresponding PCR product by sequencing.

Canine whole blood was incubated with colcemid in order to arrest the cultured cells in metaphases. The verified BAC DNA was digoxigenin labeled and used as a probe in fluorescence *in situ* hybridization (FISH). Ten well spread metaphases were examined indicating a signal on canine chromosome 10 on both chromatids. A detailed fine mapping was performed indicating the canine *THADA* gene locus on the q-arm of chromosome 10.

Results: The canine *THADA* gene locus was mapped on chromosome 10q25. Our mapping results obtained in this study following the previously described nomenclature for the canine karyotype.

Conclusion: We analysed whether the *THADA* gene locus is a hotspot of canine chromosomal rearrangements in canine neoplastic lesions of the thyroid and in addition might play a role as a candidate gene for a possible malignant transformation of canine thyroid adenomas. Although the available cytogenetic data of canine thyroid adenomas are still insufficient the chromosomal region to which the canine *THADA* has been mapped seems to be no hotspot of chromosomal aberrations seen in canine thyroid adenomas.

Background

In human thyroid adenomas chromosomal translocations involving the regions 19q13 and 2p21 have frequently been described [1,2]. Chromosomal aberrations showing 2p21 rearrangements belong to the most common abnormalities in benign epithelial tumours with an observed frequency of 10% [3]. Recently, a gene named *THADA* (thyroid adenoma associated) [GenBank: NM_022065] which is directly affected by this cytogenetic rearrangement, could be identified within the 2p21 breakpoint region [3].

In terms of animal cancer models, the dog has lately been attracting significant interest due to the fact that the malignancies of humans and dogs show various similarities [4]. Among the striking arguments for the dog as an animal model for man are spontaneous appearance of the tumours, comparable histological variance, similar cancer types and similar biological behaviour of the observed neoplasias, including metastasis [5-7].

In man the majority of tumours affecting the thyroid gland are benign, whereas in dogs the situation is quite different. Thyroid carcinomas are rare in the human population, the overall incidence is <1% [8,9]. A total of 1.2% of all canine tumours affects the thyroid gland with thyroid carcinomas occurring more frequently than adenomas [9,10]. Carcinomas of follicular origin are the most common form of canine thyroid neoplasias [11].

In order to elucidate whether human genes which are involved in the pathogenesis of benign thyroid adenomas could play a role as orthologous candidate genes for a possible malignant transformation of thyroid tumours in dogs, we have mapped the canine *THADA* gene and analysed if the canine gene locus is involved in cytogenetic rearrangements.

Methods

BAC library screening

A PCR reaction for PCR-based screening of the *Canis familiaris* DogBAC library [12] (Institute of Animal Genetics, Nutrition and Housing, University of Berne, Berne, Switzerland) for a BAC clone containing *THADA* was established using canine genomic DNA derived from blood. The primers T1: 5'GCATTTTTCGATTGTCATAAC'3 and T2: 5'TCAGCCAAAACTAGATAACAC'3 were designed using the predicted canine *THADA* gene sequence of canine chromosome 10, [GeneBank: NC_006592]. PCR parameters were: 95°C for 5 min, followed by 35 cycles of 95°C 30 sec, 55°C 30 sec, 72°C 30 sec, and a final elongation of 72°C for 10 min. The corresponding 601 bp PCR product was cloned into the pGEM-T Easy vector system (Promega) and verified by sequencing. The obtained canine sequence contained the 97 bp of exon 2 with a 92% similarity to human exon 2 of *THADA* [GenBank: NM_022065]. The sequence was submitted to the NCBI database [GenBank DQ836130]. The DNA contigs and alignments were done with Lasergene software (DNAstar, Madison, USA) and various sequences from the NCBI database [GeneBank: AC_000045, NM_022065].

For verification and secondary screening a semi-nested PCR reaction was established, using the T1 primer and a nested primer T1B (5'TCAGTACTATTGGCATTTGGAG'3) generating a 147 bp amplicon. A positive BAC clone (DogBAC library ID S011P24K05RE) was identified and verified by PCR. The obtained PCR products were cloned into the pGEM-T Easy vector system (Promega) and verified by sequencing. The verified clone was used as probe for following FISH experiments.

Slide Preparation

1 ml of canine whole blood was incubated for 72 h in Chromosome Medium B (Biochrom). Subsequently, colcemide (0.1 μg/ml) (Biochrom) was added for 2 hours. The cells were centrifuged at 135 × g for 10 min and incubated for 20 min in 0.05 M KCl. Finally, the cells were fixed overnight with methanol/glacial acetic acid. This suspension was dropped on ice-cold slides and dried for at least 7 days at 37°C. The chromosomes were stained by GTG banding for karyotype description. Prior to use in FISH investigations, the slides were destained with 70% ethanol.

Fluorescence in situ hybridization

BAC-DNA was digoxigenin labeled (Dig-Nick-Translation-Kit, Roche). The hybridization mixture contained 200 ng probe, 40 ng ssDNA, 600 ng sonicated dog DNA, 2 × SSC, 2 × SSPE, 50% formamide and 10% dextran sulfate. 50 μl of this mixture were applied to each slide and the cover slips were sealed with rubber cement. Probe and chromosomes were denatured at 75°C on an Eppendorf thermocycler gradient, using the in situ adapter. Afterwards, the slides were incubated in a moist chamber at 37°C over night. Cover slips were carefully removed and the slides were incubated in 0.1 × SSC at 61°C and 1 × PBS at RT. Slides were then covered with 100 μl NFDM for 20 min. at 37°C in a moist chamber. For signal detection 100 μl NFDM containing 3 μg of anti-digoxigenin-rhodamine, fab fragments (Roche) were added to each slide and again incubated for 20 min at 37°C in a moist chamber, followed by washes with 1 × PBS, 3 × 3 min at RT. Slides were air dried before chromosome staining was performed with 25 μl of Vectashield mounting medium with DAPI (Vector Laboratories).

Ten well spread metaphases were examined indicating a signal on canine chromosome 10 on both chromatids of both chromosomes of canine chromosome 10 (Fig. 1).

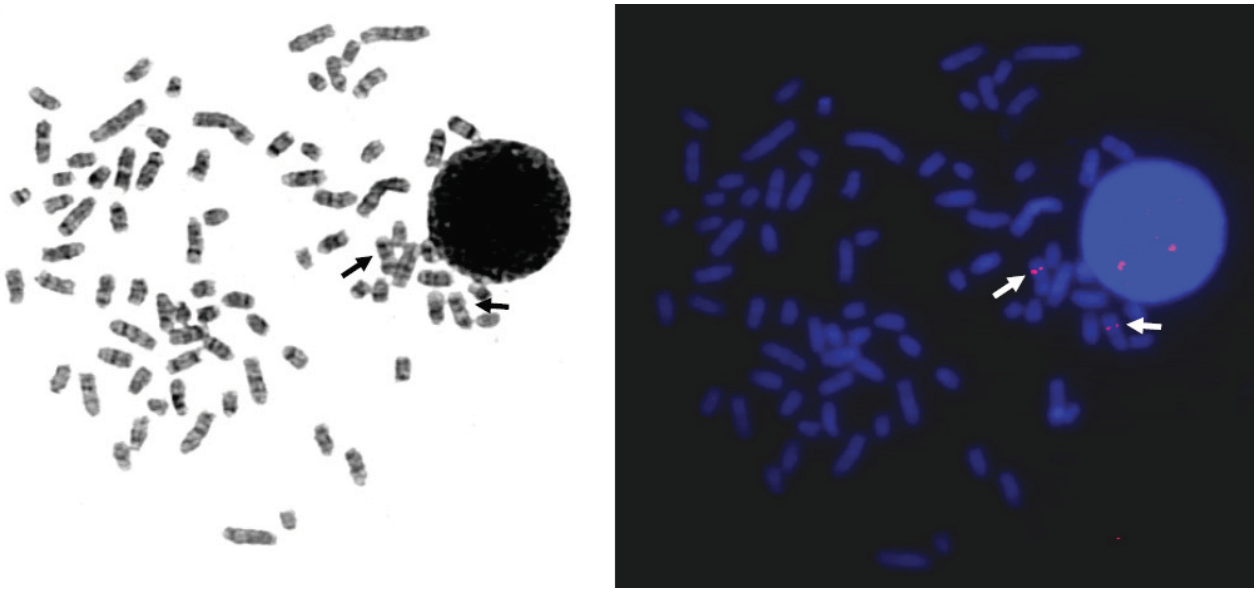

Figure 1
FISH mapping of canine THADA. Metaphase spread after fluorescence *in situ* hybridisation with signals on CFA 10q25 (right) of both chromosomes, the same metaphase after GTG-banding (left).

The determination of chromosomes followed the nomenclature of the canine karyotype as described previously [13].

Results and Discussion

In humans 10% of all chromosomal rearrangements in benign thyroid tumours involve a 450 kb breakpoint region on 2p21 [14]. These 2p21 rearrangements are the most commonly detected cytogenetic aberrations in benign thyroid adenomas. Within the mentioned breakpoint region the *THADA* gene was identified as a target gene for translocation events. *THADA* transcripts fused downstream to ectopic sequences of human chromosome 3 and 7 have been detected in thyroid adenoma cell lines S325/TSV40 and S533/TSV40 [3] (Centre for Human Genetics, University of Bremen, Bremen, Germany). The loss of parts of the *THADA* coding sequence is proposed to play a major role in the pathogenesis of these lesions affecting the thyroid gland due to the truncation of the gene and its deduced protein sequence [3,15]. Rippe et al. (2003) proposed an involvement of THADA in a death receptor pathway and characterized the human *THADA*. The mRNA of *THADA* contains 6090 bp (ORF 5862 bp) and 38 exons and encodes a hypothetical protein of 1954 amino acids.

The UCSC genome browser on Dog May 2005 [16] assembly showed the canine *THADA* chromosomal location on CFA 10 at region 48,883,266 to 49,209,580 and the gene encompasses a sequence of 326,315 bp. The genome browser also described that the canine *THADA* region is highly conserved between the homologous gene locations of man, mouse and rat. Particularly the *THADA* region seems to be more evolutionarily conserved between man and dog than in rodents. In detail NCBI Blast analyses [17] were performed in order to show similarities between various mammalian and avian *THADA* nucleotide sequences from the NCBI databases. The similarities of the canine *THADA* [GenBank: EF222204] coding sequence (CDS) to the CDS of other species vary between human CDS [GenBank: NM_022065] 87%, mouse CDS 80% [GenBank: EF222207], rat predicted CDS 80% [GenBank XM_001060686.1] and chicken 69% [Genbank EF222206]. Respectively the similarities of the canine proposed THADA protein sequence to the deduced protein sequence of other species vary between human protein 83% [GenBank: NP_071348], mouse protein 75% [GenBank: ABQ10601], rat predicted protein 76% [XP_233829] and chicken protein 59% [GenBank: NP_001103529]. Also all deducted mammalian and avian THADA proposed protein sequence have in common one highly conserved domain termed COG5543 [CDD: 35102], the clusters of orthologous groups protein motif with yet unknown function, identified by the NCBI Conserved Domain Database (CDD) [18].

The mapping of *THADA* to canine chromosome 10 shows that the chromosomal region to which the canine *THADA* has been mapped is not a hotspot of chromosomal aberrations seen in canine thyroid adenomas. Previous case

reports of canine thyroid adenomas showed either a trisomy of chromosome 18 as a sole cytogenetic abnormality [19], or a rather complex karyotype of chromosomal fusions [20]. However, the available cytogenetic data of canine thyroid adenomas are still insufficient.

In 1999, reciprocal chromosome painting probes were established for a comparative chromosome map between human, red fox and dog showing the hybridisation pattern of canine probes onto human chromosomes [21,22]. Corresponding to the data obtained by the painting probes conserved syntheny exists between canine chromosome 10 and the human chromosomes 2, 12, and 22. Our mapping result obtained in this study is in accordance with the described homology of the canine and human chromosomes allowing a fine mapping of the *THADA* gene locus on canine chromosome 10q25 (Fig 1.) which corresponds to the 2p21 region of the p-arm of human chromosome 2.

Conclusion

In dogs malignant thyroid carcinomas occur more often than adenomas but interestingly no cytogenetic reports of canine thyroid carcinomas have been published until now (NCBI, Pubmed 2008). In order to elucidate whether canine *THADA* could be a candidate gene for a possible malignant transformation of canine thyroid adenomas further cytogenetic studies of the tumours could be of significant value.

Competing interests

The authors declare that they have no competing interests.

Authors' contributions

JTS and CB carried out the molecular genetic studies, established the PCR condition, performed the *in silico* analyses and drafted the manuscript, SW and ND carried out the FISH, SW and NRB determined the gene locus and performed the fine-mapping following the nomenclature of the canine karyotype, GD and CS screened the DogBAC library for a BAC clone containing gene of interest, HME, IN and JB conceived the study, participated in the experimental design and coordination, and helped to draft the manuscript. All authors read and approved the final manuscript.

References

1. Bartnitzke S, Herrmann ME, Lobeck H, Zuschneid W, Neuhaus P, Bullerdiek J: **Cytogenetic findings on eight follicular thyroid adenomas including one with a t(10;19).** *Cancer genetics and cytogenetics* 1989, **39(1):**65-68.
2. Belge G, Roque L, Soares J, Bruckmann S, Thode B, Fonseca E, Clode A, Bartnitzke S, Castedo S, Bullerdiek J: **Cytogenetic investigations of 340 thyroid hyperplasias and adenomas revealing correlations between cytogenetic findings and histology.** *Cancer Genet Cytogenet* 1998, **101(1):**42-48.
3. Rippe V, Drieschner N, Meiboom M, Murua Escobar H, Bonk U, Belge G, Bullerdiek J: **Identification of a gene rearranged by 2p21 aberrations in thyroid adenomas.** *Oncogene* 2003, **22(38):**6111-6114.
4. Khanna C, Hunter K: **Modeling metastasis in vivo.** *Carcinogenesis* 2005, **26(3):**513-523.
5. Hahn KA, Bravo L, Adams WH, Frazier DL: **Naturally occurring tumors in dogs as comparative models for cancer therapy research.** In *Vivo* 1994, **8(1):**133-143.
6. Ostrander EA, Galibert F, Patterson DF: **Canine genetics comes of age.** *Trends Genet* 2000, **16(3):**117-124.
7. Ostrander EA, Wayne RK: **The canine genome.** *Genome Res* 2005, **15(12):**1706-1716.
8. Pacini F, Schlumberger M, Dralle H, Elisei R, Smit JW, Wiersinga W: **European consensus for the management of patients with differentiated thyroid carcinoma of the follicular epithelium.** *European journal of endocrinology / European Federation of Endocrine Societies* 2006, **154(6):**787-803.
9. Harari J, Patterson JS, Rosenthal RC: **Clinical and pathologic features of thyroid tumors in 26 dogs.** *Journal of the American Veterinary Medical Association* 1986, **188(10):**1160-1164.
10. Klein MK, Powers BE, Withrow SJ, Curtis CR, Straw RC, Ogilvie GK, Dickinson KL, Cooper MF, Baier M: **Treatment of thyroid carcinoma in dogs by surgical resection alone: 20 cases (1981-1989).** *Journal of the American Veterinary Medical Association* 1995, **206(7):**1007-1009.
11. Ramos-Vara JA, Miller MA, Johnson GC, Pace LW: **Immunohistochemical detection of thyroid transcription factor-1, thyroglobulin, and calcitonin in canine normal, hyperplastic, and neoplastic thyroid gland.** *Vet Pathol* 2002, **39(4):**480-487.
12. Schelling C, Schläpfer J, Billaut A, Guziewicz K, Gmür A, Katmann I, Pineroli B, Colomb B, Rickli O, Wittwer C, Piasecka A, Dolf G: **Construction of a canine artificial chromosome library for screening with PCR.** *Journal of Animal Breeding and Genetics* 2002, **119(6):**400-401.
13. Reimann N, Bartnitzke S, Bullerdiek J, Schmitz U, Rogalla P, Nolte I, Ronne M: **An extended nomenclature of the canine karyotype.** *Cytogenet Cell Genet* 1996, **73(1-2):**140-144.
14. Bol S, Belge G, Rippe V, Bullerdiek J: **Molecular cytogenetic investigations define a subgroup of thyroid adenomas with 2p21 breakpoints clustered to a region of less than 450 kb.** *Cytogenet Cell Genet* 2001, **95(3-4):**189-191.
15. Drieschner N, Belge G, Rippe V, Meiboom M, Loeschke S, Bullerdiek J: **Evidence for a 3p25 breakpoint hot spot region in thyroid tumors of follicular origin.** *Thyroid* 2006, **16(11):**1091-1096.
16. **Dog (Canis familiaris) Genome Browser Gateway** [http://genome.ucsc.edu/cgi-bin/hgGateway]
17. **Basic Local Alignment Search Tool** [http://www.ncbi.nlm.nih.gov/blast/Blast.cgi]
18. **NCBI Conserved Domain Database** [http://www.ncbi.nlm.nih.gov/Structure/cdd/cdd.shtml]
19. Reimann N, Nolte I, Bonk U, Werner M, Bullerdiek J, Bartnitzke S: **Trisomy 18 in a canine thyroid adenoma.** *Cancer Genet Cytogenet* 1996, **90(2):**154-156.
20. Mayr B, Schleger W, Loupal G, Burtscher H: **Characterisation of complex karyotype changes in a canine thyroid adenoma.** *Research in veterinary science* 1991, **50(3):**298-300.
21. Breen M, Thomas R, Binns MM, Carter NP, Langford CF: **Reciprocal chromosome painting reveals detailed regions of conserved synteny between the karyotypes of the domestic dog (Canis familiaris) and human.** *Genomics* 1999, **61(2):**145-155.
22. Yang F, O'Brien PC, Milne BS, Graphodatsky AS, Solanky N, Trifonov V, Rens W, Sargan D, Ferguson-Smith MA: **A complete comparative chromosome map for the dog, red fox, and human and its integration with canine genetic maps.** *Genomics* 1999, **62(2):**189-202.

3.3 Molekulargenetische Charakterisierung der 19q13.4-Bruchpunktregion bei benignen follikulären Läsionen der Schilddrüse

V. Delineation of a 150-kb breakpoint cluster in benign thyroid tumors with 19q13.4 aberrations (Belge *et al.*, 2001)

Obwohl in früheren Arbeiten der Bruchpunktbereich bei benignen Läsionen der Schilddrüse mit 19q13.4-Rearrangierungen auf eine Region von 400 kb eingegrenzt (Belge *et al.*, 1995; Belge *et al.*, 1997) und ein Kandidatengen (*ZNF331*) in der Nähe dieses Bruchpunktbereiches identifiziert und charakterisiert werden konnte (Rippe *et al.*, 1999), sollte eine weitere Analyse des Bruchpunktbereiches erfolgen, da die bisherigen Daten ausschließlich auf Untersuchungen zweier Zelllinien (S40.2/TSV40 und S121/TSV40) mit entsprechenden chromosomalen Veränderungen der Region 19q13.4 beruhen. Hierzu wurden weiterführende molekularzytogenetische Untersuchungen unter Verwendung zusätzlicher BAC- und PAC-Klone an den beiden Zelllinien sowie vier Primärtumoren durchgeführt. Dabei konnten die Bruchpunkte auf eine Region von 150 kb weiter eingegrenzt werden, wobei in den beiden Zelllinien S40.2/TSV40 und S121/TSV40 die Bruchpunkte jeweils innerhalb der Klone BAC 41372 und PAC 13174 lokalisiert sind, wohingegen die Bruchpunkte bei den Primärtumoren S141.2, S172, S476.2 und S532.1 vom Klon BAC 280723 überspannt werden. Unter Erstellung eines 470 kb Contigs, der aus vier BAC-Klonen, einem PAC-Klon und vier Cosmid-Klonen besteht und in dem 10 neue Sequence Tagged Sites (STS)-Marker lokalisiert wurden, war es möglich, die genaue genomische Lokalisation des Bruchpunktclusters sowie die transkriptionelle Orientierung und Lage von *ZNF331* zum Bruchpunktcluster zu bestimmen. Neben der Identifizierung möglicher 3‘-regulatorischer Elemente von *ZNF331* im Bruchpunktcluster ist auch die Identifizierung anderer Gene innerhalb bzw. in der Nähe des 150 kb-Bruchpunktclusters von Bedeutung.

V

Delineation of a 150-kb breakpoint cluster in benign thyroid tumors with 19q13.4 aberrations

G. Belge, V. Rippe, M. Meiboom, N. Drieschner, E. Garcia, J. Bullerdiek

(Cytogenetic and Cell Genetics 93(1-2): 48-51)

Eigenanteil:

- Durchführung und Auswertung der molekularzytogenetischen Untersuchungen
- Präparation der für die molekularzytogenetischen Untersuchungen verwendeten DNA-Sonden.

Gene Mapping, Cloning and Sequencing

Cytogenet Cell Genet 93:48–51 (2001)

Cytogenetics and Cell Genetics

Delineation of a 150-kb breakpoint cluster in benign thyroid tumors with 19q13.4 aberrations

G. Belge,[a] V. Rippe,[a] M. Meiboom,[a] N. Drieschner,[a] E. Garcia,[b] and J. Bullerdiek[a]

[a] Center for Human Genetics and Genetic Counseling, University of Bremen, Bremen (Germany);
[b] Lawrence Livermore National Laboratory, Livermore, California (USA)

Abstract. Structural rearrangements involving the long arm of chromosome 19 characterize a cytogenetic subgroup of benign thyroid tumors and constitute one of the most frequent specific chromosome abnormalities in epithelial tumors. Recently, we have been able to narrow down the breakpoint region affected in two cell lines to a region covered by a single PAC clone. Close to that region a candidate gene has been identified which we tentatively referred to as RITA (Rearranged In Thyroid Adenomas) now named ZNF331 according to HUGO nomenclature. However, the results had been obtained on two cell lines only making it necessary to extend the studies to a larger number of tumors including primary material. Herein, we have used four further primary tumors showing translocations involving 19q13 for fluorescence in situ hybridization (FISH) mapping studies using a variety of molecular probes from a 470-kbp cosmid/BAC contig. Ten new STSs were characterized and physically mapped within an *Eco*RI restriction map. The results enabled us to define an approximately 150-kbp breakpoint cluster region of the 19q13 aberrations in benign thyroid tumors flanked by two newly established STS markers.

Chromosome aberrations involving 19q13 first described 10 years ago (Bartnitzke et al., 1989) are the most frequent structural alterations in follicular thyroid adenomas and hyperplasias (Belge et al., 1998). Recently, we have been able to narrow down the breakpoints of several primary tumors and cell lines derived from thyroid tumors and hyperplasias with 19q13 translocations to a region of about 400 kbp between the two cosmid clones 30316 and 20019 (Belge et al., 1995; 1997). Further analyses allowed us to establish the cDNA sequence and the genomic structure of a candidate gene which we tentatively referred to as RITA (Rearranged In Thyroid Adenomas) now named ZNF331 according to HUGO nomenclature. Nevertheless, the identification of that candidate gene so far is based on the results obtained from only two cell lines not allowing for a clear delineation of the breakpoint region. Thus, further studies on primary tumors would be helpful to characterize in depth these very frequent chromosome aberrations in human tumors. We have therefore extended our studies to the molecular cytogenetic analysis of the 19q13 breakpoints observed in four primary benign thyroid tumors.

Material and methods

For cell culturing and chromosome analyses, a method previously described for pleomorphic adenomas of the parotid gland (Bullerdiek et al., 1987) was used. Karyotypes were described according to ISCN (1995).

The cell lines were obtained by transfection with a construct containing the SV40 "early region" as reported previously (Kazmierczak et al., 1990; Belge et al., 1992). Four primary tumors were used for FISH studies and compared to the results obtained on the two previously reported SV40-transformed cell lines with 19q13 aberrations (Rippe et al., 1999). Karyotype descriptions of the tumors are summarized in Table 1.

Supported by the Deutsche Forschungsgemeinschaft by grant BE 1942/1-3. G.B. and V.R. contributed equally to this paper and should thus both be considered first authors.

Received 21 December 1999; revision accepted 6 February 2001.

Request reprints from Dr. J. Bullerdiek, Center for Human Genetics, University of Bremen, Leobenerstrasse ZHG, D–28359 Bremen (Germany); telephone: +49 421 218 4239; fax: +49 421 218 4239; email: bullerd@uni-bremen.de

KARGER

Fax + 41 61 306 12 34
E-mail karger@karger.ch
www.karger.com

0301–0171/01/0932–0048$17.50/0

Accessible online at:
www.karger.com/journals/ccg

To map the breakpoints we used PAC clone 13174 (Genome Systems, USA), a PAC clone previously described in detail (Rippe et al., 1999), cosmid clones 15841 and 29573, and the BAC clones 41372, 280723, and 829651 identified according to the Livermore National Laboratory nomenclature (LLNL) (Ashworth et al., 1995). The cosmid clones were derived from the human chromosome 19 flow-sorted library prepared at LLNL (de Jong et al., 1989; Trask et al., 1992; Ashworth et al., 1995). The BAC clones were derived from the human library CIT-HSPC and isolated at LLNL. Cosmid/BAC fragments were *Eco*RI-digested, separated in a 0.8 % agarose gel, cut out, purified from gel slices by glass bead techniques (QIAExII, QIAGEN, Hilden, Germany) and cloned in the pGEM11zf(+) vector (Promega, Madison, WI). The plasmid, cosmid, PAC and BAC DNA were isolated using a standard alkaline lysis protocol and purified by anion-exchange columns (QIAGEN, Hilden, Germany). DNA digestions were performed following the standard procedures according to the manufacturers (Sambrook et al., 1989). Sequencing was performed on a 373 DNA sequencer (Applied Biosystem, Weiterstadt, Germany) using standard and internal primers. To map the new STSs, cosmids, PACs and BACs, DNA was digested with *Eco*RI, *Bam*HI and *Hin*dIII, respectively, separated on a 0.8 % agarose gel, and transferred onto a Hybond-N^+ nylon membrane (Amersham Pharmacia, Freiburg, Germany). PCR-amplified STS or plasmid DNAs were labeled by random primed incorporation of DIG-dUTP (Roche, Mannheim, Germany) and used as molecular probes. For both prehybridization and hybridization the ExpressHyb hybridization solution (Clontech Laboratories, Palo Alto, USA) was used. Probes were detected by chemiluminescence (Roche, Mannheim, Germany). Polymerase chain reaction was performed using primers and annealing temperatures reported in Table 2. PCR analyses were carried out following standard procedures in a final volume of 50 µl. About 60 ng template was amplified in a standard PCR reaction with 400 nM of each primer, 300 µM dNTPs, 1 × PCR buffer (containing 1.5 mM $MgCl_2$) and 2.5 U AmpliTaq (Perkin Elmer Applied Biosystems, Weiterstadt, Germany). PCR products were separated in a 1.5 % agarose gel, cut out, purified from gel slices by glass bead techniques (QIAExII, QIAGEN, Hilden, Germany), and cloned into the pCR2.1 vector (Invitrogen, San Diego, CA).

Table 1. Location of the DNA probes (cosmid, PAC, BAC) used for the FISH studies on four benign primary thyroid tumors and two SV40-transformed cell lines derived from benign thyroid tumors all showing aberrations affecting 19q13.

Tumor no	DNA probes	Translocation	Location of FISH signals relative to the breakpoint
S141.2	c15841	t(2;19)(p12;q13)	proximal
	c29573		proximal
	BAC 41372		proximal
	BAC 280723		across
	BAC 829651		distal
	PAC 13174		proximal
S172	c29573	t(2;19)(p12;q13)	proximal
	BAC 41372		proximal
	BAC 280723		across
	BAC 829651		distal
	PAC 13174		proximal
S476.1	c29573	t(5;19)(q13;q13)	proximal
	BAC 41372		proximal
	BAC 280723		across
	BAC 829651		distal
	PAC 13174		proximal
S121/SV40	c15841[a]	t(5;19)(q13;q13)	proximal
	c29573[a]		distal
	BAC 41372		across
	BAC 280723		distal
	PAC 13174[a]		across
S40.2/SV40	c15841[a]	t(1;19)(p35→36.1;q13)	proximal
	c29573[a]		distal
	BAC 41372		across
	BAC 280723		distal
	PAC 13174[a]		across
S532.1	BAC 280723	t(14;19)(q22;q13)	across

[a] FISH results obtained from a previously described study (Rippe et al., 1999).

Fluorescence in situ hybridization (FISH) analyses were performed after GTG banding of the same metaphase spreads. Treatment of metaphases and subsequent FISH experiments were performed using the protocol of Kievits et al. (1990). Cosmid, PAC and BAC DNAs were labeled with biotin-14-dATP by nick translation (Gibco BRL, Life Technologies GmbH, Eggenstein, Germany). For every cosmid, PAC or BAC probe 20 metaphases were examined except for case S532.1 where only two metaphases were scored. Chromosomes were counterstained with propidium iodide, analyzed on a Zeiss Axiophot fluorescence microscope using an FITC filter (Zeiss, Oberkochem, Germany) and recorded with the Power Gene Karyotyping System (PSI, Halladale, U.K.).

Total RNA was isolated from the two cell lines and non-neoplastic adult thyroid tissue and fibroblasts using TRIzol reagent (Gibco BRL, Life Technologies GmbH, Eggenstein, Germany) based on the single-step acid-phenol RNA isolation method (Chomczynski and Sacchi, 1987). Poly(A)$^+$ RNAs were purified by Oligotex $dC_{10}T_{30}$ adsorption (QIAGEN, Hilden, Germany). Approximately 5 µg of poly(A)$^+$ RNAs were denatured and fractionated on a 1 % agarose, 6 % formaldehyde gel, and transferred onto a Hybond-N^+ nylon membrane (Amersham Pharmacia, Freiburg, Germany). As a molecular probe we used a partial cDNA clone (bp 17–1108) of ZNF331. The probe was labeled with ^{32}P using a random primer extension protocol (Feinberg and Vogelstein, 1983). For both prehybridization and hybridization the ExpressHyb hybridization solution (Clontech Laboratories, Palo Alto, USA) was used. Prehybridization was carried out for 30 min and hybridization for 1 h at 68 °C. The membranes were washed twice for 20 min at room temperature in 2 × SSC, 0.05 % SDS, and twice for 20 min at 68 °C in 0.1 × SSC, 0.1 % SDS. Signals were visualized by using a STORM imager (Molecular Dynamics, Sunnyvale, USA).

Table 2. Primers for PCR amplification of STS markers which were physically mapped

Marker	GenBank Acc No	Forward primer	Reverse primer	Product (bp)
RSTS1	G64894	TCCTGGCTCATAATTCCATAACCCTTGGT	GTGCGCCACCTTTTCAGAGTTCTTTTGT	423
RSTS2	G64900	TTATGCCTGATTCAGTGACACTACTTTTTC	CGGCTGCCTCTAACATACGGAAGATTC	397
RSTS3	G64895	GAGGCTGACGCGGCGGCTCTATCTC	AGCGGTTGCGTCACCGGTGCAGAAG	113
RSTS4	AF260531	ATATACGTGTATCAGTTTCAGAATGC	TATTTTAAAGTCAGACATGAAAAAGG	188
RSTS5	AF260970	GGGCCAGGAAAATGCACGGAAGTGAAG	CCCGGGCTTGTGGAATTAACTGAGCAG	360
RSTS6	G64896	TTATGTGGGCCCCAAACCATTACTGATACTC	CTCATGCCCATAAACCCCTAAATTCCTTGT	385
RSTS7	G64897	GCCTGCTAAGCCTCTGTGCCTAGTAAAG	GGTATCAGAAAGGTACAATCCCTATGTCTC	189
RSTS8	G64901	CCCAAAAGATCCCAAGTCCAGGCAGAAAG	CCTGGGAAGCTCACAAGGGTGGAAGAC	397
RSTS9	G64898	GTACATTGGCATCCGCAGGGGTAAC	CCTCTCAAGGCGTGCTTTTTCGTAAGA	406
RSTS10	G64899	AGCCCGCTCGTATCTATGG	TGAGGACTACTTGGGCACAGG	301

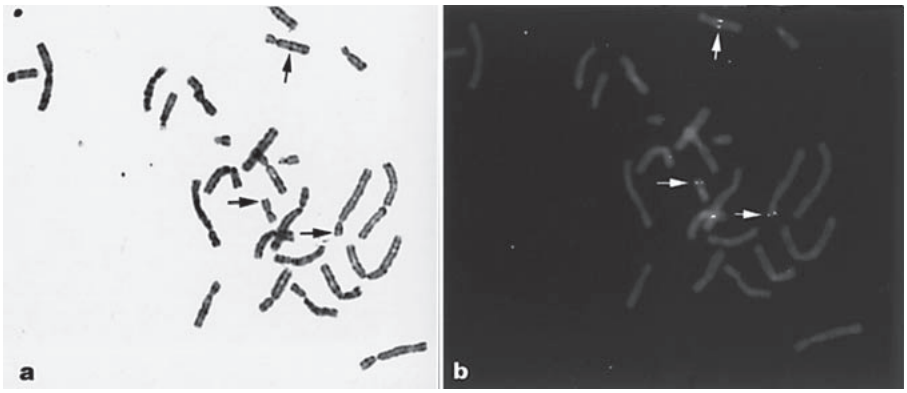

Fig. 1 . (**a**) Metaphase of the cell line S141.2 with t(2;19)(p12;q13) after G-banding; the chromosomes 19, der(19), and der(2) are marked (arrows). (**b**) The same metaphase after FISH with the BAC clone 280723; the hybridization signals are located on chromosome 19, der(19), and der(2) (arrows).

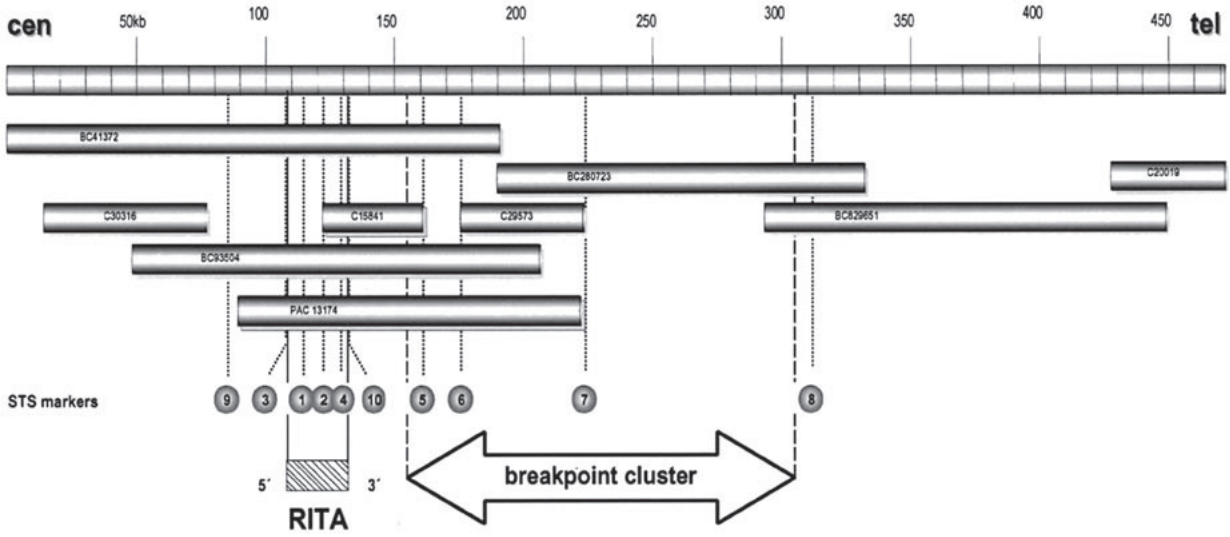

Fig. 2. Schematic representation of the breakpoint cluster region in benign thyroid tumors with 19q13 aberrations. The FISH mapping data obtained for the six tumors tested in this study show that the breakpoints of the benign thyroid tumors with 19q13 translocations map in a region of about 150 kb 3′ of RITA (ZNF331). The cosmid, BAC, and PAC clones are in accordance with the chromosome 19-physical map of Lawrence Livermore National Laboratory. Circled numbers refer to newly established STS markers RSTS1–RSTS10 (for comparison see Table 2).

Results

FISH studies were performed on four primary thyroid tumors with 19q13 aberrations. The results of the FISH experiments revealed that in all newly investigated tumors (S476.1, S141.2, S172, S532.1) the breakpoints map within a region covered by a single BAC clone, i.e. 280723. With this BAC clone hybridization signals were obtained on the normal chromosome 19 and on both derivative chromosomes (Fig. 1, Table 1). In contrast, further FISH studies with cosmids 15841 and 29573, PAC 13174 and BAC 41372 on cells of these tumors showed hybridization signals proximal to the breakpoint, whereas BAC 829651 showed signals distal to the breakpoint. As for the two cell lines previously described (Rippe et al., 1999) FISH results obtained with the cosmid and BAC clones are also given in Table 1.

The results of these FISH analyses revealed that the breakpoint of chromosome 19 in all tumors investigated mapped within a segment of about 150 kbp close to the 3′ region of ZNF331 between the cosmid clone 15841 and BAC clone 829651 (Fig. 2).

Based on an assembled contig (for details of restriction maps see http://www-bio.llnl.gov/rmap/) four BACs, one PAC and four cosmids were finally retained for further characterization and were assembled in an *Eco*RI and STS content based contig shown in Fig. 2. Ten new STSs were generated from sequence data obtained either from plasmid/cosmid clone insert-end or cosmid, PAC or BAC internal sequencing. Oligo-

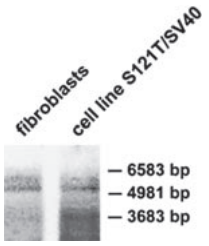

Fig. 3. Results of Northern blot hybridization on RNA isolated from the thyroid adenoma cell line S121/SV40 and fibroblasts using a 1,092-bp cDNA probe from exon 1 to exon 5. The 5.5-kb and 6.2-kb transcripts were found in the fibroblasts and adenoma cell line.

nucleotide sequences for these PCR assays as well as the size of the product generated from template are presented in Table 2. The contig spans 470 kb in length and most of the newly defined STS markers are located within ZNF331 or the breakpoint cluster, respectively. The analyses of these sequence data and comparison with the chromosome 19 *Eco*RI restriction maps of LLNL enabled us to revise the transcriptional orientation of ZNF331 (Fig. 2).

Northern blot analyses were performed using RNA isolated from the cell lines S121/SV40, S325/SV40, normal thyroid tissue, and fibroblasts from a healthy normal donor. Whereas the 5.5-kb and 6.2-kb transcripts were found in the fibroblasts and adenoma cell line (Fig. 3) the normal thyroid tissue (data not shown) revealed 4.7 kb and 5 kb transcripts akin to those previously described in many other human tissues (Rippe et al., 1999).

Discussion

Interestingly, so far specific chromosome translocations have been described in many more leukemias, lymphomas, and soft tissue tumors than in epithelial neoplasms. Consequently, the number of genes found to be affected by the latter aberrations is still low. Certainly, 19q13 translocations constitute one of the most frequent types of specific chromosomal translocations in human epithelial tumors (Mitelman, 1998). In an attempt to elucidate the molecular background of these rearrangements we were recently able to map the breakpoint of two cell lines derived from thyroid tumors showing t(1;19)(p35 → 36.1;q13) and t(5;19)(q13;q13) between the two cosmids 15841 and 29573 in a region of approximately 25 kbp. Sequence analysis of PAC clone 13174 crossing the breakpoint region led us to identify ZNF331, a KRAB zinc finger protein encoding gene, as a possible candidate gene affected by the 19q13 rearrangements in thyroid hyperplasias and neoplasias. Now we have established a 470-kbp BAC, PAC and cosmid contig by physical STS mapping and mapped the breakpoints of four primary thyroid tumors with chromosome changes in 19q13. The results indicate that all breakpoints map within a narrow region of about 150 kbp including the previously identified breakpoint region. The results revealed by these additional FISH experiments offer further evidence that ZNF331 is a likely candidate gene for the 19q13 aberrations and implicate a clustering of breakpoints 3′ of ZNF331. The transcripts detected in a cell line with the typical 19q13 translocation did not differ from those in cell cultures derived from normal fibroblasts and thus most likely indicates no more than the expression pattern of ZNF331 in rapidly dividing cells. Future studies will be aimed at possible 3′ regulatory elements of ZNF331 located within the breakpoint cluster region identified herein but will also address the identification of other genes within or close to that region.

References

Ashworth LK, Batzer MA, Brandriff B, Brandscomp E, de Jong P, Garcia E, Garnes JA, Gordon LA, Lamardin JE, Lennon G, Mohrenweiser H, Olsen AS, Slezak T, Carrano AV: An integrated metric physical map of human chromosome 19. Nature Genet 11:422–427 (1995).

Bartnitzke S, Hermann ME, Lobeck H, Zuschneid W, Neuhaus P, Bullerdiek J: Cytogenetic findings on eight follicular thyroid adenomas including one with a t(10;19). Cancer Genet Cytogenet 39:65–68 (1989).

Belge G, Kazmierczak B, Meyer-Bolte K, Bartnitzke S, Bullerdiek J: Expression of SV40 T-antigen in lipoma with a chromosomal translocation t(3;12) is not sufficient for direct immortalization. Cell Biol Int Rep 16:339–347 (1992).

Belge G, de Jong P, Bartnitzke S, Bullerdiek J: FISH analyses of a newly established thyroid tumor cell line showing a t(1;19)(p35 or p36.1;q13) reveal that the breakpoint lies between 19q13.3 → q13.4 and 19q13.4. Cytogenet Cell Genet 69:220–222 (1995).

Belge G, Garcia E, Rippe V, Fusco A, Bartnitzke S, Bullerdiek J: Breakpoints of 19q13 translocations of benign thyroid tumors map within a 400 kilobase region. Genes Chrom Cancer 20:201–203 (1997).

Belge G, Roque L, Soares J, Bruckmann S, Thode B, Fonseca E, Clode A, Bartnitzke S, Castedo S, Bullerdiek J: Cytogenetic investigations of 340 thyroid hyperplasias and adenomas revealing correlations between cytogenetic findings and histology. Cancer Genet Cytogenet 101:42–48 (1998).

Bullerdiek J, Böschen C, Bartnitzke S: Aberrations of chromosome 8 in mixed salivary gland tumors: cytogenetic findings on seven cases. Cancer Genet Cytogenet 24:205–212 (1987).

Chomczynski P, Sacchi N: Single-step method of RNA isolation by acid guanidinium thiocyanate-phenol-chloroform extraction. Anal Biochem 162:156–159 (1987).

de Jong PJ, Yokabata K, Chen C, Lohman F, Pederson L, McNinch J, van Dilla M: Human chromosome-specific partial digest libraries in lambda and cosmid vectors. Cytogenet Cell Genet 51:985 (1985).

Feinberg AP, Vogelstein B: A technique for radiolabeling DNA restriction endonuclease fragments to high specific activity. Anal Biochem 132:6–13 (1983).

ISCN (1995): An International System for Cytogenetic Nomenclature. Mitelman F (ed) (S Karger, Basel 1995).

Kazmierczak B, Bartnitzke S, Hartl M, Bullerdiek J: In vitro transformation by the SV 40 "early region" of cells from a human benign salivary gland tumor with a 12q13 → q15 rearrangement. Cytogenet Cell Genet 53:37–39 (1990).

Kievits T, Dauwerse JG, Wiegant J, Devilee P, Breuning MH, Cornelisse CJ, van Ommen GJB, Pearson PL: Rapid subchromosomal localization of cosmids by nonradioactive in situ hybridization. Cytogenet Cell Genet 53:134–136 (1990).

Mitelman F: Catalog of chromosome aberrations in cancer [catalog on CD-ROM, producers version 1]. (Wiley-Liss, New York 1998).

Rippe V, Belge G, Meiboom M, Kazmierczak B, Fusco A, Bullerdiek J: A KRAB zinc finger protein gene is the potential target of 19q13 translocation in benign thyroid tumors. Genes Chrom Cancer 26: 299–336 (1999).

Sambrook J, Fritsch EF, Maniatis T: Molecular Cloning: A laboratory manual, 2nd ed. (Cold Spring Harbor Laboratory Press, Cold Spring Harbor 1989).

Trask B, Christensen M, Fertitta A, Bergmann A, Ashworth L, Branscomp E, Carrano A, Van den Engh G: Fluorescence in situ hybridization mapping of human chromosome 19: Mapping and verification of cosmid contigs formed by random restriction enzyme fingerprinting. Genomics 14:162–167 (1992).

VI. The two stem cell microRNA gene clusters C19MC and miR-371-3 are activated by specific chromosomal rearrangements in a subgroup of thyroid adenomas (Rippe *et al.*, 2010)

Neuere Untersuchungen zeigten, dass sich in der Region 19q13.4 der bisher größte menschliche miRNA-Cluster C19MC befindet (Bentwich *et al.*, 2005). Dieser umfasst ca. 100 kb mit 46 primaten-spezifischen miRNA-Genen und liegt zu einem Großteil innerhalb des 19q13.4-Bruchpunktclusters. Zudem befindet sich ein weiterer wesentlich kleinerer miRNA-Cluster miR-371-3 in Telomerrichtung außerhalb des Bruchpunktclusters (Suh *et al.*, 2004). Um einen möglichen Einfluss der 19q13.4-Rearrangierungen auf die Expression von miRNAs beider Cluster zu bestimmen, erfolgten RT-PCR-Analysen ausgewählter miRNAs (miR-512-5p, miR-517a und miR-519a) sowie eine quantitative Real Time-PCR (qRT-PCR) von miR-520c aus dem Cluster C19MC an fünf Zelllinien mit und drei Zelllinien ohne 19q13.4-Rearrangierungen. Mit Ausnahme der Zelllinie S121/TSV40 mit einer Translokation t(5;19)(q13;q13) wiesen alle Zelllinien mit 19q13.4-Rearrangierungen eine Expression der getesteten miRNAs auf, wohingegen in den Zelllinien ohne 19q13.4-Rearrangierungen keine oder nur eine geringe Expression messbar war. Für S121/TSV40 wird angenommen, dass die geringe Expression auf Deletionen im Bruchpunktcluster bedingt durch die chromosomale Rearrangierung zurückzuführen ist.

Ein entsprechendes Ergebnis zeigte sich an Primärmaterial von benignen Schilddrüsenläsionen. Hierzu erfolgte die Auswahl von Tumoren mit 19q13.4-Rearrangierungen mittels I-FISH an Touch-Präparaten von 70 benignen Schilddrüsenläsionen unter Verwendung der Dual-Color, Break-Apart Sonde Thyroid Breakpoint Cluster 19 (TBPC19). Insgesamt konnten fünf Tumoren mit 19q13.4-Rearrangierungen erfasst werden. Diese zeigten ebenfalls eine erhöhte Expression der o.g. miRNAs im Vergleich zu fünf Adenomen sowie zu drei Proben aus umliegendem Normalgewebe, die keine 19q13.4-Rearrangierungen aufwiesen.

Für den Cluster miR-371-3 konnte an denselben Zelllinien sowie Primärtumoren und Normalgeweben gleichfalls eine differente Expression der miRNAs miR371-3p, miR-372 und miR-373 festgestellt werden. Hierbei zeigte sich eine erhöhte Expression auch in der Zelllinie S121/TSV40, was die Annahme stützt, dass die geringe Expression von miRNAs des Clusters

C19MC in dieser Zelllinie auf Deletionen in diesem Cluster bedingt durch die 19q13.4-Rearrangierungen zurückzuführen ist.

An einer ausgewählten Zelllinie S40.2/TSV40 mit einer Translokation t(1;19)(p35.2;q13.4) erfolgte eine Bruchpunktkartierung für die Region 1p35.2 mit dem Ziel, die zugrundeliegenden Mechanismen der Aktivierung beider miRNA-Cluster zu erfassen. Dazu wurde der Bruchpunkt mittels FISH-Analysen unter Verwendung von BAC-Klonen innerhalb des Introns 10 des *Pumilio Homolog 1* (*PUM1*)-Gens in der Region 1p35.2 lokalisiert. Zudem konnte gezeigt werden, dass entsprechend die Exons 1 – 10 im Zuge der Translokation vor beiden miRNA-Clustern lokalisiert sind.

Mittels 3‘-RACE-PCR und RT-PCR wurden daraufhin in S40.2/TSV40 Fusionstranskripte nachgewiesen (*PUM1-FUS-19q-I* und *PUM-FUS-19q-II*), die neben den Exons 1 – 10 von *PUM1* zudem Sequenzen aus der 19q13.4-Bruchpunktregion enthielten. Aufgrund dessen wird angenommen, dass beide Cluster, C19MC und miR-371-3, in der Zelllinie S40.2/TSV40 durch die Translokation t(1;19)(p35.2;q13.4) Bestandteil eines Polymerase-II Transkripts sind, dessen Expression vom Promotor des an der Translokation beteiligtem *PUM1* ausgeht.

VI

The two stem cell microRNA gene clusters C19MC and miR-371-3 are activated by specific chromosomal rearrangements in a subgroup of thyroid adenomas

Volkhard Rippe, Lea Dittberner, Verena N. Lorenz, Norbert Drieschner, Rolf Nimzyk, Wolfgang Sendt, Klaus Junker, Gazanfer Belge, Jörn Bullerdiek

(PLoS ONE 5(3): e9485)

Eigenanteil:

- Durchführung und Auswertung der molekularzytogenetischen Untersuchungen.

OPEN ACCESS Freely available online

PLoS one

The Two Stem Cell MicroRNA Gene Clusters C19MC and miR-371-3 Are Activated by Specific Chromosomal Rearrangements in a Subgroup of Thyroid Adenomas

Volkhard Rippe[1], Lea Dittberner[1], Verena N. Lorenz[1], Norbert Drieschner[1], Rolf Nimzyk[1], Wolfgang Sendt[2], Klaus Junker[3], Gazanfer Belge[1], Jörn Bullerdiek[1,4]*

1 Center for Human Genetics, University of Bremen, Bremen, Germany, **2** Department of General and Visceral Surgery, St. Joseph Stift, Bremen, Germany, **3** Department of Pathology, Hospital Bremen-Mitte, Bremen, Germany, **4** Small Animal Clinic and Research Cluster of Excellence "REBIRTH", University of Veterinary Medicine, Hanover, Germany

Abstract

Thyroid adenomas are common benign human tumors with a high prevalence of about 5% of the adult population even in iodine sufficient areas. Rearrangements of chromosomal band 19q13.4 represent a frequent clonal cytogenetic deviation in these tumors making them the most frequent non-random chromosomal translocations in human epithelial tumors at all. Two microRNA (miRNA) gene clusters i.e. C19MC and miR-371-3 are located in close proximity to the breakpoint region of these chromosomal rearrangements and have been checked for a possible up-regulation due to the genomic alteration. In 4/5 cell lines established from thyroid adenomas with 19q13.4 rearrangements and 5/5 primary adenomas with that type of rearrangement both the C19MC and miR-371-3 cluster were found to be significantly overexpressed compared to controls lacking that particular chromosome abnormality. In the remaining cell line qRT-PCR revealed overexpression of members of the miR-371-3 cluster only which might be due to a deletion accompanying the chromosomal rearrangement in that case. In depth molecular characterization of the breakpoint in a cell line from one adenoma of this type reveals the existence of large Pol-II mRNA fragments as the most likely source of up-regulation of the C19MC cluster. The up-regulation of the clusters is likely to be causally associated with the pathogenesis of the corresponding tumors. Of note, the expression of miRNAs miR-520c and miR-373 is known to characterize stem cells and in terms of molecular oncology has been implicated in invasive growth of epithelial cells in vitro and in vivo thus allowing to delineate a distinct molecular subtype of thyroid adenomas. Besides thyroid adenomas rearrangements of 19q13.4 are frequently found in other human neoplasias as well, suggesting that activation of both clusters might be a more general phenomenon in human neoplasias.

Citation: Rippe V, Dittberner L, Lorenz VN, Drieschner N, Nimzyk R, et al. (2010) The Two Stem Cell MicroRNA Gene Clusters C19MC and miR-371-3 Are Activated by Specific Chromosomal Rearrangements in a Subgroup of Thyroid Adenomas. PLoS ONE 5(3): e9485. doi:10.1371/journal.pone.0009485

Editor: Alfons Navarro, University of Barcelona, Spain

Received August 11, 2009; **Accepted** February 3, 2010; **Published** March 3, 2010

Funding: The work was supported by the University of Bremen. The funders had no role in study design, data collection and analysis, decision to publish, or preparation of the manuscript.

Competing Interests: The authors declare competing financial interests because of a patent application claiming the expression level of the miRNA miR371–373 and miR C19MC clusters for the diagnosis of thyroid tumors (EP 09011141.0, applicant: University of Bremen).

* E-mail: bullerd@uni-bremen.de

Introduction

Thyroid adenomas are highly frequent human tumors that can be distinguished from their malignant counterparts i.e. follicular carcinomas by an encapsulated growth and a lack of invasiveness, respectively. Even in iodine sufficient areas thyroid adenomas occur in 4–7% of adults and in iodine deficient areas this number can rise to about 50%. The pathogenesis of these frequent benign tumors is only poorly understood but clonal chromosomal aberrations can be observed in roughly 40% of the nodules and are likely to pinpoint genomic regions and genes relevant for the development of the disease [1]. About 20% of the tumors with clonal cytogenetic aberrations show abnormalities involving chromosomal band 19q13 [2]. Given the extremely high prevalence of thyroid adenomas in Europe and the U.S. alone four to five million people can be estimated to be affected by this genomic alteration in their thyroid. So far, by positional cloning and *in silico* analyses the breakpoints have been found to cluster within a segment of 150 kb (kilobases) [3] that is located in close proximity to the genes encoding two miRNA clusters i.e. C19MC and miR-371-3 (Figure 1). The 100 kb long C19MC cluster with 46 tandemly repeated, primate-specific miRNA genes accounts for about 8% of all known human miRNA genes making it the largest human miRNA gene cluster discovered to date [4]. Ren et al. [5] have predicted 4,691 targets for this cluster. Recent evidence suggests that its miRNAs are encoded by an intron of a non-protein coding Pol-II transcript which is mainly expressed in the placenta [4]. In contrast to that large cluster the miR-371-3 cluster is much smaller spanning a region of approximately 1,050 bp where five miRNAs are encoded. The miRNAs of both clusters belong to a large miRNA family sharing a similar seed sequence [6]. Of note, several groups recently have linked the expression of members of the C19MC as well as the miR-371-3 cluster with the miRNA signature characteristic for human embryonic stem cells (hESC) [5,6,7]. First evidence for an oncogenic potential of miR-373 has been obtained in human testicular germ cell tumors where it was shown to allow tumorigenic growth in the presence of wild-type p53 [8]. In prostate cancer both miR-373 and miR-520c

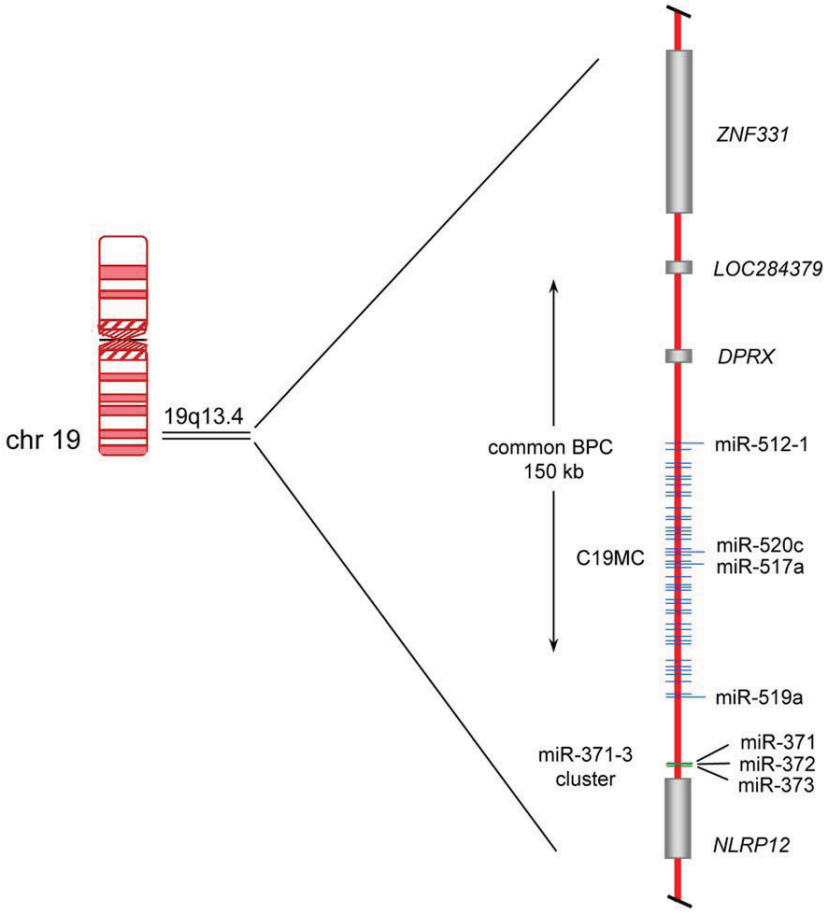

Figure 1. Scheme of the chromosomal region 19q13.4 with the two miRNA clusters C19MC and miR-371-3. Protein coding genes are represented by gray bars whereas genes of miRNA clusters are given as blue (C19MC cluster) and green (miR-371-3 cluster) lines, respectively. The common breakpoint cluster (BPC) of benign thyroid tumors of about 150 kb is indicated by a vertical arrow. miR-512-1 (pre-miR) is coding for mature-miR-512-5p, miR-371 (pre-miR) is coding for mature-miR371-3p. Gene symbols refer to the following protein coding genes: *ZNF331 = zinc finger protein 331*, *DPRX = divergent-paired related homeobox*, *NLRP12 = NLR family, pyrin domain containing 12.*
doi:10.1371/journal.pone.0009485.g001

although found to be downregulated stimulated migration and invasion *in vitro* [9]. Recently, Huang et al. [10] were able to demonstrate that miR-373 and miR-520c promote tumor invasion and metastasis *in vivo* and *in vitro* by the suppression of CD44. Interestingly, qualitative and quantitative changes of CD44 expression have been implicated in the growth and progression of thyroid tumors. Because invasive behavior is of pivotal significance in the differential diagnosis of thyroid tumors we have addressed this study on a possible up-regulation of both miRNA clusters in thyroid adenomas.

Results

Cell Lines from Thyroid Adenomas with 19q13-Rearrangement Show Upregulated Expression of miRNAs of the C19MC Cluster

To evaluate the role of either of the two miRNA clusters located in close proximity to the breakpoint region as possible targets of the 19q13 translocations in thyroid adenomas, we have first used RT-PCR to compare the expression of three members of the C19MC cluster, i.e. miR-512-5p, miR-517a, and miR-519a in five cell lines established from thyroid adenomas with 19q13 rearrangements and three cell lines from adenomas with other clonal abnormalities (Table 1). All cell lines had been established from primary tumors by using a SV40 derived subgenomic fragment. The three miRNAs chosen were spread over the whole cluster and served as examples for the more than 46 different but similar cluster members. Four of the five cell lines with 19q13 rearrangements expressed detectable levels of the three miRNAs whereas in the remaining cell line (S121, Table 1) and all cell lines with other aberrations no expression of any of the three miRNAs was noted (Figure 2).

We have then used these cell lines to quantify the expression of another member of the C19MC cluster i.e. miR-520c by real-time PCR (qRT-PCR). Akin to the results obtained for the other members of that cluster high expression was noted only in the same four cell lines with 19q13 rearrangements expressing miR-512-5p, miR-517a, and miR-519a (Figure 3a) whereas a significantly lower expression was seen in the remaining cell lines ($p = 0.001659$; for details see Table 2). Most likely, the exceptionally low expression of all examined members of the C19MC cluster in cell line S121 may result from a deletion of that part of the breakpoint region resulting from the chromosomal translocation the breakpoint of which had previously been mapped at a

Table 1. Used tissue samples and cell lines.

sample no.	thyroid material	cytogenetic subtype/FISH karyotype
S40.2*	cell line	46,XX,t(1;19)(p35 or p36;q13)[19]
S121*	cell line	46,XX,t(5;19)(q13;q13)[52]
S141.2*	cell line	46,XX,t(2;19)(p12 or p13;q13)[59]
S211#	cell line	46,XX,inv(4)(p15.2q12),t(5;19)(p14 or 15.1;q13),t(9;18)(q12;q22)[25]
S270.2	cell line	46,XX,t(2;3)(q21;q27 or q28)[13]
S290.1	cell line	46,XX,t(11;19)(q23;q13)[19]
S325π	cell line	46,XX,t(2;20;3)(p21;q11.2;p25)[17]
S533π	cell line	46,XX,t(2;7)(p21;p15)[16]
S805	adenoma	46,XX
S806	adenoma	46,XX
S889	adenoma	46,XX
S920	adenoma	46,XX
S925	adenoma	46,XX
S801	adenoma	46,XY,t(2;4),t(2;14;19)
		nuc ish(5′-tbpc19,3′-tbpc19)x2(5′-tbpc19 sep 3′-tbpc19x1)
S814	adenoma	46,XX,del(6)(q21∼22)
		nuc ish(5′-tbpc19,3′-tbpc19)x2(5′-tbpc19 sep 3′-tbpc19x1)
S842	adenoma	46,XX,t(1;19)(q32;q13)[8]/46,XX[24]
		nuc ish(5′-tbpc19,3′-tbpc19)x2(5′-tbpc19 sep 3′-tbpc19x1)
S846	adenoma	46,XY
		nuc ish(5′-tbpc19,3′-tbpc19)x2(5′-tbpc19 sep 3′-tbpc19x1)
S849	adenoma	not evaluable by cc
		nuc ish(5′-tbpc19,3′-tbpc19)x2(5′-tbpc19 sep 3′-tbpc19x1)

Cytogenetic details of the analyzed samples from follicular thyroid tumors and the cell lines used with their genetic subgroups determined by conventional cytogenetics and/or by interphase fluorescence in situ hybridization (I-FISH) with break-apart, dual-color rearrangement probe (tbpc-19). In case of the cell lines only the clonal aberrations found in the original tumors the cell lines have been established from are given.
Ref.: (*) [30]; (#) [2]; (π) [31].
doi:10.1371/journal.pone.0009485.t001

position between the C19MC and the miR 371-3 cluster. Thus, in all cell lines with breakpoints upstream of the C19MC cluster evidence for an upregulation of four cluster members was obtained. Because of a common regulation of that cluster, no further members were examined.

Thyroid Adenomas with 19q13 Rearrangements Show Upregulation of miRNAs of the C19MC Cluster and the miR-371-73 Cluster

To see if comparable results can be obtained for primary tumors as well we have characterized 70 thyroid nodules by interphase

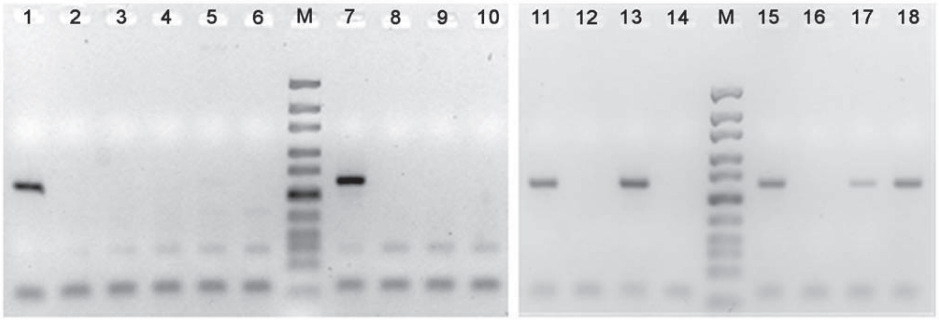

Figure 2. Expression analysis of miR-517a by RT-PCR. PCR reactions were performed and then analyzed in 4% small DNA Agarose. The expected DNA-fragment has a size of 62 bp, Ultra low range Ladder (Fermentas) was used as Marker (M). Lane 1: S40.2, 2: S40.2 without reverse transcriptase (–RT), 3: S121, 4: S121–RT, 5: thyroid (normal), 6: thyroid–RT, 7: placenta, 8: placenta-RT, 9: S270.2, 10: S270.2–RT, 11: S290.1, 12: S290.1–RT, 13: S141.2, 14: S325, 15: S211, 16: S211–RT, 17: fetal RNA, 18: adult testis, 19: fetal RNA-RT, 20: S141.2-RT, 21: adult testis-RT, 22: S325-RT (for details of the cell lines and tumor samples see Table 1).
doi:10.1371/journal.pone.0009485.g002

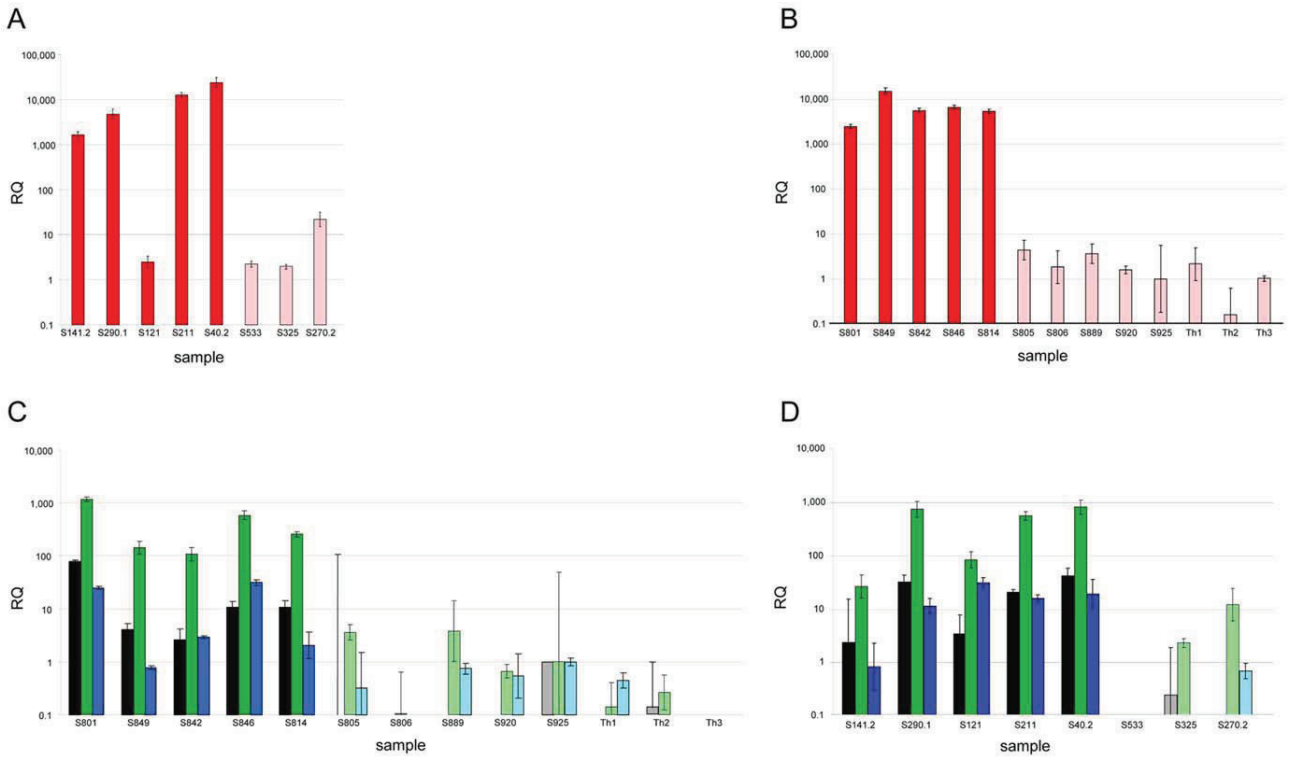

Figure 3. Expression of miR-520c, miR-371-3p, miR-372 and miR-373 in cell lines and primary tumors. Relative expression of miRNAs was determined by real-time PCR (mean s.d. from three independent experiments). Values of miRNA were normalized to *RNU6B (RNA, U6 small nuclear 2)* (**A**) miR-520c expression in thyroid cell lines, five cell lines derived from adenomas with 19q13.4 rearrangements (S141.2, S290.1, S121, S211, S40.2) (red bars) and three cell lines derived from thyroid adenomas with other structural rearrangements (S533, S325, S270.2) (light red bars). (**B**) miR-520c expression in three samples of non-neoplastic thyroid tissues (Th1, Th2, Th3) (light red bars), five adenomas with 19q13.4 rearrangement (S801, S849, S842, S846, S814) (red bars) and five adenomas without cytogenetically detectable aberrations (S805, S806, S889, S920, S925) (light red bars). (**C**) miR-371-3 expression in three samples of non-neoplastic thyroid tissues (gray (miR-371-3p), light green (miR-372) and light blue (miR-373)), five adenomas with 19q13.4 rearrangement (black (miR-371-3p), green (miR-372) and blue (miR-373)) and five adenomas without cytogenetically detectable aberrations (gray, light green and light blue bars) (for case numbers refer to Table 1). (**D**) miR-371-3 expression in thyroid cell lines, five cell lines derived from adenomas with 19q13.4 rearrangements (black (miR-371-3p), green (miR-372) and blue (miR-373)) and three cell lines derived from thyroid adenomas with other structural rearrangements (gray (miR-371-3p), light green (miR-372) and light blue (miR-373)) (for case numbers refer to Table 1).
doi:10.1371/journal.pone.0009485.g003

fluorescence in situ hybridization (I-FISH) on cytologic samples obtained prior to cell culturing. The results were usually supplemented by conventional cytogenetics. FISH screening/conventional cytogenetic analysis of the nodules detected five tumors with clonal rearrangements of chromosomal band 19q13 (Figure 4). Akin to the cell lines semi-quantitative RT-PCR revealed an upregulation of 3 miRNAs and again, as further example of that cluster, results were supplemented with qRT-PCR analyses for miR-520. We have shown that all thyroid adenomas with 19q13 rearrangements express significantly higher levels ($p \leq 0.003133$) of miR-520 than samples without 19q13 rearrangements (adenomas and surrounding thyroid tissue; for details see Table 1) (Figure 3b).

To see if the 19q13 rearrangements also activate the expression of the miR-371-3 cluster we have studied the expression of three members of this cluster in the same samples used before. All tumors with 19q13 rearrangements were shown to express significantly higher levels of miR-371-3p, miR-372, and miR-373 than three samples of surrounding histologically normal thyroid tissue ($p \leq 0.02236$) and the five cytogenetically normal adenomas ($p \leq 0.01428$) (Figure 3c). We then quantified the expression of miR-371-3p, miR-372, and miR-373 in the cell lines where comparable results were obtained (Figure 3d). Interestingly, cell line S121 with absent or very low expression of the C19MC cluster members showed a high expression of the miR-371-3 cluster thus further strengthening the idea that in this cell line part of the C19MC cluster is deleted.

In a Thyroid Adenoma Cell Line the C19MC Cluster Becomes Part of a Pol-II Fusion mRNA

In order to further understand the mechanisms involved in the activation of the miRNA clusters one cell line of the 19q13 group has been investigated in more detail. This cell line shows a rearrangement of chromosomal band 19q13.4 resulting from an apparently balanced translocation t(1;19)(1p35.2;q13.4) (Figure 5). By appropriate FISH analyses using BAC (bacterial artificial chromosome) probes the breakpoint on chromosome 1 was mapped within *pumilio homolog 1* (*PUM1*) (Figure 6). *PUM1* encodes a RNA-binding protein and shows a widespread expression in adult tissues. It has 22 exons and spans about 150 kb on chromosomal band 1p35.2 [11,12]. To further characterize the breakpoint region at the molecular level additional FISH studies were performed allowing to narrow down the 1p35.2 breakpoint to the 6,144 kbp intron 10 of *PUM1*. By the translocation the

Table 2. Statistical analysis of the qRT-PCR data.

19q translocation	without 19q translocation	microRNA	p-value	d.f.	t
Adenoma	normal thyroid and adenoma	mir371-3p	0.005355	4.48	5.0446
		mir372	2.232e-06	10.996	8.9445
		mir373	0.006122	8.522	3.6176
		mir520c	1.722e-09	10.977	17.9765
Adenoma	adenoma	mir371-3p	0.004623	5.203	4.745
		mir372	0.0001681	7.043	7.2279
		mir373	0.01428	7.9	3.128
		mir520c	4.312e-08	7.978	19.941
Adenoma	normal thyroid	mir371-3p	0.005471	4.159	5.2956
		mir372	0.008832	2.826	6.5061
		mir373	0.02236	4.122	3.5632
		mir520c	0.003133	2.573	10.9875
adenoma cell line	adenoma cell line	mir371-3p	0.004041	4.446	5.4488
		mir372	0.1121	2.4893	2.344
		mir373	0.08229	2.311	2.9573
		mir520c	0.001659	4.029	7.4811

Statistical analysis (t-test, two-tailed) of the expression of miRNAs from the cluster C19MC and miR-371-3 in tissues or cell lines containing 19q13 rearrangements compared to normal thyroid tissue and/or adenomas without 19q13 rearrangements. The data were obtained using statistical software R (www.r-project.org). (d.f. = degrees of freedom, t = Student's t-value)

doi:10.1371/journal.pone.0009485.t002

proximal part of *PUM1* including exons 1–10 was found to be juxtaposed to the miRNA clusters (Figure 7). In addition, we have therefore used 3′RACE-PCR to detect possible fusion transcripts between the proximal part of *PUM1* and sequences from chromosome 19. Among several aberrant transcripts a fusion transcript consisting of exon 1–10 of *PUM1* followed by an ectopic sequence of the chromosome 19 breakpoint region was detected (Figure 8) and sequenced (Genbank Accession number GQ334687). This transcript further confirms that the chromosomal break in this cell line is indeed located within intron 10 of *PUM1*. Accordingly, we have performed RT-PCR experiments using a sequence within exon 10 as the forward primer by which we were able to detect part of one fusion transcript (Figure 8) (Genbank Accession number GQ334688) with a border clearly extending the distal border of C19MC (Figure 7). The 5′ splice site of intron 10 is not completely homologous to the consensus sequence of human introns (Figure 9c)[13]. But the 3′splice sites on either site of the fusion are in line with the conserved consensus sequence and a upstream region known as the polypyrimidine tract (Figure 9a,b). However, from these results it seems reasonable to assume that in the cell line S40.2 both clusters become part of large Pol-II transcript driven by the *PUM1* promoter. An *in silico* analysis of intron 10 of *PUM-1* as well as the chromosome 19 breakpoint region did not reveal obvious sequence homologies pointing to homologous recombination as a mechanism underlying the chromosomal rearrangement seen in that cell line.

Discussion

Specific structural chromosome abnormalities have turned out to be valuable signposts indicating the position of protein-coding genes with oncogenic potential. Recently, in addition some evidence for a causal association of some chromosomal rearrangements with the activity of microRNA coding genes has been presented [14,15,16]. Herein, we were able to show that a highly frequent translocation in benign thyroid tumors i.e. the 19q13.4 rearrangement targets and activates two microRNA clusters in close proximity to the chromosomal breakpoint cluster the expression of which is otherwise almost exclusively confined to embryonic and fetal development. Activation by an ectopic Pol-II promoter may generally be the mechanism by which the translocations activate both miRNA clusters and fits with the apparent "natural" generation of the miRNAs of the C19MC cluster from a large Pol-II driven transcript as witnessed by the results of a recent study [4]. From the histologic analyses performed herein no evidence for invasiveness of the corresponding tumors has been found that by definition would lead to the diagnosis of a follicular carcinoma but this does not rule out a higher risk of these tumors to become malignant. Generally, members of both clusters have been implicated in malignant growth. In human testicular germ cell tumors evidence for an oncogenic potential of miR-373 has been obtained. In these tumors the expression of miR-373 was shown to allow tumorigenic growth in the presence of wild-type p53 [8]. As another example in a recent paper hsa-miR-518c and hsa-miR-373 were among the microRNAs associated with the tumorigenesis of retinoblastomas [17]. In breast cancer, miR-373 and miR-520c promote tumor invasion and metastasis *in vivo* and *in vitro* by the suppression of CD44 [10]. Interestingly, the expression of a miRNA of the C19MC cluster i.e. miR-516-3p recently has been linked to higher aggressiveness of breast cancer as well. Based on a large-scale screen for miRNA expression patterns associated with distant metastasis Foekens et al. [17] were able to show that miR-516-3p belongs to four miRNAs the expression of which is associated with an adverse prognosis in estrogen receptor-positive, lymph node-negative primary breast cancer [18]. Moreover, forced expression of miR-373 leads to a reduction in the nucleotide excision repair (NER) protein, RAD23B, as well as in RAD52 [19] thereby possibly contributing to a higher genome instability.

Based on these data it may be hypothesized that activation of both clusters by chromosomal rearrangements might be not restricted to thyroid tumors. Balanced translocations involving 19q13.4 have also been described in mesenchymal hamartoma of

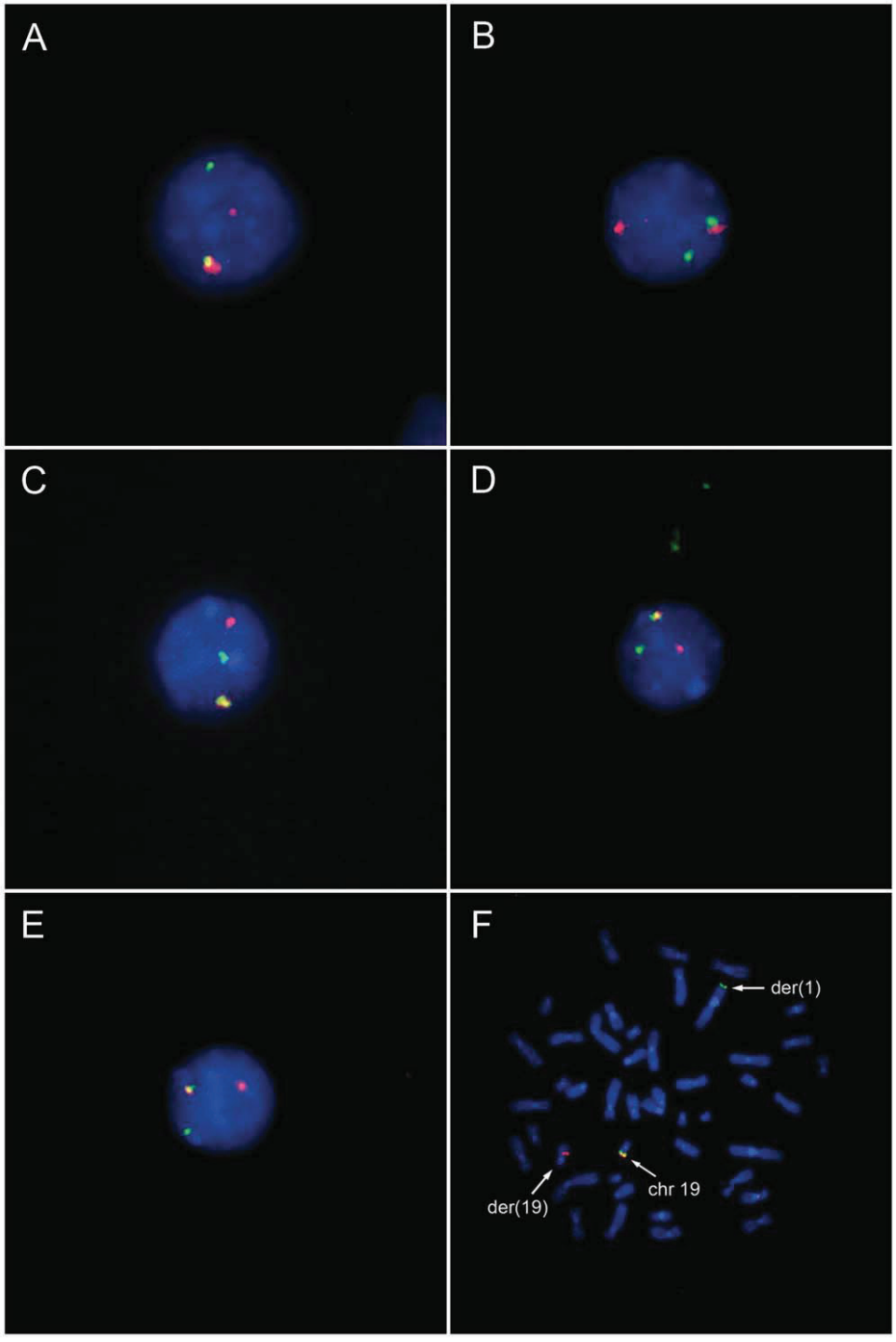

Figure 4. Fluorescence in situ hybridization (FISH) with dual-color, break-apart rearrangement probe (tbpc19). (**A**)–(**E**) I-FISH showing 19q13 rearrangements detected using touch-preparations of five thyroid adenomas (**A:** S801, **B:** S814, **C:** S842, **D:** S846, **E:** S849) indicated by separated green (3′-tbpc19) and red signals (5′-tbpc19); (**F**) Metaphase of case S842 with a t(1;19)(q32;q13) after FISH with tbpc19. The 19q13 rearrangement is indicated also by separated signals on der(1) and der(19).
doi:10.1371/journal.pone.0009485.g004

the liver (MHL), a rare benign tumor-like lesion of childhood [20]. Of note, quite recently, genomic amplifications including the C19MC cluster have been detected by array CGH and FISH as recurrent genomic imbalances in an aggressive subgroup in primitive neuroectodermal brain tumors. Functional studies implicated two miRNAs of the cluster i.e. miR-517c and 520 g as oncogenes causally linked to the development of the disease [21]. More generally, breaks of chromosomal band 19q13 have been reported in a variety of human neoplasms. Furthermore, according to the CancerChromosomes/Mitelman database (NCBI) chromosomal band 19q13 belongs to the areas most frequently targeted by chromosomal aberrations at all in the

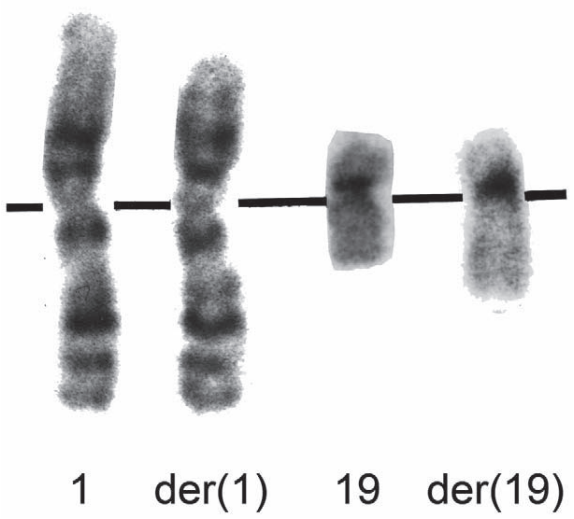

Figure 5. Partial karyotype of cell line S40.2. Partial G-banded karyotype showing chromosome 1 and 19 as well as their derivatives resulting from t(1;19)(p35.2;q13.4).
doi:10.1371/journal.pone.0009485.g005

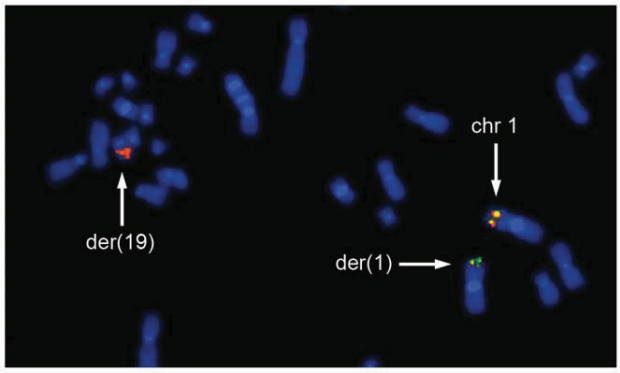

Figure 6. Delineation of *PUM1* breakpoint by metaphase FISH. Part of metaphase of cell line S40.2 after FISH with two overlapping BAC clones RP11-201O14 (green) and RP11-1136E4 (red) both spanning the whole genomic sequence of *PUM1* in 1p35.2. The breakpoint in 1p35.2 is located within *PUM1* indicated by a separation of RP11-201O14 and RP11-1136E4. Because of weak signals of RP11-1136E4 remaining on the der(1) the breakpoint is located within RP11-1136E4 distal to RP11-201O14.
doi:10.1371/journal.pone.0009485.g006

genome. Thus, it remains to be determined whether or not some of these do also target either of the two or both miRNA clusters investigated herein. However, there is ample evidence that within the thyroid epithelium the clonal re-expression of two important "embryonic" miRNA clusters with thousands of potential targets is causally linked to the development of a large subgroup of thyroid adenomas. Effects of individual of these miRNAs with single targets have been associated with human tumors but mechanistically the effects observed are more likely to result from global changes of gene expression than from the de-regulation of single targets of the corresponding miRNAs.

Methods

Ethics Statement

The use of human thyroid tumors for this study (including the preparation of the cell lines S270.2 and S290.1) was approved by the local medical ethics committee and followed the guidelines of the declaration of Helsinki. Only samples that were initially taken for diagnostic purposes were secondarily used for the present study. Because the samples were de-identified and were considered as samples normally discarded, the committee felt that there was no specific patient consent necessary.

Tissue and Cell Lines

All samples were obtained from patients undergoing thyroid resection in the Department of General and Visceral Surgery of the St. Joseph Stift, Bremen (Germany). One piece of each tumor was stored in Hank's solution for cell culture and a second piece was stored in liquid nitrogen for gene expression studies. The cell lines were derived from thyroid adenoma cells as reported previously [22]. Archival RNAs from fetal, placental and testicular tissue were used as controls.

Cell Culture and Cytogenetic Analyses

Tissue digestion, cultivation of primary cell lines, and cytogenetic analyses were performed according to previously described methods [2,23]. Before digestion, each sample was touched onto slides to get samples for FISH screening.

Isolation of RNA, Reverse Transcription and Real-Time PCR (qRT-PCR) Quantification

Total RNA was extracted from tissue as well as from immortalized cell lines using TRIzol (Invitrogen, Karlsruhe, Germany) reagent, or mirVana (Ambion, Woodward, USA)

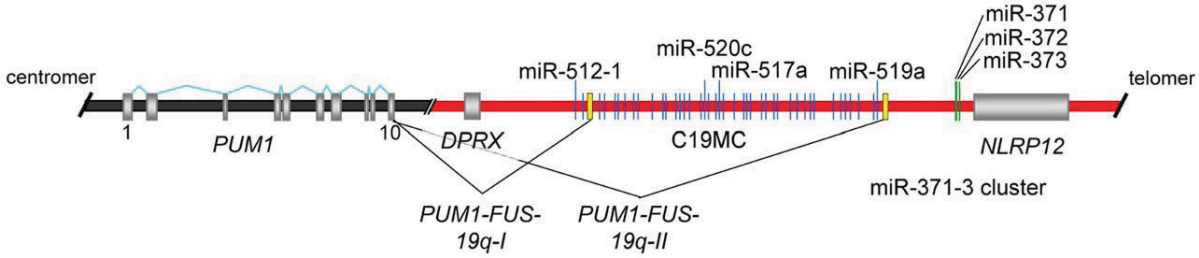

Figure 7. Genomic organization of the fusion gene on the derivative chromosome 1 resulting from a translocation t(1;19)(p35.2;13.4) in cell line S40.2. Detailed schematic overview illustrating the origin of the fusion transcripts *PUM1-FUS-19q-I* (Genbank Accession number GQ334687) and PUM1-FUS-19q-II (Genbank Accession number GQ334688) identified in cell line S40.2. The genomic region of PUM1 in 1p35.2 (horizontal gray bar) fuses after exon 10 of *PUM1* (exons: vertical light gray bars) to the genomic region of *C19MC* in 19q13.4 (horizontal red bar). The two vertical yellow bars indicate 3′-sequences located after exon 1–10 of *PUM1* in *PUM1-FUS-19q-I* and *PUM1-FUS-19q-II*, respectively, both originating from alternative splicing. The fusion transcripts were detected either by 3′-RACE-PCR (*PUM1-FUS-19q-I*) or RT-PCR (*PUM1-FUS-19q-II*) experiments. The quantified miRNAs have been highlighted by their names.
doi:10.1371/journal.pone.0009485.g007

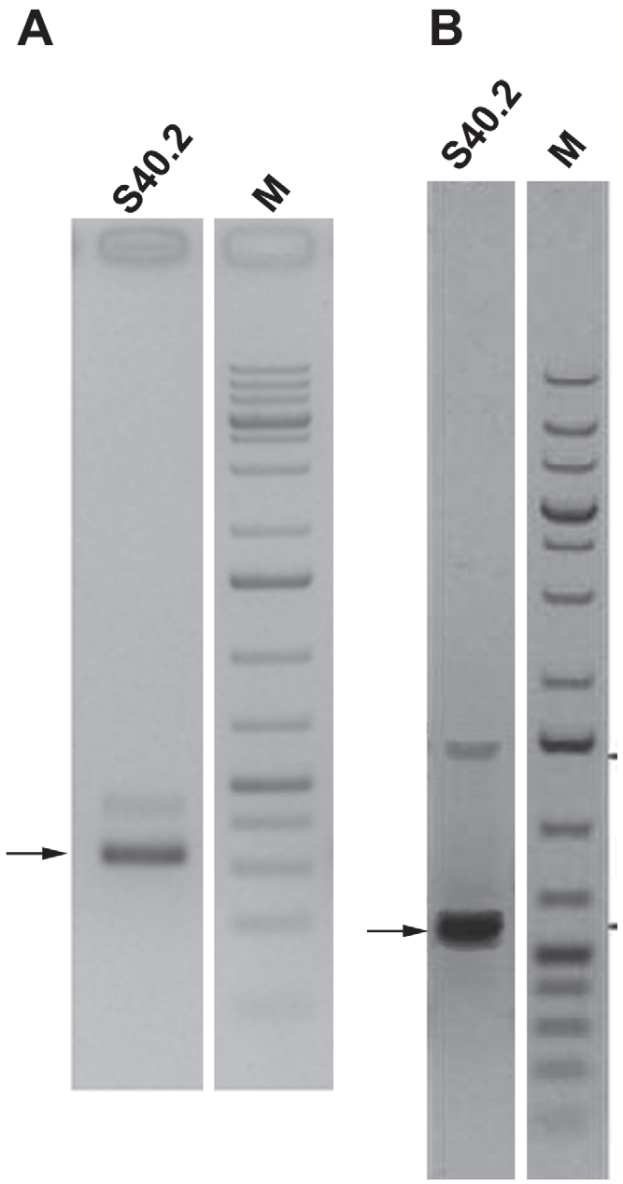

Figure 8. Cloning of fusion transcripts PUM1-FUS-19q-I and PUM1-FUS-19q-II. Fusion transcripts resulting from the t(1;19) in cell line S40.2 were detected by RT-PCR and analyzed by gel electrophoresis. M = Marker DNA (1 kb+, Fermentas). S40.2 = Thyroid adenoma cell line S40.2. The arrows point to the corresponding bands that were excised. Isolated DNA was sequenced and analyzed. Weak bands above may represent splice variants. **A**) Transcript PUM1-FUS-19q-I generated with primers Ex9_up and 19_2. **B**) Transcript PUM1-FUS-19q-II generated with primers Ex9_up and 500_Cluster_polyA_I.
doi:10.1371/journal.pone.0009485.g008

miRNA isolation kit according to the manufacturer's instructions. miRNA (miR-371-3p, miR-372, miR-373 and miR-520c) and *RNU6B* (*RNA, U6 small nuclear 2*; internal control for relative quantification)-specific cDNA were generated from 10 ng of total RNA using the *Taq*Man microRNA RT Kit and the gene-specific RT primers from the *Taq*Man microRNA Assays (Applied Biosystems, Foster City, CA, USA) according to the manufacturer's instructions. The reactions were incubated in a thermal cycler for 30 min at 16°C, 30 min at 42°C, 5 min at 85°C and then stored at 4°C. All reverse transcriptions included no-template controls and minus RT controls (–RT).

Real-time PCR was performed using an Applied Biosystems 7300 Fast Real Time PCR system with miRNA and *RNU6B*-specific probes and TaqMan Universal PCR Master Mix (Applied Biosystems, Foster City, CA, USA). The reactions were incubated in 96-well plates at 95°C for 10 min followed by 40 cycles of 15 s at 95°C and one min at 60°C. All reactions were run in triplicate. Relative quantification (RQ) was calculated using Applied Biosystems SDS software based on the RQ = 2_DDCt 2(–Delta Delta C(T)) method [24]. Ct data were normalized to the internal control, *RNU6B* [25].

Detection of Fusion Transcripts via 3′RACE-PCR

3′RACE-PCR was performed on cell line S40.2. Total RNA was isolated using RNeasy Mini Kit (Qiagen, Hilden, Germany). cDNA syntheses were carried out with slight modifications following the instructions for the M-MLV reverse transcriptase using oligo(dT) primer as anchor primer (Invitrogen, Karlsruhe, Germany). 3′RACE-PCRs and Nested 3′RACE-PCRs were performed as described in the Gene Racer Kit (Invitrogen, Karlsruhe, Germany) adjusted to the conditions for Go*Taq* Flexi DNA Polymerase (Promega, Mannheim, Germany). Southern Blots were carried out as mentioned by Fehr et al. [26] with *PUM1*-specific probe labelled with digoxigenin-11-dUTP (Roche Diagnostics, Penzberg, Germany). Fragments of interest were excised and extracted with the QIAquick Gel Extraction Kit (Qiagen, Hilden, Germany) and were then cloned into the pGEM-T Easy Vector (Promega, Mannheim, Germany). The plasmid DNA from the clones of interest was isolated via QIAprep Spin Miniprep Kit (Qiagen, Hilden, Germany) and sequenced by Eurofins MWG, Ebersberg, Germany.

Detection of Fusion Transcripts via RT-PCR

With the program polyadq [27], the possible PolyA-site of the C19MC-cluster was detected. Nearby a primer was designed which was later used together with a *PUM1*-specific primer. Total RNA of S40.2 isolated via TRIzol reagent (Invitrogen, Karlsruhe, Germany) was used for cDNA syntheses as previously described. PCR was done with the Go*Taq* Flexi DNA-Polymerase (Promega, Mannheim, Germany) followed by a semi-nested PCR. Fragments of interest were excised and extracted as described above and sequenced by Eurofins MWG, Ebersberg, Germany.

Validation of the Fusion Transcript

To confirme the former results, different primers localized within the fusion transcript were utilized. The PCRs were carried out as described above. Fragments of the expected size were excised, extracted and sequenced (see above).

RT-PCR

miRNA-specific-primers for miR-512-5p, miR-517a and miR-519a were designed, as described by Chen et al. [28]. cDNA was generated from 1 µg total RNA according to Chen et al. [28] with small modifications in stem-loop-primer concentration (5 nM), as well as the PCR-reactions that were modified in annealing-temperature (68°C) and -duration (10 s). The RT-PCR was performed with Go*Taq* Flexi DNA-Polymerase (Promega GmbH, Mannheim, Germany). Elongation was run at 72°C for 15 s.

Primers

See Table 3.

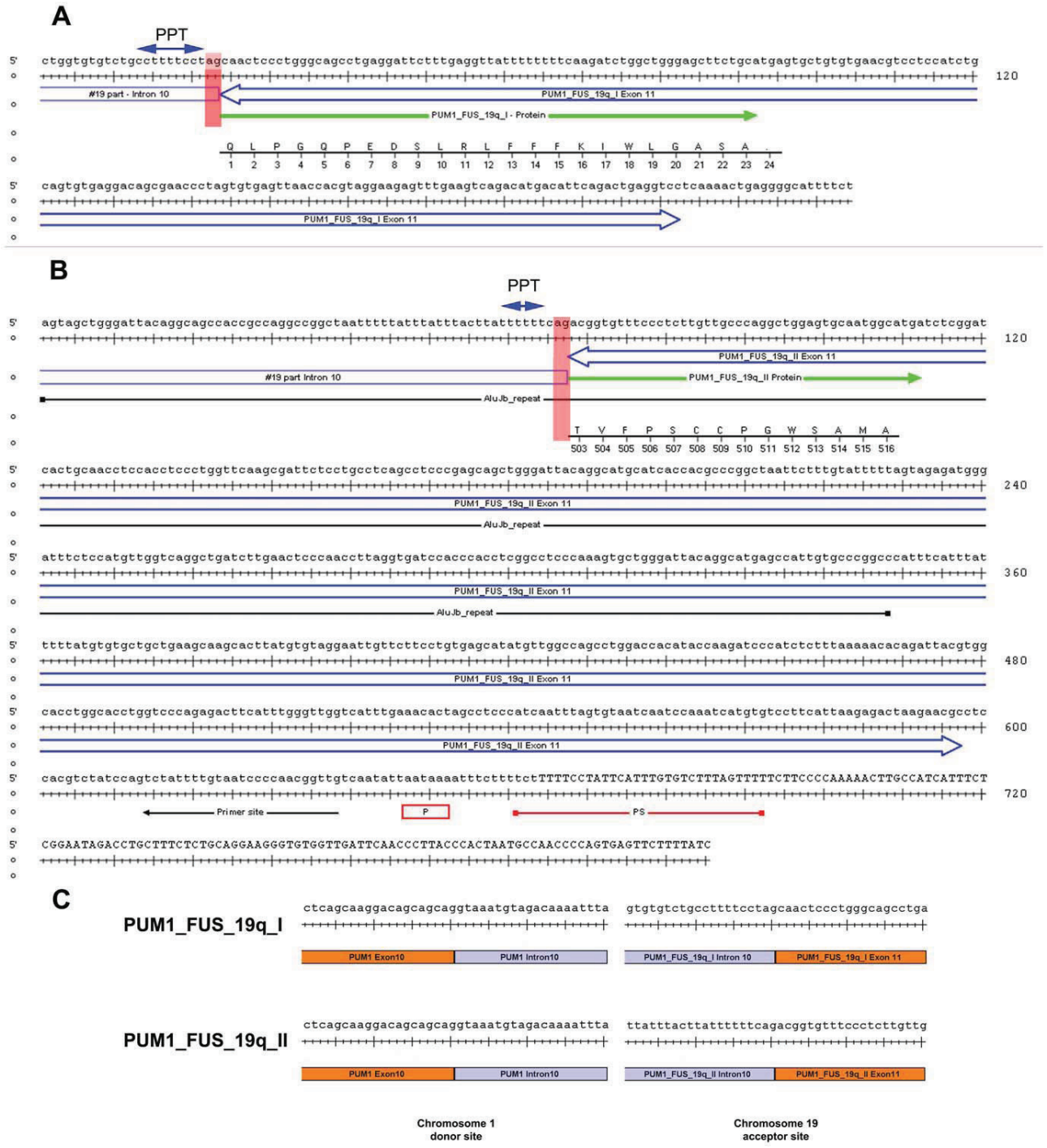

Figure 9. Sequence analysis of the genomic structure of *PUM1-FUS-19q*. Genomic organization of part of *FUS-19q*. Blue double arrows indicate exon 11 of *PUM1-FUS*-19q. The green arrow marks the final part of the fusion protein. The underlying ruler shows the final amino acid sequence. The bases ag (red) correspond to the intron 10 (chromosome 19 part) splice site. Solid blue double arrows indicate the polypyrimidine tract (PPT). **A**) Chromosome 19 derived part of the genomic sequence of *PUM1-FUS-19q-I*. **B**) Chromosome 19 derived part of the genomic sequence of *PUM1-FUS-19q-II*. Black line indicates the Alu–repeat. Site of Primer 500-Cluster_PolyA_I is shown by a black arrow. Red line (PS) and red box (P) indicates predicted poly (A) signals. **C**) Intron 10 splice sites of the two *PUM1-FUS-19q* variants.
doi:10.1371/journal.pone.0009485.g009

Fluorescence In Situ Hybridization (FISH)

Interphase FISH (I-FISH) analyses were performed on touch-preparations of thyroid tumors. For detection of 19q13.4 rearrangements a dual-color, break-apart rearrangement probe (PanPath, Budel, Netherlands) referred to as tbpc19 (thyroid breakpoint cluster 19q13) was used. The rearrangement probe is a mixture of two probes located distal (3′-tbpc19; labeled by Alexa Fluor 488) and proximal (5′-tbpc19; labeled by Alexa-

Table 3. Used Primers.

PUM 1		
Primer (Exon)	**sequence (5′ -3′)**	**company**
Ex1_Up (Exon 2)	CCCTCAAGAACCAGCTAATCCCAACA	Invitrogen
Ex3_Up (Exon 4)	TTCCTGGGTGATCAATGGCGAGA	Invitrogen
Ex4_Up (Exon 5)	TCCCCGGGCGATTCCTGTCT	Invitrogen
Ex5_Lo (Exon 6)	TCCATCACATCACCCTCCTCCTTCAA	Invitrogen
Ex7_Up (Exon 8)	ACCTAATGCGCTTGCTGTCCA	Invitrogen
Ex8_Up (Exon 9)	GCTCCCGCTGCGTTTGTCC	Invitrogen
Ex9_Up (Exon 10)	CAACAGACCACCCCACAGGCTCAG	Invitrogen
Ex11_Lo (Exon 12)	ATTTCTCGCGCCTGCATTCACTAC	Invitrogen
Ex12_Up (Exon 13)	CCAGTTCTTTCTACGGCAACAACTCTCTG	Invitrogen
Ex14_Up (Exon 15)	AACTGCGGGAGATTGCTGGACATA	Invitrogen
Ex14_Lo (Exon 15)	CCATTATATGTCCAGCAATCTCCCGC	Invitrogen
Ex17_Lo (Exon 18)	CGATGATAAATTGCAAAGACTGGGGC	Invitrogen
Ex19_Up (Exon 20)	TGAGGATAAAAGCAAAATTGTAGCAGAA	Invitrogen
Ex20_Up (Exon 21)	GGAGCCAGGCCAGCGGAAGATC	Invitrogen
Ex21_Lo (Exon 22)	GCCAGTGAGGTCAGCGGGAATG	Invitrogen
3′UTR_Lo (Exon 22)	AATCCAGTAGGCAGTAAACAATCACACC	Invitrogen
5′UTR_Up (Exon 1)	AGAGAGAAGATCGGGGGGCTGAAAT	Invitrogen
cDNA/3′RACE		
AP2	AAGGATCCGTCGACATC(T)17	Invitrogen
Oligo dT	GCTGTCAACGATACGCTACGTAACGGC	Invitrogen
	ATGACAGTG(T)24	
UAP2	CTACTACTACTAAAGGATCCGTCGACATC	Invitrogen
Gene Racer 3′	GCTGTCAACGATACGCTACGTAACG	Invitrogen
Gene Racer 3′Nested	CGCTACGTAACGGCATGACAGTG	Invitrogen
GAPDH2_Up	GTGAAGGTCGGAGTCAACG	Invitrogen
GAPDH5_Lo	AGGAGGCATTGCTGATGAT	Invitrogen
Chromosome 19 miRNA cluster C19MC		
19_1	GGCTGCCCAGGGAGTTGCT	Invitrogen
19_2	GCAGAAGCTCCCAGCCAGATCTT	Invitrogen
19_3	CTAGGGTTCGCTGTCCTCACACTGC	Invitrogen
500-Cluster_PolyA_I	CAACCGTTGGGGATTACAAAATAGA	Invitrogen
Stem-loop-Primers		
miR-371-5p a sl	GTCGTATCCAGTGCAGGGTCCGAGGTAT	Invitrogen
	TCGCACTGGATACGACACACTC	
miR-371-5p sl	GTCGTATCCAGTGCAGGGTCCGAGGTAT	Invitrogen
	TCGCACTGGATACGACAGTGCC	
miR-372 sl	GTCGTATCCAGTGCAGGGTCCGAGG	Invitrogen
	TATTCGCACTGGATACGACACGCTC	
miR-373 sl	GTCGTATCCAGTGCAGGGTCCGAGGTAT	Invitrogen
	TCGCACTGGATACGACACACCC	
miR-512-5p sl	GTCGTATCCAGTGCAGGGTCCGAGG	Invitrogen
	TATTCGCACTGGATACGACGAAAGT	
miR-517a sl	GTCGTATCCAGTGCAGGGTCCGAGG	Operon
	TATTCGCACTGGATACGACACACTC	
miR-520c-3p sl	GTCGTATCCAGTGCAGGGTCCGAGGTAT	Invitrogen
	TCGCACTGGATACGACACCCTC	
miR-520c-5p sl	GTCGTATCCAGTGCAGGGTCCGAGGTAT	Invitrogen
	TCGCACTGGATACGACCAGAAA	

Table 3. Cont.

Forward and Reverse Primers (PCR)		
miR-371-3p fw	ACCGCTAAGTGCCGCCATCTTTTG	Invitrogen
miR-371-5p fw	GCCGCCACTCAAACTGTGGGG	Invitrogen
miR-372 fw	GGTCATAAAGTGCTGCGACATTTG	Invitrogen
miR-373 fw	TTCATGAAGTGCTTCGATTTTGG	Invitrogen
miR-512-5p fw	AGTCTACACTCAGCCTTGAGGGCA	Invitrogen
miR-517a fw	CGGCGGATCGTGCATCCCTTTA	Operon
miR-519a fw	CCGGCTAAAGTGCATCCTTTTAG	Invitrogen
miR-520c-3p fw	GCCGCCAAAGTGCTTCCTTTTAG	Invitrogen
miR-520c-5p fw	ACCGCTCTCTAGAGGGAAGCAC	Invitrogen
Reverse Primer	GTGCAGGGTCCGAGGT	Operon

Primer sequences for PCR and cDNA synthesis.
doi:10.1371/journal.pone.0009485.t003

Fluor 555), respectively, of the common breakpoint-cluster region in 19q13.4 in benign thyroid lesions. 10 µl of the break-apart probe were used per slide. Co-denaturation was performed on a Mastercycler gradient (Eppendorf, Hamburg, Germany) for 3 min at 80°C followed by overnight hybridization in a humidified chamber at 37°C. Post-hybridization was performed at 61°C for 5 min in 0.1xSSC. Interphase nuclei were counterstained with DAPI (0.75 µg/ml). Slides were examined with a Axioskop 2 plus fluorescence microscope (Carl Zeiss, Göttingen, Germany). Images were captured with an AxioCam MRm digital camera and were edited with AxioVision (Carl Zeiss, Göttingen, Germany). For each case 200 non-overlapping nuclei were scored. Co-localized signals (green/red) indicate a non-rearranged breakpoint region, whereas separated green and red signals indicate a rearrangement of the chromosomal region 19q13.4. Metaphase-FISH with tbpc-19 on case S842 was performed as described above for I-FISH on touch-preparations. Treatment of metaphases was carried out as described by Kievits et al. [29].

For determination of the breakpoint on chromosome 1 FISH was performed on metaphase preparations of the cell line S40.2. As probes two overlapping clones RP11-1136E4 (Genbank Accession number AQ707626 and AQ733864) and RP11-201O14 (Genbank Accession number AL356320.8) (imaGenes, Berlin, Germany) both spanning the whole genomic sequence of *PUM1* were used. DNA was isolated using Qiagen Plasmid Midi Kit (Qiagen, Hilden, Germany). 1 µg of isolated plasmid DNA was labeled by nick translation (Roche, Mannheim, Germany) either with digoxigenin-11-dUTP (RP11-201O14) or biotin-16-dUTP (RP11-1136E4). Treatment of metaphases and subsequent FISH experiments were carried out as described previously by Kievits et al. [29] with exception for co-denaturation and post-hybridization which were performed as described above.

Statistical Analysis

Results are presented as the mean ± standard error (SE). Statistical comparisons were performed by a nonpaired Student's t -test. A p-value of less than 0.05 was considered significant.

Data Deposition

The complete fusion transcript sequences has been deposited in GenBank, PUM1-FUS-19q-I (Genbank Accession number

GQ334687) and PUM1-FUS-19q-II (Genbank Accession number GQ334688).

Acknowledgments

We thank M. Grund, A. Laabs, J. Papprott, T. Sommerfeld, A. Bogaczewicz, I. Flor, and C. Kuntze for their technical help. For help with cytogenetic analyses we thank Y. Kiefer and B. Rommel.

Author Contributions

Conceived and designed the experiments: VR JB. Performed the experiments: VNL. Analyzed the data: VR JB. Wrote the paper: VR LD ND JB. Did the expression analyses: LD VNL. Characterized the genomic fusion and the fusion transcripts in cell line S40.2: LD VNL. Carried out the FISH analyses on the primary tumors as well as the cell lines: ND. Performed the bioinformatics and statistics: RN. Carried out the clinical workout: WS KJ. Performed the pathological analyses: WS KJ. Cytogenetically characterized the cell lines: GB.

References

1. DeLellis RA (2004) Pathology and genetics of tumours of endocrine organs: [… editorial and consensus conference in Lyon, France, April 23 - 26, 2003]. Lyon: IARC Press. 320 S. p.
2. Belge G, Roque L, Soares J, Bruckmann S, Thode B, et al. (1998) Cytogenetic investigations of 340 thyroid hyperplasias and adenomas revealing correlations between cytogenetic findings and histology. Cancer Genet Cytogenet 101: 42–48.
3. Belge G, Rippe V, Meiboom M, Drieschner N, Garcia E, et al. (2001) Delineation of a 150-kb breakpoint cluster in benign thyroid tumors with 19q13.4 aberrations. Cytogenet Cell Genet 93: 48–51.
4. Bortolin-Cavaille ML, Dance M, Weber M, Cavaille J (2009) C19MC microRNAs are processed from introns of large Pol-II, non-protein-coding transcripts. Nucleic Acids Res 37: 3464–3473.
5. Ren J, Jin P, Wang E, Marincola FM, Stroncek DF (2009) MicroRNA and gene expression patterns in the differentiation of human embryonic stem cells. J Transl Med 7: 20.
6. Laurent LC, Chen J, Ulitsky I, Mueller FJ, Lu C, et al. (2008) Comprehensive microRNA profiling reveals a unique human embryonic stem cell signature dominated by a single seed sequence. Stem Cells 26: 1506–1516.
7. Li SS, Yu SL, Kao LP, Tsai ZY, Singh S, et al. (2009) Target identification of microRNAs expressed highly in human embryonic stem cells. J Cell Biochem 106: 1020–1030.
8. Voorhoeve PM, le Sage C, Schrier M, Gillis AJ, Stoop H, et al. (2006) A genetic screen implicates miRNA-372 and miRNA-373 as oncogenes in testicular germ cell tumors. Cell 124: 1169–1181.
9. Yang K, Handorean AM, Iczkowski KA (2009) MicroRNAs 373 and 520c Are Downregulated in Prostate Cancer, Suppress CD44 Translation and Enhance Invasion of Prostate Cancer Cells in vitro. Int J Clin Exp Pathol 2: 361–369.
10. Huang Q, Gumireddy K, Schrier M, le Sage C, Nagel R, et al. (2008) The microRNAs miR-373 and miR-520c promote tumour invasion and metastasis. Nat Cell Biol 10: 202–210.
11. Spassov DS, Jurecic R (2002) Cloning and comparative sequence analysis of PUM1 and PUM2 genes, human members of the Pumilio family of RNA-binding proteins. Gene 299: 195–204.
12. Szabo A, Perou CM, Karaca M, Perreard L, Palais R, et al. (2004) Statistical modeling for selecting housekeeper genes. Genome Biol 5: R59.
13. Lomelin D, Jorgenson E, Risch N (2009) Human genetic variation recognizes functional elements in non-coding sequence. Genome Res.
14. Bousquet M, Quelen C, Rosati R, Mansat-De Mas V, La Starza R, et al. (2008) Myeloid cell differentiation arrest by miR-125b-1 in myelodysplastic syndrome and acute myeloid leukemia with the t(2;11)(p21;q23) translocation. J Exp Med 205: 2499–2506.
15. Calin GA, Croce CM (2006) MicroRNAs and chromosomal abnormalities in cancer cells. Oncogene 25: 6202–6210.
16. Calin GA, Dumitru CD, Shimizu M, Bichi R, Zupo S, et al. (2002) Frequent deletions and down-regulation of micro- RNA genes miR15 and miR16 at 13q14 in chronic lymphocytic leukemia. Proc Natl Acad Sci U S A 99: 15524–15529.
17. Zhao JJ, Yang J, Lin J, Yao N, Zhu Y, et al. (2009) Identification of miRNAs associated with tumorigenesis of retinoblastoma by miRNA microarray analysis. Childs Nerv Syst 25: 13–20.
18. Foekens JA, Sieuwerts AM, Smid M, Look MP, de Weerd V, et al. (2008) Four miRNAs associated with aggressiveness of lymph node-negative, estrogen receptor-positive human breast cancer. Proc Natl Acad Sci U S A 105: 13021–13026.
19. Crosby ME, Kulshreshtha R, Ivan M, Glazer PM (2009) MicroRNA regulation of DNA repair gene expression in hypoxic stress. Cancer Res 69: 1221–1229.
20. Speleman F, De Telder V, De Potter KR, Dal Cin P, Van Daele S, et al. (1989) Cytogenetic analysis of a mesenchymal hamartoma of the liver. Cancer Genet Cytogenet 40: 29–32.
21. Li M, Lee KF, Lu Y, Clarke I, Shih D, et al. (2009) Frequent amplification of a chr19q13.41 microRNA polycistron in aggressive primitive neuroectodermal brain tumors. Cancer Cell 16: 533–546.
22. Belge G, Kazmierczak B, Meyer-Bolte K, Bartnitzke S, Bullerdiek J (1992) Expression of SV40 T-antigen in lipoma cells with a chromosomal translocation T(3;12) is not sufficient for direct immortalization. Cell Biol Int Rep 16: 339–347.
23. Roque L, Castedo S, Gomes P, Soares P, Clode A, et al. (1993) Cytogenetic findings in 18 follicular thyroid adenomas. Cancer Genet Cytogenet 67: 1–6.
24. Livak KJ, Schmittgen TD (2001) Analysis of relative gene expression data using real-time quantitative PCR and the 2(-Delta Delta C(T)) Method. Methods 25: 402–408.
25. Yu SL, Chen HY, Chang GC, Chen CY, Chen HW, et al. (2008) MicroRNA signature predicts survival and relapse in lung cancer. Cancer Cell 13: 48–57.
26. Fehr A, Roser K, Belge G, Loning T, Bullerdiek J (2008) A closer look at Warthin tumors and the t(11;19). Cancer Genet Cytogenet 180: 135–139.
27. Tabaska JE, Zhang MQ (1999) Detection of polyadenylation signals in human DNA sequences. Gene 231: 77–86.
28. Chen C, Ridzon DA, Broomer AJ, Zhou Z, Lee DH, et al. (2005) Real-time quantification of microRNAs by stem-loop RT-PCR. Nucleic Acids Res 33: e179.
29. Kievits T, Devilee P, Wiegant J, Wapenaar MC, Cornelisse CJ, et al. (1990) Direct nonradioactive in situ hybridization of somatic cell hybrid DNA to human lymphocyte chromosomes. Cytometry 11: 105–109.
30. Belge G, Garcia E, Rippe V, Fusco A, Bartnitzke S, et al. (1997) Breakpoints of 19q13 translocations of benign thyroid tumors map within a 400 kilobase region. Genes Chromosomes Cancer 20: 201–203.
31. Bol S, Belge G, Rippe V, Bullerdiek J (2001) Molecular cytogenetic investigations define a subgroup of thyroid adenomas with 2p21 breakpoints clustered to a region of less than 450 kb. Cytogenet Cell Genet 95: 189–191.

3.4 Molekulargenetische und molekularzytogenetische Untersuchungen des *PAX8/PPARγ*-Fusionsgens sowie der 3p25-Bruchpunktregion bei follikulären Schilddrüsentumoren

VII. Evidence for a 3p25 Breakpoint Hot Spot Region in Thyroid Tumors of Follicular Origin (Drieschner *et al.*, 2006)

In dieser Arbeit lag der Fokus auf der näheren Charakterisierung der Bruchpunktregion 3p25 bei einem follikulären Adenom der Schilddrüse mit einer Translokation t(2;20;3)(p21;q11.2,p25), in dem neben der Region 3p25 zudem die chromosomale Region 2p21 bzw. das dort lokalisierte *THADA* involviert sind. Innerhalb der Region 3p25 ist das Gen *PPARγ* lokalisiert, welches in follikulären Neoplasien der Schilddrüse mit einer Translokation t(2;3)(q13;p25) gemeinsam mit dem in 2q13 lokalisiertem *PAX8* das Fusionsgen *PAX8/PPARγ* bildet. Um eine mögliche Beteiligung der genomischen Region um *PPARγ* bzw. von *PPARγ* selbst nachzuweisen, wurden zum einem FISH-Analysen an der Zelllinie S325/TSV40 mit der Translokation t(2;20;3)(p21;q11.2;q25) mit BAC-Klonen durchgeführt, die die genomische Region mit *PPARγ* in 3p25 überspannen. Zum anderen erfolgten 3‘ RACE- und RT-PCR-Analysen sowie Real-Time PCR-Analysen zur quantitativen Bestimmung der Expression von *THADA*.

Anhand der 3‘-RACE- und RT-PCR Analysen konnte gezeigt werden, dass die auf Exon 28 von *THADA* folgenden Sequenzen des in der Zelllinie S325/TSV40 nachgewiesenen Fusionstranskripts *THADA-FUS3p* innerhalb des BAC-Klons RP11-167M22 bzw. des Intron 2 von *PPARγ* in 3p25 lokalisiert sind. Insgesamt ließen sich vier verschiedene Exons (I, Ia, II und III) sowie neben der Variante *THADA-FUS3p* drei weitere Spleißvarianten (*THADA-FUS3pA, -B* und *-C*) nachweisen. Mittels *in silico*-Analysen konnte gezeigt werden, dass es sich hier um nicht-kodierende Sequenzen handelt, da sich keine Homologien zu bekannten Genen bzw. ESTs fanden. Weiterhin konnte ein mögliches Fusionsgen *THADA/PPARγ* ausgeschlossen werden, da die vier nachgewiesenen Exons auf dem Minusstrang entgegen der Leserichtung von *PPARγ* orientiert sind.

FISH-Analysen mit zwei BAC-Klonen (RP11-167M22 und RP11-30G23), die die gesamte genomische Region von *PPARγ* überspannen, bestätigten die Bruchpunktlokalisation innerhalb *PPARγ*.

Insgesamt weisen die Ergebnisse auf eine Beteiligung der genomischen Region mit *PPARγ* bei follikulären Läsionen der Schilddrüse hin, unabhängig von einer Translokation t(2;3)(q13;p25) bzw. einer Beteiligung von *PAX8* in 2q13.

Die Expressionsanalysen mittels quantitativer Real-Time PCR wurden an insgesamt sieben Zelllinien von benignen Schilddrüsenläsionen, darunter neben der Zelllinie S325/TSV40 auch die Zelllinie S533/TSV40 mit einer 2p21- bzw. *THADA*-Rearrangierung, sowie an fünf Schilddrüsenkarzinom-Zelllinien durchgeführt. Dabei zeigte sich kein signifikanter Unterschied hinsichtlich der Expression in allen analysierten Zelllinien.

VII

Evidence for a 3p25 breakpoint hot spot region in thyroid tumors of follicular origin

Norbert Drieschner, Gazanfer Belge, Volkhard Rippe, Maren Meiboom, Siegfried Loeschke, J. Bullerdiek

(Thyroid 16(11): 1091-1096)

Eigenanteil:

- Planung und Durchführung der molekularzytogenetischen Untersuchungen einschließlich Etablierung eines FISH-Assays zum Nachweis von 3p25-Rearrangierungen.
- *In silico*-Analyse der 3p25-Bruchpunktregion.
- Verfassen des Artikels gemeinsam mit Jörn Bullerdiek.

THYROID
Volume 16, Number 11, 2006

Evidence for a 3p25 Breakpoint Hot Spot Region in Thyroid Tumors of Follicular Origin

N. Drieschner, G. Belge, V. Rippe, M. Meiboom, S. Loeschke, and J. Bullerdiek

Epithelial tumors of the thyroid are cytogenetically well-investigated tumors. So far, the main cytogenetic subgroups, characterized by trisomy 7 and by rearrangements of either 19q13 or 2p21, respectively, have been described. Recently, we have been able to describe the involvement of a novel gene called *THADA* in benign thyroid lesions with 2p21 rearrangements. Other fusion genes found in thyroid lesions are *RET/PTC* and *PAX8/PPARγ*. The latter occurs in follicular thyroid carcinomas with a t(2;3)(q13;p25). Here we present molecular–cytogenetic and cytogenetic investigations on a follicular thyroid adenoma with a t(2;20;3)(p21;q11.2;p25). In this case, an intronic sequence of *PPARγ* is fused to exon 28 of *THADA*. We used BAC clones containing the genomic sequence of *PPARγ* for fluorescence in situ hybridization to confirm the localization of the breakpoint within intron 2 of *PPARγ*. Our findings suggest that the close surrounding of *PPARγ* is a breakpoint hot spot region, leading to recurrent alterations of this gene in thyroid tumors of follicular origin including carcinomas as well as adenomas with or without involvement of *PAX8*.

Introduction

Benign epithelial tumors of the thyroid are cytogenetically well-investigated tumors with different cytogenetic subgroups.[1–7] Of these, translocations involving either of the two chromosomal regions 19q13 and 2p21 do not co-occur, thus indicating independent subgroups.[1,3,6,8] In addition, these translocations represent rare examples of specific cytogenetic rearrangements found in epithelial tumors.

Fluorescence in situ hybridization (FISH) studies on benign thyroid lesions with 2p21 rearrangements showed that the breakpoint is located within a chromosomal region of about 316kb.[9] Further in silico and reverse transcriptase polymerase chain reaction (RT-PCR) analyses revealed a novel gene called *THADA* (thyroid adenoma associated) located within the breakpoint region in 2p21.[10] *THADA* is rearranged in benign thyroid tumors leading to a *THADA*-fusion gene in which the 3′-part is truncated and ectopic sequences derived from the translocation partners are fused to *THADA*.[10] Other fusion genes found in thyroid tumors are *RET/PTC*[11–15] and *PAX8/PPARγ*.[16–19] *PPARγ* maps to chromosomal region 3p25, which is frequently affected by rearrangements in different thyroid tumors including papillary carcinomas, follicular carcinomas, and follicular adenomas,[5,20–22] indicating that this region represents a breakpoint hot spot region predominantly in thyroid tumors of follicular cell origin.

Here, we describe a follicular thyroid adenoma with a t(2;20;3)(p21;q11.2;p25) in which beside an involvement of *THADA* the 3p25 breakpoint was found to be involved. In order to detect whether the 3p25 breakpoint casually coincides with the mapping of *PPARγ* or if the gene itself might be rearranged, we have performed a series of molecular–cytogenetic and molecular investigations.

Materials and Methods

Tissue specimen

The tissue sample was obtained after a bilobular subtotal goiter-resection of a 49-year-old woman. Macroscopically there were several nodules (diameter up to 1.5 cm) in the right lobe and two yellowish, well-encapsulated tumors measuring up to 4.5-cm diameter in the left. From the larger of the latter tumors, an approximately 1×1×0.5-cm tissue-sample was taken and stored into Hank's solution prior to cell culture. It was prepared according to standard procedures for routine histopathologic examination, cell culture, and chromosome analysis. Histologic sections of the tumors have been checked by three experienced endocrine pathologists.

Chromosome analysis and fluorescence in situ hybridization (FISH)

For chromosome analyses and FISH studies, the cell line S325/TSV40 derived from a thyroid adenoma was used. The cell line was obtained by transfection with a construct containing the SV40 large T antigen, as reported previously.[23] Cell culture of the cell line and karyotyping of Giemsa-banded metaphases were performed as previously described for

Center for Human Genetics, University of Bremen, Bremen, Germany.

pleomorphic adenomas of the parotid gland.[24] For FISH analyses, BAC clones (167M22 and 30G23 located within *PPARγ* in 3p25) were obtained from the RP-11-Library (RZPD, Heidelberg, Germany). DNA of BAC clones was isolated using the QIAGEN Plasmid Midi Kit (QIAGEN, Hilden, Germany). FISH analyses were performed after GTG banding of the same metaphase spreads. Treatment of metaphases and subsequent FISH experiments were performed as described previously.[25] For FISH studies, BAC DNA was labeled with dig-11-dUTP by nick translation (Roche Diagnostics, Mannheim, Germany). For FISH experiments, the labeled BAC DNA was pooled (concentration: 4 ng/μL). Detection was performed with anti-dig-fluorescein fab-fragments (Roche Diagnostics). Chromosomes were counterstained with DAPI (0.025 mg/mL). For the cell line, 10 metaphases were examined. Slides were analyzed on a Zeiss Axiophot fluorescence microscope using a fluorescein isothiocyanate and DAPI filter set. Metaphases were recorded with the Power Gene Karyotyping System (Applied Imaging, Newcastle, UK).

3′ RACE and RT-PCR analysis

3′-RACE and RT-PCR experiments were performed as described previously.[10]

Real-time PCR expression analysis

Total RNA from cell cultures was isolated using the TRIzol reagent (Invitrogen, Karsruhe, Germany). Reverse transcription into cDNA was done with M-MLV Reverse Transcriptase (Invitrogen, Karsruhe, Germany). Real-time PCR was performed using the Applied Biosystems 7300 Sequence Detection System according to TaqMan Gene Expression Assay Protocol (Applied Biosystems, 2004). The amplicon spans the boundary of exon 31 to exon 32 of *THADA* and is about 60 bp in length.

Results

Histological patterns of the thyroid tissue sample

As to their predominant architectural pattern, both tumors of the left lobe were referred to as microfollicular adenomas, with few cells showing enlarged hyperchromatic nuclei. There were no mitoses seen. Also, there was no evidence for capsular or vascular invasion (Fig. 1). Accordingly, both tumors were classified as follicular adenomas.

Detection of THADA-FUS3p spliceforms and description of ectopic sequences derived from 3p25

RT-PCR with primers derived from exon 28 of *THADA* and from the sequence located in 3p25 revealed three amplification products indicating three spliceforms of *THADA-FUS3p*.[10] The splice variants are *THADA-FUS3p* with exon I (118 bp) and exon II (258 bp) derived from 3p25, *THADA-FUS3pA* with exon II, and *THADA-FUS3pB* with exons I, Ia (165 bp), and II. A fourth splice variant (*THADA-FUS3pC*) was detected by 3′-RACE analyses on S325/TSV40 and consists of exon I and exon III (321 bp) out of 3p25 (Fig. 3).

The last four exons (I, Ia, II, and III) of *THADA-FUS3p* map to the BAC clone 167M22 and are located within intron

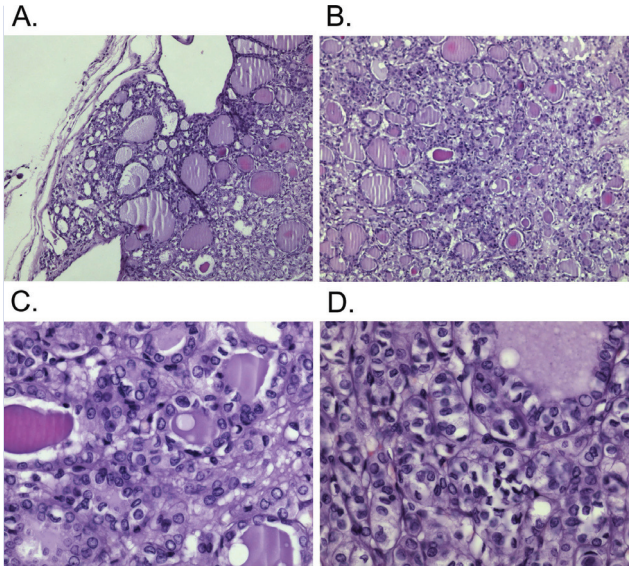

FIG. 1. Follicular thyroid adenoma with a t(2;3;20)(p21;p25;q11.2). **A:** Intact capsule and unaffected blood vessels in the periphery of the described follicular adenoma. **B:** Typical structures of the follicular adenoma. **C:** Polymorphic nuclei and cells with prominent nucleoli. **D:** Solid growth pattern.

2 of *PPARγ* (Fig. 3). Sequence analysis[26] revealed that exon Ia, II, and III do not show homologies with any described gene structure (including ESTs), whereas exon I is only homologous to Alu repetitive elements. Thus, there is no evidence for a novel gene located within intron 2 of *PPARγ*. The exons are located within a genomic region of 5681 bp on the minus strand whereas *PPARγ* is located on the plus strand indicating that a *THADA/PPARγ* fusion gene can be excluded. The localization of the breakpoint in 3p25 in the cell line S325/TSV40 is shown in Figure 3.

Chromosome analysis of S325/TSV40 and delineation of the breakpoint located within 3p25

Karyotyping of metaphases of S325/TSV40 revealed that the cell line S325/TSV40 is characterized by a translocation t(2;20;3)(p21;q11.2;p25) (Fig. 2A) as described previously.[9,10]

FISH was performed with two BAC clones (167M22 and 30G23) containing the complete genomic sequence of *PPARγ* (Fig. 3) to confirm the results based on RT-PCR and in silico analyses. Signals were seen on der(2), der(3), and the normal chromosome 3 (Fig. 2B), thus confirming that the breakpoint lies within *PPARγ* without involvement of chromosomal region 2q13 and *PAX8*, respectively.

Expression analysis of wild-type THADA

Expression of wild-type *THADA* was analyzed with real-time PCR. The analysis included beneath the cell line S325/TSV40 six additional cell lines from benign thyroid lesion (including another one with a previously described *THADA* fusion gene[10]) as well as five cell lines deriving from malignant thyroid lesions. Besides the two benign thyroid lesions with 2p21 rearrangements, respectively, *THADA*

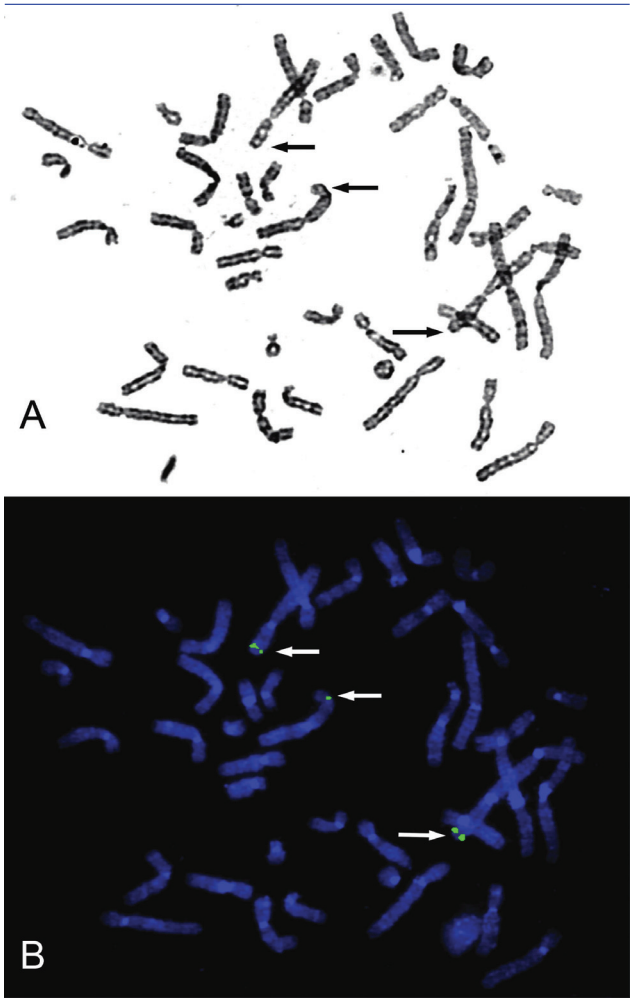

FIG. 2. 3p25 rearrangement in a thyroid adenoma. **A:** G-banded metaphase of the cell line S325/TSV40 with a t(2;20;3)(p21;q11.2;p25) (arrows indicate the derivative chromosomes). **B:** The same metaphase after fluorescence in situ hybridization with *PPARγ* containing BAC clones 167M22 and 30G23 (signals are marked by arrows) demonstrating rearrangement of *PPARγ*.

fusion genes, there was no cell line with 2p21 rearrangement. As control, a cell line deriving from fibroblasts was used. In comparison, between all cell lines no significant difference of the *THADA* expression was found (data not shown).

Discussion

Recently, we were able to describe fusion genes between *THADA*, a putative death receptor interacting protein, and ectopic sequences derived from the chromosomal translocation partners in benign thyroid lesions with rearrangements of chromosomal band 2p21.[10] In the cell line S325/TSV40 with a t(2;20;3)(p21;q11.2;p25) as well as in the cell line S533/TSV40 with a t(2;7)(p21;p15), sequences located within the translocation partners of 2p21 are fused to exon 28 of *THADA (THADA-FUS3p* and *THADA-FUS7p)*. The occurrence of similar fusion genes involving *THADA* in two different benign thyroid lesions and the truncation of the ORF in both fusion genes directly after exon 28 suggests that truncation of the 3′-part of *THADA* is the critical event in the investigated benign thyroid tumors.[10] This will be supported by the suggestion that tumor type-specific chromosomal rearrangements leading to fusion genes are involved in the early development of many neoplasias, including solid tumors.[27] Thus, 2p21 rearrangements and *THADA* rearrangements, respectively, as solely changes observed in benign thyroid tumors, seem to be an important event in the early development in these tumors.

Expression analysis of the unaltered *THADA* mRNA by real-time PCR revealed no significant changes of the expression level in the cell lines with 2p21 rearrangements compared to thyroid cell lines without 2p21 rearrangements (data not shown). This seems to be evidence that the truncated THADA protein has no influence on the expression of the wild-type THADA.

Interestingly, the breakpoint in the cell line S325/TSV40 derived from a follicular thyroid adenoma maps to chromosomal region 3p25, in which *PPARγ*, a gene encoding for the peroxisome proliferator-activated receptor, is located.[28] The sequences fused to *THADA* are located within intron 2 of *PPARγ*. They do not have homologies to any described gene structure and are located on the minus strand within 3p25, whereas *PPARγ* is located on the plus strand. Thus, there is no evidence for fusion of *PPARγ* with *THADA* in accordance with the results from 3′RACE analysis showing no evidence of a *THADA/PPARγ* fusion.

Specific chromosomal translocations encoding fusion oncogenes are common in leukemias/lymphomas and sarcomas.[29] Chromosomal rearrangements in epithelial tumors are well described for lesions of the thyroid including carcinomas and adenomas.[3,6,8,21,27,30] Of those, t(2;3)(q13;p25) is a recurrent finding in human follicular thyroid adenomas and carcinomas.[5,21,22,31] Fine mapping and molecular characterization of the 2q13 and 3p25 translocation breakpoint regions revealed fusion between exons 1 to 7, 1 to 8, or 1 to 9 of *PAX8* (2q13) and exons 1 to 6 of *PPARγ* (3p25).[17] The occurrence of *PAX8/PPARγ* seems to be restricted to follicular thyroid carcinomas, suggesting that the molecular pathogenesis of follicular thyroid carcinomas with *PAX8/PPARγ* fusion is different compared to other thyroid lesions and that *PAX8/PPARγ* may aid as marker for differential diagnosis, e.g., in fine needle aspiration biopsies.[17,19,32–34] However, other publications describe the detection of *PAX8/PPARγ* in follicular thyroid carcinomas as well as in adenomas.[16,18] The authors conclude that *PAX8/PPARγ* fusion genes are not specific for follicular carcinomas, corresponding to previous cytogenetic studies revealing the t(2;3)(q13;p25) in follicular adenomas.[5,21,31]

Nevertheless the involvement of 3p25 in chromosomal aberrations (including t(2;3)(q13;p25)) is a common finding in tumors of the thyroid.[4,5,9,20–22,31,35,36] Our findings suggest that alterations of 3p25 affecting *PPARγ* could occur without involvement of 2q13 and *PAX8*, respectively. On the basis of our FISH results we can exclude that the translocation of part of *PPARγ* on chromosome 2 is indeed part of a more complex translocation leading to the typical t(2;3)(q13;p25) as well. *PPARγ* rearrangements without involvement of 2q13 detected by FISH have been described previously.[17] In another

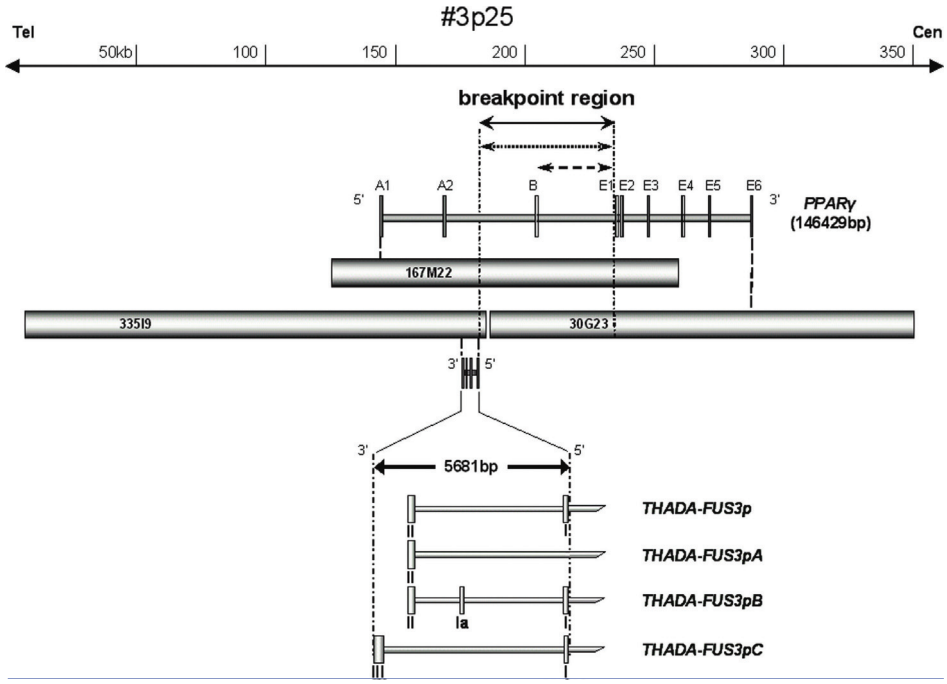

FIG. 3. Genomic organization of *PPARγ* and last exons of *THADA-FUS3p* (splice forms enlarged) in relation to BAC clones (gray bars) located within breakpoint region in #3p25. The breakpoint region (continuous line) consists of the breakpoint localization in S325/TSV40 within intron 2 to 3 of *PPARγ* (dotted line) and the putative breakpoint localization in cases with *PAX8/PPARγ* fusion (dashed line).[17] Note that the orientation of *PPARγ* is opposite to the last exons of *THADA-FUS3p* and *THADA*, respectively, indicating the exclusion of a *THADA/PPARγ* fusion.

study, Western analysis identified an altered protein size for PPARγ in 7 of 86 thyroid tumors studied, whereas PAX8 was expressed unaltered in these tumors, suggesting the involvement of alternative PPARγ fusion partners.[34] This indicates that this region located within *PPARγ* is prone to breakage and maps to intron 2 to 3 of *PPARγ*.

The region 3p25-26 was previously described as a novel breakpoint cluster region in papillary thyroid carcinomas.[22] We suggest that a common breakpoint region in 3p25 is located within *PPARγ*, because of the several described rearrangements of 3p25 found in the literature.[4,5,9,20–22,31,35,36] Besides the t(2;3)(q13;p25), which results in the fusion of *PAX8* and *PPARγ*, other translocations involving 3p25 were detected in thyroid tumors.[4,35,36] In our case, S325/TSV40 with a t(2;20;3)(p21;q11.2;p25), we were able to map the breakpoint in 3p25 within intron 2 to 3 of *PPARγ*, a site that corresponds with the previously described breakpoint location in cases with *PAX8/PPARγ* fusion genes.[17] To our knowledge, it is the second described follicular tumor but the first follicular thyroid adenoma in which *PPARγ* is rearranged without involvement of 2q13. Interestingly, two chromosomal regions, i.e., 2p21 and 3p25, respectively, two genes, *THADA* and *PPARγ*, are both affected in this follicular thyroid adenoma. Rearrangements of 2p21 characterize a main cytogenetic subgroup in benign thyroid lesions.[3,4] For this reason, and because of the involvement of *THADA* in two different benign thyroid lesions,[10] the *THADA*-rearrangement seems to be the critical event in this follicular thyroid adenoma. Another reason may be the finding that *PAX8/PPARγ* fusion genes seem to be restricted to follicular thyroid carcinomas.[17,19,32–34] Nevertheless, the occurrence of a fusion gene involving *PPARγ* and an unknown gene located in 20q11.2 cannot be excluded in the present case. An altered expression level of *PPARγ* due to the rearrangement of *PPARγ* resulting from the 3p25 alteration was not tested. In a recent publication, only a downregulation of *PPARγ* expression in papillary thyroid carcinomas as well as Graves' disease was noted,[37] whereas benign thyroid lesions as well as follicular thyroid carcinomas did not show alteration of *PPARγ* expression. Furthermore, the expression level in adenomas broadly varied among the analyzed samples.[37]

It will be of interest to see whether different *PPARγ* rearrangements occur in other tumors as well. These rearrangements could lead to fusion of *PPARγ* and other genes than *PAX8* located on the translocation partners. FISH studies with BAC clones containing *PPARγ* on such cases are an appropriate method for detection of *PPARγ* rearrangements. This will be helpful to uncover the molecular mechanisms leading to accumulation of breakpoints located within intron 2 to 3 of *PPARγ* in tumors of the thyroid.

References

1. Bartnitzke S, Herrmann ME, Lobeck H, Zuschneid W, Neuhaus P, Bullerdiek J 1989 Cytogenetic findings on eight follicular thyroid adenomas including one with a t(10;19). Cancer Genet Cytogenet **39:**65–68.
2. Belge G, Thode B, Rippe V, Bartnitzke S, Bullerdiek J 1994 A characteristic sequence of trisomies starting with trisomy 7 in benign thyroid tumors. Hum Genet **94:**198–202.

3. Belge G, Roque L, Soares J, Bruckmann S, Thode B, Fonseca E, Clode A, Bartnitzke S, Castedo S, Bullerdiek J 1998 Cytogenetic investigations of 340 thyroid hyperplasias and adenomas revealing correlations between cytogenetic findings and histology. Cancer Genet Cytogenet **101:**42–48.
4. Bol S, Belge G, Thode B, Bartnitzke S, Bullerdiek J 1999 Structural abnormalities of chromosome 2 in benign thyroid tumors. Three new cases and review of the literature. Cancer Genet Cytogenet **114:**75–77.
5. Bondeson L, Bengtsson A, Bondeson AG, Dahlenfors R, Grimelius L, Wedell B, Mark J 1989 Chromosome studies in thyroid neoplasia. Cancer **64:**680–685.
6. Roque L, Castedo S, Clode A, Soares J 1992 Translocation t(5;19): a recurrent change in thyroid follicular adenoma. Genes Chromosomes Cancer **4:**346–347.
7. Teyssier JR, Liautaud-Roger F, Ferre D, Patey M, Dufer J 1990 Chromosomal changes in thyroid tumors. Relation with DNA content, karyotypic features, and clinical data. Cancer Genet Cytogenet **50:**249–263.
8. Cigudosa JC, Pedrosa Guerra A, Otero Gomez A, Carrasco Juan JL, Perez Gomez JA, Ferrer Roca OF, Garcia Miranda JL 1995 Translocation (5;19)(q13;q13) in a multinodular thyroid goiter. Cancer Genet Cytogenet **82:**67–69.
9. Bol S, Belge G, Rippe V, Bullerdiek J 2001 Molecular cytogenetic investigations define a subgroup of thyroid adenomas with 2p21 breakpoints clustered to a region of less than 450 kb. Cytogenet Cell Genet **95:**189–191.
10. Rippe V, Drieschner N, Meiboom M, Escobar HM, Bonk U, Belge G, Bullerdiek J 2003 Identification of a gene rearranged by 2p21 aberrations in thyroid adenomas. Oncogene **22:** 6111–6114.
11. Rabes HM, Klugbauer S 1998 Molecular genetics of childhood papillary thyroid carcinomas after irradiation: high prevalence of RET rearrangement. Recent Results Cancer Res **154:**248–264.
12. Sarasin A, Bounacer A, Lepage F, Schlumberger M, Suarez HG 1999 Mechanisms of mutagenesis in mammalian cells. Application to human thyroid tumours. C R Acad Sci III **322:**143–149.
13. Schlumberger M, Cailleux AF, Suarez HG, de Vathaire F 1999 Irradiation and second cancers. The thyroid as a case in point. C R Acad Sci III **322:**205–213.
14. Sozzi G, Bongarzone I, Miozzo M, Borrello MG, Blutti MG, Pilotti S, Della Porta G, Pierotti MA 1994 A t(10;17) translocation creates the RET/PTC2 chimeric transforming sequence in papillary thyroid carcinoma. Genes Chromosomes Cancer **9:**244–250.
15. Tallini G 2002 Molecular pathobiology of thyroid neoplasms. Endocr Pathol **13:**271–288.
16. Cheung L, Messina M, Gill A, Clarkson A, Learoyd D, Delbridge L, Wentworth J, Philips J, Clifton-Bligh R, Robinson BG 2003 Detection of the PAX8-PPARgamma fusion oncogene in both follicular thyroid carcinomas and adenomas. J Clin Endocrinol Metab **88:**354–357.
17. Kroll TG, Sarraf P, Pecciarini L, Chen CJ, Mueller E, Spiegelman BM, Fletcher JA 2000 PAX8-PPARgamma1 fusion oncogene in human thyroid carcinoma [corrected]. Science **289:**1357–1360.
18. Marques AR, Espadinha C, Catarino AL, Moniz S, Pereira T, Sobrinho LG, Leite V 2002 Expression of PAX8-PPAR gamma 1 rearrangements in both follicular thyroid carcinomas and adenomas. J Clin Endocrinol Metab **87:**3947–3952.
19. Nikiforova MN, Biddinger PW, Caudill CM, Kroll TG, Nikiforov YE 2002 PAX8-PPARgamma rearrangement in thyroid tumors: RT-PCR and immunohistochemical analyses. Am J Surg Pathol **26:**1016–1023.
20. Rodrigues-Serpa A, Catarino A, Soares J 2003 Loss of heterozygosity in follicular and papillary thyroid carcinomas. Cancer Genet Cytogenet **141:**26–31.
21. Sozzi G, Miozzo M, Cariani TC, Bongarzone I, Pilotti S, Pierotti MA, Della Porta G 1992 A t(2;3)(q12-13;p24-25) in follicular thyroid adenomas. Cancer Genet Cytogenet **64:**38–41.
22. Roque L, Nunes VM, Ribeiro C, Martins C, Soares J 2001 Karyotypic characterization of papillary thyroid carcinomas. Cancer **92:**2529–2538.
23. Belge G, Kazmierczak B, Meyer-Bolte K, Bartnitzke S, Bullerdiek J 1992 Expression of SV40 T-antigen in lipoma cells with a chromosomal translocation T(3;12) is not sufficient for direct immortalization. Cell Biol Int Rep **16:**339–347.
24. Bullerdiek J, Boschen C, Bartnitzke S 1987 Aberrations of chromosome 8 in mixed salivary gland tumors—cytogenetic findings on seven cases. Cancer Genet Cytogenet **24:**205–212.
25. Kievits T, Dauwerse JG, Wiegant J, Devilee P, Breuning MH, Cornelisse CJ, van Ommen GJ, Pearson PL 1990 Rapid subchromosomal localization of cosmids by nonradioactive in situ hybridization. Cytogenet Cell Genet **53:**134–136.
26. Altschul SF, Madden TL, Schaffer AA, Zhang J, Zhang Z, Miller W, Lipman DJ 1997 Gapped BLAST and PSI-BLAST: a new generation of protein database search programs. Nucleic Acids Res **25:**3389–3402.
27. Aman P 1999 Fusion genes in solid tumors. Semin Cancer Biol **9:**303–318.
28. Greene ME, Blumberg B, McBride OW, Yi HF, Kronquist K, Kwan K, Hsieh L, Greene G, Nimer SD 1995 Isolation of the human peroxisome proliferator activated receptor gamma cDNA: expression in hematopoietic cells and chromosomal mapping. Gene Expr **4:**281–299.
29. Rabbitts TH 1994 Chromosomal translocations in human cancer. Nature **372:**143–149.
30. Herrmann ME, Mohamed A, Talpos G, Wolman SR 1991 Cytogenetic study of a papillary thyroid carcinoma with a rearranged chromosome 10. Cancer Genet Cytogenet **57:** 209–217.
31. Roque L, Castedo S, Clode A, Soares J 1993 Deletion of 3p25→pter in a primary follicular thyroid carcinoma and its metastasis. Genes Chromosomes Cancer **8:**199–203.
32. Fuhrer D 2001 A nuclear receptor in thyroid malignancy: Is PAX8/PPARgamma the Holy Grail of follicular thyroid cancer? Eur J Endocrinol **144:**453–456.
33. Nikiforova MN, Lynch RA, Biddinger PW, Alexander EK, Dorn GW 2nd, Tallini G, Kroll TG, Nikiforov YE 2003 RAS point mutations and PAX8-PPARgamma rearrangement in thyroid tumors: Evidence for distinct molecular pathways in thyroid follicular carcinoma. J Clin Endocrinol Metab **88:** 2318–2326.
34. Dwight T, Thoppe SR, Foukakis T, Lui WO, Wallin G, Hoog A, Frisk T, Larsson C, Zedenius J 2003 Involvement of the PAX8/peroxisome proliferator-activated receptor gamma rearrangement in follicular thyroid tumors. J Clin Endocrinol Metab **88:**4440–4445.
35. Lui WO, Kytola S, Anfalk L, Larsson C, Farnebo LO 2000 Balanced translocation (3;7)(p25;q34): another mechanism of tumorigenesis in follicular thyroid carcinoma? Cancer Genet Cytogenet **119:**109–112.

36. Jenkins RB, Hay ID, Herath JF, Schultz CG, Spurbeck JL, Grant CS, Goellner JR, Dewald GW 1990 Frequent occurrence of cytogenetic abnormalities in sporadic nonmedullary thyroid carcinoma. Cancer **66:**1213–1220.
37. Karger S, Berger K, Eszlinger M, Tannapfel A, Dralle H, Paschke R, Fuhrer D 2005 Evaluation of peroxisome proliferator-activated receptor-gamma expression in benign and malignant thyroid pathologies. Thyroid **15:**997–1003.

Address reprint request to:
Jörn Bullerdiek
Center for Human Genetics
University of Bremen
Leobenerstr/ZHG
D-28359 Bremen, Germany

E-mail: bullerd@uni-bremen.de

VIII. On the prevalence of the *PAX8/PPARγ* fusion resulting from the chromosomal translocation t(2;3)(q13;p25) in adenomas of the thyroid (Klemke *et al.*, 2011b)

Ziel dieser Arbeit war der Nachweis und die Bestimmung der Häufigkeit der Translokation t(2;3)(q13;p25) bei follikulären Adenomen der Schilddrüse.

Zytogenetisch konnte unter 192 follikulären Adenomen der Schilddrüse eine t(2;3)(q13;p25) insgesamt in zwei Fällen nachgewiesen werden. Zudem wurde in beiden Tumoren eine Rearrangierung von *PPARγ* mittels I-FISH an Touchpräparaten unter Verwendung einer *PPARγ* Break-Apart Sonde molekularzytogenetisch bestätigt. Beide Tumoren wurden histologisch als follikuläre Adenome klassifiziert, was auch gestützt wird durch eine quantitative Real-Time PCR von *HMGA2*, die gegenüber histologisch unauffälligem Schilddrüsengewebe nicht erhöht war. Gemäß Belge *et al.* (2008) ist das Expressionslevel von *HMGA2* geeignet zur Differenzierung follikulärer Adenome von follikulären Karzinomen der Schilddrüse, die eine signifikant erhöhte Expression von *HMGA2* gegenüber Adenomen und Normalgewebe der Schilddrüse aufweisen.

RT-PCR-Untersuchungen zum molekulargenetischen Nachweis des Fusionsgen *PAX8*/*PPARγ* wurden an insgesamt 21 Tumoren durchgeführt, darunter die beiden mit der zytogenetisch und molekularzytogenetisch nachgewiesenen Translokation t(2;3)(q13;p25) sowie 19 zytogenetisch unauffällige Adenome. Beide Fälle mit einer t(2;3)(q13;p25) waren hierbei positiv bezüglich des Fusionsgen *PAX8*/*PPARγ*, wohingegen in keinem der zytogenetisch unauffälligen Adenome ein Fusionstranskript nachweisbar war.

VIII

On the prevalence of the *PAX8/PPARγ* fusion resulting from the chromosomal translocation t(2;3)(q13;p25) in adenomas of the thyroid

Markus Klemke, Norbert Drieschner, Anne Laabs, Volkhard Rippe, Gazanfer Belge, Jörn Bullerdiek, Wolfgang Sendt

(Cancer Genetics 204(6): 334-339)

Eigenanteil:

- Planung, Durchführung und Auswertung der molekularzytogenetischen Untersuchungen.

ELSEVIER

Cancer Genetics 204 (2011) 334–339

Cancer Genetics

BRIEF COMMUNICATION

On the prevalence of the *PAX8-PPARG* fusion resulting from the chromosomal translocation t(2;3)(q13;p25) in adenomas of the thyroid

Markus Klemke [a], Norbert Drieschner [a], Anne Laabs [a], Volkhard Rippe [a], Gazanfer Belge [a], Jörn Bullerdiek [a,b,*], Wolfgang Sendt [c]

[a] *Center for Human Genetics, University of Bremen, Leobener Strasse ZHG, Bremen, Germany;* [b] *Clinic for Small Animals and Research Cluster REBIRTH, University of Veterinary Medicine, Hannover, Germany;* [c] *Department of General and Visceral Surgery, St. Joseph-Stift Hospital Bremen, Bremen, Germany*

The chromosomal translocation t(2;3)(q13;p25) characterizes a subgroup of tumors originating from the thyroid follicular epithelium and was initially discovered in a few cases of adenomas. Later, a fusion of the genes *PAX8* and *PPARG* resulting from this translocation was frequently observed in follicular carcinomas and considered as a marker of follicular thyroid cancer. According to subsequent studies, however, this rearrangement is not confined to carcinomas but also occurs in adenomas, with considerably varying frequencies. Only five cases of thyroid adenomas with this translocation detected by conventional cytogenetics have been documented. In contrast, studies using reverse-transcription polymerase chain reaction (RT-PCR) detected fusion transcripts resulting from that translocation in an average of 8.2% of adenomas. The aim of this study was to determine the frequency of the *PAX8-PPARG* fusion in follicular adenomas and to use the *HMGA2* mRNA level of such tumors as an indicator of malignancy. In cytogenetic studies of 192 follicular adenomas, the t(2;3)(q13;p25) has been identified in only two cases described herein. Histopathology revealed no evidence of malignancy in either case, and, concordantly, *HMGA2* mRNA levels were not elevated. In summary, the fusion is a rare event in follicular adenomas and its prevalence may be overestimated in many RT-PCR–based studies.

Keywords Follicular thyroid neoplasia, t(2;3)(q13;p25), *PAX8-PPARG* fusion, *HMGA2*

Distinguishing follicular thyroid carcinomas (FTC) from adenomas cytologically represents a major diagnostic challenge because of their similar appearance, so there is a need for specific markers (1). The chromosomal t(2;3)(q13;p25) is a recurrent cytogenetic aberration in follicular neoplasias of the thyroid leading to a fusion of the genes encoding the thyroid-specific transcription factor PAX8 and the peroxisome proliferator–activated receptor gamma (PPARγ). Although the translocation had been reported before in adenomas as well (2–4), the *PAX8-PPARG* rearrangement was considered a marker of FTC in a study by Kroll et al., who detected *PAX8-PPARG* fusion transcripts in 5/8 FTCs but in none of 20 follicular adenomas (FA), 10 papillary carcinomas, and 10 multinodular hyperplasias (5). Accordingly, it was proposed that the *PAX8-PPARG* fusion may aid the differential diagnosis of follicular neoplasias. The presence of the fusion gene in follicular thyroid carcinomas has been confirmed by several studies, even though its prevalence seems to be lower than initially reported (Table 1A). It occurs in FA, however, with a prevalence reported to range between 0.0 and 54.5% (for references, see Table 1A). Herein, we present two novel cases of thyroid adenomas that harbor the t(2;3)(q13;p25) and express low levels of *HMGA2*, a molecular marker to distinguish between benign and malignant thyroid tumors (6–9).

Materials and methods

Tissue samples

Tumor samples were snap-frozen in liquid nitrogen immediately after surgery and stored at −80°C for RNA isolation.

Received October 18, 2010; received in revised form April 28, 2011; accepted May 3, 2011.

* Corresponding author.
E-mail address: bullerd@uni-bremen.de

2210-7762/$ - see front matter © 2011 Elsevier Inc. All rights reserved.
doi:10.1016/j.cancergen.2011.05.001

Table 1 Prevalence of *PAX8-PPARG* rearrangements in follicular neoplasias of the thyroid

A. Prevalence of *PAX8-PPARG* fusion transcripts according to RT-PCR–based studies

Reference	FA with fusion of *PAX8–PPARG*	Total number of FA	Frequency (%)	FTC with fusion of *PAX8–PPARG*	Total number of FTC	Frequency (%)	FISH performed in addition to PCR
Kroll et al. (5)	0	20	0.0	5	8	62.5	Yes
Marques et al. (22)[a]	2	16	12.5	5	9	55.6	No
Nikiforova et al. (21)	2	25	8.0	8	15	53.3	No
Martelli et al. (23)	–	–	–	0	5	0.0	No
Cheung et al. (19)	6	11	54.5	6	17	35.3	No
Aldred et al. (24)	–	–	–	2	19	10.5	No
Nikiforova et al. (25)	1	23	4.3	5	17	29.4	No[b]
Dwight et al. (26)	1	40	2.5	4[c]	34	11.8	Yes
Hibi et al. (27)	0	12	0.0	0	6	0.0	Yes
Lacroix et al. (28)	1	26	3.8	4	21	19.0	No
Nakabashi et al. (29)	3	10	30.0	4	12	33.3	No
Sahin et al. (30)[a]	–	–	–	8	10	57.4	No
Giordano et al. (31)	0	10	–	8	13	61.5	No
Di Cristofaro et al. (32)	0	9	0.0	9	21	42.9	No
Banito et al. (33)[d]	5	40	12.5	7	17	41.2	Yes
Algeciras-Schimnich et al. (20)	2	39	5.1	13	21	61.9	Yes
Overall prevalence	23	281	8.2	88	245	35.9	

B. Prevalence of the chromosomal t(2;3)(q13;p25) according to cytogenetic studies

Reference	FA with t(2;3)	Total number of FA	Frequency of translocation (%)	Translocation	Case no.
Teyssier et al. (2)	1	42	2.4	t(2;3)(q12;p24)	43
Antonini et al. (13)	0	6	0.0	–	–
Sozzi et al. (3)	2	5	40.0	t(2;3)(q12-13;p24-25)	1 and 2
Roque et al. (4)	1	18	5.6	t(2;3)(q13;p25)	6
Belge et al. (14)	0	69	0.0	–	–
Roque et al. (15)	1	6	16.7	t(2;3)(q13;p25)	10
Overall prevalence	5	146	3.4		

C. Prevalence of the *PAX8–PPARG* rearrangement according to FISH-based studies

Reference	FA with *PAX8–PPARG* rearrangement	Total number of FA	Frequency of rearrangement (%)
French et al. (16)	0	40	0.0
Castro et al. (17)	3	9	33.3
Chia et al. (18)	0	24	0.0
Overall prevalence	3	73	4.1

(A) Summary of 16 RT-PCR–based studies on follicular adenomas as well as carcinomas. Some studies additionally performed FISH experiments, as indicated in the last column. [a]Immunohistochemical results excluded. [b]FISH was performed on 16 additional carcinomas, but not on the 40 cases listed here. [c]Six FTCs were positive for rearrangement in FISH analysis. [d]Authors do not state the results of FISH and RT-PCR separately. (B) Cytogenetic studies on the chromosomal t(2;3)(q13;p25) in follicular thyroid adenomas. (C) Summary of studies in which the *PAX8-PPARG* rearrangement was detected by FISH.

For cell cultures, tissues were kept in Hank's solution with 200 IU/mL penicillin and 200 μg/mL streptomycin.

Cell culture and chromosome analyses

Tissue samples of surgically removed thyroid tumors were minced and treated with 0.26% (200 U/mL) collagenase (Serva, Heidelberg, Germany) for 3–5 hours. After centrifugation, the pellet was re-suspended in culture medium (TC 199 with Earle's salts supplemented with 20% fetal bovine serum, 200 IU/mL penicillin, 200 μg/ml streptomycin) and incubated at 37°C and 5% CO_2. Exponentially growing cultures of thyroid cells were used for GTG banding and chromosome analyses according to routine methods. Karyotype description followed ISCN 2009 (10). A total of 192 tumor samples were karyotyped successfully.

Fluorescence in situ hybridization (FISH)

For the detection of rearrangements of the *PPARG* gene, interphase FISH (I-FISH) with a PPARG break-apart probe (PanPath, Budel, The Netherlands) was performed on touch preparations. For one slide, 10 μL of the PPARG break-apart probe was used. Co-denaturation was performed on

a Mastercycler gradient (Eppendorf, Hamburg, Germany) for 3 minutes at 80°C followed by overnight hybridization in a humidified chamber at 37°C. Post-hybridization was performed at 61°C for 5 minutes in 0.1 × standard saline citrate (SSC). Interphase nuclei were finally counterstained with DAPI (0.75 μg/mL; Vector Laboratories, Burlingame, CA). Slides were examined with an Axioskop 2 plus fluorescence microscope (Zeiss, Göttingen, Germany). Images were captured with an AxioCam MRm digital camera and edited with AxioVision (Zeiss, Göttingen, Germany). At least 200 non-overlapping nuclei were scored. For determination of cut-off values, signal patterns of 200 non-overlapping nuclei of control specimens (i.e., touch preparations of four previously frozen normal thyroid tissue samples) were determined. Cut-off values were defined as the mean plus three standard deviations (M + 3SD) of the number of nuclei with abnormal signal patterns in control specimens (11). Nuclei with two co-localized red/green signals (RG) were scored as normal. Nuclei with one co-localized red/green signal, one single red, and one single green signal (1RG1R1G) were scored as positive for a *PPARG* rearrangement.

RNA isolation and reverse-transcription polymerase chain reaction (RT-PCR)

RNA was isolated from frozen tissue samples with the RNeasy Mini Kit (Qiagen, Hilden, Germany). Reverse transcription was performed using M-MLV RT (Invitrogen, Darmstadt, Germany) according to the manufacturer's instructions. For the detection of fusion transcripts, three different primers specific for *PAX8* (5′-GCC ACC AAG TCC CTG AGT CC-3′, exon 5; 5′-GCA TTG ACT CAC AGA GCA GCA-3′, exon 7; 5′-GCT CAA CAG CAC CCT GGA-3′, exon 8) were used in combination with a *PPARG*-specific reverse primer (5′-CAT TAC GGA GAG ATC CAC GG-3′). PCR was performed with DreamTaq DNA polymerase (Fermentas, St. Leon-Rot, Germany). Reaction conditions were as follows: 5 minutes at 95°C followed by 41 cycles of 30 seconds at 95°C, 30 seconds at 60°C, and 1 minute at 72°C, and a final elongation at 72°C for 5 minutes. PCR products were separated by agarose gel electrophoresis, distinct bands were excised from the gel, and the DNA was extracted with the Gel Extraction Kit (Qiagen). The purified PCR products were sequenced directly (Eurofins MWG Operon, Ebersberg, Germany). Two tumors with a known chromosomal t(2;3)(q13;p25) and 19 karyotypically normal tumors were used for RT-PCR.

Quantitative real-time PCR

The relative quantification of *HMGA2* expression was performed with the *HMGA2*-specific TaqMan assay Hs00171569_m1 (Applied Biosystems, Darmstadt, Germany), as described elsewhere (6), on a 7300 Real-Time PCR System (Applied Biosystems). For the detection of the endogenous control *HPRT1*, primers 5'-GGC AGT ATA ATC CAA AGA TGG TCA A-3′ and 5′-GTC TGG CTT ATA TCC AAC ACT TCG T-3′ were used in combination with the *HPRT1*-specific hydrolysis probe 6FAM-CAA GCT TGC TGG TGA AAA GGA CCC C-TAMRA.

Results

Cytogenetic analyses identified a chromosomal t(2;3)(q13;p25) as the sole clonal aberration in two thyroid tumors classified as follicular adenomas by routine histological examinations (Figure 1A): The first tumor (case 1) was 2.5 cm in diameter and was removed from the right thyroid lobe of a 25-year-old female patient. The second tumor harboring the translocation (case 2) measured 3.7 cm in diameter and was found during pathologic examination of a nodular goiter of a 36-year-old female patient. In addition to hematoxylin and eosin staining, sections were also Elastica van Gieson (EvG)-stained. A microfollicular growth pattern but no invasive growth of the tumor was noted, which was accordingly classified as microfollicular adenoma. The t(2;3)(q13;p25) was also confirmed by FISH on interphase nuclei (Figure 1B).

RT-PCR was performed on both tumors with the chromosomal translocation, as well as on 19 adenomas with an apparently normal karyotype, to detect *PAX8-PPARG* fusion transcripts. It was positive in both cases with the translocation, but in none of the cases with an apparently normal karyotype. The PCR products of the two positive cases were sequenced directly to confirm their identity. In case 1, two different fusion transcripts consisting of exons 1−7 and 1−10, respectively, of *PAX8* fused to *PPARG* were found. Three different fusion transcripts consisting of *PAX8* exons 1−7, 1−8, and 1−9, respectively, fused to *PPARG* were identified in case 2 (Figure 1C).

Finally, we have quantified the *HMGA2* mRNA level, which was not elevated in the two adenomas with the *PAX8-PPARG* fusion, compared to histologically normal thyroid tissue (data not shown).

Discussion

When *PAX8-PPARG* fusion transcripts were discovered in follicular thyroid carcinomas with a t(2;3), it was suggested that this gene fusion was a useful marker for the diagnosis of follicular neoplasias of the thyroid (5). Subsequent studies, however, reported lower occurrence rates of the fusion transcripts in follicular carcinomas than initially reported. While this gene fusion seems to characterize a distinct subgroup of follicular thyroid tumors, it is not specific for malignant tumors, because it has also been detected in follicular adenomas (Table 1A).

In our series of 192 follicular adenomas, the t(2;3)(q13;p25) was detected in only two tumors by conventional cytogenetics. Histologic examination revealed no evidence for malignancy in either case. In addition, *HMGA2* mRNA levels (6−9) were not elevated in the two tumors with the translocation, compared to histologically normal thyroid tissue. By RT-PCR and sequencing of PCR products, fusion transcripts of *PAX8* and *PPARG* were detected in both cases. Hence, it was shown that the chromosomal translocation led to the same gene fusion that was initially described for FTC.

Based on cytogenetic analyses, the translocation leading to the *PAX8-PPARG* fusion is a rare finding in thyroid adenomas. The Mitelman Database (12) was searched for cases of FA harboring a t(2;3)(q12~13;p24~25) chromosomal translocation (last checked on February 25, 2011). Previous

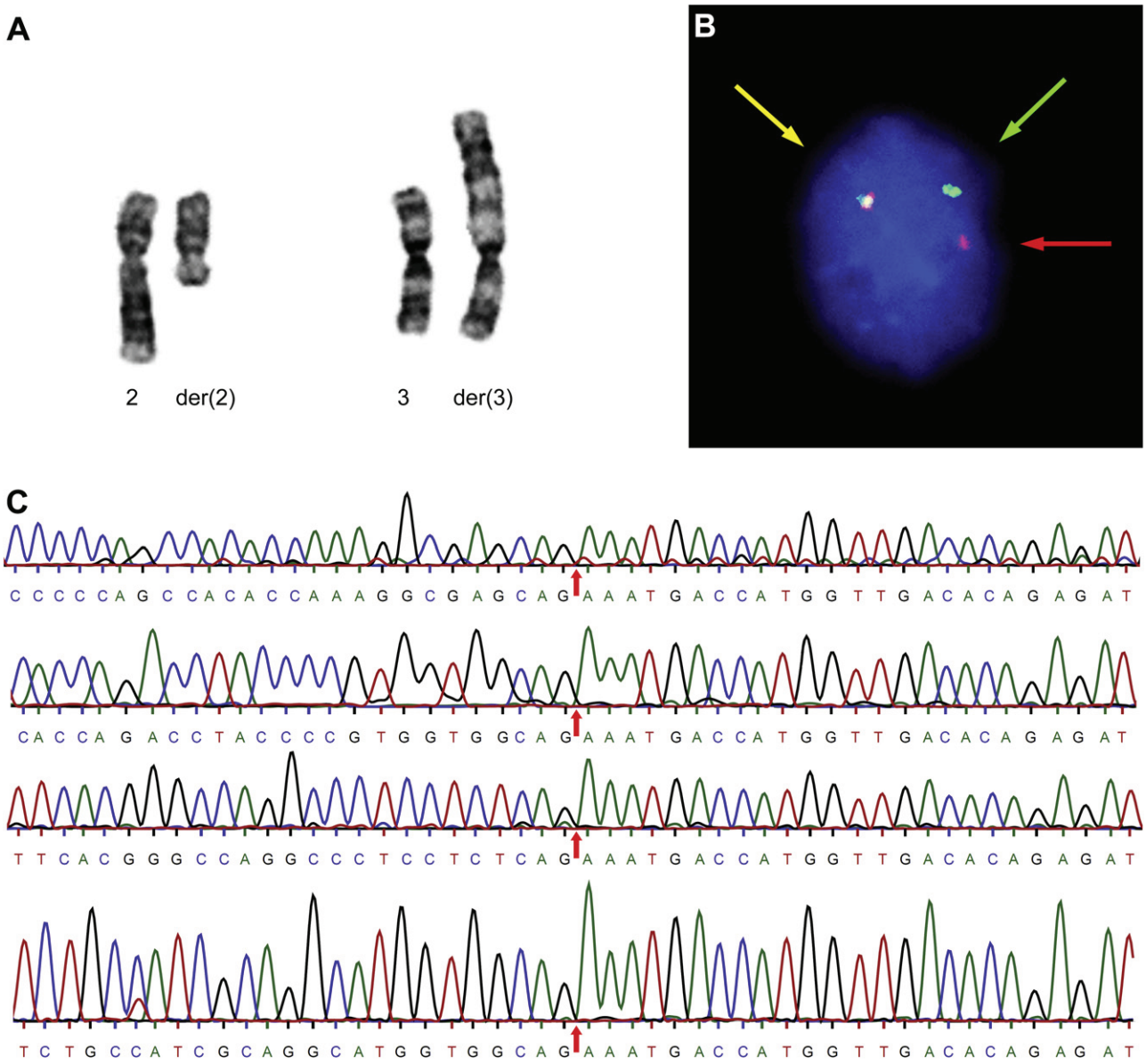

Figure 1 (A) Partial G-banded karyotype of case 1 with a t(2;3)(q13;q15) as the sole chromosomal aberration. (B) Interphase-FISH with a PPARG break-apart probe (PanPath, Budel, Netherlands) on a touch preparation of case 2 showing a rearrangement of *PPARG* as indicated by a split of the *PPARG* surrounding probes (signals marked by green and red arrow). The non-rearranged region appears as a red/green fusion signal (yellow arrow). (C) Sequences of four different *PAX8-PPARG* fusion transcripts. The fusion sites are indicated by arrows. From top to bottom: exons 1−7, 1−8, 1−9a, and 1−10 of *PAX8* are fused to *PPARG*. The first three fusion transcripts are from case 2, the fusion of *PAX8* exon 10 (in addition to exon 7) to *PPARG* was found in case 1. *PAX8* exon numbering is based on GenBank accession number NM_003466.

studies based on cytogenetic analysis (2−4,13−15) reported the t(2;3)(q13;p25) leading to a fusion of *PAX8* and *PPARG* in only 5/146 cases (Table 1B), corresponding to a prevalence of 3.4%. In three more recent studies, FISH was used to detect the rearrangement in 73 follicular adenomas (16−18; Table 1C), but only three cases were positive (4.1%). These data indicate that the prevalence of the chromosomal aberration in adenomas is low and does not coincide with the more frequently reported occurrence of *PAX8-PPARG* fusion transcripts. In contrast to the relatively low prevalence observed in the present series, several other studies, though usually based on smaller series, have identified this aberration by RT-PCR at a much higher frequency (Table 1A). The highest frequency of this gene fusion reported in follicular adenomas was 54.5% (19). Summing up the results of several studies, *PAX8-PPARG* fusion transcripts were detected by RT-PCR in 23/281 adenomas (8.2%; for references, see Table 1A). As a possible explanation for the clear discrepancy in the prevalence of the gene fusion in adenomas, we considered the use of different methods for its detection. Mosaicism of aberrant and cytogenetically normal cells in thyroid adenomas might cause discrepant results between cytogenetic analyses and RT-PCR−based studies. Interphase

FISH analyses of tumors harboring the rearrangement revealed that the proportion of fusion-positive tumor cells varied between 16 and 93% (20). If only a small fraction of cells in a tumor is aberrant, they might escape detection by chromosome analysis. The fusion transcripts, however, would still be detectable by RT-PCR on native tissue samples. As another explanation, the rearrangement may not always be detectable at the cytogenetic level, as reported for many other chromosomal translocations in tumors. In the present study, however, *PAX8-PPARG* fusion transcripts were not detected in any of the 19 adenomas with an apparently normal karyotype that were subjected to RT-PCR.

Another conceivable reason for the relatively high prevalence of the gene fusion in adenomas in some studies may be the possible mis-identification of follicular thyroid carcinomas, in which the rearrangement is known to be more common than in follicular adenomas. As discussed by Nikiforova et al. (21), tumors classified as adenomas and harboring the *PAX8-PPARG* fusion may in fact be follicular carcinomas that were removed at a preinvasive stage.

Nevertheless, in follicular carcinomas as well, the frequency of the fusion gene varies over a broad range among different studies. In a recent study based on FISH (18), the authors discuss the role of the patients' ethnic background and geographic location as possible explanations for the relatively low frequency they observed in follicular thyroid carcinomas. Future studies should address the question of whether these factors also may cause diverging frequencies of the gene fusion in adenomas.

In summary, our results indicate that the chromosomal t(2;3)(q13;p25) and the resulting fusion of *PAX8* and *PPARG* is rare in follicular adenomas. The diverging rates of occurrence in adenomas between different studies could be explained by a high rate of hidden translocations, a minority of positive cells in the samples, or by the use of different methodologies. In addition, the influence by other factors such as ethnic background or geographic location still remains to be elucidated.

Acknowledgments

We thank Dr. Birgit Rommel for critically reading the manuscript.

References

1. Schmid KW, Farid NR. How to define follicular thyroid carcinoma? Virchows Arch 2006;448:385–393.
2. Teyssier JR, Liautaud-Roger F, Ferre D, et al. Chromosomal changes in thyroid tumors. Relation with DNA content, karyotypic features, and clinical data. Cancer Genet Cytogenet 1990;50: 249–263.
3. Sozzi G, Miozzo M, Cariani TC, et al. A t(2;3)(q12-13;p24-25) in follicular thyroid adenomas. Cancer Genet Cytogenet 1992;64: 38–41.
4. Roque L, Castedo S, Gomes P, et al. Cytogenetic findings in 18 follicular thyroid adenomas. Cancer Genet Cytogenet 1993;67: 1–6.
5. Kroll TG, Sarraf P, Pecciarini L, et al. PAX8-PPARγ1 fusion oncogene in human thyroid carcinoma. Science 2000;289: 1357–1360.
6. Belge G, Meyer A, Klemke M, et al. Upregulation of HMGA2 in thyroid carcinomas: a novel molecular marker to distinguish between benign and malignant follicular neoplasias. Genes Chromosomes Cancer 2008;47:56–63.
7. Chiappetta G, Ferraro A, Vuttariello E, et al. HMGA2 mRNA expression correlates with the malignant phenotype in human thyroid neoplasias. Eur J Cancer 2008;44:1015–1021.
8. Prasad NB, Somervell H, Tufano RP, et al. Identification of genes differentially expressed in benign versus malignant thyroid tumors. Clin Cancer Res 2008;14:3327–3337.
9. Lappinga PJ, Kip NS, Jin L, et al. HMGA2 gene expression analysis performed on cytologic smears to distinguish benign from malignant thyroid nodules. Cancer Cytopathol 2010;118: 287–297.
10. Schaffer LG, Slovak ML, Campbell LJ, editors. ISCN 2009: An International System for Human Cytogenetic Nomenclature. Basel: Karger; 2009.
11. Castagné C, Muhlematter D, Beyer V, et al. Determination of cutoff values to detect small aneuploid clones by interphase fluorescence in situ hybridization: the Poisson model is a more appropriate approach. Should single-cell trisomy 8 be considered a clonal defect? Cancer Genet Cytogenet 2003;147: 99–109.
12. Mitelman Database of Chromosome Aberrations and Gene Fusions in Cancer (2011). Mitelman F, Johansson B, Mertens F, editors. Available at: http://www.cgap.nci.nih.gov/Chromosomes/Mitelman. Accessed on February 25, 2011.
13. Antonini P, Vénuat AM, Linares G, et al. Cytogenetic abnormalities in thyroid adenomas. Cancer Genet Cytogenet 1991;52: 157–164.
14. Belge G, Roque L, Soares J, et al. Cytogenetic investigations of 340 thyroid hyperplasias and adenomas revealing correlations between cytogenetic findings and histology. Cancer Genet Cytogenet 1998;101:42–48.
15. Roque L, Rodrigues R, Pinto A, et al. Chromosome imbalances in thyroid follicular neoplasms: a comparison between follicular adenomas and carcinomas. Genes Chromosomes Cancer 2003; 36:292–302.
16. French CA, Alexander EK, Cibas ES, et al. Genetic and biological subgroups of low-stage follicular thyroid cancer. Am J Pathol 2003;162:1053–1060.
17. Castro P, Rebocho AP, Soares RJ, et al. PAX8-PPARγ rearrangement is frequently detected in the follicular variant of papillary thyroid carcinoma. J Clin Endocrinol Metab 2006;91: 213–220.
18. Chia WK, Sharifah NA, Reena RM, et al. Fluorescence in situ hybridization analysis using PAX8- and PPARG-specific probes reveals the presence of PAX8-PPARG translocation and 3p25 aneusomy in follicular thyroid neoplasms. Cancer Genet Cytogenet 2010;196:7–13.
19. Cheung L, Messina M, Gill A, et al. Detection of the PAX8-PPARγ fusion oncogene in both follicular thyroid carcinomas and adenomas. J Clin Endocrinol Metab 2003;88:354–357.
20. Algeciras-Schimnich A, Milosevic D, McIver B, et al. Evaluation of the PAX8/PPARG translocation in follicular thyroid cancer with a 4-color reverse-transcription PCR assay and automated high-resolution fragment analysis. Clin Chem 2010;56: 391–398.
21. Nikiforova MN, Biddinger PW, Caudill CM, et al. PAX8-PPARγ rearrangement in thyroid tumors: RT-PCR and immunohistochemical analyses. Am J Surg Pathol 2002;26:1016–1023.
22. Marques AR, Espadinha C, Catarino AL, et al. Expression of PAX8-PPARγ1 rearrangements in both follicular thyroid carcinomas and adenomas. J Clin Endocrinol Metab 2002;87: 3947–3952.
23. Martelli ML, Iuliano R, Le Pera I, et al. Inhibitory effects of peroxisome poliferator-activated receptor γ on thyroid carcinoma cell growth. J Clin Endocrinol Metab 2002;87:4728–4735.

24. Aldred MA, Morrison C, Gimm O, et al. Peroxisome proliferator-activated receptor gamma is frequently downregulated in a diversity of sporadic nonmedullary thyroid carcinomas. Oncogene 2003;22:3412–3416.
25. Nikiforova MN, Lynch RA, Biddinger PW, et al. RAS point mutations and PAX8-PPARγ rearrangement in thyroid tumors: evidence for distinct molecular pathways in thyroid follicular carcinoma. J Clin Endocrinol Metab 2003;88:2318–2326.
26. Dwight T, Thoppe SR, Foukakis T, et al. Involvement of the PAX8/peroxisome proliferator-activated receptor γ rearrangement in follicular thyroid tumors. J Clin Endocrinol Metab 2003; 88:4440–4445.
27. Hibi Y, Nagaya T, Kambe F, et al. Is thyroid follicular cancer in Japanese caused by a specific t(2;3)(q13;p25) translocation generating Pax8-PPARγ fusion mRNA? Endocr J 2004;51: 361–366.
28. Lacroix L, Mian C, Barrier T, et al. PAX8 and peroxisome proliferator-activated receptor gamma 1 gene expression status in benign and malignant thyroid tissues. Eur J Endocrinol 2004; 151:367–374.
29. Nakabashi CC, Guimarães GS, Michaluart P Jr, et al. The expression of *PAX8-PPARγ* rearrangements is not specific to follicular thyroid carcinoma. Clin Endocrinol (Oxf) 2004;61: 280–282.
30. Sahin M, Allard BL, Yates M, et al. PPARγ staining as a surrogate for PAX8/PPARγ fusion oncogene expression in follicular neoplasms: clinicopathological correlation and histopathological diagnostic value. J Clin Endocrinol Metab 2005;90:463–468.
31. Giordano TJ, Au AY, Kuick R, et al. Delineation, functional validation, and bioinformatic evaluation of gene expression in thyroid follicular carcinomas with the PAX8-PPARG translocation. Clin Cancer Res 2006;12:1983–1993.
32. Di Cristofaro J, Silvy M, Lanteaume A, et al. Expression of tpo mRNA in thyroid tumors: quantitative PCR analysis and correlation with alterations of ret, Braf, ras and pax8 genes. Endocr Relat Cancer 2006;13:485–495.
33. Banito A, Pinto AE, Espadinha C, et al. Aneuploidy and RAS mutations are mutually exclusive events in the development of well-differentiated thyroid follicular tumours. Clin Endocrinol (Oxf) 2007;67:706–711.

IX. Detection of *PAX8-PPARG* Fusion Transcripts in Archival Thyroid Carcinoma Samples by Conventional RT-PCR (Klemke *et al.*, 2012)

Da ein Großteil der bisherigen Untersuchungen zum Nachweis des Fusionsgen *PAX8*/*PPARγ* in follikulären Schilddrüsenkarzinomen mittels RT-PCR an frischem Material bzw. an Gefrierschnitten durchgeführt wurde, erfolgte in dieser Studie der Nachweis an FFPE-Gewebe von 21 FTC, sieben follikulären Varianten des papillären Schilddrüsenkarzinoms (FV-PTC) sowie einer Knochenmetastase eines FTC.

Die RT-PCR zur Detektion von *PAX8*/*PPARγ* erfolgte unter Verwendung von insgesamt fünf Forward-Primern lokalisiert in den Exons 5, 7, 8, 9 und 10 von *PAX8* sowie einem Reverse-Primer lokalisiert in Exon 5 von *PPARγ*. In zwei Fällen (Nr. 10 und Nr. 16) der 21 FTC konnte das Fusionstranskript *PAX8*/*PPARγ* nachgewiesen werden. In einem Fall (Nr. 16) lag nur eine Transkriptvariante vor, in der Exon 10 von *PAX8* mit *PPARγ* fusioniert ist, wohingegen in dem zweitem Fall (Nr. 10) verschiedene Transkriptvarianten nachweisbar waren.

Die Knochenmetastase (Fall Nr. 15) war ebenfalls positiv hinsichtlich des Fusionstranskripts *PAX8*/*PPARγ*, wohingegen zwei FFPE-Proben des entsprechenden Primärtumors negativ hinsichtlich *PAX8*/*PPARγ* waren.

Molekularzytogenetische Analysen erfolgten zur Verifizierung in Form einer I-FISH an FFPE-Gewebeschnitten unter Verwendung einer *PPARγ* Break-Apart Sonde. In Fall Nr. 16 wies nur ein Zellkern unter 100 ausgewerteten Zellkernen ein positives Signalmuster auf, was unterhalb der für die I-FISH entsprechenden Nachweisgrenze für das Vorliegen einer *PPARγ*-Rearrangierung lag. Die I-FISH an Fall Nr. 15 ergab keine auswertbaren Signale. Bei Fall Nr. 10 konnte in 79% der analysierten Zellkerne ein positives Signalmuster entsprechend einer *PPARγ*-Rearrangierung detektiert werden.

IX

Detection of *PAX8-PPARG* Fusion Transcripts in Archival Thyroid Carcinoma Samples by Conventional RT-PCR

Markus Klemke, Norbert Drieschner, Gazanfer Belge, Käte Burchardt, Klaus Junker, Jörn Bullerdiek

(Genes, Chromosomes & Cancer 51(4): 402-408)

Eigenanteil:

- Planung, Durchführung und Auswertung der molekularzytogenetischen Untersuchungen.

GENES, CHROMOSOMES & CANCER 51:402–408 (2012)

Detection of *PAX8–PPARG* Fusion Transcripts in Archival Thyroid Carcinoma Samples by Conventional RT-PCR

Markus Klemke,[1] Norbert Drieschner,[1] Gazanfer Belge,[1] Käte Burchardt,[2] Klaus Junker,[2] and Jörn Bullerdiek[1]*

[1]Center for Human Genetics, University of Bremen, Bremen, Germany
[2]Institute of Pathology, Clinical Center Bremen-Mitte, Bremen, Germany

The t(2;3)(q13;p25) occurs in a subgroup of follicular-patterned thyroid tumors and leads to a fusion of the genes encoding for the thyroid-specific transcription factor paired box 8 (PAX8) and the peroxisome proliferator-activated receptor gamma (PPARγ). Although initially discovered in follicular carcinomas (FTC), the fusion transcripts were also detected in a small fraction of follicular adenomas and rarely in follicular variants of papillary carcinomas (FV-PTC). In most RT-PCR based studies, fresh or snap-frozen tissue samples were used. The aim of the present study was to develop a method for the detection of chimeric *PAX8–PPARG* transcripts in formalin-fixed paraffin-embedded (FFPE) thyroid tumor samples by conventional RT-PCR. For this purpose, RNA from FFPE samples of 21 FTC, seven FV-PTC, and one bone metastasis derived from an FTC was subjected to RT-PCR with subsequent gel electrophoretic separation of the products. Fusion transcripts were detected in 2/21 primary FTC (9.5%) and in the bone metastasis, but they were undetectable in all seven FV-PTC under investigation. The RT-PCR approach described herein allows to detect all known variants of *PAX8–PPARG* fusion transcripts and is applicable to FFPE tissues. Thus, it can be used to screen archival thyroid tumor samples for the gene fusion.

INTRODUCTION

Eleven years ago, a fusion of the genes *PAX8* and *PPARG* resulting from the t(2;3)(q13;p25) was described in follicular thyroid carcinomas (FTC) (Kroll et al., 2000), and it was assumed that it might be specific for FTC. However, in later studies, the presence of *PAX8–PPARG* fusion transcripts was reported in follicular adenomas (FA) as well. Besides conventional cytogenetic analysis and fluorescence in situ hybridization (FISH) to detect the translocation, RT-PCR is a commonly used method for the detection of the fusion transcripts. However, for most RT-PCR approaches published so far intact RNA from fresh or snap-frozen tissues is required and they cannot be performed on degraded RNA isolated from formalin-fixed paraffin-embedded (FFPE) tissue samples. In a recently published approach, fluorescently labeled primers were used in combination with high-resolution fragment analysis (Algeciras-Schimnich et al., 2010). Herein, we describe a method to detect chimeric *PAX8–PPARG* transcripts in RNA from FFPE samples using a conventional RT-PCR with gel electrophoretic separation of PCR products. Of note, an additional sense primer for the detection of a fusion transcript, which is not included in the recently published RT-PCR based analysis of *PAX8–PPARG* fusions in FFPE samples (Algeciras-Schimnich et al., 2010) was used. Since there have been reports on tumors harboring the *PAX8–PPARG* rearrangement, which express this additional variant as the sole fusion transcript (Cheung et al., 2003), it is important to include specific primers for this variant. Otherwise such tumors would escape the RT-PCR based detection of the fusion. The RT-PCR described in the present study offers a reliable tool to screen archives of FFPE thyroid tumors for the presence of *PAX8–PPARG* fusion transcripts.

MATERIALS AND METHODS

Tissue Samples

FFPE tissue samples of two FA of the thyroid that were recently described in detail (Klemke et al., 2011) were used to ascertain the feasibility of the RT-PCR approach for the detection of *PAX8–PPARG* fusion transcripts. One tumor (Case 1) is known to express three different chimeric

*Correspondence to: Jörn Bullerdiek, Center for Human Genetics, University of Bremen, Leobener Strasse ZHG, 28359 Bremen, Germany. E-mail: bullerd@uni-bremen.de

Received 21 April 2011; Accepted 20 November 2011
DOI 10.1002/gcc.21925
Published online 16 December 2011 in Wiley Online Library (wileyonlinelibrary.com).

TABLE I. Clinicopathological Parameters of all Thyroid Tumors Included in the Present Study

Case No.	Type of tumor	Tumor size (cm)	Patient's age	Sex	pTNM classification	*PAX8* exons juxtaposed to *PPARG*	Remarks/clinical outcome
1	FA	3.7	36	F		7, 8, 9	
2	FA	2.5	25	F		7, 10	
3	FTC	3.0	69	M	pT4	Negative	Bone metastases (3.7 and 5.6 years)
4	FTC	2.8	37	F	pT2 pN0	Negative	
5	FTC (m. i.)	2.0	66	F	pT1	Negative	
6	FTC (w. i.)	5.5	67	M	pT3 pN1 (1/8) pM1	Negative	Regional lymph node metastasis, bone metastasis at the time of surgery
7	FTC (w. i.)	1.0	68	M	pT3 pN0 (0/17) pMX R1	Negative	Liver metastasis (1.5 years)
8	FTC (m. i.)	3.3	62	F	pT2 pN0 (0/31) R0	Negative	
9	FTC (w. i.)	extensive growth	81	F	pT4a pN1a (1/2) (pN1b) M1 (PUL) R1	Negative	Multiple lung metastases and mediastinal lymphomas (at the time of surgery)
10	FTC (w. i.)	6.0	53	M	pT3 pNX pMX V1 R0	7, 8, 9, 9 + 10, 8 + 10	Vascular invasion
11	FTC (w.i.)	2.5	24	F	pT2 N0 (0/44) pN0 pMX V1 RX	Negative	Vascular invasion
12	FTC (m.i.)	1.5	39	M	pT1 pN0 (0/3) pMX R0	Negative	
13	FTC (w.i.)	1.8	41	F	pT1 pN0 (0/8) R0	Negative	
14	FTC (w. i.)	8.0	61	M	pT4	Negative	
15	FTC	1.2	53	F	pT1 (M)	8 (Detected in a bone metastasis but not in the primary tumor) 10	Bone metastasis at the time of surgery, additional bone metastases after 2.0 and 2.4 years
16	FTC (m.i.)	1.5	48	F	pT1 pN0 (0/12) pMX R0	Negative	
17	FTC (m.i.)	4.5	63	M	pT3 pN0 (0/2)	Negative	
18	FTC (m.i.)	3.6	46	M	pT2 pN0 (0/15) R0	Negative	
19	FTC (m.i.)	1.3	65	F	pT1 pN0 (0/14) pMX R0	Negative	
20	FTC (m.i.)	6.0	72	F	pT3 pN0 (0/50)	Negative	
21	FTC (m.i.)	1.0	58	M	pT1 pN0 (0/24) L0 V0 R0	Negative	
22	FTC (m.i.)	3.6	41	M	pT2 pN0 (0/13) R0	Negative	
23	FTC (m.i.)	2.2	35	F	pT2 pN0 (0/14) pMX R0	Negative	
24	FV-PTC	3.3	74	F	pT3	Negative	
25	FV-PTC	1.2	47	M	pT1 R0	Negative	
26	FV-PTC	0.7	38	F	pT1 pN1a (1/20) R0	Negative	Regional lymph node metastasis
27	FV-PTC	1.5	50	M	pT1 pN0 (0/30) R0	Negative	
28	FV-PTC	1.8	33	F	pT1 pN1a (3/26) pMX R0	Negative	Regional lymph node micrometastases
29	FV-PTC	1.6	66	M	pT1 pN1 (4/11) R0	Negative	Regional lymph node metastases
30	FV-PTC	3.5	23	F	pT3 pN1 (3/25) L1 V1 pMX R0	Negative	Regional lymph node metastases, vascular invasion

FA, follicular adenoma; FTC, follicular thyroid carcinoma; m.i., minimally invasive; w.i., widely invasive; FV-PTC, follicular variant of a papillary thyroid carcinoma.

TABLE 2. Sequences and Locations of the Primers Used for the Detection of the Positive Control (*PAX8* exons 5 and 6) and the *PAX8–PPARG* Fusion Transcripts

Primer	Sequence (5′–3′)	Location	Product length (bp)
E5	TCA ACC TCC CTA TGG ACA GC	*PAX8*, exon 5	125
E6-as	GGA GTA GGT GGA GCC CAG G	*PAX8*, exon 6	
E7	CCG CTC GAG TGC CCA TTT GA	*PAX8*, exon 7	124
E8	CCT CTC GAC TCA CCA GAC CT	*PAX8*, exon 8	84
E9	GCC CTT CAA TGC CTT TCC CCA TG	*PAX8*, exon 9	117
E10	AGC GGA CAG GGC AGC TAT GC	*PAX8*, exon 10	98
PPARG-as	CCA AAG TTG GTG GGC CAG AAT	*PPARG*, exon 5	

For the primers E7–E9 in combination with the *PPARG* specific antisense primer, the length of the shortest amplicon is indicated. All primer sequences except primer E7 located in exon 7 of *PAX8* were reported previously (Algeciras-Schimnich et al., 2010). as: antisense.

PAX8–PPARG transcripts consisting of exons 1–7, 1–8, and 1–9 of *PAX8* juxtaposed to exon 5 (the first coding exon) of *PPARG*. In the second tumor (Case 2) two fusion transcripts consisting of exons 1–7 and 1–10 fused to *PPARG* were detected earlier. After the RT-PCR was established using the FA samples, it was performed on 21 FTC as well as on seven FV-PTC, which have not been karyotyped or analyzed by FISH previously. All carcinomas were diagnosed by routine histological classification of hematoxylin and eosin stained tissue sections. In addition, a bone metastasis that had developed in one FTC patient (Case 15) was also included in the study. Clinicopathological parameters of the tumors included in the study are given in Table 1.

RT-PCR

Six 5 μm sections of each tumor were deparaffinized with xylene and rehydrated with ethanol. RNA was isolated with the RNeasy FFPE kit (Qiagen, Hilden, Germany) according to the manufacturer's instructions. In a total reaction volume of 20 μl, 1 μg RNA was reverse transcribed with M-MLV Reverse Transcriptase (Invitrogen, Darmstadt, Germany). The final concentrations of the reaction components were as follows: 1× first strand buffer (50 mM Tris–HCl, 75 mM KCl, 3 mM $MgCl_2$), 0.5 mM dNTPs (each) 2 U/μl RNaseOUT recombinant ribonuclease inhibitor, 10 U/μl M-MLV reverse transcriptase, 10 mM dithiothreitol, and 7.5 ng/μl random hexamers. The reaction tubes were incubated at 25°C for 10 min, at 37°C for 50 min, and finally at 70°C for 15 min.

In each PCR reaction, 4 μl of cDNA was used as template. PCR was performed with 2.5 U DreamTaq DNA polymerase (Fermentas, St. Leon-Rot, Germany) per reaction in a total reaction volume of 25 μl with the following final concentrations: 2 mM $MgCl_2$, 0.2 mM dNTPs (each), and 0.1 μM sense as well as antisense primer. The initial denaturation was performed at 95°C for 10 min followed by 41–43 cycles of 95°C for 30 sec, 65°C for 30 sec, and 72°C for 30 sec. The final extension was performed at 72°C for 7 min.

The sequences of the primers used for the detection of the positive control (exons 5–6 of *PAX8*) and the different *PAX8–PPARG* transcripts are given in Table 2. All primer sequences except the sense primer in exon 7 of *PAX8* were published recently (Algeciras-Schimnich et al., 2010). In contrast to the method described by Algeciras-Schimnich et al. (2010), unmodified oligonucleotides were used in the present study. PCR products were separated on 4% agarose gels with 0.5× TBE buffer and stained with ethidium bromide.

FISH

For the detection of rearrangements of the *PPARG* gene, interphase-FISH (I-FISH) with a *PPARG* break-apart probe (PanPath, Budel, Netherlands) was performed on FFPE tissue sections. Pretreatment of 4 μm tissue sections was performed as described previously for FFPE tissue sections (Hopman and Ramaekers, 2001) with a few modifications. Digestion with a pepsin ready-to-use solution (DCS, Hamburg, Germany) was performed at 37°C for 2 × 30 min. Fifteen microliters of the *PPARG* break-apart probe was used per slide. Co-denaturation was performed on a ThermoBrite (Abbott Molecular, Wiesbaden, Germany) for 5 min at 85°C followed by overnight hybridization in a humidified chamber at 37°C. Posthybridization was performed at 42°C for 2 min in 0.4× SSC/0.3% NP-40. Interphase nuclei were counterstained with DAPI (0.75 μg/ml) and slides were examined with an Axioskop 2

plus fluorescence microscope (Carl Zeiss, Göttingen, Germany). Images were captured with a high performance CCD-camera (Visitron Systems, Puchheim, Germany) and were edited with FISH View (Applied Spectral Imaging, Migdal HaEmek, Israel). 100 nonoverlapping nuclei from different (at least four) areas of the tumor were scored.

RESULTS

Samples of two well characterized FA with t(2;3)(q13;p25) were used to check the performance of the RT-PCR. *PAX8–PPARG* fusion transcripts were detected in both cases as reported previously (Klemke et al., 2011). The gel electrophoretic separation of the PCR products (Fig. 1, left) resulted in distinct bands for the positive control as well as for fusions of exons 7, 8, 9, and 10 of *PAX8* to *PPARG*. The identity of the PCR products was confirmed by direct sequencing. In the PCR with the forward primer located in *PAX8* exon 7 an additional longer band was visible. By sequencing of this PCR product, its origin from the fusion of *PAX8* exon 8 to *PPARG* was shown.

The positive controls with primers located in *PAX8* exons 5 and 6 resulted in distinct bands with an expected length of 125 bp in all 21 FTC and 7 FV-PTC under investigation.

Of the 21 primary FTC screened for fusion transcripts, two cases were positive (9.5%). The first of them (No. 16) expressed only one type of chimeric transcript in which exon 10 of *PAX8* was fused to *PPARG*. Several PCR products were visible in the second case (No. 10, Fig. 1, right). Strong bands resulted from the PCRs with forward primers located in *PAX8* exon 7 and 10, respectively. Interestingly, the PCRs with forward primers located in exons 8 and 9 resulted in weak bands with the expected length of 84 and 117 bp, but strong bands of a higher molecular weight appeared in both cases. These PCR products were sequenced directly, and the product generated with the forward primer in exon 9 also contained exon 10 of *PPARG*, the same variant that was also detected with the forward primer in exon 10. The longer product of the PCR with the forward primer located in exon 8, however, indicated the presence of an additional transcript variant. Sequencing revealed a fusion of exon 10 to *PPARG* as well, while exon 9 was completely deleted in this case.

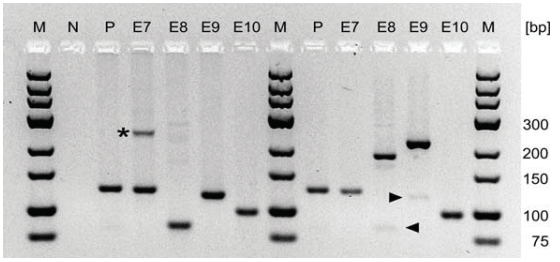

Figure 1. Gel electrophoretic separation of RT-PCR products using RNA templates extracted from FFPE samples of two adenomas (left, E7–E9 from Case 1, E10 from Case 2) and one follicular carcinoma (right, Case 10). M: Fragment length marker (GeneRuler Low Range DNA Ladder, Fermentas, St. Leon-Rot, Germany), N: no template control, P: positive control (*PAX8* exons 5 and 6). Lanes E7–E10: PCR with primers specific for *PAX8–PPARG* fusion transcripts. The names of the forward primers used in combination with the reverse primer (*PPARG*-as) are indicated above the lanes (see also Table 2). Asterisk: the fusion transcript in which *PAX8* exon 8 is juxtaposed to *PPARG* is also detected with a primer located in exon 7 (product length: 245 bp). Triangles: weak bands in the RT-PCR with RNA from a follicular carcinoma corresponding to *PAX8* exon 8 and 9 joined to *PPARG*. The longer PCR products in this case correspond to *PAX8* exons 8 + 10 (E8, 186 bp) and 9 + 10 (E9, 219 bp) juxtaposed to *PPARG*.

A bone metastasis derived from a follicular carcinoma (Case 15) was also analyzed, and a chimeric transcript consisting of *PAX8* exon 8 juxtaposed to *PPARG* was detected. Two samples of the primary tumor, which was multifocal, were available for RT-PCR, but chimeric transcripts were detected in neither of them. Therefore, this case was regarded as negative when calculating the frequency of the rearrangement.

To verify the results obtained by RT-PCR, I-FISH with a *PPARG* break-apart probe was performed on FFPE sections. In Case no. 10, 79/100 nuclei showed one co-localized signal corresponding to the unaffected chromosome 3 and split red and green signals, indicating a translocation targeting *PPARG* (Fig. 2) in accordance with the positive PCR result. In a second follicular carcinoma with positive PCR result (No. 16), FISH revealed a break affecting the *PPARG* locus in only 1/100 nuclei. In case of the bone marrow metastasis (Case No. 15), FISH did not result in appropriate signals.

DISCUSSION

In all 28 FFPE samples under investigation, the positive control was successfully amplified indicating a sufficient quality of all RNA samples for RT-PCR analysis. Using FFPE tissue samples of two FA for which the presence of *PAX8–PPARG* fusion transcripts was shown previously, it was possible to detect the transcripts by

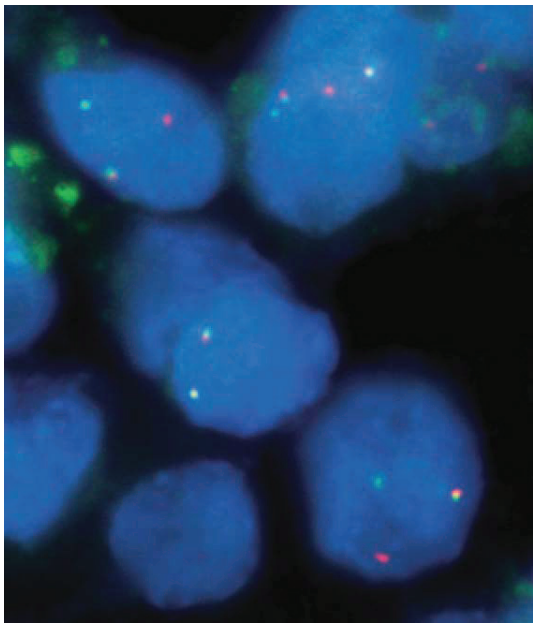

Figure 2. I-FISH with a *PPARG* break-apart probe on an FFPE section of Case 10. A rearrangement of *PPARG* is indicated by a split of the *PPARG* break-apart probes. The nonrearranged region appears as a red/green fusion signal. Two nuclei with aberrations affecting *PPARG* are visible (upper left and lower right corner).

RT-PCR. Thus, it was demonstrated that conventional RT-PCR is suitable for the detection of chimeric *PAX8–PPARG* transcripts in FFPE tissue samples.

Of the 21 FFPE tissue samples from FTC, fusion transcripts were found in two cases. One of them (Case 16) expressed only one transcript variant, but in the second case (No. 10) five different variants were detected. Exons 7, 8, 9, and 10 of *PAX8* were juxtaposed to *PPARG* in this case, and the fusion of exon 10 occurred with as well as without a complete deletion of exon 9. Partial deletions of exon 9 that have been reported in previous studies (Marques et al., 2002) were not found. Of note, this second case of FTC was a rather large tumor with a diameter of 6.0 cm and did not only show capsular invasion but was angioinvasive as well. It is tempting to speculate that the transcript with exon 10 of *PAX8* juxtaposed to *PPARG* accompanied by a deletion of exon 9, which was not observed in any other of the cases, contributes to aggressiveness of thyroid tumors. While exons 10 and 11 of *PAX8* encode an activating domain of the protein, an inhibitory domain is encoded by exon 9, which is rich in proline, serine, and threonine residues (PST domain). It has been demonstrated that removal of this domain results in a strong increase in the transactivating potential of the corresponding protein (Poleev et al., 1995, 1997). Likewise, a PAX8–PPARγ fusion protein lacking the region encoded by *PAX8* exon 9 but containing the transactivating domain encoded by exon 10 may as well exhibit a strong transactivating potential due to the lost repression of function of the activating domain. Further studies are required to elucidate whether tumors expressing fusion transcripts with partial or complete deletions of exon 9 exhibit a more aggressive behavior in general. Regardless of whether fusion proteins lacking the domain encoded by exon 9 of *PAX8* display a significant but as yet unknown effect, this second case is an unusual tumor, because the presence of five different fusion transcripts in a single carcinoma is a rare finding and may account for the aggressiveness of the tumor.

The incidence of the rearrangement observed in our series of FTC (9.5%) is relatively low when compared with the average rates observed by other investigators. However, similarly low rates were also reported in some studies. In a study by Aldred et al. (2003), the fusion transcripts were detected by RT-PCR in 2/19 cases of FTC (10.5%). The authors discussed the possibility of a geographical variation in the incidence of the translocation among FTC but could not confirm this hypothesis. Instead, they speculated that the frequency of the translocation may be generally lower than reported in earlier studies. As in the present study, their FTC samples were collected in a German Hospital. Considered together, these results indicate that at least in Germany, the gene fusion is less common in FTC.

Interestingly, a chimeric *PAX8–PPARG* transcript was detected in a bone metastasis originating from an FTC (Case 15) located in the lower jaw of the patient. In this case, *PAX8* exon 8 is juxtaposed to *PPARG*. Samples of the primary tumor located in the thyroid were also analyzed by RT-PCR, but no chimeric transcript was found. The tumor was multifocal, and unfortunately the available FFPE samples did not cover all foci. Thus, the bone metastasis is likely to originate from one of the nodules unavailable for RT-PCR analysis.

All seven FFPE tissue samples from FV-PTC under investigation were negative with respect to chimeric *PAX8–PPARG* transcripts. This observation is in good agreement with previous work because fusion transcripts have been detected by RT-PCR in only two FV-PTC cases so far (Castro et al., 2006).

Figure 3. Four variants of *PAX8–PPARG* fusion transcripts. Exons 8 (B), 9 (C), and 10 (D) are fused in-frame to *PPARG* (Kroll et al., 2000). A fourth transcript variant with exon 7 juxtaposed to *PPARG* described later (Marques et al., 2002; Cheung et al., 2003) is not translated into a fusion protein (A). Due to a premature stop codon, it is translated into a truncated PAX8 protein. The start codon of *PPARG* is underlined and the fusion junctions are indicated by vertical lines.

The rearrangement affecting chromosome band 3p25 was also detected by I-FISH in the tumor in which multiple fusion transcripts were detected (No. 10). In this case, the rate of translocation-positive nuclei was high (79%). In a tumor expressing a single fusion transcript variant (No. 16), the chromosomal translocation was detected in only 1/100 nuclei by FISH. By FISH alone this case would be scored as negative for a *PPARG* rearrangement because the fraction of positive nuclei is below the detection limit. However, a small fraction of cells harboring the translocation and expressing *PAX8–PPARG* fusion transcripts seems to be sufficient to induce positive RT-PCR signals and could thus lead to discrepant results between both methods. Moreover, the paucity of positive cells may indicate that in this case the rearrangement had occurred as a secondary event.

Recently, the detection of *PAX8–PPARG* transcripts by a four-color RT-PCR assay and automated high-resolution fragment analysis was reported (Algeciras-Schimnich et al., 2010). We were able to demonstrate that fusion transcripts in RNA from FFPE samples can also be successfully amplified by conventional RT-PCR and visualized by standard gel electrophoresis with ethidium bromide staining without the use of fluorescently labeled primers and capillary electrophoresis. We identified one FTC expressing five variants, but often only a single transcript variant can be detected. In the study by Algeciras-Schimnich et al. (2010), no primer located in exon 7 of *PAX8* was used, although fusion transcripts consisting of exons 1–7 joined to *PPARG* were described earlier (Marques et al., 2002; Cheung et al., 2003). Thus, translocation-positive tumors would escape detection by the RT-PCR assay if they would express a transcript consisting of *PAX8* exons 1–7 fused to *PPARG* exclusively. Therefore, we have designed an additional primer with a binding site in exon 7 and were able to detect the transcript with exon 7 of *PAX8* as the fusion partner in adenomas as well as in one follicular carcinoma. The use of primers specific for all known chimeric *PAX8–PPARG* transcripts is recommended, because a given tumor may express any one of them as the sole fusion transcript. Unlike the three transcripts described by Kroll et al. (2000), no fusion protein is encoded by the transcript in which exon 7 is joined to *PPARG*. While exons 8, 9, and 10 are fused in-frame to their partner, the fusion of exon 7 induces an early stop codon directly after the junction and results in a truncated PAX8 protein (Fig. 3).

In summary, it was demonstrated that conventional RT-PCR is feasible and well-suited for the detection of chimeric *PAX8–PPARG* transcripts in FFPE samples as well. The RT-PCR was performed on FFPE samples of 28 follicular-patterned thyroid tumors. Whereas no fusion was detectable in seven cases of FV-PTC, fusion transcripts were detected in 9.5% of FTC. To detect all known variants of fusion transcripts, the RT-PCR described in the present study uses an additional forward primer located in exon 7 of *PAX8*. Since it is applicable to partially degraded RNA from FFPE tissues, our approach enables the RT-PCR based detection of *PAX8-PPARG* fusion transcripts in archival thyroid tumor samples, which are more easily available than fresh or cryopreserved tissues.

ACKNOWLEDGMENTS

The authors thank Caroline Zeiser for excellent technical assistance.

REFERENCES

Aldred MA, Morrison C, Gimm O, Hoang-Vu C, Krause U, Dralle H, Jhiang S, Eng C. 2003. Peroxisome proliferator-activated receptor gamma is frequently downregulated in a diversity of sporadic nonmedullary thyroid carcinomas. Oncogene 22:3412–3416.

Algeciras-Schimnich A, Milosevic D, McIver B, Flynn H, Reddi HV, Eberhardt NL, Grebe SK. 2010. Evaluation of the PAX8/PPARG translocation in follicular thyroid cancer with a 4-color reverse-transcription PCR assay and automated high-resolution fragment analysis. Clin Chem 56:391–398.

Castro P, Rebocho AP, Soares RJ, Magalhães J, Roque L, Trovisco V, Vieira de Castro I, Cardoso-de-Oliveira M, Fonseca E, Soares P, Sobrinho-Simões M. 2006. PAX8-PPARγ rearrangement is frequently detected in the follicular variant of papillary thyroid carcinoma. J Clin Endocrinol Metab 91:213–220.

Cheung L, Messina M, Gill A, Clarkson A, Learoyd D, Delbridge L, Wentworth J, Philips J, Clifton-Bligh R, Robinson BG. 2003. Detection of the PAX8-PPARγ fusion oncogene in both follicular thyroid carcinomas and adenomas. J Clin Endocrinol Metab 88:354–357.

Hopman AH, Ramaekers FC. 2001. Processing and staining of cell and tissue material for interphase cytogenetics. Curr Protoc Cytom 8.5.1–8.5.22. DOI: 10.1002/0471142956.cy0805s05.

Klemke M, Drieschner N, Laabs A, Rippe V, Belge G, Bullerdiek J, Sendt W. 2011. On the prevalence of the *PAX8–PPARG* fusion resulting from the chromosomal translocation t(2;3)(q13;p25) in adenomas of the thyroid. Cancer Genet 204:334–339.

Kroll TG, Sarraf P, Pecciarini L, Chen CJ, Mueller E, Spiegelman BM, Fletcher JA. 2000. PAX8–PPARγ1 fusion oncogene in human thyroid carcinoma. Science 289:1357–1360.

Marques AR, Espadinha C, Catarino AL, Moniz S, Pereira T, Sobrinho LG, Leite V. 2002. Expression of PAX8-PPARγ1 rearrangements in both follicular thyroid carcinomas and adenomas. J Clin Endocrinol Metab 87:3947–3952.

Poleev A, Wendler F, Fickenscher H, Zannini MS, Yaginuma K, Abbott C, Plachov D. 1995. Distinct functional properties of three human paired-box-protein, PAX8, isoforms generated by alternative splicing in thyroid, kidney and Wilms' tumors. Eur J Biochem 228:899–911.

Poleev A, Okladnova O, Musti AM, Schneider S, Royer-Pokora B, Plachov D. 1997. Determination of functional domains of the human transcription factor PAX8 responsible for its nuclear localization and transactivating potential. Eur J Biochem 247:860–869.

3.5 Molekulargenetische bzw. molekularzytogenetische Untersuchungen bei benignen mesenchymalen Tumoren im Hinblick auf *HMGA1*, *HMGA2* und *RAD51L1*

X. Intragenic breakpoint within RAD51L1 in a t(6;14)(p21.3;q24) of a pulmonary chondroid hamartoma (Blank *et al.*, 2001)

Um eine mögliche Beteiligung des in 14q24 lokalisiertem *RAD51L1*, dessen Rearrangierung durch eine Translokation t(12;14)(q15;q23~24) in uterinen Leiomyomen bereits gezeigt worden ist (Schoenmakers *et al.*, 1999), auch in benignen mesenchymalen Tumoren mit der Translokation t(6;14)(p21.3;q24) nachzuweisen, wurde an einem chondroiden Hamartom der Lunge mit einer t(6;14)(p21;q24) eine FISH mit *RAD51L1*-spezifischen BAC-Klonen durchgeführt.

Hierfür wurden insgesamt drei BAC-Klone verwendet (CTD-3225F7, CITB-135H17 und CTD-2325P2), die den genomischen Bereich von *RAD51L1* komplett umfassen. In einer zwei-Farben FISH an Metaphasen des o.g. chondroiden Hamartoms unter Verwendung aller drei BAC-Klone konnte der Bruchpunkt innerhalb einer Region von *RAD51L1,* abgedeckt durch die beiden BAC-Klone CITB-135H17 und CTD-2325P2, eingegrenzt werden.

In anschließenden FISH-Analysen jeweils separat mit CITB-135H17 und CTD-2325P2 konnte dann gezeigt werden, dass der Bruchpunkt innerhalb CITB-135H17 und somit in der genomischen Region von *RAD51L1*, die Exon 10, 11a und 11b einschließt, liegt.

Somit konnte eine Beteiligung von *RAD51L1* auch in benignen mesenchymalen Tumoren mit einer t(6,14)(p21;q24) nachgewiesen werden. Weiterführende Untersuchungen sollten demnach auf die Bedeutung von *RAD51L1* aber auch von dem in 6p21 lokalisiertem HMGA1 hinsichtlich der Tumorgenese bzw. –entwicklung von benignen mesenchymalen Tumoren ausgerichtet sein.

X

Intragenic breakpoint within RAD51L1 in a t(6;14)(p21.3;q24) of a pulmonary chondroid hamartoma

C. Blank, E.F.P.M. Schoenmakers, P. Rogalla, E.H. Huys, A.A. Van Rijk, N. Drieschner, J. Bullerdiek

(Cytogenetics and Cell Genetics 95(1-2): 17-19)

Eigenanteil:

- Durchführung und Auswertung der molekularzytogenetischen Untersuchungen.
- Etablierung eines FISH-Assays zum Nachweis von *RAD51L1*-Rearrangierungen.

Gene Mapping, Cloning and Sequencing

Cytogenet Cell Genet 95:17–19 (2001)

Cytogenetics and Cell Genetics

Intragenic breakpoint within RAD51L1 in a t(6;14)(p21.3;q24) of a pulmonary chondroid hamartoma

C. Blank,[a] E.F.P.M. Schoenmakers,[b] P. Rogalla,[a] E.H.L.P.G. Huys,[b] A.A.F. van Rijk,[b] N. Drieschner[a] and J. Bullerdiek[a]

[a] Center for Human Genetics, University of Bremen, Bremen (Germany)
[b] Department of Human Genetics, University Medical Centre Nijmegen, Nijmegen (The Netherlands)

Abstract. Rearrangements involving chromosome region 14q23→q24 represent a main cytogenetic subgroup in a variety of benign solid tumors. Recently, in uterine leiomyomas containing the classical t(12;14)(q15;q23→q24), the primary chromosome 14 target gene was identified as the protein kinase-encoding gene RAD51L1. In this report we show that RAD51L1 is also involved in the frequently ocurring t(6;14)(p21;q23→q24) in pulmonary chondroid hamartomas.

Pulmonary chondroid hamartomas (PCHs) are the most common benign lung tumors consisting of cartilage, undifferentiated mesenchymal cells, smooth muscle cells, adipocytes, and non-neoplastic epithelium. Cytogenetic studies of this histologically heterogeneous tumor entity revealed a "hot spot" in chromosome band 14q23→q24 mostly affected by aberrations involving 6p21 or 12q15 (Johansson et al., 1993; Kazmierczak et al., 1999), chromosome regions harboring two closely related members of the high mobility group protein gene family A, i.e. HMGIY and HMGIC. Interestingly, similarly frequent rearrangements of 14q24 were also found in the cytogenetically well-characterized uterine leiomyomas (ULs) (Nilbert and Heim, 1990) making it tempting to hypothesize that a common target gene within this chromosome band plays a crucial role in the development of both tumor entities. Recently, in ULs showing a t(12;14)(q15;q23→q24) this candidate gene has been identified as the human RAD51L1 (formerly also known as RAD51B) involved in various fusion transcripts with its preferential translocation partner HMGIC (Schoenmakers et al., 1999). Nevertheless, it remains to be established whether this gene is also targeted by the t(6;14)(p21.3;q24) which is known to involve the HMGIY gene, the other member of the HMGA gene family.

In order to test our hypothesis that RAD51L1 is also affected in a primary PCH showing a typical t(6;14) we performed FISH experiments using RAD51L1-specific BAC probes.

Materials and methods

A primary pulmonary chondroid hamartoma index case from a 71-year-old male patient was used for cytogenetic and molecular investigations and was cultured following standard methods. Metaphase chromosome spreads were obtained by standard cytogenetic procedures. After GTG-banding of the metaphase spreads FISH analyses and treatment of metaphases were performed using standard protocols.

The following RAD51L1-specific BAC clones derived from the CalTech-D library were used for FISH: C-3225F7 (GenBank accession number: AL121595; insert size of 172 kb) containing 14 kb of the 5′ region, and exon 1 to 90 kb of intron 7; CITB-135H17 (AC004518; 124 kb) spanning 10 kb of intron 9 to 84 kb of intron 11b, and C-2325P2 (AL121820; 117 kb) harboring 35 kb of intron 11b to exon 11c, and 82 kb of 3′ region. The latter two BAC

Supported in part by the Deutsche Forschungsgemeinschaft (Bu 592/4-3).

Received 26 September 2001; manuscript accepted 23 October 2001.

Request reprints from Dr. Jörn Bullerdiek, Center for Human Genetics
University of Bremen, Leobenerstr. ZHG, D–28359 Bremen (Germany)
telephone: 49-421-218-3589; fax: 49-421-218-4239
e-mail: bullerdiek@uni-bremen.de

KARGER
Fax + 41 61 306 12 34
E-mail karger@karger.ch
www.karger.com

0301–0171/01/0952–0017$17.50/0

Accessible online at:
www.karger.com/journals/ccg

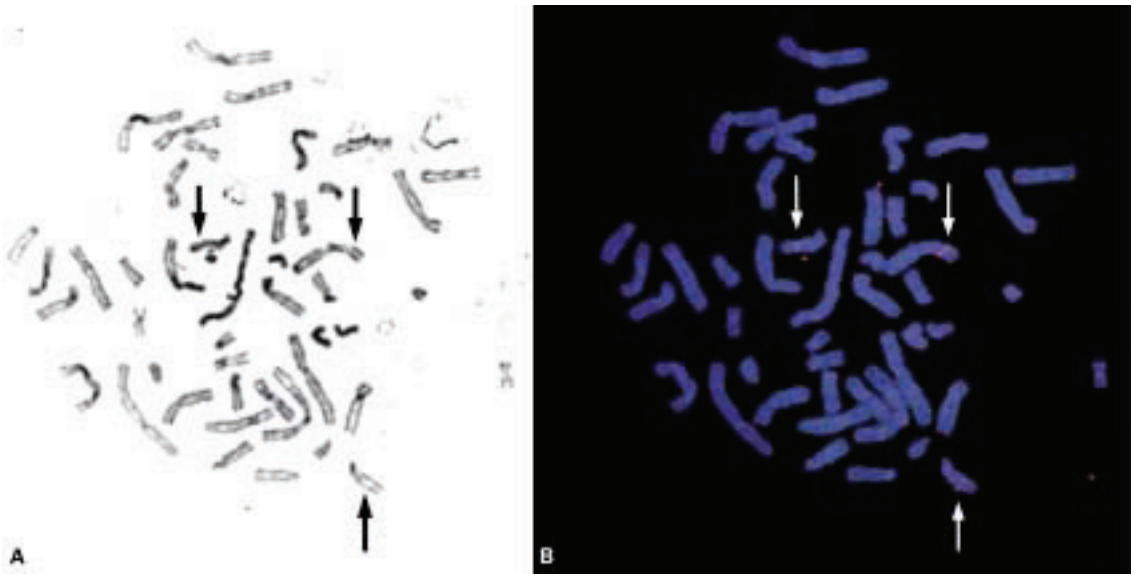

Fig. 1. (**A**) Metaphase of a hamartoma with t(6;14)(p21.3;q24) after GTG-banding; the chromosomes 14, der(6) and der(14) are marked (arrows). (**B**) The same metaphase after FISH with BAC clone CITB-135H17 revealing red signals on chromosome 14, der(6), and der(14) (arrows).

clones share an overlapping sequence within intron 11b of 5 kb. DNA of BAC clones was isolated using the QIAGEN Plasmid Midi Kit (QIAGEN, Hilden, Germany).

BAC DNA was labeled either with dig-11-dUTP (C-3225F7) or biotin-16-dUTP (CITB-135H17 and C-2325P2) by nick-translation (Roche Diagnostics, Mannheim, Germany) and pooled (concentration: 4 ng/µl) for bi-color FISH experiments. Chromosomes were counterstained with DAPI (0.025 µg/ml). For each FISH experiment at least 10 metaphases were examined. Slides were analyzed on a Zeiss Axiophot fluorescence microscope using an FITC, Cy3 and DAPI filter set. Metaphases were recorded with the Power Gene Karyotyping System (PSI, Halladale, U.K.).

Results and discussion

In the present study a primary PCH index case with a typical t(6;14)(p21;q24) was analyzed by FISH experiments using three BAC clones mapping at precisely defined positions within RAD51L1. By bi-color FISH analyses using all three BAC clones the breakpoint was found to be residing within the genomic interval covered by the overlapping and pooled BACs CITB-135H17 and C-2325P2. In order to map the breakpoint region more precisely within this interval, the latter two BAC clones were used separately in subsequent FISH experiments. As a result the genomic breakpoint was mapped within CITB-135H17 (Fig. 1), a clone overspanning exon 10, 11a, and 11b of RAD51L1.

Aberrations involving 14q23→q24 are found in two of the major cytogenetic subgroups in ULs (Nilbert and Heim, 1990) and PCHs (Johansson et al., 1993; Kazmierczak et al., 1999) and can be considered as one of the main karyotypic similarities between these two tumor entities (Johansson et al., 1993). Recently, RAD51L1 currently consisting of 14 exons of which the last four represent alternative exons (Schoenmakers, personal communication) was identified as the target gene of t(12;14) both in primary UL as well as in leiomyoma-derived cell lines (Schoenmakers et al., 1999; Takahashi et al., 2001). Here, we could clearly demonstrate that this gene is also involved in a t(6;14) of another benign tumor entity, i.e. PCHs.

In the literature different, but related genetic pathways are suggested for tumor initiation and progression of ULs and PCHs due to their overlapping cytogenetic subgroups (Johansson et al, 1993; Kazmierczak et al., 1999).

Recently, in primary tumors and UL-derived cell lines showing t(12;14), 3′ RACE analysis and RT-PCR experiments revealed fusion transcripts containing RAD51L1 and HMGIC sequences (Schoenmakers et al., 1999; Takahashi et al., 2001). Interestingly, in a subgroup of tumors variantly truncated RAD51L1 cDNA was fused 3′ to frameshifted sequences of HMGIC. According to our data, a similar truncated RAD51L1 cDNA can be predicted. Furthermore, it should be noted that previous FISH experiments revealed breaks 3′ of HMGIY in PCHs containing 6p21 aberrations suggesting a dysregulation by the loss of its possible 3′ regulatory elements (Kazmierczak et al., 1999). However, despite the absence of intragenic breaks truncated transcripts of HMGIY were found by 3′ RACE (Kazmierczak et al., 1998). Interestingly, proteins deriving from tuncated transcripts of HMGA genes show an enhanced activity compared to the native protein (Nissen and Reeves, 1995; Fedele et al., 1998). In addition, the reactivation and enhancement of HMGIY transcription is discussed as a mechanism of tumor initiation (Xiao et al., 1997). Alternatively, fusion transcripts consisting of sequences of RAD51L1 and HMGIY might be plausible when these aberrations would lead to the same orientation of both target genes.

Therefore, expression studies are planned in order to elucidate the relevance of RAD51L1 and HMGIY to tumor development. Furthermore, molecular genetic studies of PCHs showing t(12;14) shall shed more light onto the primary – and perhaps identical – mechanism in the tumorigenesis of UL and PCHs.

Acknowledgements

The authors thank Prof. Dr. K. Kayser, Thorax-Klinik GmbH Heidelberg, Germany, for collaboration.

References

Fedele M, Berlingieri MT, Scala S, Chiariotti L, Viglietto G, Rippe V, Bullerdiek J, Santoro M, Fusco A: Truncated and chimeric *HMGI-C* genes induce neoplastic transformation of NIH3T3 murine fibroblasts. Oncogene 17:413–418 (1998).

Johansson M, Dietrich C, Mandahl N, Hambraeus G, Johansson L, Clausen PP, Mitelman F, Heim S: Recombinations of chromosomal bands 6p21 and 14q24 characterise pulmonary hamartomas. Br J Cancer 67:1236–1241 (1993).

Kazmierczak B, Dal Cin P, Wanschura S, Borrmann L, Fusco A, Van den Berghe H, Bullerdiek J: *HMGIY* is the target of 6p21.3 rearrangements in various benign mesenchymal tumors. Genes Chrom Cancer 23:279–285 (1998).

Kazmierczak B, Meyer-Bolte K, Tran KH, Wockel W, Breightman I, Rosigkeit J, Bartnitzke S, Bullerdiek J: A high frequency of tumors with rearrangements of genes of the *HMGI(Y)* family in a series of 191 pulmonary chondroid hamartomas. Genes Chrom Cancer 26:125–133 (1999).

Nilbert M, Heim S: Uterine leiomyoma cytogenetics. Genes Chrom Cancer 2:3–13 (1990).

Nissen MS, Reeves R: Changes in superhelicity are introduced into closed circular DNA by binding of high mobility group protein I/Y. J biol Chem 270:4355–4360 (1995).

Schoenmakers EF, Huysmans C, Van de Ven WJ: Allelic knockout of novel splice variants of human recombination repair gene *RAD51B* in t(12;14) uterine leiomyomas. Cancer Res 59:19–23 (1999).

Takahashi T, Nagai N, Oda H, Ohama K, Kamada N, Miyagawa K: Evidence for *RAD51L1/HMGIC* fusion in the pathogenesis of uterine leiomyoma. Genes Chrom Cancer 30:196–201 (2001).

Xiao S, Lux ML, Reeves R, Hudson TJ, Fletcher JA HMGI(Y) activation by chromosome 6p21 rearrangements in multilineage mesenchymal cells from pulmonary hamartoma [comment]. Am J Pathol 150:901–910 (1997).

XI. 6p21 rearrangements in uterine leiomyomas targeting *HMGA1* (Nezhad *et al.*, 2010)

Rearrangierungen der chromosomalen Region 6p21 finden sich in einem kleinen Anteil uteriner Leiomyome. Obwohl eine erhöhte Expression von dem in 6p21 lokalisiertem *HMGA1* in uterinen Leiomyomen mit 6p21-Rearrangierungen bereits gezeigt worden ist (Sornberger *et al.*, 1999), sind quantitative Expressionsanalysen von *HMGA1* in uterinen Leiomyomen mit 6p21-Rearrangierungen bisher noch nicht durchgeführt worden.

In dieser Arbeit wurde daher an sieben uterinen Leomyomen mit Aberrationen unter Beteiligung von Chromosom 6 eine quantitative Real-Time PCR zur Bestimmung des Expressionslevels von *HMGA1* sowie *HMGA2* im Vergleich zu zytogenetisch unauffälligen Myomen sowie dem umliegenden Normalgewebe des Myometriums. Zudem erfolgte neben der zytogenetischen Analyse aller untersuchten Gewebe auch eine FISH-Analyse zum molekularzytogenetischen Nachweis einer *HMGA1*-Rearrangierung an ausgewählten uterinen Leiomyomen.

Die quantitative Bestimmung der *HMGA1*-Expression zeigte ein um das durchschnittlich 45-fach erhöhtes Expressionslevel in der Gruppe der uterinen Leiomyome mit Chromosom 6-Aberrationen im Vergleich zu dem Myometrium-Gewebe, welches als Kalibrator verwendet wurde. Die zytogenetisch unauffällige Kontrollgruppe wies ein um das durchschnittlich 8,2-fach erhöhtes Expressionslevel auf, wobei sich der Unterschied bezüglich der *HMGA1*-Expression zwischen beiden Gruppen als signifikant erwies.

Eine Korrelation zwischen dem Expressionslevel von *HMGA1* sowie dem von *HMGA2* konnte in beiden Gruppen nicht nachgewiesen werden.

Die FISH wurde an insgesamt 5 Tumoren durchgeführt, von denen vier Fälle zytogenetisch entweder eine 6p-Rearrangierung oder eine Monosomie 6 aufwiesen. Der fünfte Tumor war zytogenetisch unauffällig. Zum Nachweis einer *HMGA1*-Rearrangierung wurden insgesamt vier BAC-Klone verwendet, von denen je zwei überlappende Klone distal (CTD-2522J1 und CTD-2510D13) sowie proximal (CTD-2524P4 und RP11-140K17) zu *HMGA1* lokalisiert sind und somit als Break-Apart Sonde eingesetzt wurden. In drei Tumoren mit einer 6p-Rearrangierung, aber auch dem Tumor mit einer Monosomie 6 konnte so eine Rearrangierung von *HMGA1* nachgewiesen werden. Der zytogenetisch unauffällige Tumor wies molekularzytogenetisch keine *HMGA1*-Rearrangierung auf.

XI

6p21 rearrangements in uterine leiomyomas targeting *HMGA1*

Maliheh Hashemi Nezhad, Norbert Drieschner, Sabrina Helms, Anke Meyer, Mahboobeh Tadayyon, Markus Klemke, Gazanfer Belge, Sabine Bartnitzke, Käte Burchardt, Christiane Frantzen, Ernst Heinrich Schmidt, Jörn Bullerdiek

(Cancer Genetics and Cytogenetics 203(2): 247-252)

Eigenanteil:

- Planung, Durchführung und Auswertung der molekularzytogenetischen Untersuchungen
- Auswahl der verwendeten DNA-Sonden und Etablierung eines FISH-Assays zum Nachweis von *HMGA1*-Rearrangierungen.

ELSEVIER

Cancer Genetics and Cytogenetics 203 (2010) 247–252

Cancer Genetics and Cytogenetics

6p21 rearrangements in uterine leiomyomas targeting *HMGA1*

Maliheh Hashemi Nezhad[a], Norbert Drieschner[a], Sabrina Helms[a], Anke Meyer[a], Mahboobeh Tadayyon[a], Markus Klemke[a], Gazanfer Belge[a], Sabine Bartnitzke[a], Käte Burchardt[b], Christiane Frantzen[c], Ernst Heinrich Schmidt[d], Jörn Bullerdiek[a,e,*]

[a]*Center for Human Genetics, University of Bremen, Leobener Str. ZHG, D-28359 Bremen, Germany*
[b]*Department of Pathology, General Hospital Bremen-Mitte, St.-Jürgen-Str. 1, D-28177 Bremen, Germany*
[c]*Women's Clinic, St. Joseph-Stift Hospital, Schwachhauser Heerstrasse 54, D-28209 Bremen, Germany*
[d]*Department of Obstetrics and Gynecology, Evang. Diakonie Hospital, Gröpelinger Heerstrasse 406-408, D-28239 Bremen, Germany*
[e]*Clinic for Small Animals, University of Veterinary Medicine, Bischofsholer Damm 15, D-30137 Hanover, Germany*

Received 7 January 2010; received in revised form 2 August 2010; accepted 5 August 2010

Abstract To quantify the expression of *HMGA1* mRNA in uterine leiomyomas, the expression of *HMGA1* was analyzed in a series including tumors with aberrations of chromosome 6 ($n = 7$) and cytogenetically normal tumors ($n = 8$) as a control group by quantitative reverse transcriptase–polymerase chain reaction. The average expression level in the 6p21 group was found to be 5.6 times higher than that in the control group, and with one exception, all cases with 6p21 alteration revealed a high expression of *HMGA1* mRNA than cytogenetically normal tumors. Nevertheless, compared to fibroids with a normal karyotype, the upregulation of the *HMGA1* mRNA in these cases was much less strong than that of *HMGA2* mRNA in case of 12q14~15 aberrations identified in previous studies.

1. Introduction

Uterine leiomyomas (ULs) belong to the cytogenetically best investigated human tumors. The cytogenetic analyses have revealed several subtypes, with a frequent group showing rearrangements of chromosomal region 12q14~15, which apparently targets the gene encoding the high-mobility group AT-hook 2 (*HMGA2)* [1,2]. Accordingly, tumors of this type show significantly higher expression of *HMGA2* than fibroids with an apparently normal karyotype [3]. HMGA2 is a protein abundantly expressed in stem cells and casually linked to their self-renewal ability. A decrease of HMGA2 has recently seen linked to the group of hematopoietic as well as neural stem cells [4]. Accordingly, it is tempting to speculate that in terms of pathogenesis, smooth muscle cells continuously expressing HMGA2 are maintaining a self-renewing program that occasionally also display multilineage potential as witnessed by variants as, for example, lipoleiomyomas or leiomyomas with cartilaginous differentiation [5,6].

Of note, a smaller subgroup of ULs shows rearrangements of 6p21 (i.e., the locus where *HMGA1,* the other gene encoding proteins of the HMGA type, has been mapped), suggesting that *HMGA1* is the relevant target gene in that subgroup of ULs [7]. In small series of ULs, it was shown that this rearrangement leads to an overexpression of *HMGA1* [8,9]. However, to our knowledge, no study quantifying the expression of *HMGA1* mRNA in ULs of this subtype has been performed. Thus, we analyzed the *HMGA1* expression in seven ULs with aberrations of chromosome 6 in comparison to myomas with normal karyotype and to the matching myometrial tissues.

2. Materials and methods

2.1. Tissue samples and chromosome analysis

For RNA isolation, samples of ULs and myometrium were snap frozen in liquid nitrogen immediately after surgery and stored at −80°C. For cell culture, samples of primary tumors were transferred to Hank's solution with antibiotics (200 IU/mL penicillin, 200 µg/mL streptomycin) after surgery. Cell culture and chromosome analyses were performed as described previously [3].

2.2. RNA isolation, reverse transcription, and quantitative reverse transcriptase–polymerase chain reaction

Total RNA was isolated from tissue samples with the RNeasy Mini Kit (Qiagen, Hilden, Germany) including

* Corresponding author. Tel.: +49-421-2184239; fax: +49-421-2184239.
E-mail address: bullerd@uni-bremen.de (J. Bullerdiek).

0165-4608/$ - see front matter
doi:10.1016/j.cancergencyto.2010.08.005

DNase 1 treatment according to the manufacturer's instructions, and quantitated by spectrophotometry. Reverse transcription of 250 ng RNA was carried out with M-MLV reverse transcriptase, RNaseOUT, and random hexamers (Invitrogen, Karlsruhe, Germany) according to the manufacturer's recommendations. Controls without reverse transcriptase were included for each sample to ensure the absence of DNA contaminations, which, as a result of the high number of *HMGA1*-related retropseudogenes, could lead to false-positive results.

Quantitative real-time reverse transcriptase–polymerase chain reaction (RT-PCR) was performed on a real-time

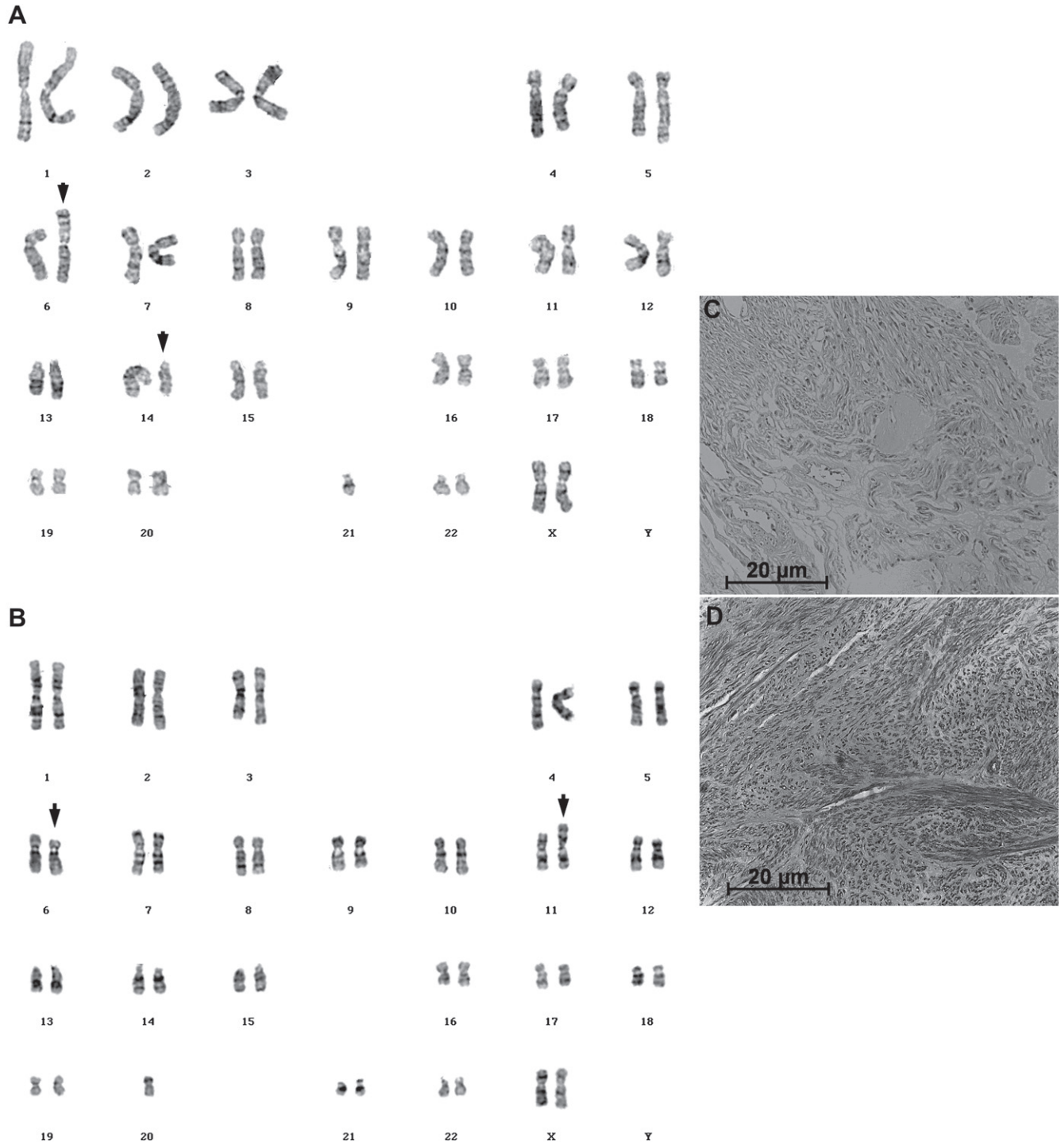

Fig. 1. Karyotypes of two ULs with 6p21 rearrangements with different levels of *HMGA1* expression and the histologic appearance of these ULs. (A) Representative G-banded karyotype of myoma 87: 46,XX,t(6;14)(p23;q24), tas(14;21)(pter;qter). (B) Representative G-banded karyotype of myoma 125A: 46,XX, t(6;11)(p21;p15), chromosomes participating in the 6p21 rearrangements are indicated by arrows. Histologic appearance of myoma 87 (C) and myoma 125A (D).

PCR cycler (Applied Biosystems, Darmstadt, Germany) with TaqMan Universal Mastermix. Of each cDNA, 2 μL served as template in a final reaction volume of 20 μL. Reaction condition were as follows: 2 minutes at 50°C, 10 minutes at 95°C, 50 cycles of 15 seconds at 95°C, and 1 minute at 60°C. For transcripts of *HMGA1,* a set of primers and probe was designed (forward primer: 5′-GGA CCA AAG GGA AGC AAA AA-3′, reverse primer: 5′-TTC CTG GAG TTG TGG TGG TTT-3′, probe: 6-FAM-AAG GGT GCT GCC AAG ACC CGG-MGB). 18S rRNA was chosen as endogenous control and detected with the following primer/probe set: forward primer: 5′-GGA TCC ATT GGA GGG CAA AGT-3′, reverse primer: 5′-AAT ATA CGC TAT TGG AGC TGG AAT TAC-3′, probe: TGC CAG CAG CCG C [10]. All reactions were run in triplicate.

2.3. Analysis of gene expression

The relative expression was calculated by the ΔC_t method, using 18S rRNA as endogenous control and choosing the *HMGA1* expression of a myometrial sample (of normal group) as calibrator. For statistical analyses, Student's *t*-test was used. *P*-values of ≤0.05 were considered to be significant.

2.4. Fluorescence in situ hybridization

For determination of rearrangements involving 6p21 and *HMGA1,* respectively, fluorescence in situ hybridization (FISH) was performed on metaphase preparations of the cases myoma 36, myoma 110, myoma 121B, myoma 125A, and myoma 166A. For FISH, two overlapping clones CTD-2522J1 (GenBank accession number AQ280064 and AQ280066) and CTD-2510D13 (GenBank accession number AQ264849 and AQ264850), both located distal to *HMGA1* in 6p21, and two overlapping clones CTD-2524P4 (GenBank accession number AQ310763 and AQ277896) and RP11-140K17 (GenBank accession number AQ385566 and AQ385568), both located proximal to *HMGA1,* in 6p21 were used. CTD clones were obtained from Invitrogen (Darmstadt, Germany); RP11-140K17 was obtained from imaGenes (Berlin, Germany). DNA was isolated with the Qiagen Plasmid Midi Kit (Qiagen, Hilden, Germany).

One microgram of isolated plasmid DNA was labeled by nick translation (Abbott Molecular, Wiesbaden, Germany) either with SpectrumOrange-dUTP (CTD-2522J1 and CTD-2510D13) or SpectrumGreen-dUTP (CTD-2524P4 and RP11-140K17) (Abbott Molecular). Treatment of metaphases and subsequent FISH experiments were carried out as described previously [11]. Twenty microliters of the

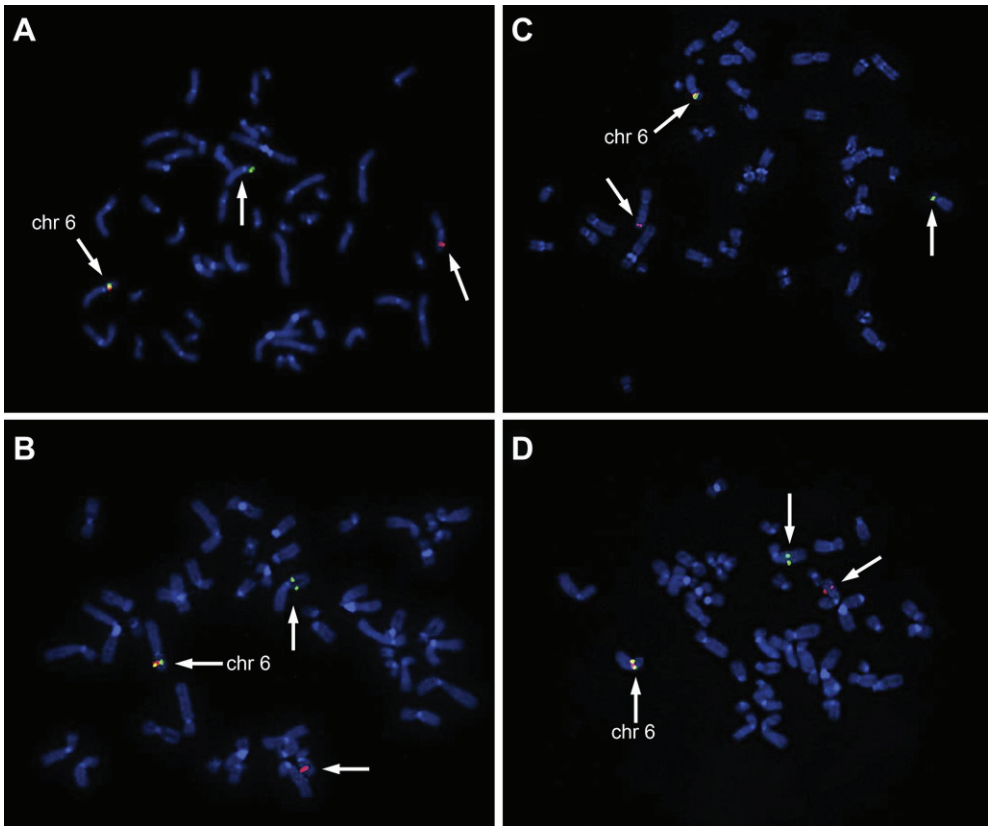

Fig. 2. FISH analysis with *HMGA1* break-apart probes in four UL with 6p21 rearrangement. (A) Myoma 125A, (B) myoma 166A, (C) myoma 121B, (D) myoma 110 (for karyotypes see Table 1). The green fluorescent probes (CTD-2524P4 and RP11-140K17) located proximal to *HMGA1*, the red fluorescent probes (CTD-2522J1 and CTD-2510D13) located distal to *HMGA1*. Arrows point to normal chromosomes 6 and the rearranged chromosomes.

Table 1
Cytogenetic and molecular-cytogenetic data, results of relative *HMGA1* and *HMGA2* expression, and clinical data of all ULs. All tumors investigated were histologically typical leiomyomas.

Case no.	Karyotype	Relative *HMGA1* expression	Relative *HMGA2* expression	Patient age (y)	Tumor size (cm)	*HMGA1* expression matching myometrium	Single or multiple	FISH analysis for *HMGA1* rearrangements
87	46,XX,t(6;14)(p23;q24)[6]/46,XX,t(6;14)(p23;q24),tas(14;21)(p13;q22)[11]/46,XX[2]/47,XX,+12[1]	0.5	0.6	63	—	1.7	Multiple	ND
125A	46,XX,t(6;11)(p21;p15)[7]/46,XX[14]	32.0	2.7	42	2.5	2.3	Multiple	Split signals
110	44,XX,der(1)t(1;?),der(3),der(5)t(5;?),−6,der(11)?t(11;15)(q25;q22),del(15)(q22),der(15)t(15;?),−19[25]	33.2	1.6	44	4	NA	Single	Split signals
113C	46,XX,t(6;10)(p23;q23)[5]/46,XX[7]	34.0	11.4	53	3.5	NA	Multiple	ND
117D	46,XX,t(6;11)(p23;q21)[4]/46,XX[12]	41.2	26.0	39	4.5	NA	Multiple	ND
121B	42~46,X,−X[6],−1[19],t(1;8)(p22;q24)[11],der(1)[6],del(3)[3],add(6)[19],−8[6],der(8)[4],−10[6],−11[6],−13[6],−14[19],−22[15],+mar1[18],+mar2[18],+mar3[6],+mar[6][cp19]/46,XX[1]	63.3	0.8	38	3	NA	Multiple	Split signals
166A	46,XX,t(6;10)(p21;q22)[13]/46,XX[8]	110.4	1.29	—	3	NA	Multiple	Split signals
14B	46,XX[10]	2.8	3.8	46	—	8.5	Multiple	ND
12B	46,XX[10]	3.1	2.4	41	—	1.0	Multiple	ND
24	46,XX[20]	3.9	0.5	44	1	7.6	Multiple	ND
27A	46,XX[10]	4.8	2.8	40	5	NA	Multiple	ND
20	46,XX[10]	5.1	0.6	36	—	1.2	Multiple	ND
37D	46,XX[15]	10.0	12.9	43	2	15.4	Multiple	ND
29	46,XX[21]	12.6	1.1	48	3.5	8.5	Multiple	ND
36	46,XX[14]	23.2	10.7	39	6	6.9	Single	No split signals

Abbreviations: −, unknown; ND, not done; NA, not available.

break-apart probe was used per slide. Co-denaturation was performed on a ThermoBrite (Abbott Molecular) for 7 minutes at 77°C, followed by overnight hybridization in a humidified chamber at 37°C. Posthybridization was performed at 70°C for 2 minutes in 0.4× standard saline citrate/0.3% NP-40. Metaphases were counterstained with DAPI (4′,6-diamidino-2-phenylindole; 0.75 μg/mL). Slides were examined with an Axioskop 2 Plus fluorescence microscope (Carl Zeiss, Göttingen, Germany). Images were captured with a high-performance CCD camera (Visitron Systems, Puchheim, Germany) and were edited with FISH View (Applied Spectral Imaging, Migdal Ha'Emek, Israel). Chromosomes were identified by inverted DAPI staining. For each case, if possible, at least 10 metaphases were analyzed, and 100 interphase nuclei were scored. Co-localized signals (green/red) indicate a nonrearranged breakpoint region, whereas separated green and orange signals indicate a rearrangement of the chromosomal region 6p21 and *HMGA1,* respectively.

3. Results

In this study, seven ULs with chromosomal rearrangements of 6p21 and eight karyotypically normal ULs as detected by chromosome analysis of GTG-banded metaphases and FISH analysis were subjected to real-time RT-PCR analysis. According to the histological examination, no sign of leiomyosarcoma or atypical leiomyoma was detected in any of the cases (Fig. 1).

For identification of 6p21 rearrangements involving *HMGA1* FISH on metaphase preparations and interphase nuclei of five myomas (four cases with 6p rearrangement or loss of one normal chromosome 6, respectively, and one with apparently normal karyotype) was performed with a *HMGA1*-specific break-apart probe. The results revealed a signal pattern corresponding to a 6p21 rearrangement involving *HMGA1* in all cases except for that with a normal karyotype (numbers 110, 121B, 125A, and 166A; Fig. 2A–D).

The expression of *HMGA1* mRNA in seven ULs with 6p21 rearrangement was compared to that in eight samples of UL with an apparently normal karyotype, which served as controls (Table 1). For nine of these samples, matching myometrium was available. Two myometrial samples belonged to fibroids of the 6p group, and the remaining tissues belonged to fibroids of the normal group. The average relative expression level in the 6p group was 45-fold compared to its expression in a myometrium sample of normal group as calibrator and differed significantly from that in the control group (8.2-fold increase). As to the expression in the individual tumors, *HMGA1* expression, with one exception, clearly distinguishes between both karyotypic groups (Fig. 3). In the exception, case 87, no unusually high percentage of metaphases with normal karyotype could be detected, which may explain the low expression of *HMGA1* observed. Regarding the expression of *HMGA1* in UL and matching myometrium, there were no significant differences in the normal group.

Next, we analyzed whether the expression of *HMGA1* correlates with the expression of *HMGA2*. No evidence for such a correlation was obtained (Fig. 3).

4. Discussion

ULs are by far the most common gynecological tumors, occurring in at least 70–80% of all women in their reproductive years [12–14]. Cytogenetic subtypes have been identified that may correlate with a different molecular pathogenesis of the disease. So far, the best-investigated group is characterized by 12q14~15 changes associated with a strong overexpression of *HMGA2* [3,15]. The

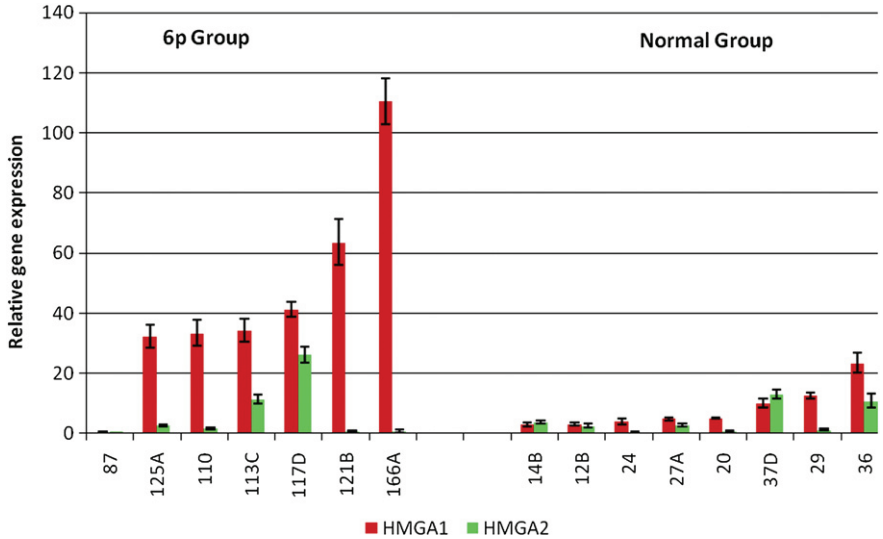

Fig. 3. Relative quantification of the *HMGA1* and *HMGA2* expression in normal and aberrant uterine leiomyomas (ULs).

overexpression of the stem-cell chromatin-associated protein HMGA2 fits well with important characteristics of UL growth. A much smaller subset of UL is characterized by 6p21 rearrangements leading to the upregulation of a closely related protein of the HMGA family (i.e., *HMGA1*). Likely activation of either of both genes and the abundance of their proteins, respectively, leads to an almost identical histopathologic phenotype of the tumors commonly referred as leiomyomas.

However, what distinguishes tumors of both types is the level of overexpression of *HMGA* genes compared to myometrium. Whereas the average upregulation of *HMGA2* in case of 12q14~15 aberrations is in range of 3,000-fold [3], even when omitting the outlier represented by case 87, upregulation of *HMGA1* due to 6p21 rearrangements is on average 45-fold and raise up to a maximum of only 52.4-fold.

We had recently been able to show that most cytogenetically normal leiomyomas show subtle changes of the *HMGA2* level compared to the matching myometrium as well [3]. Some recent studies have correlated HMGA2 with stemness of mesenchymal cells and stem cell self-renewal [4,16]. Although similar studies are lacking for HMGA1, it is tempting to assume that the translocation products of both genes can shift mesenchymal stem cells or progenitors of smooth muscle cells and other mesenchyme-derived cells back to a higher self-renewing potential. Nevertheless, we were recently able to show that there is no correlation between the expression of *Ki-67* and *HMGA2* [17]. Thus, the exact mechanism by which increased levels of HMGA proteins contribute to benign tumorigenesis still remains to be elucidated. However, HMGA1 can be assumed to have the ability to replace, at least in part, the function of HMGA2 and vice versa. The proteins of both genes are highly charged DNA-binding proteins that show abundant expression in embryonic cells but greatly decreased expression in most adult cells. They share a high homology in their DNA-interacting domains; despite their apparent differences in interaction partners [18], this may explain why knockout for neither gene alone is lethal.

Acknowledgments

This study was supported by grant from the Tönjes-Vagt-Foundation, Bremen. We acknowledge the valuable technical support of Tanja Schwarz and Lisa Imbiel.

References

[1] Ashar HR, Fejzo MS, Tkachenko A, Zhou X, Fletcher JA, Weremowicz S, et al. Disruption of the architectural factor HMGI-C: DNA-binding AT hook motifs fused in lipomas to distinct transcriptional regulatory domains. Cell 1995;82:57–65.

[2] Schoenmakers EF, Wanschura S, Mols R, Bullerdiek J, Van den Berghe H, Van de Ven WJ. Recurrent rearrangements in the high mobility group protein gene, HMGI-C, in benign mesenchymal tumours. Nat Genet 1995;10:436–44.

[3] Klemke M, Meyer A, Hashemi Nezhad M, Bartnitzke S, Drieschner N, Frantzen C, et al. Overexpression of HMGA2 in uterine leiomyomas points to its general role for the pathogenesis of the disease. Genes Chromosomes Cancer 2009;48:171–8.

[4] Nishino J, Kim I, Chada K, Morrison SJ. Hmga2 promotes neural stem cell self-renewal in young, but not old, mice by reducing p16Ink4a and p19Arf expression. Cell 2008;135:227–39.

[5] Willén R, Gad A, Willén H. Lipomatous lesions of the uterus. Virchows Arch A Pathol Anat Histol 1978;377:351–61.

[6] Yamadori I, Kobayashi S, Ogino T, Ohmori M, Tanaka H, Jimbo T. Uterine leiomyoma with a focus of fatty and cartilaginous differentiation. Acta Obstet Gynecol Scand 1993;72:307–9.

[7] Kazmierczak B, Bol S, Wanschura S, Bartnitzke S, Bullerdiek J. PAC clone containing the HMGI(Y) gene spans the breakpoint of a 6p21 translocation in a uterine leiomyoma cell line. Genes Chromosomes Cancer 1996;17:191–3.

[8] Sornberger KS, Weremowicz S, Williams AJ, Quade BJ, Ligon AH, Pedeutour F, et al. Expression of HMGIY in three uterine leiomyomata with complex rearrangements of chromosome 6. Cancer Genet Cytogenet 1999;114:9–16.

[9] Tallini G, Vanni R, Manfioletti G, Kazmierczak B, Faa G, Pauwels P, et al. HMGI-C and HMGI(Y) immunoreactivity correlates with cytogenetic abnormalities in lipomas, pulmonary chondroid hamartomas, endometrial polyps, and uterine leiomyomas and is compatible with rearrangement of the HMGI-C and HMGI(Y) genes. Lab Invest 2000;80:359–69.

[10] Antonov J, Goldstein DR, Oberli A, Baltzer A, Pirotta M, Fleischmann A, et al. Reliable gene expression measurements from degraded RNA by quantitative real-time PCR depend on short amplicons and a proper normalization. Lab Invest 2005;85:1040–50.

[11] Kievits T, Devilee P, Wiegant J, Wapenaar MC, Cornelisse CJ, van Ommen GJ, et al. Direct nonradioactive in situ hybridization of somatic cell hybrid DNA to human lymphocyte chromosomes. Cytometry 1990;11:105–9.

[12] Cramer SF, Patel A. The frequency of uterine leiomyomas. Am J Clin Pathol 1990;94:435–8.

[13] Day Baird D, Dunson DB, Hill MC, Cousins D, Schectman JM. High cumulative incidence of uterine leiomyoma in black and white women: ultrasound evidence. Am J Obstet Gynecol 2003;188:100–7.

[14] Heinemann K, Thiel C, Möhner S, Lewis MA, Raff T, Kühl-Habich D, et al. Benign gynecological tumors: estimated incidence. Results of the German Cohort Study on Women's Health. Eur J Obstet Gynecol Reprod Biol 2003;107:78–80.

[15] Gross KL, Neskey DM, Manchanda N, Weremowicz S, Kleinman MS, Nowak RA, et al. HMGA2 expression in uterine leiomyomata and myometrium: quantitative analysis and tissue culture studies. Genes Chromosomes Cancer 2003;38:68–79.

[16] Li O, Li J, Dröge P. DNA architectural factor and proto-oncogene HMGA2 regulates key developmental genes in pluripotent human embryonic stem cells. FEBS Lett 2007;581:3533–7.

[17] Markowski DN, von Ahsen I, Nezhad MH, Wosniok W, Helmke BM, Bullerdiek J. HMGA2 and the p19Arf-TP53-CDKN1A axis: a delicate balance in the growth of uterine leiomyomas. Genes Chromosomes Cancer 2010;49:661–8.

[18] Arlotta P, Rustighi A, Mantovani F, Manfioletti G, Giancotti V, Tell G, et al. High mobility group I proteins interfere with the homeodomains binding to DNA. J Biol Chem 1997;272:29904–10.

XII. Overexpression of *HMGA2* in Uterine Leiomyomas Points to its General Role for the Pathogenesis of the Disease (Klemke *et al.*, 2009)

Chromosomale Rearrangierungen der Region 12q14~15 unter Beteiligung von *HMGA2* stellen die häufigste strukturelle chromosomale Veränderung innerhalb mesenchymaler Tumoren dar und gehen i.d.R. mit einer erhöhten *HMGA2*-Expression einher. Für uterine Leiomyome konnte bereits gezeigt werden, dass *HMGA2*-Rearrangierungen eine bedeutende Rolle hinsichtlich der Pathogenese einnehmen (Hennig *et al.*, 1999). In dieser Studie lag der Fokus auf der quantitativen Bestimmung der *HMGA2*-Expression in uterinen Leiomyomen unter der Fragestellung, ob in diesen Tumoren ein generell erhöhtes Expressionslevel unabhängig von einer *HMGA2*-Rearrangierung vorliegt.

Entsprechend wurde eine quantitative Real-Time PCR zur Bestimmung des *HMGA2*-Expressionslevels an 180 Gewebeproben aus uterinen Leiomyomen sowie Myometrien durchgeführt. Parallel erfolgte eine zytogenetische Analyse aller uterinen Leiomyome sowie eine molekularzytogenetische Analyse an ausgewählten Tumoren.

Unter den zytogenetisch untersuchten uterinen Leiomyomen fanden sich in insgesamt 13 Tumoren chromosomale Aberrationen unter Beteiligung der Region 12q14~15.

Die quantitative Real-Time PCR zeigte, dass das relative Expressionslevel von *HMGA2* innerhalb der uterinen Leiomyome mit 261,41 deutlich über dem in der Gruppe der Myometrien lag (1,99). Zudem wies die Gruppe uteriner Leiomyome mit 12q14~15-Rearrangierungen (relatives *HMGA2*-Expressionlevel: 3213,78) im Vergleich zu der Gruppe ohne 12q14~15-Rearrangierung (31,59) einen signifikanten Unterschied bezüglich des durchschnittlichen *HMGA2*-Expressionslevels auf.

Eine I-FISH zum Nachweis einer *HMGA2*-Rearrangierung erfolgte an HOPE-fixierten Gewebeschnitten von drei uterinen Leiomyomen mittels einer *HMGA2* Break-Apart Sonde unter Einsatz der distal zu *HMGA2* lokalisierten Klone RP11-745O10 und RP11-293H23 sowie dem proximal zu *HMGA2* lokalisierten Klon RP11-269K4. In einem Fall lag trotz einer zytogenetisch nachgewiesenen Translokation t(12;14)(q15;q24) ein vergleichsweise niedriges *HMGA2*-Expressionslevel vor. Hier zeigte die I-FISH in 98% der ausgewerteten Interphase-Kerne einen intakten, d.h. nicht-rearrangierten *HMGA2*-Lokus. In einem zweiten Fall, der durch einen unauffälligen Karyotyp charakterisiert war, jedoch ein deutlich erhöhtes *HMGA2*-Expressionslevel aufwies, konnte in 23% der Interphase-Kerne am Gewebeschnitt

eine *HMGA2*-Rearrangierung nachgewiesen werden. In einem dritten Fall, für den kein zytogenetisches Ergebnis vorlag, der aber durch ein hohes *HMGA2*-Expressionslevel charakterisiert war, waren 51% der Interphase-Kerne positiv hinsichtlich einer *HMGA2*-Rearrangierung.

Eine Metaphase-FISH erfolgte an einem weiteren Tumor mit einer Translokation t(12;14)(q15;q24) und einem entsprechend hohen *HMGA2*-Expressionslevel. Hier konnte der Bruchpunkt innerhalb des Klons RP11-269K4 und somit außerhalb (5‘) von *HMGA2* nachgewiesen werden.

XII

Overexpression of *HMGA2* in Uterine Leiomyomas Points to its General Role for the Pathogenesis of the Disease

Markus Klemke, Anke Meyer, Maliheh Hashemi Nezhad, Sabine Bartnitzke, Norbert Drieschner, Christiane Frantzen, Ernst Heinrich Schmidt, Gazanfer Belge, Jörn Bullerdiek

(Genes Chromosomes & Cancer 48(2): 171-178)

Eigenanteil:

- Planung, Durchführung und Auswertung der molekularzytogenetischen Untersuchungen
- Auswahl der verwendeten DNA-Sonden und Etablierung eines FISH-Assays zum Nachweis von *HMGA2*-Rearrangierungen.
- Optimierung der FISH-Methode an HOPE-fixiertem, paraffin-eingebetteten Gewebeschnitten.

GENES, CHROMOSOMES & CANCER 48:171–178 (2009)

Overexpression of *HMGA2* in Uterine Leiomyomas Points to its General Role for the Pathogenesis of the Disease

Markus Klemke,[1†] Anke Meyer,[1†] Maliheh Hashemi Nezhad,[1] Sabine Bartnitzke,[1] Norbert Drieschner,[1] Christiane Frantzen,[2] Ernst Heinrich Schmidt,[3] Gazanfer Belge,[1] and Jörn Bullerdiek[1,4*]

[1]Center for Human Genetics, University of Bremen, 28359 Bremen, Germany
[2]Women's Clinic, St. Joseph-Stift Hospital, 28209 Bremen, Germany
[3]Department of Obstetrics and Gynecology, DIAKO Evang. Diakonie Hospital, 28239 Bremen, Germany
[4]Clinic for Small Animals and Research Cluster REBIRTH, University of Veterinary Medicine, 30137 Hanover, Germany

An overexpression of *HMGA2* is supposed to be a key event in the genesis of leiomyoma with chromosomal rearrangements affecting the region 12q14-15 targeting the *HMGA2* gene, but gene expression data regarding differences between uterine leiomyomas with and those without 12q14-15 aberrations are insufficient. To address the question whether *HMGA2* is only upregulated in the 12q14-15 subgroup, the expression of *HMGA2* was analyzed in a comprehensive set of leiomyomas ($n = 180$) including tumors with 12q14-15 chromosomal aberrations ($n = 13$) and matching myometrial tissues ($n = 51$) by quantitative RT-PCR. The highest expression levels for *HMGA2* were observed in tumors with rearrangements affecting the region 12q14-15, but although *HMGA2* is expressed at lower levels in leiomyomas without such aberrations, the comparison between the expression in myomas and matching myometrial tissues indicates a general upregulation of *HMGA2* regardless of the presence or absence of such chromosomal abnormalities. The significant ($P < 0.05$) overexpression of *HMGA2* also in the group of fibroids without chromosomal aberrations of the 12q14-15 region suggests a general role of *HMGA2* in the development of the disease.

INTRODUCTION

Uterine leiomyomas (UL, fibroids) are the most frequent gynecological tumors and, despite being benign, constitute an enormous public health burden. Among the symptoms caused by uterine leiomyomas are menorrhagia, abdominal pain, and infertility (Stewart, 2001). Their actual prevalence is still a matter of debate and seems to vary among populations, but at least one third of women aged 30 years or older have one or more UL (Cramer and Patel, 1990; Baird et al., 2003; Heinemann et al., 2003). Their incidence seems to be higher in African American than in European American or European women (Marshall et al., 1998).

Currently, mutations of the two human genes encoding high mobility group proteins of the HMGA type, i.e., *HMGA1* and *HMGA2* have been assumed to be causally linked with the development of subsets of uterine leiomyomas. Both genes encode members of the so-called high mobility group proteins. HMGA proteins are capable of binding to the minor groove of AT-rich DNA with three DNA-binding domains (so-called AT-hooks), thus inducing conformational changes in chromatin structure and enabling the regulation of the expression of various target genes. In addition, they can interact with other proteins by means of their acidic domain (Fusco and Fedele, 2007). *HMGA1* and *HMGA2* map to chromosomal bands that are targeted by nonrandom structural chromosomal abnormalities found in uterine leiomyomas, i.e., 6p21 for *HMGA1* (Kazmierczak et al., 1996) and 12q14-15 for *HMGA2* (Ashar et al., 1995; Schoenmakers et al., 1995). Usually, these regions are affected by chromosomal translocations but inversions can occur as well with structural chromosomal aberrations affecting 12q14-15 being much more frequent than those affecting 6p21 (Nilbert and Heim, 1990). The molecular alterations resulting from the cytogenetic deviations generally seem to

Supported by: Tönjes-Vagt-Stiftung, Bremen.

[†]Markus Klemke and Anke Meyer contributed equally to this work.

*Correspondence to: Jörn Bullerdiek, Center for Human Genetics, University of Bremen, Leobener Str. ZHG, 28359 Bremen, Germany. E-mail: bullerd@uni-bremen.de

Received 9 May 2008; Accepted 18 September 2008
DOI 10.1002/gcc.20627
Published online 3 November 2008 in Wiley InterScience (www.interscience.wiley.com).

include an upregulation of the genes (Tallini et al., 2000; Gross et al., 2003). With regard to *HMGA2*, a considerable fraction of the chromosomal breakpoints has been assigned to regions outside the open reading frame of the gene, thus primarily affecting its expression rather than its protein sequence (Quade et al., 2003). Thus, overexpression of *HMGA2* seems to be sufficient to trigger tumorigenesis. It is obvious that an enhanced level of *HMGA2* is pathogenetically relevant in a subset of some 10–20% of uterine leiomyomas (Hennig et al., 1999), but it remains an open question whether or not an increased level of *HMGA2*, compared to normal myometrium, may characterize also leiomyomas that do not have *HMGA2* rearrangements. A recent study by Peng et al., (2008) suggests that upregulation of *HMGA2* may be a more general phenomenon in UL but the analyzed tumors were not genetically classified and no matched samples were analyzed individually by quantitative RT-PCR. Herein, we have quantitated the level of *HMGA2* mRNA in a large series of uterine leiomyomas.

MATERIALS AND METHODS

Tissue Samples

Samples of uterine leiomyomas and myometrium were snap frozen in liquid nitrogen immediately after surgery and stored at −80°C. In case of UL another part of the tumor was used for cell culturing and karyotyping. Informed consent was obtained from all patients.

For fluorescence in situ hybridization (FISH) analyses HOPE (HEPES-glutamic acid buffer mediated organic solvent protection effect)-fixed, paraffin-embedded tissue sections were used. The tissues were cut into 5 μm sections which were subsequently used for FISH analyses.

RNA Isolation, Reverse Transcription, and Quantitative RT-PCR

RNA was isolated from fresh-frozen tissue samples with the RNeasy Mini Kit (Qiagen, Hilden, Germany) including DNase treatment according to the manufacturer's instructions and quantitated by spectrophotometry. After reverse transcription of 250 ng of total RNA using M-MLV RT (Invitrogen, Karlsruhe, Germany) and random hexamers, the *HMGA2* mRNA levels were determined by relative quantification referring to the expression of 18S rRNA. Real-time PCR was performed on a 7300 Real-Time PCR System with Assay No. Hs00171569_m1 (Applied Biosystems, Darmstadt, Germany) for the detection of *HMGA2* and primers and probe for 18S rRNA as described previously (Belge et al., 2008).

Analysis of Gene Expression

The relative expression was calculated by the ΔC_t method, using 18S rRNA as endogenous control and by choosing the *HMGA2* expression of a myometrial sample as calibrator. The significance of differential *HMGA2* expression between the different groups (myometrium, myoma with and without 12q14-15 aberrations) was determined by Student's *t*-test.

Cell Culture

After surgery, samples of primary tumors were stored in Hank's solution with antibiotics (200 IU/ml penicillin, 200 μg/ml streptomycin). For cell culture the tumor samples were minced and treated with 0.26% (200U/ml) collagenase (Serva, Heidelberg, Germany) for 5–8 hr. After centrifugation, the pellet was resuspended in culture medium (TC 199 with Earle's salts supplemented with 20% fetal bovine serum, 200 IU/ml penicillin, 200 μg/ml streptomycin) and incubated at 37°C and 5% CO_2.

Chromosome Analyses

For chromosome analyses exponentially growing cultures of leiomyoma cells were used. Metaphase chromosome spreads were prepared by using colcemid (0.06 μg/ml for 1 hr) to arrest cultured cells during mitosis. A hypotonic solution (culture medium and aqua bidest in a 1:6 ratio) and the fixative (methanol and acetic acid in a 3:1 ratio) were then applied sequentially. Finally, the chromosome suspension was dropped onto glass slides. The chromosomes were GTG-banded according to routine techniques. Karyotype description followed ISCN (2005).

HMGA2-Specific Break-Apart Probes and FISH

For FISH three BAC clones were used as break-apart probes. RP11-745O10 (AC078927) and RP11-293H23 (AC012264) are located distal (3′) to *HMGA2*. RP11-269K4 (AQ478964 and AZ516203) is located proximal (5′) to *HMGA2*. Labeling was performed by nick translation (Roche Diagnostics, Mannheim, Germany) either with digoxigenin (RP-269K4) or biotin (RP11-

745O10 and RP11-293H23). For each FISH experiment 2 ng/μl of the distally located probes (RP11-745O10 and RP11-293H23) and 3 ng/μl of RP11-296K4 were used in 15 μl hybridization solution containing 50% formamide, 2×SSC, 10% dextrane sulfate and 105 ng/μl COT human DNA.

FISH analysis on metaphase preparations was performed after GTG banding of the metaphase spreads. Treatment of metaphases and subsequent FISH experiments were performed as described previously (Kievits et al., 1990) with a few modifications. For one slide 25 μl of hybridization mixture were used. Codenaturation was performed on a Mastercycler gradient (Eppendorf, Hamburg, Germany) for 3 min at 80°C followed by O/N hybridization in a humidified chamber at 37°C. Posthybridization was performed at 61°C for 5 min in 0.1×SSC. Subsequent treatment of slides was performed as described previously (Kievits et al., 1990). For detection of the hybridized probes antidigoxigenin fluorescein fab fragments (Roche Diagnostics) and Cy3-conjugated streptavidin (Dianova, Hamburg, Germany) were used. Slides were counterstained with DAPI (0.75 μg/ml) (Vector Laboratories, Burlingame, CA).

For FISH, formalin-fixed, paraffin-embedded (FFPE) tissue sections were deparaffinized with diethylether. Protease digestion was done with a pepsin ready-to-use solution (DCS, Hamburg, Germany) for 12–17 min. After dehydration in a 70%, 80%, and 95% ethanol series the sections were postfixed with 1% formaldehyde in 1×PBS for 15 min. Prior to codenaturation the sections were dehydrated again. Codenaturation was performed on a Mastercycler gradient (Eppendorf) for 5 min at 85°C followed by O/N hybridization in a humidified chamber at 37°C. Posthybridization was performed at 42°C or 61°C for 2 min in 0.4×SSC/0.3%NP-40. Subsequent treatment of slides and detection of hybridized probes were performed as described for FISH on metaphase preparations.

Slides were examined in an Axioskop 2 plus fluorescence microscope (Zeiss, Göttingen, Germany). Images were captured with an AxioCam MRm digital camera and were edited with AxioVision (Zeiss). For metaphase preparations, 10 metaphases were examined. For analysis of FFPE tissue sections at least 100 nonoverlapping nuclei from different (at least three) areas of the tumors were scored. Nuclei with two colocalized red/green signals (RG) were scored as normal. Nuclei with one colocalized red/green signal, one single red, and one single green signal (1RG1R1G) were scored as positive for *HMGA2* rearrangement.

RESULTS

For this study 180 uterine leiomyomas from 100 patients have been investigated by qRT-PCR for the expression level of *HMGA2*. A total of 57 myometrium samples from uteri removed because of the occurrence of UL were investigated as well. For 51 of these samples, matching tissue from one or more leiomyomas was available. All UL have been karyotyped successfully based on at least 10 G-banded metaphases showing a resolution of 400 bands per haploid set or higher.

Based on cytogenetics the group of UL was further subdivided into those showing aberrations of chromosomal region 12q14-15 ($n = 13$; Table 1) and those with an apparently normal karyotype or other clonal aberrations ($n = 167$), respectively.

As to these three groups, i.e., myometrium, UL with 12q14-15 changes, and other UL *HMGA2* expression was determined by qRT-PCR using fresh-frozen samples. The average relative *HMGA2* mRNA expression was 1.99 for the myometria and 261.41 for all UL. When distinguishing between both subgroups of UL outlined above average expression levels were 3213.78 for UL with aberrations in the chromosomal region 12q14-15 and 31.59 for those without changes in this region, respectively.

Thus, even within the group of UL without cytogenetically detectable rearrangements of the *HMGA2* locus at 12q14-15 *HMGA2* mRNA was expressed at a higher level than in myometrium (Fig. 1). Differences between all leiomyomas and myometrium as well as between leiomyomas without 12q14-15 aberrations and myometrium were statistically significant ($P < 0.005$ and $P < 0.05$, respectively). Furthermore, an individual analysis of the matched samples (51 myometrial tissues and 107 corresponding UL) was performed. The mean *HMGA2* expression was 11.37 in karyotypically normal UL ($n = 101$) and 1.77 in the corresponding myometrial tissues ($n = 51$).

The results clearly show that in nearly all cases within each of the paired samples the leiomyomas showed higher *HMGA2* expression than the corresponding myometrium (Fig. 2).

One case with a normal karyotype and an unexpectedly high *HMGA2* expression as well as

TABLE 1. Karyotypes of the 13 Leiomyomas with Chromosome 12 Aberrations and Results of Interphase FISH with *HMGA2* Specific Break-Apart Probes

Karyotype	Relative *HMGA2* expression	FISH results (2RG/1RG1R1G)[a]
46,XX,inv(5)(q15q31∼ 33),t(12;14)(q15;q24)[13]	8.6	98/1
46,XX,t(12;15;14)(q15;q26;q24)[20]/46,XX[1]	302.3	–
46,XX[36]	894.5	72/23
–	993.3	41/51
46,XX,der(1)r(1;2),t(12;14)(q15;q24)[4]/46,XX,t(12;14)(q15;q24)[13]	1047.8	m
46,XX,t(12;14)(q15;q24)[9]/46,XX[3]	1327.3	–
46,XX,r(1),t(1;12;14)(p36.3;q14;q24)[19]	1722.5	–
46,XX,t(2;12)(q33;q13)[17]	2381.6	–
46,XX,der(12),der(14)?ins(14;12)[8]/46,idem,r(1)[4]	3444.3	–
46,XX,t(3;5;12)(q23∼ 25;p13∼ 15;q13∼ 15)[11]/45,XX,idem,-22 [10]	4450.7	–
46,XX,t(12;14)(q15;q24)[5]/46,XX[9]	5906.1	–
45,XX,t(12;14)(q15;q24),der(14)t(12;14)(q15;q24),-22[15]	7760.3	–
45,XX,t(12;14)(q15;q24),der(14)t(12;14)(q15;q24),-22[15]	11539.7	–

[a]Percentage of nuclei either with two colocalized signals (2RG) or with one colocalized, one single red and one single green signal (1RG1R1G) indicating a *HMGA2* rearrangement.
m, FISH was performed on metaphase preparations (Fig. 4). All 10 metaphases showed a breakpoint upstream of *HMGA2*.

a second myoma with a cytogenetically visible t(12;14) and a rather low *HMGA2* expression were checked by interphase FISH. In the cytogenetically normal myoma, FISH showed *HMGA2* disruption in 23% of the cells (Fig. 3, Table 1). The tumor with visible t(12;14) but low expression of *HMGA2* showed two colocalized signals in 98% of the nuclei, indicating an intact *HMGA2* locus.

Metaphase FISH was also done on one case with a t(12;14)(q15;q24) (Fig. 4). Interestingly, the probe located proximal to *HMGA2* (RP11-269K4) showed three signals: on the normal chromosome 12, the derivative chromosome 12, and the derivative chromosome 14 (Fig. 4C), indicating a breakpoint located 5′ of *HMGA2*. The approximately 16kb distance between the probe RP11-269K4 and the 5′ end of *HMGA2* suggests that the breakpoint was located approximately 20kb upstream of *HMGA2*.

DISCUSSION

Despite their high prevalence the etiology and pathogenesis of UL remain poorly understood. Mutations of the gene encoding the high mobility group protein HMGA2 have been suggested to cause a subset of uterine leiomyomas (Schoenmakers et al., 1995; Hennig et al., 1999). As a

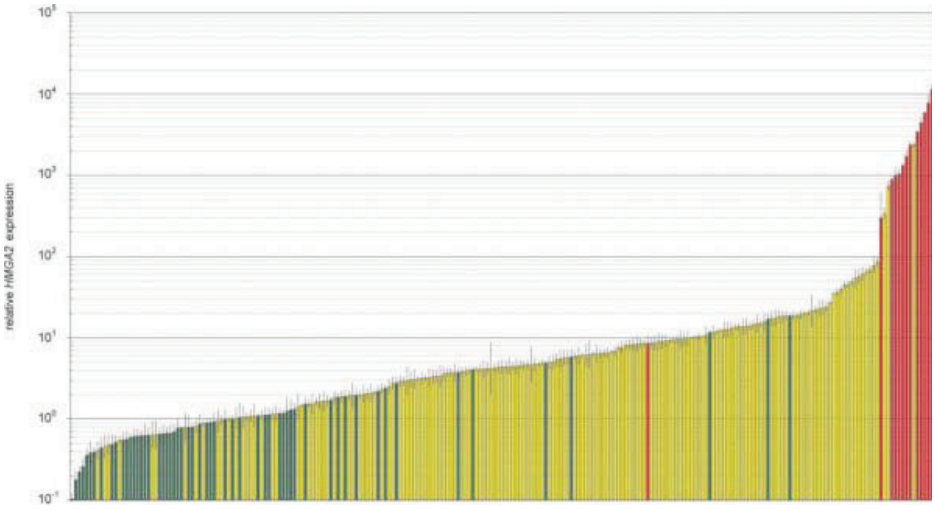

Figure 1. Relative quantification of the *HMGA2* expression in uterine leiomyomas and myometrial tissues. Green bars: Myometrium; yellow bars: UL without cytogenetically detectable aberrations of chromosomal region 12q14-15; red bars: UL with 12q14-15 aberrations.

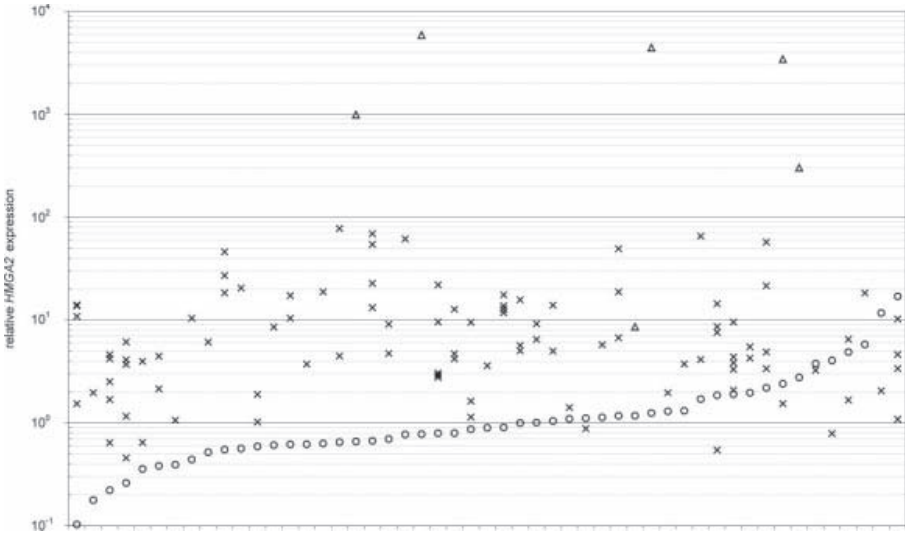

Figure 2. *HMGA2* expression in UL (crosses) and matching myometrial tissues (open circles) in increasing order of expression in myometrial tissues. Triangles indicate UL with 12q14-15 aberrations.

rule, this subset is characterized by cytogenetically visible structural chromosome alterations affecting chromosomal region 12q14-15. *HMGA2* has been identified as the target of these alterations (Schoenmakers et al., 1995) and despite a wide distribution of breakpoints, intragenic as well as extragenic (Kazmierczak et al., 1995; Hennig et al., 1996; Schoenmakers et al., 1999; Kurose et al., 2000; Mine et al., 2001; Takahashi et al., 2001; Quade et al., 2003), the key mechanism by which the chromosomal alterations contribute to tumorigenesis seems to be an upregulation of the *HMGA2* gene leading to overexpression of the full-length transcript or a truncated or chimeric protein. Nevertheless, the majority of UL lack cytogenetically visible chromosome alterations and also by molecular-cytogenetic methods there is no evidence that submicroscopic alterations of the *HMGA2* locus occur in a considerable number of these cases (Weremowicz and Morton, 1999). On the other hand, *HMGA2* overexpression could play a more general role in the development of UL, and not only in the subgroup characterized by 12q14-15 alterations. Roughly 10 years ago the hypothesis was advanced that *HMGA2* overexpression induces an embryonic chromatin configuration in cells, thus re-endowing them with a stem-cell like behavior (Bullerdiek, 1997). This assumption was further supported by recent studies on the *HMGA2* expression in embryonic stem cells (Li et al., 2006, 2007).

Here, we have shown that also UL without cytogenetically detectable 12q14-15 rearrangements overexpress *HMGA2*. This supports the assumption that an elevated level of a stem-cell chromatin associated protein is one of the key events in the genesis of UL. Of particular note, the expression of *HMGA2* in myomas almost always exceeded that of the corresponding myometrium (Fig. 2). Apparently, the basic level of *HMGA2* varies among the samples. Possibly, this could reflect changes throughout the menstrual

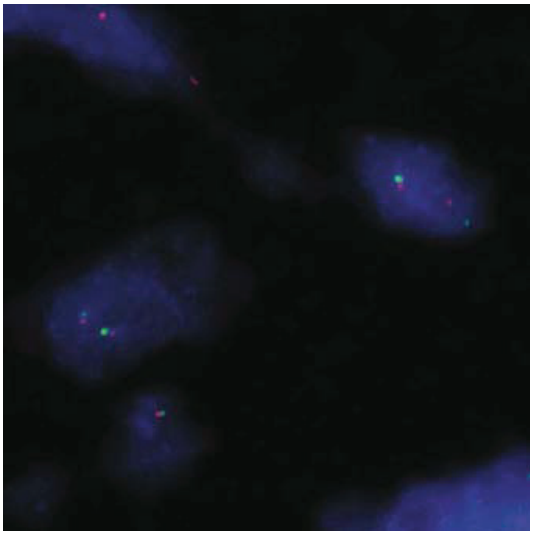

Figure 3. Dual-color FISH performed on interphase nuclei of a leiomyoma with cytogenetically normal karyotype. One nucleus showing two colocalized red/green signals (2RG, left) and a second nucleus with one colocalized red/green and one single red and green signal (1RG1R1G, right), respectively, indicating a rearrangement of *HMGA2*.

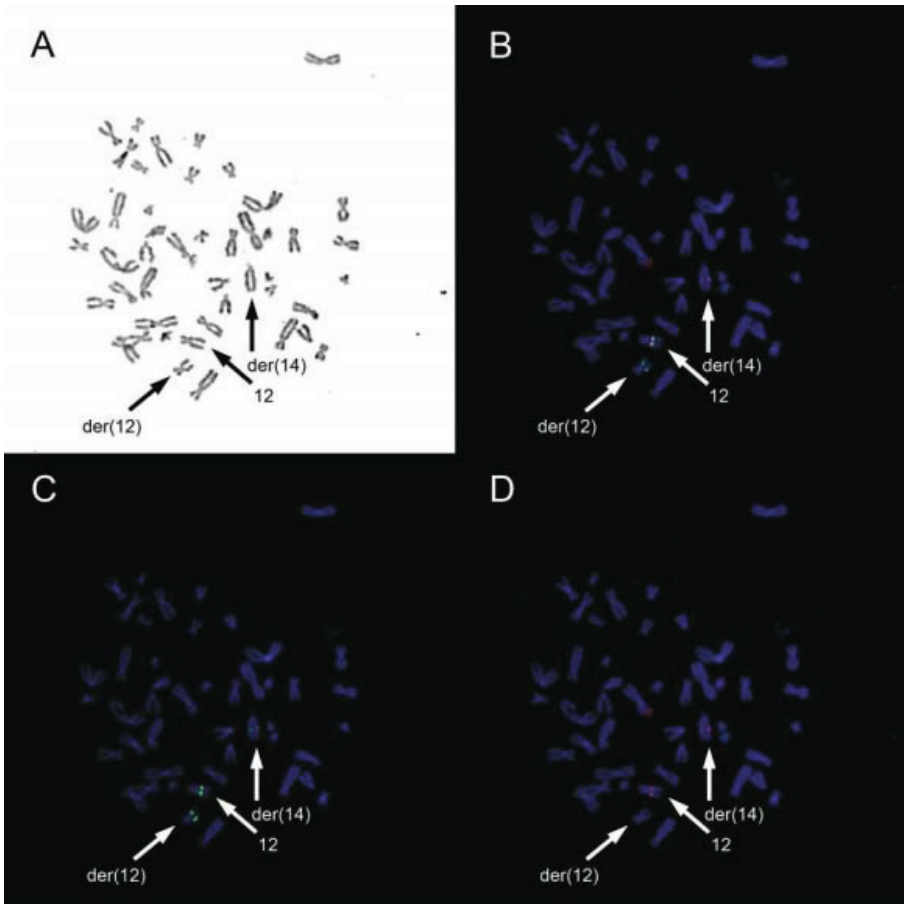

Figure 4. FISH with *HMGA2* break-apart probes in a UL with t(12;14)(q15;q24). A: G-banded metaphase prior to FISH. B: The same metaphase after dual-color FISH indicating a rearrangement of the *HMGA2* locus. C: Corresponding figure only showing the green fluorescent probe (RP11-269K4) located proximal (5′) to *HMGA2*. D: Corresponding figure only showing the red fluorescent probes (RP11-745O10 and RP11-293H23) located distal (3′) to *HMGA2*.

cycle. Such alterations in gene expression patterns have been described, e.g., by Kayisli et al. (2007). Herein, the term overexpression refers to an expression exceeding that of the matching myometrium. Despite the monoclonal origin of UL (Townsend et al., 1970; Mashal et al., 1994; Hashimoto et al., 1995; Zhang et al., 2006) overexpression of *HMGA2* must not necessarily be due to mutations affecting the gene itself. It has recently been described that *HMGA2* is regulated by microRNAs of the let-7 family (Lee and Dutta, 2007; Mayr et al., 2007; Park et al., 2007; Shell et al., 2007; Kumar et al., 2008; Motoyama et al., 2008; Peng et al., 2008). Thus, having now identified the overexpression of *HMGA2* also in UL without 12q14-15 alterations being visible at the microscopic level, future studies should also address mutations of let-7 genes and their binding sites within the 3′ UTR of *HMGA2*.

To further validate the cytogenetic results in cases with high *HMGA2* expression and no visible translocation or vice versa, FISH was performed with *HMGA2* break-apart probes. In the first case, separate signals from BAC clones located 5′ and 3′ of *HMGA2* occurred in 23% of the cells, indicating a translocation with a breakpoint within or in close proximity of *HMGA2*. Besides a cryptic *HMGA2* rearrangement undetectable by classical cytogenetics, a selection of cells without translocation during cell culture may explain the observation that the karyotype was apparently normal. However, the fact that chromosome 12 was found to be aberrant in almost one fourth of the cells by FISH is concordant with the high *HMGA2* expression despite an apparently normal karyotype.

In the second case showing a low *HMGA2* expression despite a visible t(12;14) the signals

were colocalized in 98% of the cells suggesting that the breakpoint was localized outside the region covered by the FISH probes. This unusually large distance between the breakpoint and *HMGA2* may explain why the observed *HMGA2* expression was unexpectedly low in one UL with a t(12;14). On the other hand, as indicated by FISH on metaphases of one UL with t(12;14)(q15;q24), an extragenic breakpoint upstream but in closer proximity of *HMGA2* can be sufficient to trigger the observed overexpression. Breakpoints located 5′ of *HMGA2* in UL with t(12;14) have also been reported by Quade et al. (2003).

The *HMGA2* expression in uterine leiomyomas has also been quantified in a study by Gross et al. (2003). Eleven karyotypically normal UL plus four matching myometrial samples as well as 10 UL with 12q14-15 rearrangements plus three myometrial tissues were analyzed by qRT-PCR, and a significantly higher *HMGA2* expression in UL with 12q14-15 rearrangements was noted. However, in contrast to the present study, no significant differences between the expression levels in karyotypically normal UL and matching myometrial samples were observed.

In summary, our results confirm the strongly increased *HMGA2* expression in UL with 12q14-15 rearrangements. Moreover, the expression levels detected in 101 UL from 51 patients and 51 matching myometrial samples indicate a general increase of *HMGA2* mRNA also in karyotypically normal tumors.

ACKNOWLEDGMENTS

We thank Karmela Sobczyk and Manuela Grund for their valuable technical support.

REFERENCES

Ashar HR, Fejzo MS, Tkachenko A, Zhou X, Fletcher JA, Weremowicz S, Morton CC, Chada K. 1995. Disruption of the architectural factor HMGI-C: DNA-binding AT hook motifs fused in lipomas to distinct transcriptional regulatory domains. Cell 82:57–65.

Baird DD, Dunson DB, Hill MC, Cousins D, Schectman JM. 2003. High cumulative incidence of uterine leiomyoma in black and white women: Ultrasound evidence. Am J Obstet Gynecol 188:100–107.

Belge G, Meyer A, Klemke M, Burchardt K, Stern C, Wosniok W, Loeschke S, Bullerdiek J. 2008. Upregulation of HMGA2 in thyroid carcinomas: A novel molecular marker to distinguish between benign and malignant follicular neoplasias. Genes Chromosomes Cancer 47:56–63.

Bullerdiek J. 1997. The molecular target of 12q14-15 aberrations in benign solid tumors. HMGIC rearrangements and beyond. Fourth International workshop on chromosome 12 mapping. Kucherlapati R, Marynen P, Turc-Carel C, editors. Book of abstracts. Nice: Organizing Comittee of the Meetings.

Cramer SF, Patel A. 1990. The frequency of uterine leiomyomas. Am J Clin Pathol 94:435–438.

Fusco A, Fedele M. 2007. Roles of HMGA proteins in cancer. Nat Rev Cancer 7:899–910.

Gross KL, Neskey DM, Manchanda N, Weremowicz S, Kleinman MS, Nowak RA, Ligon AH, Rogalla P, Drechsler K, Bullerdiek J, Morton CC. 2003. HMGA2 expression in uterine leiomyomata and myometrium: Quantitative analysis and tissue culture studies. Genes Chromosomes Cancer 38:68–79.

Hashimoto K, Azuma C, Kamiura S, Kimura T, Nobunaga T, Kanai T, Sawada M, Noguchi S, Saji F. 1995. Clonal determination of uterine leiomyomas by analyzing differential inactivation of the X-chromosome-linked phosphoglycerokinase gene. Gynecol Obstet Invest 40:204–208.

Heinemann K, Thiel C, Möhner S, Lewis MA, Raff T, Kühl-Habich D, Heinemann LA. 2003. Benign gynecological tumors: Estimated incidence. Results of the German Cohort Study on Women's Health. Eur J Obstet Gynecol Reprod Biol 107:78–80.

Hennig Y, Wanschura S, Deichert U, Bartnitzke S, Bullerdiek J. 1996. Rearrangements of the high mobility group protein family genes and the molecular genetic origin of uterine leiomyomas and endometrial polyps. Mol Hum Reprod 2:277–283.

Hennig Y, Deichert U, Bonk U, Thode B, Bartnitzke S, Bullerdiek J. 1999. Chromosomal translocations affecting 12q14-15 but not deletions of the long arm of chromosome 7 associated with a growth advantage of uterine smooth muscle cells. Mol Hum Reprod 5:1150–1154.

ISCN. 2005. An International System for Human Cytogenetic Nomenclature. In: Shaffer LG, Tommerup N, editors. Basel, Switzerland: S. Karger AG.

Kayisli UA, Berkkanoglu M, Kizilay G, Senturk L, Arici A. 2007. Expression of proliferative and preapoptotic molecules in human myometrium and leiomyoma throughout the menstrual cycle. Reprod Sci 14:678–686.

Kazmierczak B, Bol S, Wanschura S, Bartnitzke S, Bullerdiek J. 1996. PAC clone containing the HMGI(Y) gene spans the breakpoint of a 6p21 translocation in a uterine leiomyoma cell line. Genes Chromosomes Cancer 17:191–193.

Kazmierczak B, Hennig Y, Wanschura S, Rogalla P, Bartnitzke S, van de Ven W, Bullerdiek J. 1995. Description of a novel fusion transcript between HMGI-C, a gene encoding for a member of the high mobility group proteins, and the mitochondrial aldehyde dehydrogenase gene. Cancer Res 55:6038–6039.

Kievits T, Dauwerse JG, Wiegant J, Devilee P, Breuning MH, Cornelisse CJ, van Ommen GJ, Pearson PL. 1990. Rapid subchromosomal localization of cosmids by nonradioactive in situ hybridization. Cytogenet Cell Genet 53:134–136.

Kumar MS, Erkeland SJ, Pester RE, Chen CY, Ebert MS, Sharp PA, Jacks T. 2008. Suppression of non-small cell lung tumor development by the let-7 microRNA family. Proc Natl Acad Sci USA 105:3903–3908.

Kurose K, Mine N, Doi D, Ota Y, Yoneyama K, Konishi H, Araki T, Emi M. 2000. Novel gene fusion of COX6C at 8q22-23 to HMGIC at 12q15 in a uterine leiomyoma. Genes Chromosomes Cancer 27:303–307.

Lee YS, Dutta A. 2007. The tumor suppressor microRNA let-7 represses the HMGA2 oncogene. Genes Dev 21:1025–1030.

Li O, Li J, Dröge P. 2007. DNA architectural factor and protooncogene HMGA2 regulates key developmental genes in pluripotent human embryonic stem cells. FEBS Lett 581:3533–3537.

Li O, Vasudevan D, Davey CA, Dröge P. 2006. High-level expression of DNA architectural factor HMGA2 and its association with nucleosomes in human embryonic stem cells. Genesis 44:523–529.

Mashal RD, Fejzo ML, Friedman AJ, Mitchner N, Nowak RA, Rein MS, Morton CC, Sklar J. 1994. Analysis of androgen receptor DNA reveals the independent clonal origins of uterine leiomyomata and the secondary nature of cytogenetic aberrations in the development of leiomyomata. Genes Chromosomes Cancer 11:1–6.

Marshall LM, Spiegelman D, Barbieri RL, Goldman MB, Manson JE, Colditz GA, Willett WC, Hunter DJ. 1998. Variation in the incidence of uterine leiomyoma among premenopausal women by age and race. Obstet Gynecol 90:967–973.

Mayr C, Hemann MT, Bartel DP. 2007. Disrupting the pairing between let-7 and Hmga2 enhances oncogenic transformation. Science 315:1576–1579.

Mine N, Kurose K, Konishi H, Araki T, Nagai H, Emi M. 2001. Fusion of a sequence from HEI10 (14q11) to the HMGIC gene at 12q15 in a uterine leiomyoma. Jpn J Cancer Res 92:135–139.

Motoyama K, Inoue H, Nakamura Y, Uetake H, Sugihara K, Mori M. 2008. Clinical significance of high mobility group A2 in

human gastric cancer and its relationship to let-7 microRNA family. Clin Cancer Res 14:2334–2340.
Nilbert M, Heim S. 1990. Uterine leiomyoma cytogenetics. Genes Chromosomes Cancer 2:3–13.
Park SM, Shell S, Radjabi AR, Schickel R, Feig C, Boyerinas B, Dinulescu DM, Lengyel E, Peter ME. 2007. Let-7 prevents early cancer progression by suppressing expression of the embryonic gene HMGA2. Cell Cycle 6:2585–2590.
Peng Y, Laser J, Shi G, Mittal K, Melamed J, Lee P, Wei JJ. 2008. Antiproliferative effects by let-7 repression of high-mobility group A2 in uterine leiomyoma. Mol Cancer Res 6:663–673.
Quade BJ, Weremowicz S, Neskey DM, Vanni R, Ladd C, Dal Cin P, Morton CC. 2003. Fusion transcripts involving HMGA2 are not a common molecular mechanism in uterine leiomyomata with rearrangements in 12q15. Cancer Res 63:1351–1358.
Schoenmakers EF, Huysmans C, van de Ven WJ. 1999. Allelic knockout of novel splice variants of human recombination repair gene RAD51B in t(12;14) uterine leiomyomas. Cancer Res 59:19–23.
Schoenmakers EF, Wanschura S, Mols R, Bullerdiek J, van den Berghe H, van de Ven WJ. 1995. Recurrent rearrangements in the high mobility group protein gene, HMGI-C, in benign mesenchymal tumours. Nat Genet 10:436–444.
Shell S, Park SM, Radjabi AR, Schickel R, Kistner EO, Jewell DA, Feig C, Lengyel E, Peter ME. 2007. Let-7 expression defines two differentiation stages of cancer. Proc Natl Acad Sci USA 104:11400–11405.
Stewart EA. 2001. Uterine fibroids. Lancet 357:293–298.
Takahashi T, Nagai N, Oda H, Ohama K, Kamada N, Miyagawa K. 2001. Evidence for RAD51L1/HMGIC fusion in the pathogenesis of uterine leiomyoma. Genes Chromosomes Cancer 30:196–201.
Tallini G, Vanni R, Manfioletti G, Kazmierczak B, Faa G, Pauwels P, Bullerdiek J, Giancotti V, van Den Berghe H, Dal Cin P. 2000. HMGI-C and HMGI(Y) immunoreactivity correlates with cytogenetic abnormalities in lipomas, pulmonary chondroid hamartomas, endometrial polyps, and uterine leiomyomas and is compatible with rearrangement of the HMGI-C and HMGI(Y) genes. Lab Invest 80:359–369.
Townsend DE, Sparkes RS, Baluda MC, McClelland G. 1970. Unicellular histogenesis of uterine leiomyomas as determined by electrophoresis by glucose-6-phosphate dehydrogenase. Am J Obstet Gynecol 107:1168–1173.
Weremowicz S, Morton CC. 1999. Is HMGIC rearranged due to cryptic paracentric inversion of 12q in karyotypically normal uterine leiomyomas? Genes Chromosomes Cancer 24: 172–173.
Zhang P, Zhang C, Hao J, Sung CJ, Quddus MR, Steinhoff MM, Lawrence WD. 2006. Use of X-chromosome inactivation pattern to determine the clonal origins of uterine leiomyoma and leiomyosarcoma. Hum Pathol 37:1350–1356.

XIII. Cell culture and senescence in uterine fibroids (Markowski *et al.*, 2010a)

Uterine Leiomyome zeigen im Vergleich zum Myometrium *in vivo* ein höheres Wachstumspotential (Dixon *et al.*, 2002), wohingegen Zellen von Myomen *in vitro* ein vergleichsweise niedrigeres Wachstumspotential bzw. eine geringere Proliferation aufweisen als Zellen des Myometriums (Carney *et al.*, 2002; Loy *et al.*, 2005). Zudem liegen keine Hinweise vor, dass es einen Bezug gibt zwischen dem *in vitro* Wachstumsverhalten und dem vorliegenden zytogenetischen Subtyp bzw. dem *HMGA2*-Expressionslevel, welches unter uterinen Leiomyomen *in vivo* eine große Variabilität aufweist.

Um eine mögliche *in vitro*-abhängige Änderung der Expression von *HMGA2* im Vergleich zu nativem Gewebe bzw. dessen Einfluss auf das Wachstumsverhalten *in vitro* zu untersuchen, erfolgte in dieser Arbeit an uterinen Leiomyomen eine quantitative Messung der *HMGA2*-Expression zur Bestimmung des Expressionslevels *in vivo* einerseits und nach *in vitro* Kultivierung andererseits. Parallel erfolgte eine quantitative Bestimmung der Expression von *Cyclin-Dependent Kinase Inhibitor 2A* (*$p14^{Arf}$*), einem Seneszenz-assoziierten Gen, welches in uterinen Leiomyomen *in vivo* ein höheres Expressionslevel im Vergleich zum Myometrium aufweist (Markowski *et al.*, 2010b) und aufgrund dessen einen Einfluss auf das Wachstumsverhalten *in vitro* nehmen könnte.

Die quantitative Real-Time PCR erfolgte an insgesamt 16 uterinen Leiomyomen, von denen 11 Translokationen unter Beteiligung der Region 12q14~15 und/oder Rearrangierungen des *HMGA2*-Lokus aufwiesen. Die Bestimmung erfolgte mittels CC bzw. in drei Fällen mit FISH unter Verwendung einer *HMGA2* Break-Apart Sonde (Klemke *et al.*, 2009). In dem Fall 646 liegt zytogenetisch eine Translokation t(2;12)(p21;p13) vor. Nach FISH zeigte sich zusätzlich eine Rearrangierung von *HMGA2* mit getrennten Signalen der *HMGA2* Break-Apart Sonde sowohl auf dem langen als auch dem kurzen Arm des derivativen Chromosoms 12. In Fall 523.2 mit dem Karyotyp 45,XX,t(12;14)(q15;q24),der(14)t(12;14)(q15,q24),-22 fanden sich neben Fusionssignalen auf beiden derivativen Chromosomen 14 ein separates Signal des distal von *HMGA2* lokalisiertem Klons 269K4, was darauf hindeutet, dass der Bruchpunkt außerhalb (5‘) von *HMGA2* lokalisiert ist. Im dritten Fall 677.3 mit komplexen zytogenetischen Aberrationen u.a. mit Beteiligung von Chromosom 7 und Chromosom 12 fanden sich getrennte Signale entsprechend einer *HMGA2*-Rearrangierung auf einem derivativen Chromosom 7.

Die *HMGA2*-Expressionsanalysen zeigten mit Ausnahme eines uterinen Leiomyoms mit einer Translokation t(12;14)(q15;q24) in allen Fällen mit einer Rearrangierung der Region 12q14~15 bzw. des *HMGA2*-Lokus ein deutlich höheres *in vivo* Expressionslevel im Vergleich zu den zytogenetisch unauffälligen Myomen. Im Vergleich der Expressionen *in vivo* und *in vitro* fand sich in Myomen mit einer hohen *in vivo HMGA2*-Expression eine Abnahme der Expression *in vitro*, wohingegen in Fällen mit einer niedrigen *in vivo HMGA2*-Expression eine Zunahme der Expression *in vitro* erfolgte. Insgesamt wiesen *in vitro* alle Tumoren unabhängig ihres zytogenetischen Subtyps ein vergleichsweise ähnliches Expressionsniveau von *HMGA2* auf. Bezüglich $p14^{Arf}$ fand sich *in vivo* mit Ausnahme von drei Fällen ein Anstieg der Expression.

XIII

Cell culture and senescence in uterine fibroids

Dominique Nadine Markowski, Sabine Bartnitzke, Gazanfer Belge, Norbert Drieschner, Burkhard Maria Helmke, Jörn Bullerdiek

(Cancer Genetics and Cytogenetics 202(1): 53-57)

Eigenanteil:

- Planung, Durchführung und Auswertung der molekularzytogenetischen Untersuchungen.

ELSEVIER

Cancer Genetics and Cytogenetics 202 (2010) 53–57

Cancer Genetics and Cytogenetics

Short communication

Cell culture and senescence in uterine fibroids

Dominique Nadine Markowski[a], Sabine Bartnitzke[a], Gazanfer Belge[a], Norbert Drieschner[a], Burkhard Maria Helmke[b], Jörn Bullerdiek[a,c,*]

[a]*Center of Human Genetics, University of Bremen, Leobener Strasse ZHG, 28359 Bremen, Germany*
[b]*Institute of Pathology, University of Heidelberg, Im Neuenheimer Feld 220/221, 69120 Heidelberg, Germany*
[c]*Small Animal Clinic, University of Veterinary Medicine/Research Cluster of Excellence "REBIRTH," Bischofsholer Damm 15, 30173 Hannover, Germany*

Received 18 February 2010; received in revised form 7 June 2010; accepted 14 June 2010

Abstract The in vitro growth of cells from uterine fibroids is characterized by an early onset of senescence. Often, an even lower growth potential than that of matching myometrial cells is noted. Also, the tremendous differences in the expression of the high mobility group protein HMGA2 seen when comparing fibroids of different genetic subtypes are surprisingly not reflected by significant differences in their growth potential in vitro. We aimed to evaluate possible changes of the HMGA2 expression level between the native tissue and cell cultures, so we performed quantitative real-time polymerase chain reaction studies that revealed a marked decrease of the *HMGA2* mRNA in culture in those cases with overexpression of HMGA2. In the two cases initially showing the highest expression, it decreased by approximately 97%. Associated with the decrease of HMGA2 was a clearly increased expression of the senescence-associated $p19^{Arf}$. Together, these findings explain the similar behavior of cell cultures from fibroids of different genetic subgroups and may also offer an explanation for the early onset of in vitro senescence in these cell cultures.

1. Introduction

Despite their high growth potential in vivo, uterine leiomyomas show a strictly limited in vitro growth that is even exceeded by that of matching myometrial samples. This holds true for karyotypically normal leiomyomas as well as those characterized by the various types of recurrent chromosomal abnormalities such as deletions of the long arm of chromosome 7 or rearrangements of 12q14∼15 [1,2]. The latter group of fibroids is characterized by a high expression of the gene-encoding high-mobility-group protein HMGA2 [3,4], which is targeted by these chromosomal rearrangements [5]. Recently, the abundant expression of that protein has been associated with an impaired DNA repair, which might also contribute to the high genomic instability seen in many malignant epithelial tumors in vivo [6] and in corresponding cell lines in vitro. On the other hand, regarding uterine fibroids, the problem of possible genomic instability has not been addressed in detail, but most, if not all, of them show a low tendency to undergo malignant transformation, which argues in favor of a relatively high genomic stability. Likewise, cell cultures from these tumors have not been reported to immortalize spontaneously and do not show gross differences in their in vitro behavior when compared to cytogenetically normal cases [7].

However, to our knowledge, no data allowing a direct comparison of the expression of HMGA2 in malignant epithelial vs. benign mesenchymal tumors and addressing changes of HMGA2 expression of leiomyomas of the 12q14∼15 group when setting up cell cultures have been published so far. Thus, we have compared the HMGA2 expression levels of several leiomyomas with and without 12q14∼15 rearrangements in native tumor samples as well as in the corresponding cell cultures. In addition, the expression has been compared to that seen in lung cancer samples and in a colon cancer cell line expressing comparably high levels of HMGA2.

2. Materials and methods

2.1. Tissue samples

Tumor samples from fibroids were taken during surgery, immediately frozen in liquid nitrogen, and stored at −80°C for RNA isolation and quantitative real-time polymerase chain reaction (qRT-PCR) analysis or transferred to Hanks

* Corresponding author. Tel.: 49-421-218-2589; fax: 49-421-218-4239.
E-mail address: bullerdiek@uni-bremen.de (J. Bullerdiek).

0165-4608/$ - see front matter © 2010 Elsevier Inc. All rights reserved.
doi:10.1016/j.cancergencyto.2010.06.010

solution for cell cultures. Samples from malignant lung tumors were also frozen in liquid nitrogen immediately after surgery. Case numbers correspond to those provided in Meyer et al. [8].

2.2. Isolation and culture of uterine leiomyoma cells

Tissue samples stored in sterile Hanks solution were minced into small pieces followed by treatment with 0.26% (200 U/mL) collagenase (Serva, Heidelberg, Germany). After 1–2 hours, the dissociated cells were transferred into sterile 25-cm^2 cell culture flasks containing 5 mL medium 199, supplemented with 20% fetal bovine serum (Invitrogen, Karlsruhe, Germany) and 2% penicillin–streptomycin (Biochrom, Berlin, Germany). The cultures were incubated in 5% CO_2 air at 37°C, and medium was changed every 2–3 days. Cultures were passaged when reaching 80% confluence with 1xTrypLE Express (Gibco, Karlsruhe, Germany) in a phosphate-buffered saline–EDTA (ethylenediaminetetraacetic acid) buffer.

2.3. RNA isolation

RNA isolation was performed with the miRNeasy mini kit (Qiagen, Hilden, Germany), and a DNase I digestion was performed following the manufacturer's instructions.

2.4. cDNA synthesis

Approximately 250 ng of total RNA were reverse transcribed with 200 U/μL of M-MLV reverse transcriptase (Invitrogen, Karlsruhe, Germany), RNase Out (Invitrogen, Karlsruhe, Germany), 150 ng random hexamers, and 10 mmol/L dNTPs according to the manufacturer's instructions. RNA was denatured at 65°C for 5 minutes and subsequently kept on ice for 1 minute. After adding the enzyme to the RNA primer mixes, samples were incubated for 10 minutes at 25°C to allow annealing of the random hexamers. Reverse transcription was performed at 37°C for 50 minutes followed by inactivation of the reverse transcriptase at 70°C for 15 minutes.

2.5. qRT-PCR

Relative quantification of transcription levels was carried out by real-time PCR analyses with a real-time PCR system (Applied Biosystems, Darmstadt, Germany). Commercially available gene expression assays (Applied Biosystems) were used for quantification of mRNA of human *HMGA2* (Hs00171569 m1) and $p19^{Arf}$ (Hs00924091). As to the transcripts from human cells and tissues, *HPRT* served as endogenous control with the primers 5′-GGC AGT ATA ATC CAA AGA TGG TCA A-3′ (forward) and 5′-GTC TGG CTT ATA TCC AAC ACT TCG T-3′ (reverse), and the fluorescence probe 5′-6-FAM-CAA GCT TGC TGG TGA AAA GGA CCC C-TAMRA-3′. All qRT-PCR experiments were performed in triplicate.

2.6. Cytogenetic and molecular–cytogenetic studies

Chromosome analyses and fluorescence in situ hybridization were performed as described recently [4]. Karyotypes are described according to the 2009 International System of Human Cytogenetic Nomenclature [9].

3. Results

For the present analysis, samples from 11 uterine leiomyomas with clonal rearrangements of 12q14∼15 and the HMGA2 locus, respectively, detected by conventional cytogenetics and/or fluorescence in situ hybridization and five leiomyomas with an apparently normal karyotype were used (Figs. 1A–1F; Table 1). The HMGA2 levels were calibrated against a myometrial tissue. In all but one case, the tumors with 12q14∼15 aberrations showed expression levels of HMGA2, exceeding those seen in the myometrial tissue by more than a hundredfold (Fig. 2A). The remaining case had an expression level close to that of the tumors with an apparently normal level. Also, the expression of HMGA2 in the cases with 12q14∼15 rearrangements clearly exceeded that seen in malignant tumors, as exemplified here for four cases of lung cancer with HMGA2 expressions varying over a broad range (Table 1).

Although the overall correlation of the HMGA2 expression with the cytogenetic subtype of the fibroids confirmed earlier findings [3,4], the expression of HMGA2 in the corresponding cell cultures was somewhat surprising. All cases with a high level of HMGA2 expression showed marked reduction of expression when put in culture. As a rule, the degree of HMGA2 overexpression was positively correlated with its decrease in vitro. Of note, the case with the highest expression of *HMGA2* showed two rearranged alleles of *HMGA2* reflected by two derivative chromosomes 14 along with one normal allele (Figs. 1C and 1D). In contrast, if low levels of *HMGA2* mRNA were expressed in the tissue, then the expression always increased, leading to similar expression rates between both groups in vitro. Nevertheless, in case of leiomyomas with high expression of HMGA2 as a result of chromosomal alterations, the lowering of HMGA2 expression may be explained by an overgrowth of normal cells present in the samples. To rule out this possibility, the cultures were checked for the presence of chromosomal rearrangements. The results show that in neither of the latter cases did such a selection cause the decreased HMGA2 expression because in none of the cases was a considerable percentage of cells lacking the specific rearrangements (Table 1). Obviously, these findings offer an explanation for the limited and similar in vitro growth potential of cells from uterine fibroids despite their cytogenetic subgroup.

Because recently the expression of HMGA2 has been shown to correlate with the self-renewal of stem cells most likely by repressing the transcription from the *Ink4a/Arf* locus [10], we next examined whether during the initiation

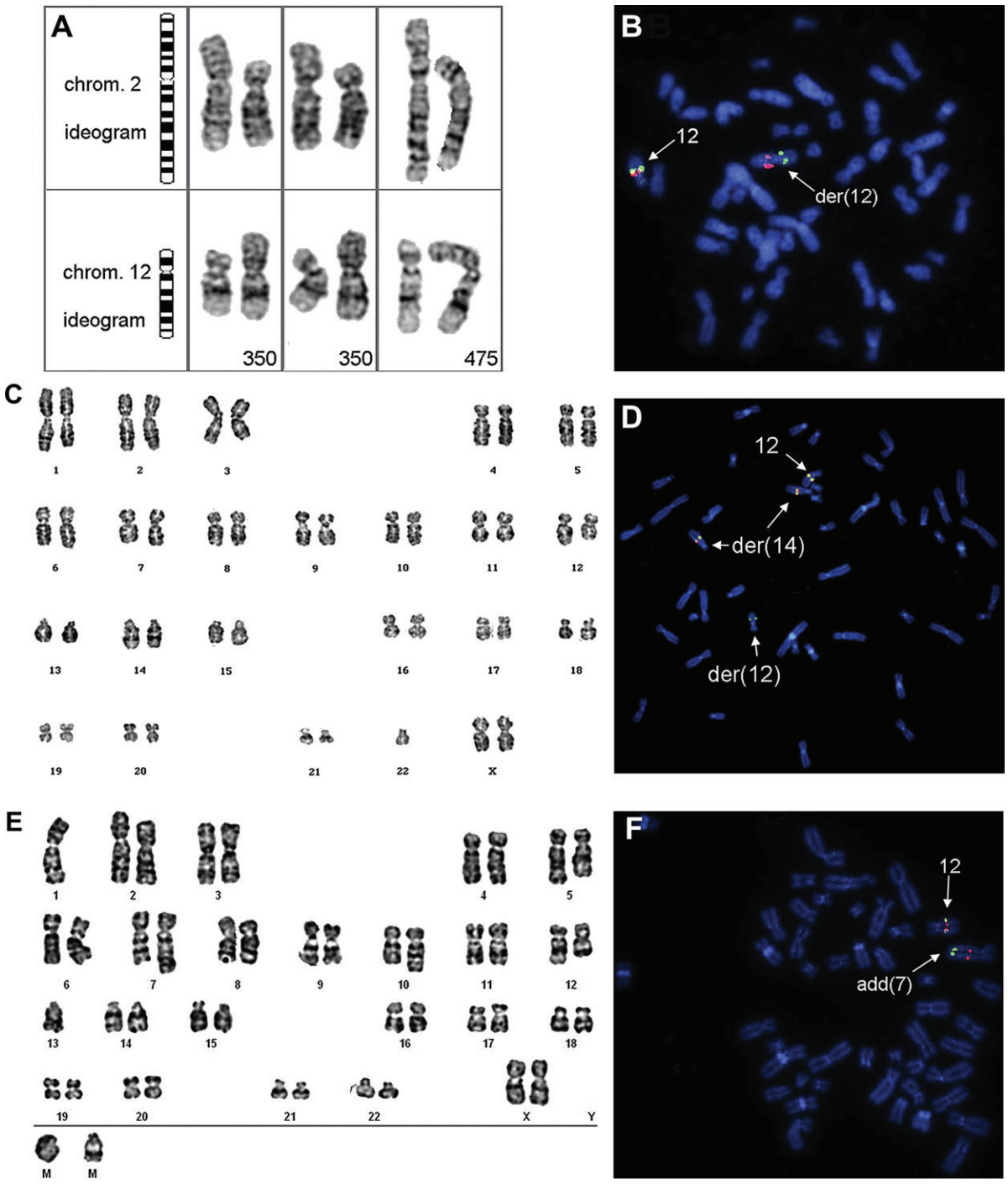

Fig. 1. Total or partial representative G-banded karyotypes and fluorescence in situ hybridization (FISH) analyses of selected cases. (A) Case 646 (see Table 1), representative partial G-banded karyotype showing chromosome pairs 2 and 12 from three metaphases does not reveal an involvement of the *HMGA2* locus on the long arm of chromosome 12. Resolution of bands is given on the bottom of each pair. (B) Case 646, FISH analysis using a break-apart probe covering the *HMGA2* locus with split signals on the long as well as the short arm of chromosome 12 reveals a hidden rearrangement of *HMGA2*. (C) Case 523.2 (see Table 1), representative G-banded karyotype showing two rearranged chromosomes 14 resulting from a t(12;14) (q15;q24). (D) Case 523.2, FISH analysis using a break-apart probe covering the *HMGA2* locus with fused signals on both rearranged chromosomes 14 as well as a single green signal on the long arm of chromosome 12. (E) Case 677.3 (see Table 1), representative G-banded karyotype showing a complex karyotypic rearrangement involving 12q14∼15. (F) Case 677.3 FISH analysis using a break-apart probe covering the *HMGA2* locus with split signals on a rearranged chromosome 7.

of cell cultures a concomitant increase of the expression of one of the genes of that locus—that is, $p19^{Arf}$—can be noted. Indeed, the establishment of cell cultures was accompanied by significant changes of $p19^{Arf}$ expression in most cases. Except for three cases (case 646, Fig. 1A), $p19^{Arf}$ expression clearly increased. By conventional cytogenetics, the

Table 1
Karyotypes of 16 uterine leiomyomas[a]

Laboratory no.	Karyotype	No. of additional metaphases checked for the aberrations (positive/negative)	*HMGA2* RQ value (tissue/culture)	$p19^{Arf}$ RQ value (tissue/culture)
503	46,XX,inv(5)(q15q31∼33),t(12;14)(q15;q24)[13]	58/0	9.075/327.974	5.164/7.42
523.2	45,XX,t(12;14)(q15;q24),der(14)t(12;14)(q15;q24), −22[15] Fig. 1C,D	100/0	74,402.695/2006.324	2.776/23.225
552.2	46,XX,t(2;12)(q33;q13)[17]	100/0	2,026.952/2451.841	0.185/14.533
643.2	46,XX,t(12;14)(q15;q24)[14]	73/0	3,187.464/295.096	0.548/2.997
646	46,XX,t(2;12)(p21;p13)[11] hidden rearrangement of HMGA2 detected by FISH Fig. 1A,B	99/1	11,146.819/389.983	17.229/4.723
677.3	46,XX,add(1)(p13),r(1)(?p36.3q25),add(7)(q22),der(10)t(1;10)(q25;q22),der(12)add(12)(p11.2)add12(q12),add(13)(q12)[20]/46,XX[3] Figs. 1E and 1F	ND	6,814.938/781.299	7.028/15.476
628.2	46,XX,?ins(12;14)(q15;q31q24)[5]/46,XX[14]	ND	2,641.862/121.667	8.737/13.646
556	46,XX,t(3;5;12)(q25;p14;q15)[15]	ND	9,713.64/622.528	1.323/5.766
580	46,XX,der(7)del(7)(p)del(7)(q),add(8)(q),add(10)(q),t(12;14)(q15;q24)[19]	ND	5,853.32/171.774	31.331/19.97
645	45,XX,r(1),der(13;14)(q10;q10)t(12;14)(q15;q24)[20]/44,XX,−1,der(13;14)(q10;q10)t(12;14)(q15;q24)[6]	ND	5,086.643/597.671	5.03/0.83
641	46,XX[12]	—	1.629/151.939	6.248/7.747
673.2	46,XX[12]	—	0.822/240.886	5.158/7.467
668.1	46,XX[12]	—	16.6/68.995	10.996/17.886
668.2	46,XX[12]	—	8.449/87.985	3.25/15.821
668.3	46,XX[12]	—	17.566/122.423	9.226/16.828
AC2	—	—	1.152	—
AC12	—	—	243.673	—
AC9	—	—	15,314.147	—
SCC4	—	—	788.485	—

Abbreviations: AC, adenocarcinoma; SCC, squamous-cell carcinoma; FISH, fluorescence in situ hybridization; ND, not done.

[a] Uterine leiomyomas were investigated according to Shaffer et al. [9] and the RQ values determined for the expression of *HMGA2* and $p19^{Arf}$, respectively, in the 16 fibroids and for the expression of *HMGA2* in four cases of lung cancer (relative quantitation). For case numbers, refer to Meyer et al. [8]. Native myometrial tissue served as calibrator (expression: 1).

breakpoint of this translocation was found to map to the short arm of chromosome 12 without any evidence for a simultaneous involvement of the long arm. Nevertheless, fluorescence in situ hybridization revealed a hidden rearrangement of the HMGA2 locus (Fig. 1B). Interestingly, in case 646, the decrease of $p19^{Arf}$ mRNA was associated with an unusual longevity of the corresponding cells and their late onset of senescence. The cells are now in their 21st in vitro passage, reflecting a quite unusual number of population doublings reached by these cells.

4. Discussion

Uterine fibroids belong to the most frequent and cytogenetically best-characterized human tumors. Although many questions remain about the pathogenesis of these highly prevalent tumors, a major point to distinguish leiomyomas from the matching myometrium is their higher proliferation rate, as revealed by PCNA and Ki-67 labeling and the mitotic count [11]. Cell cultures from fibroids display remarkable differences to what is seen in vivo, suggesting that cell cultures are not as useful when attempting to understand the development of fibroids and deducing possible therapeutic concepts. Accordingly, a good in vitro system for human leiomyomas does not exist [12]. Several reasons may account for this unmet challenge. First, despite their marked cytogenetic heterogeneity [13], cells from these tumors show a very similar in vitro behavior characterized by a limited growth potential and the absence of spontaneous immortalization [7,12]. Second, as to the growth potential of the cells in vitro, it has been shown that the colony-forming ability is lower than that of cell from the matching myometrium [13], and correspondingly, leiomyoma cells in vitro exhibit slower proliferation patterns than matched myometrial cells [14].

The results obtained herein offer an explanation for the similar number of population doublings obtained with cell cultures from leiomyomas regardless of their highly different HMGA2 expression in the tumor tissue. Obviously, the expression converges at a much more narrow range in vitro than in vivo. As an explanation for these findings, it can be hypothesized that as a rule, by chromosomal rearrangements, *HMGA2* becomes juxtaposed to transcriptional activators that are specific for the cell of origin and

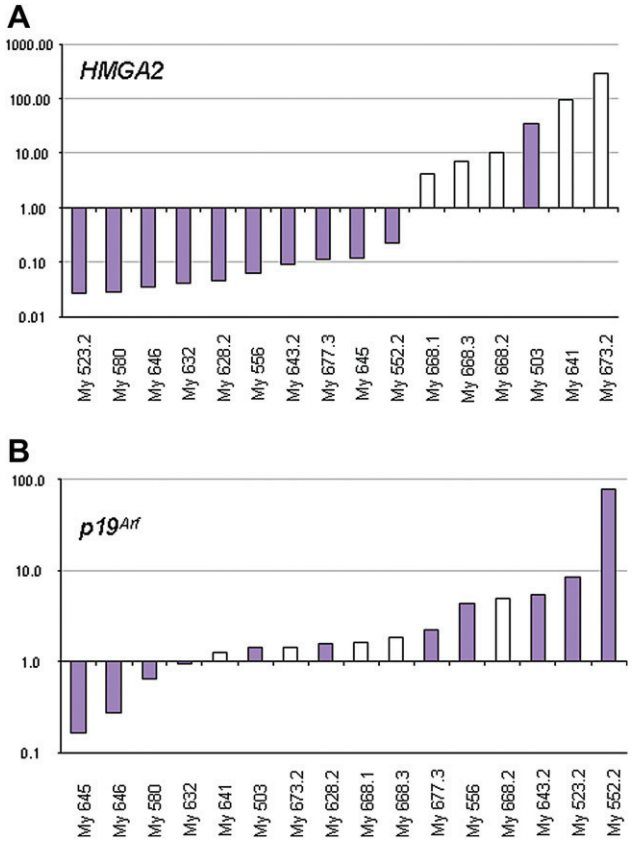

Fig. 2. Changes of *HMGA2* (A) and $p19^{Arf}$ (B) mRNA expression in cell culture compared to native tumor tissue in 16 leiomyomas. For direct comparison the logarithm of the quotient of $RQ_{native\ tissue}$ and $RQ_{cell\ culture}$ (see Table 1) is shown. Native myometrial tissue served as calibrator (expression: 1). Cases with 12q14∼15 rearrangement are given by pink bars.

their differentiation status, respectively. In most cases, the marked alterations of the extracellular milieu accompanying the change to the in vitro environment may reduce the activity of these activators. On the other hand, the normal transcriptional control in leiomyomas without chromosomal alterations targeting HMGA2 becomes stimulated, most likely by serum components, as hypothesized by Gattas et al. [15].

Furthermore, the results also offer an explanation for the clearly limited growth potential of the cells in vitro. Except for three cases, analyzed cell culturing of leiomyoma cells was accompanied by an increase of the expression of the senescence-associated $p19^{Arf}$. Basically, the inverse correlation of the increase of $p19^{Arf}$ and the decrease of *HMGA2* overexpression fits with the possible repression of the *Ink4a/Arf* locus as described for neural stem cells [10]. Nevertheless, other explanations may also be possible. An increasing number of cells undergoing senescence that are highly expressing $p19^{Arf}$ with low levels of *HMGA2* mRNA would have the same results when analyzing the whole in vitro cell population without a necessary correlation between these two parameters.

In summary, unexpected changes of the expression levels of genes importantly involved in the development of uterine leiomyomas and cellular senescence offer an explanation for the behavior of leiomyoma cells in vitro and may help improve in vitro models of fibroid development and proliferation.

Acknowledgments

This work was supported by the Tönjes-Vagt-Stiftung, Bremen, Germany. We thank Nadja Schwochow for technical assistance.

References

[1] Sandberg AA. Updates on the cytogenetics and molecular genetics of bone and soft tissue tumors: leiomyoma. Cancer Genet Cytogenet 2005;158:1–26.
[2] Lobel MK, Somasundaram P, Morton CC. The genetic heterogeneity of uterine leiomyomata. Obstet Gynecol Clin North Am 2006;33:13–39.
[3] Gross KL, Neskey DM, Manchanda N, Weremowicz S, Kleinman MS, Nowak RA, et al. HMGA2 expression in uterine leiomyomata and myometrium: quantitative analysis and tissue culture studies. Genes Chromosomes Cancer 2003;38:68–79.
[4] Klemke M, Meyer A, Nezhad MH, Bartnitzke S, Drieschner N, Frantzen C, et al. Overexpression of HMGA2 in uterine leiomyomas points to its general role for the pathogenesis of the disease. Genes Chromosomes Cancer 2009;48:171–8.
[5] Schoenmakers EF, Wanschura S, Mols R, Bullerdiek J, Van den Berghe H, Van de Ven WJ. Recurrent rearrangements in the high mobility group protein gene, HMGI-C, in benign mesenchymal tumours. Nat Genet 1995;10:436–44.
[6] Li AY, Boo LM, Wang SY, Lin HH, Wang CC, Yen Y, et al. Suppression of nonhomologous end joining repair by overexpression of HMGA2. Cancer Res 2009;69:5699–706.
[7] Stern C, Kazmierczak B, Thode B, Rommel B, Bartnitzke S, Dal Cin P, et al. Leiomyoma cells with 12q15 aberrations can be transformed in vitro and show a relatively stable karyotype during precrisis period. Cancer Genet Cytogenet 1991;54:223–8.
[8] Meyer B, Loeschke S, Schultze A, Weigel T, Sandkamp M, Goldmann T, et al. HMGA2 overexpression in non–small cell lung cancer. Mol Carcinog 2007;46:503–11.
[9] Shaffer LG, Slovak ML, Cambel LJ, editors. ISCN: An International System for Human Cytogenetic Nomenclature. Basel: S. Karger, 2009.
[10] Nishino J, Kim I, Chada K, Morrison SJ. Hmga2 promotes neural stem cell self-renewal in young but not old mice by reducing p16Ink4a and p19Arf expression. Cell 2008;135:227–39.
[11] Dixon D, Flake GP, Moore AB, He H, Haseman JK, Risinger JI, et al. Cell proliferation and apoptosis in human uterine leiomyomas and myometria. Virchows Arch 2002;441:53–62.
[12] Carney SA, Tahara H, Swartz CD, Risinger JI, He H, Moore AB, et al. Immortalization of human uterine leiomyoma and myometrial cell lines after induction of telomerase activity: molecular and phenotypic characteristics. Lab Invest 2002;82:719–28.
[13] Chang HL, Senaratne TN, Zhang L, Szotek PP, Stewart E, Dombkowski D, et al. Uterine leiomyomas exhibit fewer stem/progenitor cell characteristics when compared with corresponding normal myometrium. Reprod Sci 2010;17:158–67.
[14] Loy CJ, Evelyn S, Lim FK, Liu MH, Yong EL. Growth dynamics of human leiomyoma cells and inhibitory effects of the peroxisome proliferator-activated receptor-gamma ligand, pioglitazone. Mol Hum Reprod 2005;11:561–6.
[15] Gattas GJ, Quade BJ, Nowak RA, Morton CC. HMGIC expression in human adult and fetal tissues and in uterine leiomyomata. Genes Chromosomes Cancer 1999;25:316–22.

4 Diskussion

Die molekulare Zytogenetik, insbesondere die Fluoreszenz *in situ* Hybridisierung (FISH), hat bei soliden wie auch nicht-soliden humanen Neoplasien maßgeblich zum Nachweis und zur weiteren Charakterisierung spezifischer, rekurrenter numerischer sowie struktureller chromosomaler Aberrationen, wie z.B. Deletionen, Amplifikationen und (balancierten) Rearrangierungen, beigetragen. So kommt der FISH insbesondere bei malignen Neoplasien mittlerweile eine hohe Bedeutung innerhalb der Differentialdiagnostik und der Einbindung in Therapieentscheidungen zu. In der vorliegenden Arbeit erfolgten molekularzytogenetische sowie molekulargenetische Untersuchungen spezifischer chromosomaler Aberrationen in follikulären Tumoren der Schilddrüse sowie benignen mesenchymalen Tumoren. Der Schwerpunkt lag dabei auf der Analyse follikulärer Tumoren der Schilddrüse und innerhalb dieser Gruppe auf der Untersuchung spezifischer chromosomaler Aberrationen, die in benignen hyperplastischen und neoplastischen Läsionen der Schilddrüse nachgewiesen werden konnten sowie auf Aberrationen, die sowohl in follikulären Adenomen als auch in follikulären Karzinomen der Schilddrüse nachweisbar sind. Im Gegensatz zu den malignen soliden Tumoren des Menschen, insbesondere mesenchymalen und epithelialen Ursprungs, zeichnen sich die benignen soliden Läsionen durch eine geringere zytogenetische Komplexität und auch Heterogenität aus, d.h. sie weisen z.T. nur einzelne klonale chromosomale Aberrationen auf, wobei diese Veränderungen spezifisch sein können, sich aber auch in den entsprechenden malignen Entitäten nachweisen lassen (Mitelman, 2000; Sandberg und Meloni-Ehrig, 2010). Die Untersuchung nicht zufälliger chromosomaler Veränderungen in benignen Neoplasien des Menschen kann zu einem besseren Verständnis der Entstehung und des Wachstums dieser Läsionen sowie weiterführend auch der grundlegenden Mechanismen der Tumorgenese und –progression beitragen.

4.1 Quantitative Untersuchungen zytogenetischer Subgruppen benigner Schilddrüsenläsionen

Unter Betrachtung der drei häufigen zytogenetischen Subgruppen in benignen follikulären Schilddrüsenläsionen erfolgte in der vorliegenden Arbeit neben einer konventionellen zytogenetischen Analyse 161 benigner Schilddrüsenläsionen eine molekularzytogenetische Untersuchung mittels I-FISH an Touchpräparaten der entsprechenden Läsionen (Drieschner

et al., 2011). Hierbei zeigte sich, dass die Anzahl der Läsionen, die positiv hinsichtlich einer der drei zytogenetischen Subgruppen waren, nach I-FISH größer war als nach der CC. Dies ist zum einen darauf zurückzuführen, dass entweder die CC im Gegensatz zur I-FISH aufgrund einer zu geringen Quantität und/oder Qualität auswertbarer Metaphasen ohne Ergebnis blieb oder die mittels I-FISH nachgewiesenen Aberrationen über die CC nicht erfasst wurden. Bezüglich des letzten Aspektes war es möglich zu zeigen, dass in Fällen, bei denen die Aberration nur mittels I-FISH nachweisbar war, *in vivo* ein signifikant geringerer Anteil positiver Zellkerne vorlag, als in jenen Fällen, für die die entsprechende Aberration über beide Methoden erfasst werden konnte. Somit erwies sich die I-FISH als sensitivere Methode zum Nachweis der drei zytogenetischen Subgruppen. Diese Resultate bestätigen die Aussage von Roque *et al.* (1999), die in einer Studie zum Nachweis numerischer Veränderungen der Chromosomen 7 und 12 zeigen konnten, dass der mittels FISH bestimmte Anteil benigner Schilddrüsenläsionen mit einer Polysomie 7 und 12 größer ist als bis dahin auf Grundlage rein zytogenetischer Daten angenommen wurde. Dies konnte in der vorliegenden Arbeit neben der Trisomie 7-Subgruppe auch für die beiden Subgruppen mit strukturellen Veränderungen der chromosomalen Regionen 19q13.4 und 2p21 erstmalig gezeigt werden, sodass der Anteil dieser zytogenetischen Subgruppen innerhalb benigner Schilddrüsenläsionen tatsächlich größer ist und diese somit eine höhere Relevanz für diese Läsionen aufweisen als die bisherigen zytogenetischen Daten vermuten ließen. Da zudem diese Subgruppen häufiger in follikulären Adenomen als in Hyperplasien nachgewiesen wurden, wird zudem die These gestützt, dass im Zuge der Pathogenese benigner Schilddrüsenläsionen follikuläre Schilddrüsenadenome aus Hyperplasien hervorgehen (Belge *et al.*, 1998; Roque *et al.*, 1999; Barril *et al.*, 2000). Aufgrund des bisher fehlenden Nachweises vor allem der 19q13.4- und 2p21-Rearrangierungen in follikulären Karzinomen stellt sich die Frage, ob Hyperplasien und follikuläre Adenome mit diesen Aberrationen ein geringes bzw. kein Malignitätspotenzial besitzen. So könnten molekularzytogenetische Untersuchungen zum Nachweis dieser strukturellen Aberrationen z.B. an Touchpräparaten maligner Neoplasien der Schilddrüse diese Vermutung bestätigen, sofern diese Aberrationen in den malignen Entitäten nicht nachweisbar sind. Welchen Einfluss die involvierten Kandidatengene auf die Pathogenese der Läsionen mit 19q13.4- bzw. 2p21-Rearrangierungen haben, lässt sich letztlich durch weiterführende Untersuchungen hinsichtlich der Funktion sowie der molekular-strukturellen Veränderungen der

entsprechenden Kandidatengene feststellen. Entsprechend erfolgten in dieser Arbeit molekularzytogenetische sowie molekulargenetische Analysen mit Hinblick auf die weitere Charakterisierung der Bruchpunktregionen 2p21 und 19q13.4 sowie der beteiligten Kandidatengene.

4.2 Chromosomale Rearrangierungen der Region 2p21 unter Beteiligung des *Thyroid Adenoma Associated* (*THADA*)-Gens

Strukturelle Veränderungen unter Beteiligung der chromosomalen Region 2p21 finden sich in benignen Läsionen der Schilddrüse mit klonalen chromosomalen Aberrationen mit einer Häufigkeit von bis zu 10% (Belge *et al.*, 1998; Bol *et al.*, 1999). In der vorliegenden Arbeit konnten anhand molekularzytogenetischer Analysen an 161 benignen Schilddrüsenläsionen 2p21-Aberrationen in 2,5% aller Läsionen bzw. in 14,7% der Läsionen mit klonalen chromosomalen Veränderungen und damit in einem größeren Anteil als auf Grundlage der CC nachgewiesen werden (Drieschner *et al.*, 2011). Mit dem Zweck der Identifizierung und Charakterisierung eines an diesen 2p21-Rearrangierungen beteiligten Kandidatengens erfolgte in der vorliegenden Arbeit eine molekularzytogenetische und molekulargenetische bzw. *in silico*-Analyse der von Bol *et al.* (2001) definierten 450 kb-Bruchpunktregion bei benignen Schilddrüsenläsionen mit 2p21-Rearrangierungen (Rippe *et al.*, 2003). Bol *et al.* (2001) sahen das in der unmittelbaren Nähe zum 450 kb-Bruchpunktcluster lokalisierte Zinkfinger-Gen *ZFP36L2* als ein mögliches Kandidatengen an, jedoch erfolgte weder für dieses noch für ein anderes Gen der Nachweis einer direkten Beteiligung an den 2p21-Rearrangierungen. Es war in der vorliegenden Arbeit zum einen möglich, den Bruchpunktcluster auf eine Region von ca. 316 kb weiter einzugrenzen, zum anderen konnte erstmalig die genomische Struktur eines bis dahin nicht bekannten Gens beschrieben werden, welches größtenteils innerhalb der 316 kb-Bruchpunktregion lokalisiert ist und als *Thyroid Adenoma Associated* (*THADA*)-Gen bezeichnet wurde (Rippe *et al.*, 2003). Es konnten zwei Spleißvarianten nachgewiesen werden (*THADA* und *THADA-A2*), von denen *THADA* mit derzeit 6.134 bp (GenBank Accession NM_022065.4) die längste Variante darstellt, deren Open Reading Frame 5.862 bp umfasst und für ein Protein mit einer Länge von 1.953 Aminosäuren bzw. einer molekularen Größe von 220 Kilodalton kodiert. Es ist zu vermuten, dass *THADA* ubiquitär exprimiert wird, da die Expression eines ca. 6,2 kb großen Transkripts mittels Northern-Blot in allen getesteten Geweben nachgewiesen werden

konnte. *THADA* ist in benignen Schilddrüsenläsionen mit 2p21-Rearrangierungen strukturell direkt von den Rearrangierungen betroffen. Die Bruchpunkte sind innerhalb des Intron 28 lokalisiert, weiterhin konnten Fusionstranskripte nachgewiesen werden, bei denen die Exons 29 – 38 von *THADA* trunkiert sind und der Bereich bis einschließlich Exon 28 mit ektopischen Sequenzen aus den Bruchpunktbereichen der jeweiligen Translokationspartner fusioniert ist. Da diese Sequenzen keinem bekannten Gen oder einer Genstruktur zugeordnet werden konnten und der kodierende Bereich innerhalb der Fusionstranskripte kurz nach Exon 28 endet, ist davon auszugehen, dass der Verlust des 3‘-Anteils von *THADA* von wesentlicher funktioneller Bedeutung ist.

Obwohl laut einem GenBank-Eintrag (GenBank AF323176.1) Hinweise auf eine Beteiligung von THADA als Death-Receptor interagierendes Protein an der Apoptose bestanden, war die genaue Funktion von THADA nicht bekannt. Daher wurden die Sequenzen der orthologen *THADA*-Gene ausgewählter Vertebraten (*Mus musculus, Canis familiaris, Chlorocebus aethiops* und *Gallus gallus*) und die Homologien untereinander und zum Menschen ermittelt, um weitere Informationen zur Struktur und Funktion von THADA zu erhalten (Drieschner *et al.*, 2007). Hierbei konnte eine hoch-konservierte Region bestimmt werden, die im Zuge der 2p21-Rearrangierungen in benignen Schilddrüsenläsionen durch die Trunkierung der Exons 29 – 38 von *THADA* direkt betroffen ist. Es ist daher anzunehmen, dass dieser Region aufgrund ihres hohen Konservierungsgrades eine funktionell besonders wichtige Bedeutung zukommt und diese in benignen Schilddrüsenläsionen durch die beschriebene Trunkierung wesentlich gestört ist. Strukturell bestehen Homologien zu Proteinen, die an einer Protein-Protein-Bindung beteiligt sind sowie zur ARM Repeat Superfamilie, die an Protein-Protein-Interaktionen beteiligt sein können (Coates, 2003). Daher weist THADA möglicherweise eine Proteinbindungsaktivität auf, die z.B. auch bei Death-Receptor interagierenden Proteinen zu finden ist (Ashkenazi und Dixit, 1998; Ashkenazi, 2002). Die Death-Rezeptoren gehören zur Familie der Tumor Necrosis Factor Rezeptoren (TNFR) und vermitteln die TL1A- (Tumor necrosis factor (ligand) Superfamily, member 15) bzw. APO2L- (APO2 Ligand) oder TRAIL- (TNF-related apoptosis-inducing ligand) induzierte Apoptose (Ashkenazi und Dixit, 1998; Ashkenazi, 2002). Ausgehend von einer möglichen Beteiligung von THADA am Death-Receptor Pathway könnte durch die Trunkierung bzw. den Verlust des C-terminalen Endes von THADA bedingt durch eine 2p21-Rearrangierung die Induktion der Apoptose gestört

sein, was letztlich zu einer gesteigerten Zellproliferation und zur Genese benigner Schilddrüsenläsionen führt.

THADA scheint den Differenzierungsgrad epithelialer Zellen der Schilddrüse mit zu beeinflussen. Wie Kloth *et al*. (2011) anhand Expressionsanalysen gezeigt haben, ist die Expression von *THADA* in undifferenzierten anaplastischen Schilddrüsenkarzinomen gegenüber Normalgewebe und benignen Schilddrüsenläsionen sowie differenzierten Schilddrüsenkarzinomen signifikant reduziert. Hierbei konnte eine Korrelation bezüglich der Expression von *THADA* und des *Sodium Iodid Symporter* (*NIS*) gezeigt werden. *NIS* ist als ein schilddrüsenspezifischer Differenzierungmarker beschrieben, welcher in gering-differenzierten Schilddrüsenkarzinomen eine verringerte Expression aufweist (Arturi *et al.*, 1998; Filetti *et al.*, 1999; Lazar *et al.*, 1999). Dementsprechend weisen die Expressionsanalysen darauf hin, dass die *THADA*-Expression mit zunehmender Dedifferenzierung der Thyreozyten abnimmt (Kloth *et al.*, 2011).

Für maligne Läsionen der Schilddrüse wie auch für andere solide Tumoren sind 2p21-Rearrangierungen unter Beteiligung von *THADA* bisher nicht beschrieben. Allerdings haben bei akuten myeloischen Leukämien (AML) mit den Translokationen t(2;3)(p15-22;q26) (Trubia *et al.*, 2006) bzw. t(2;13)(p21;q14.11) (Poitras *et al.*, 2011) molekularzytogenetische Analysen zeigen können, dass die Bruchpunkte in zumindest drei Fällen innerhalb von *THADA* (Trubia *et al.*, 2006) bzw. distal von *THADA* lokalisiert sind (Trubia *et al.*, 2006; Poitras *et al.*, 2011). Für die Translokation t(2;3)(p15-22;q26) schließen die Autoren die Bildung eines Fusionsgens unter Beteiligung von *THADA* und des in 3q26 lokalisierten *Ecotropic Viral Integration Site 1* (*EVI1*)-Gens aufgrund der entgegengesetzten Orientierung beider Gene auf dem derivativen Chromosom 3 aus (Trubia *et al.*, 2006). Der Bruchpunktbereich bei der von Poitras *et al.* (2011) beschriebenen Translokation t(2;13)(p21;q14.11.) ist wie in einem Fall bei Trubia *et al.* (2006) distal von *THADA* lokalisiert, einhergehend mit einer Deletion eines 195 kb großen Bereichs, in dem die Autoren u.a. die Lokalisation regulatorischer Elemente vermuten (Poitras *et al.*, 2011). Inwiefern hier ein Einfluss dieser Aberrationen z.B. auf die Expression von *THADA* besteht ist ungeklärt, wobei nicht auszuschließen ist, dass chromosomale Aberrationen der Region 2p21 unter direkter Beteiligung von *THADA* oder regulatorischer Elemente in Nähe des genomischen *THADA*-Lokus im Zusammenhang mit der Pathogenese zumindest innerhalb einer Subgruppe der AML stehen.

Eine Meta-Analyse von drei Assoziationsstudien an Populationen europäischer Abstammung hat einen Zusammenhang eines in Exon 24 von *THADA* lokalisierten Single Nukleotid Polymorphismus (SNP) (rs7578597) und Typ 2 Diabetes Mellitus (T2DM) festgestellt (Zeggini *et al.*, 2008). Eine entsprechende Assoziation dieses SNPs und T2DM konnte für eine indische Population (Gupta *et al.*, 2011) bestätigt werden, wohingegen andere Studien keinen Zusammenhang zwischen THADA und T2DM zeigen konnten (Grarup *et al.*, 2008; Staiger *et al.*, 2008; Boesgaard *et al.*, 2009; Hu *et al.*, 2009; Kang *et al.*, 2009; Sanghera *et al.*, 2009; Stancakova *et al.*, 2009; Vangipurapu *et al.*, 2011). Ob eine Assoziation zwischen THADA und T2DM besteht, ist daher unklar, wobei zumindest eine funktionelle Bedeutung von THADA in den β-Zellen der Langerhans-Inseln nicht auszuschließen ist (Parikh *et al.*, 2009; Simonis-Bik *et al.*, 2010). Des Weiteren besteht ein Zusammenhang weiterer SNP-Varianten von *THADA* mit einem erhöhten Risiko für die Entstehung des polyzystischen Ovarialsyndroms, welches auch einhergeht mit einem erhöhten Risiko für T2DM (Chen *et al.*, 2011; Goodarzi *et al.*, 2011; Zhao *et al.*, 2012).

Auf Grundlage molekularzytogenetischer Analysen war es bei benignen Läsionen der Schilddrüse mit 2p21-Rearrangierungen möglich, das an dieser chromosomalen Aberration beteiligte Gen *THADA* nachzuweisen und weiter zu charakterisieren. So weisen die vorliegenden Ergebnisse auf eine Beteiligung von THADA an der Apoptose hin sowie auf einen Verlust einer bedeutenden funktionellen Domäne bedingt durch die 2p21-Rearrangierungen in benignen Läsionen der Schilddrüse. Darüber hinaus scheint ein Zusammenhang zwischen der Dedifferenzenzierung anaplastischer Schilddrüsenkarzinome und der Expression von *THADA* zu bestehen. Hinsichtlich einer Beteiligung von THADA in einer Subgruppe der AML sowie der T2DM und des polyzystischen Ovarialsyndroms scheinen ebenfalls Zusammenhänge zu bestehen, sodass letztlich weiterführende Analysen von THADA hinsichtlich dessen Funktionalität und dessen Beteiligung an neoplastischen und nicht-neoplastischen Erkrankungen zu neuen Erkenntnissen bezüglich der Pathogenese dieser Erkrankungen sowie auch benigner und ggf. maligner follikulärer Neoplasien der Schilddrüse führen könnten.

Die Bestimmung der chromosomalen Lokalisation von tumorassoziierten Genen des Menschen mittels der FISH in anderen Organismen kann zur Klärung, ob dieselben Gene in zytogenetische Veränderungen bei entsprechenden Tumorerkrankungen ebendieser

Organismen involviert sind, beitragen. Unter Verwendung *THADA*-spezifischer humaner BAC-Klone konnte das *THADA*-Gen in der vorliegenden Arbeit auf dem Chromosom 14 der Grünen Meerkatze (*Chlorocebus aethiops*) lokalisiert werden (Drieschner *et al.*, 2007). Des Weiteren erfolgte eine molekularzytogenetische Kartierung des caninen *THADA*-Gens beim Hund (Soller *et al.*, 2008). Auch wenn mit ca. 2% unter allen Tumoren die Schilddrüsenneoplasien beim Hund eher selten sind und von den klinisch erfassten Schilddrüsentumoren mit über 85% die Karzinome den deutlich überwiegenden Anteil einnehmen (Ogilvie, 1996; Rijnberk *et al.*, 2003), ist grundsätzlich der Hund als Tiermodell für die Erforschung tumorassoziierter Gene insbesondere aufgrund der vergleichbaren Pathogenese und Ätiologie humaner und caniner Tumorerkrankungen geeignet (Khanna *et al.*, 2006; Paoloni und Khanna, 2007). Genomisch ist das canine *THADA* in der zur humanen chromosomalen Region 2p21 homologen Bande q25 auf dem caninen Chromosom (CFA) 10 lokalisiert und weist zudem eine hohe Homologie zum humanen *THADA* bezüglich Open Reading Frame (ORF), kodierender Sequenz (CDS) und der Proteinsequenz auf (Drieschner *et al.*, 2007). Obwohl strukturelle Veränderungen der chromosomalen Region CFA10q25 bei caninen Schilddrüsenadenomen bisher nicht beschrieben sind, ist eine Beteiligung von *THADA* in Folge von chromosomalen Rearrangierungen in diesen benignen Neoplasien beim Hund dennoch nicht auszuschließen, da zytogenetische Daten bisher nur für eine geringe Anzahl caniner Schilddrüsenadenome bekannt sind (Mayr *et al.*, 1991; Reimann *et al.*, 1996).

4.3 19q13.4-Rearrangierungen und die miRNA-Cluster C19MC und miR371-3 in benignen follikulären Schilddrüsenläsionen

Die häufigste in benignen Schilddrüsenläsionen beschriebene strukturelle Chromosomenaberration sind Rearrangierungen unter der Beteiligung der Region 19q13.4, die als eigene zytogenetische Subgruppe in ca. 20% der Fälle mit klonalen chromosomalen Aberrationen auftreten (Belge *et al.*, 1998), wobei anhand molekularzytogenetischer Analysen gezeigt werden konnte, dass diese Veränderungen noch einen größeren Anteil innerhalb der benignen Schilddrüsenläsionen auszumachen scheinen und entsprechend eine noch größere Relevanz innerhalb benigner Schilddrüsenläsionen einnehmen (Drieschner *et al.*, 2011). Im Rahmen einer molekularzytogenetischen Bruchpunktcharakterisierung konnten die Bruchpunkte auf einen Bereich von ca. 400 kb (Belge *et al.*, 1995; Belge *et al.*, 1997) sowie im Rahmen dieser Arbeit weiter auf einen Bereich von 150 kb eingegrenzt

werden (Belge *et al.*, 2001). Als ein Kandidatengen wurde ursprünglich *ZNF331* identifiziert, welches für das Zinkfinger-Protein 331 kodiert und proximal zum 150 kb-Bruchpunktcluster lokalisiert ist (Rippe *et al.*, 1999; Belge *et al.*, 2001). Obwohl die Expression eines aberranten 3,4 kb-Transkripts exklusiv in Schilddrüsenadenom-Zelllinien mit 19q13.4-Rearrangierungen nachgewiesen werden konnte (Meiboom *et al.*, 2003), ist ungeklärt, ob dieses aberrante *ZNF331*-Transkript eine hinsichtlich der Pathogenese benigner Schilddrüsenläsionen mit 19q13.4-Rearrangierungen funktionelle Relevanz besitzt.

Expressionsanalysen ausgewählter miRNAs aus den innerhalb der chromosomalen Region 19q13.42 lokalisierten miRNA-Clustern C19MC und mir-317-3 zeigten sowohl in Zelllinien als auch in Primärtumoren mit molekularzytogenetisch nachgewiesenen 19q13.4-Rearrangierungen eine gegenüber 19q13.4-Rearrangierungen negativen Proben signifikant erhöhte Expression der miRNAs der beiden Cluster (Rippe *et al.*, 2010). Aufgrund ihrer Lage zum 150 kb-Bruchpunktcluster ist ein kausaler Zusammenhang zwischen den 19q13.4-Rearrangierungen und einer aberranten Expression von miRNAs der beiden Cluster naheliegend. Der von Bentwich *et al.* (2005) identifizierte, innerhalb der chromosomalen Region 19q13.42 distal zu *ZNF331* lokalisierte und mit ca. 100 kb größte humane miRNA-Cluster (C19MC) kodiert für ca. 8% aller bisher bekannten humanen miRNAs. Die miRNAs dieses Clusters sind innerhalb eines Introns eines nicht-Protein-kodierenden Polymerase II-Transkripts lokalisiert und werden überwiegend in der Plazenta exprimiert (Bortolin-Cavaille *et al.*, 2009; Tsai *et al.*, 2009). Zudem liegt ca. 25 kb distal zu C19MC ein weiterer, mit ca. 1 kb deutlich kleinerer miRNA-Cluster (mir-371-3), welcher wie auch C19MC in humanen embryonalen Stammzellen exprimiert wird (Suh *et al.*, 2004; Li *et al.*, 2009b; Ren *et al.*, 2009). Eine aberrante Expression von miRNAs ist in verschiedenen humanen Neoplasien beschrieben (Gregory und Shiekhattar, 2005; Lee und Dutta, 2009). Für miRNAs der Cluster C19MC oder miR-371-3 ist eine erhöhte Expression im Hepatoblastom (Cairo *et al.*, 2010) und hepatozellulären Karzinom (HCC) (Wu *et al.*, 2011; Fornari *et al.*, 2012) nachgewiesen, wohingegen ein vermindertes Expressionslevel in Prostata- (Yang *et al.*, 2009) und Colonkarzinomen (Tanaka *et al.*, 2011) beschrieben ist. Funktionell konnte gezeigt werden, dass miRNAs beider Cluster in Neoplasien an der Zellproliferation und –migration (Yang *et al.*, 2009; Tanaka *et al.*, 2011) bzw. an der Tumorinvasion und –metastasierung beteiligt sind (Huang *et al.*, 2008). Mittels einer molekularzytogenetischen Charakterisierung der Bruchpunktregion 1p35.2 in einer Zelllinie mit einer Translokation t(1;19)(p35.2;q13.4)

konnte der Bruchpunkt innerhalb Intron 10 des *PUM1*-Gens lokalisiert werden. *PUM1* umfasst 22 Exons, weist genomisch eine Größe von 150 kb auf und wird in einer Vielzahl adulter humaner Gewebe exprimiert (Spassov und Jurecic, 2002). Anhand molekulargenetischer Analysen konnten zwei Fusionstranskripte (*PUM1-FUS-19q-I* und *-II*) nachgewiesen werden, in denen auf den Exons 1-10 von *PUM1* ektopische Sequenzen aus der Bruchpunktregion 19q13.4 folgen. Dies lässt darauf schließen, dass bedingt durch die 19q13.4-Rearrangierung ein Polymerase II-Fusionstranskript entsteht, dessen Expression durch den Promotor des *PUM1*-Gens reguliert wird und es in Folge dessen zur Aktivierung und Expression der Cluster C19MC und miR-371-3 kommt. Die Expression von C19MC wird epigenetisch reguliert und steht in Zusammenhang mit dem Methylierungsstatus distal lokalisierter CpG-Inseln. So sind diese in Plazentagewebe hypomethyliert, in Tumorzelllinien, in denen C19MC inaktiv ist, hingegen hypermethyliert, wobei eine Aktivierung nach Zugabe demethylierender Agenzien induzierbar war (Tsai *et al.*, 2009). Zudem konnte in HCCs mit einer erhöhten Expression der dem C19MC-Cluster zugehörigen miR-519c gezeigt werden, dass in diesen C19MC hypomethyliert ist (Fornari *et al.*, 2012). Einen anderen Aktivierungsmechanismus haben Li *et al.* (2009a) in primitiv neuroektodermalen Tumoren (PNET) beschrieben, in denen sie anhand Microarray- und FISH-Analysen ein 19q13.41-Amplikon einschließlich der beiden Cluster C19MC und miR-371-3 nachweisen konnten. Tumoren mit diesem Amplikon weisen eine erhöhte Expression vor allem von miRNAs des Clusters C19MC auf (Li *et al.*, 2009a). Die Beteiligung der Cluster C19MC und miR-371-3 an einem Polymerase II-Fusionstranskript bei 19q13.4-Rearrangierungen und die damit einhergehende Aktivierung beider Cluster stellt somit einen neuen Aktivierungsmechanismus für diese Cluster dar. Eine durch eine Hypomethylierung bedingte Aktivierung der beiden Cluster konnte zudem an 50 follikulären Adenomen der Schilddrüse ohne 19q13.4-Rearrangierung nachgewiesen werden (persönliche Mitteilung, Dr. V. Rippe, ZHG). Dies deutet darauf hin, dass follikuläre Adenome der Schilddrüse mit einer aberranten bzw. erhöhten Expression von miRNAs der beiden Cluster C19MC und miR-371-3 die größte eigenständige Gruppe innerhalb der benignen Läsionen der Schilddrüse darstellen. Aberrante Expressionsmuster von miRNAs sind in Schilddrüsenneoplasien follikulären Ursprungs bereits in mehreren Untersuchungen beschrieben (Braun und Huttelmaier, 2011). Die bisherigen Daten hinsichtlich der miRNA-Expressionsmuster werden allerdings als noch nicht ausreichend für eine eindeutige Differenzierung follikulärer Adenome von follikulären

Schilddrüsenkarzinomen und auch der verschiedenen Karzinome untereinander angesehen, sodass weitere Untersuchungen mit Blick auf eine tumorcharakteristische miRNA-Expression in Neoplasien der Schilddrüse als notwendig erachtet werden (Braun und Huttelmaier, 2011).

4.4 Charakterisierung und Nachweis von 3p25-Rearrangierungen und des *PAX8/PPARγ*-Fusionsgens in follikulären Schilddrüsenneoplasien

Eine weitere in follikulären Neoplasien der Schilddrüse beschriebene zytogenetische Veränderung ist die Translokation t(2;3)(q13;p25) und das daraus resultierende Fusionsgen *PAX8/PPARγ*, welche sowohl in follikulären Adenomen als auch follikulären Karzinomen der Schilddrüse beschrieben worden sind (Sozzi *et al.*, 1992; Roque *et al.*, 1993a; Kroll *et al.*, 2000; Marques *et al.*, 2002; Nikiforova *et al.*, 2002; Cheung *et al.*, 2003). Die molekular-zytogenetischen Untersuchungen dieser Arbeit hinsichtlich *PPARγ*- bzw 3p25-Rearrangierungen geben Hinweise auf die quantitative und vor allem pathogenetische Relevanz dieser Aberrationen in follikulären Schilddrüsenneoplasien. Das Auftreten einer t(2;3)(q13;p25) bzw. der *PAX8/PPARγ*-Fusion scheint innerhalb follikulärer Schilddrüsenadenome nur gering zu sein, da sich im Rahmen dieser Arbeit unter 192 benignen follikulären Neoplasien der Schilddrüse in nur zwei Fällen zytogenetisch und auch molekularzytogenetisch eine Translokation t(2;3)(q13;p25) nachweisen ließ (Klemke *et al.*, 2011b). In beiden Fällen war es möglich, das Fusionsgen *PAX8/PPARγ* molekulargenetisch nachzuweisen. Eine Analyse zur Bestimmung des *HMGA2*-Expressionslevels in beiden Fällen ergab keine gegenüber normalem Schilddrüsengewebe signifikant erhöhte *HMGA2*-Expression, was die Klassifizierung der beiden Tumoren als follikuläre Adenome auf Grundlage histomorphologischer Kriterien zusätzlich stützt. *HMGA2* gilt als molekularer Marker hinsichtlich der Differenzierung benigner und maligner follikulärer Schilddrüseneoplasien, da eine gegenüber follikulären Adenomen signifikant erhöhte *HMGA2*-Expression in follikulären Schilddrüsenkarzinomen nachgewiesen werden kann (Belge *et al.*, 2008; Chiappetta *et al.*, 2008; Prasad *et al.*, 2008; Lappinga *et al.*, 2010). Somit stützen die vorliegenden Ergebnisse zwar nicht die These, dass es sich bei *PAX8/PPARγ*-positiven follikulären Adenomen tatsächlich um nicht-invasive (Cheung *et al.*, 2003) oder prä-invasive follikuläre Karzinome (Marques *et al.*, 2002; Nikiforova *et al.*, 2002) handelt, hingegen aber die Annahme, dass eine *PAX8/PPARγ*-Fusion als frühes Ereignis der

Tumorgenese follikulärer Schilddrüsenneoplasien angesehen werden kann (Cheung *et al.*, 2003). Das geringe Auftreten einer t(2;3)(q13;p25) bzw. *PAX8/PPARγ*-Fusion in follikulären Schilddrüsenadenomen in der vorliegenden Arbeit findet sich wieder in weiteren zytogenetischen (Teyssier *et al.*, 1990; Roque *et al.*, 1993b; Roque *et al.*, 2003) bzw. molekularzytogenetischen Untersuchungen (French *et al.*, 2003; Castro *et al.*, 2006; Chia *et al.*, 2010), allerdings besteht eine Diskrepanz hinsichtlich des Anteils *PAX8/PPARγ*-positiver Fälle zu RT-PCR-Analysen in anderen Untersuchungen (Marques *et al.*, 2002; Cheung *et al.*, 2003), was für eine unterschiedliche Sensitivität der verschiedenen Nachweismethoden spricht und abhängig sein kann von dem Anteil positiver Zellen innerhalb des Tumorgewebes bzw. dem Vorliegen zytogenetisch nicht erfassbarer Aberrationen. Eine Diskrepanz bezüglich des Anteils positiver Fälle in Abhängigkeit der Untersuchungsmethode konnte im Rahmen der vorliegenden Arbeit anhand zytogenetischer und molekularzytogenetischer Untersuchungen zum Nachweis der häufigen zytogenetischen Subgruppen in benignen Schilddrüsenläsionen bereits gezeigt werden (Drieschner *et al.*, 2011). Weiterhin geht aus Untersuchungen zum Nachweis einer t(2;3)(q13;p25) bzw. der *PAX8/PPARγ*-Fusion mittels I-FISH bzw. RT-PCR hervor, dass in Fällen, die positiv nach I-FISH sind, eine *PAX8/PPARγ*-Fusion nicht über RT-PCR nachweisbar war und umgekehrt (Dwight *et al.*, 2003; Algeciras-Schimnich *et al.*, 2010). In der vorliegenden Arbeit konnte an FFPE-Gewebe follikulärer Schilddrüsenkarzinome gezeigt werden, dass in einem Fall, bei dem mittels RT-PCR eine *PAX8/PPARγ*-Fusion nachweisbar war, der Anteil positiver Zellkerne nach I-FISH unterhalb der Nachweisgrenze lag und dieser Fall entsprechend auf Grundlage ausschließlich der I-FISH als negativ hinsichtlich einer *PAX8/PPARγ*-Fusion eingestuft worden wäre (Klemke *et al.*, 2011a). Dies spricht für eine unterschiedliche Sensitivität der beiden Methoden. Andererseits werden aber auch variierende Bruchpunkte in *PAX8* oder *PPARγ* als Ursache diskrepanter Ergebnisse verschiedener Nachweismethoden diskutiert (Dwight *et al.*, 2003). Im Rahmen der vorliegenden Arbeit konnte auf Basis einer molekularzytogenetischen Charakterisierung der Bruchpunktregion 3p25 eine Beteiligung der genomischen Region von *PPARγ* unabhängig von einer 2q13- bzw. *PAX8*-Beteiligung gezeigt werden (Drieschner *et al.*, 2006). Aus dieser und weiteren Untersuchungen (Kroll *et al.*, 2000; Roque *et al.*, 2001; Marques *et al.*, 2002; Chia *et al.*, 2010) geht hervor, dass die Region 3p25 bzw. *PPARγ* unabhängig von einer t(2;3)(q13;p25) betroffen sein und somit als Hot Spot Region in Schilddrüsentumoren follikulären Ursprungs angesehen werden kann. Welche

pathogenetische Relevanz 2q13- bzw. *PAX8*-unabhängige 3p25- und *PPARγ*-Aberrationen haben bzw. ob diese hinsichtlich der Tumorgenese äquivalent zur t(2;3)(q13;p25) und der *PAX8/PPARγ*-Fusion sind, ist ungeklärt und sollte Gegenstand weiterer Untersuchungen sein.

4.5 *HMGA1*- und *HMGA2*-Rearrangierungen in benignen mesenchymalen Tumoren

Charakteristische zytogenetische Veränderungen finden sich auch in humanen mesenchymalen Tumoren. So zählen in benignen uterinen Leiomyomen und auch chondroiden Hamartomen der Lunge strukturelle Veränderungen der chromosomalen Region 12q14~15 und 6p21 unter Beteiligung der Gene *HMGA2* (12q14~15) und *HMGA1* (6p21) zu den häufigen zytogenetischen Aberrationen in diesen Tumoren (Nilbert und Heim, 1990; Kazmierczak *et al.*, 1996b; Kazmierczak *et al.*, 1999; Ligon und Morton, 2001; Sandberg, 2005). Im Rahmen der vorliegenden Arbeit erfolgte die Etablierung einer FISH-Sonde zum molekularzytogenetischen Nachweis einer *HMGA2*-Rearrangierung, die den Nachweis von Rearrangierungen sowohl mit intragenisch als auch proximal lokalisierten Bruchpunkten ermöglicht, wobei je nach Signalmuster eine Differenzierung der Bruchpunktlokalisation möglich ist (Klemke *et al.*, 2009). *HMGA2*-Rearrangierungen können entweder durch Translokationen oder (parazentrische) Inversionen verursacht sein. In uterinen Leiomyomen findet sich am häufigsten die Translokation t(12;14)(q15;q23~24) (Heim *et al.*, 1988), welche i.d.R. zu einer Fusion zwischen *HMGA2* und dem in 14q23~24 lokalisiertem *RAD51L1* führt (Schoenmakers *et al.*, 1999; Takahashi *et al.*, 2001), wobei die Bruchpunkte vorwiegend im Intron 3 von *HMGA2* (Schoenmakers *et al.*, 1995) und seltener proximal, d.h. 5‘ von *HMGA2*, lokalisiert sein können (Schoenberg Fejzo *et al.*, 1996). Insgesamt wurden in der vorliegenden Arbeit im Rahmen von zwei Studien zur *HMGA2*-Expression in uterinen Leiomyomen (Klemke *et al.*, 2009; Markowski *et al.*, 2010a) an sieben ausgewählten Fällen begleitend molekularzytogenetische Untersuchungen hinsichtlich einer *HMGA2*-Rearrangierung durchgeführt. In zwei Fällen mit einer erhöhten *HMGA2*-Expression konnten Rearrangierungen mit Bruchpunkten proximal von *HMGA2* nachgewiesen werden, wie dies bereits von Schoenberg Fejzo *et al.* (1996) in uterinen Leiomyomen oder von Wanschura *et al.* (1996) und Kazmierczak *et al.* (1999) in chondroiden Hamartomen der Lunge beschrieben worden ist. Dies weist auf eine transkriptionelle Aktivierung von *HMGA2* bedingt durch den Verlust negativ regulatorischer Elemente oder die Translokation positiv

regulatorischer Elemente hin. In drei weiteren Fällen mit einer erhöhten *HMGA2*-Expression, jedoch ohne zytogenetisch nachweisbare 12q14~15-Aberration, konnte eine *HMGA2*-Rearrangierung molekularzytogenetisch an Metaphasepräparaten (Markowski *et al.*, 2010a) bzw. HOPE-fixierten Gewebeschnitten (Klemke *et al.*, 2009) nachgewiesen werden. Ursächlich dafür können kryptische Rearrangierungen sein oder eine *in vitro* Selektion bzw. der Verlust zytogenetisch aberranter Tumorzellklone, die infolge dessen zytogenetisch nicht mehr nachweisbar sind.

Ähnlich wie bei *HMGA2*-Rearrangierungen können auch bei *HMGA1*-Rearrangierungen die Bruchpunkte in benignen mesenchymalen Tumoren mit 6p21-Aberrationen entweder intragenisch lokalisiert sein oder außerhalb des Gens liegen, wobei hier im Gegensatz zu *HMGA2* die Bruchpunkte 3‘ (proximal) von *HMGA1* lokalisiert sind (Kazmierczak *et al.*, 1998). Zytogenetisch sind in uterinen Leiomyomen u.a. die t(1;6)(q23;p21), t(6;10)(p21;q22) und die t(6;14)(p21;q24) beschrieben (Kiechle-Schwarz *et al.*, 1991; Ozisik *et al.*, 1995; Hennig *et al.*, 1996; Sandberg, 2005). Für die t(6;14)(p21;q24) konnte in der vorliegenden Arbeit an einem chondroiden Hamartom der Lunge im Rahmen einer molekularzytogenetischen Charakterisierung der Bruchpunktregion 14q24 eine Bruchpunktlokalisation innerhalb von *RAD51L1* nachgewiesen werden (Blank *et al.*, 2001). Eine Beteiligung von *RAD51L1* an der Translokation t(12;14)(q14~15;q24) ist in uterinen Leiomyomen bereits gezeigt worden (Schoenmakers *et al.*, 1999; Takahashi *et al.*, 2001). In chondroiden Hamartomen der Lunge tritt neben der t(12;14)(q14~15;q24) die t(6;14)(p21;q24) mit einer ähnlichen Häufigkeit auf, sodass bereits diskutiert wurde, dass an beiden Translokationen jeweils dasselbe Gen in 14q24 beteiligt sein könnte (Kazmierczak *et al.*, 1999).

Zum molekularzytogenetischen Nachweis einer *HMGA1*-Rearrangierung wurde in der vorliegenden Arbeit eine Break-Apart Sonde etabliert und im Rahmen einer quantitativen Bestimmung der *HMGA1*-Expression in uterinen Leiomyomen eingesetzt (Nezhad *et al.*, 2010), bei der eine erhöhte *HMGA1*-Expression in Abhängigkeit des Vorliegens einer 6p21-Rearrangierung nachgewiesen werden konnte. In vier Tumoren mit strukturellen oder numerischen Aberrationen unter Beteiligung von Chromosom 6 und signifikant erhöhter *HMGA1*-Expression konnte jeweils molekularzytogenetisch eine *HMGA1*-Rearrangierung an Metaphasen der entsprechenden Tumoren nachgewiesen werden, darunter ein Fall mit einer kryptischen 6p21- bzw. *HMGA1*-Rearrangierung.

4.6 Fazit

„In cancer, the combination of cytogenetic and molecular studies (FISH, SKY, PCR, CGH, and related methodologies) can more clearly define pathogenetic pathways and the biologic functions of molecular markers than either approach alone." (Sandberg und Meloni-Ehrig, 2010)

Die molekulare Zytogenetik ermöglicht einerseits den Nachweis nicht zufälliger, spezifischer chromosomaler Aberrationen in humanen Neoplasien. Anderseits dient sie auch der weiteren Charakterisierung dieser Veränderungen insbesondere im Hinblick auf die Identifizierung der beteiligten Kandidatengene und schafft somit die Grundlage, die molekularen Mechanismen chromosomaler Aberrationen zu verstehen und mit Blick auf die Entstehung und Pathogenese der betroffenen Tumorentitäten einzuordnen. In diesem Kontext tragen die hier dargestellten Ergebnisse molekularzytogenetischer sowie darauf gründender molekulargenetischer Analysen zu einem besseren Verständnis der Molekularbiologie follikulärer Schilddrüsenläsionen und benigner mesenchymaler Tumoren bei. So ist die Identifizierung und die molekulargenetische Charakterisierung von *THADA* bzw. die in Läsionen mit 2p21-Rearrangierungen beschriebene Aberration von *THADA* sowie die Beschreibung eines kausalen Zusammenhangs zwischen 19q13.4-Rearrangierungen und der Expression der miRNA-Cluster C19MC und miR371-3 von grundlegender Bedeutung hinsichtlich der pathogenetischen Rolle dieser Veränderungen in benignen follikulären Schilddrüsenläsionen. Dass diesen Veränderungen eine größere Relevanz in diesen Tumorentitäten zukommt als bisherige zytogenetische Daten vermuten ließen, haben die quantitativen molekularzytogenetischen Analysen an benignen follikulären Schilddrüsenläsionen zeigen können. Die Ergebnisse der molekularzytogenetischen Analysen zum Nachweis von 3p25- bzw. *PPARγ*-Rearrangierungen bei follikulären Schilddrüsenneoplasien sowie *HMGA1*- und *HMGA2*-Rearrangierungen bei benignen mesenchymalen Tumoren bekräftigen die Bedeutung dieser Veränderungen in diesen Tumoren und zeigen, dass somit die molekulare Zytogenetik im allgemeinen und die FISH im Besonderen neben der CC und der Molekulargenetik eine besondere Stellung in der Analyse nicht zufälliger, spezifischer Chromosomenaberrationen für diese Tumorentitäten einnimmt. Weiterführende Untersuchungen auf Grundlage der hier präsentierten Ergebnisse, u.a. bezüglich der Häufigkeit, Spezifität sowie der funktionalen Rolle der hier analysierten

chromosomalen Veränderungen sowie der beteiligten Kandidatengene in den entsprechenden Tumorentitäten, können hinsichtlich Differentialdiagnostik und Therapie epithelialer follikulärer Schilddrüsenneoplasien und benigner mesenchymaler Tumoren beim Menschen von Nutzen sein.

5 Zusammenfassung

Die molekulare Zytogenetik, besonders die Fluoreszenz *in situ* Hybridisierung (FISH), ermöglicht den Nachweis sowie die Charakterisierung spezifischer, rekurrenter chromosomaler Aberrationen in humanen Neoplasien. Neben einer größeren Sensitivität zeichnet sich die FISH auch durch eine höhere Auflösung gegenüber der konventionellen Zytogenetik aus, was die nähere Charakterisierung der entsprechenden Veränderungen, insbesondere die Identifizierung und Beschreibung der beteiligten Gene, ermöglicht.

In der vorliegenden Arbeit lag der Schwerpunkt auf der molekularzytogenetischen Analyse zytogenetischer Subgruppen in follikulären Schilddrüsenläsionen. Anhand einer quantitativen Studie an 161 benignen follikulären Schilddrüsenläsionen war es möglich zu zeigen, dass den drei häufigen zytogenetischen Subgruppen, Trisomie 7 sowie 2p21- und 19q13.4-Rearrangierungen, eine größere Bedeutung in diesen Entitäten zukommt als bisher anhand zytogenetischer Analysen angenommen wurde.

Um die molekularbiologischen Hintergründe der beiden häufigen strukturellen Veränderungen in benignen follikulären Schilddrüsenläsionen in Bezug auf die Pathogenese dieser Läsionen zu verstehen, erfolgte eine molekularzytogenetische Charakterisierung der Bruchpunktregionen sowie darauf gründend molekulargenetische Analysen der in diesen Regionen lokalisierten Kandidatengene. Im Rahmen dieser Untersuchungen konnte das an 2p21-Rearrangierungen beteiligte Kandidatengen, *THADA*, identifiziert und charakterisiert werden. Weitere Analysen, die u.a. Hinweise auf funktionell relevante Strukturen innerhalb THADAs ergaben, stützen die Vermutung, dass die in Folge der 2p21-Rearrangierung auftretende Trunkierung THADAs im Zusammenhang steht mit der Proliferation epithelialer Zellen und der Genese benigner Schilddrüsenläsionen.

Bei benignen Schilddrüsenläsionen mit 19q13.4-Rearrangierungen konnten die Bruchpunkte mit Hilfe der FISH auf eine Region von 150 kb eingegrenzt werden. In Folge der Rearrangierung werden zwei in Nähe zu diesem 150 kb-Bruchpunktcluster lokalisierte miRNA-Cluster, C19MC und mir-371-3, aktiviert. In Läsionen mit einer t(1;19)(p35.2;q13.4) erfolgt dies durch Bildung eines Polymerase-II-Fusionstranskriptes unter Beteiligung der beiden miRNA-Cluster und des in 1p35.2 lokalisiertem *PUM1*-Gens.

Die in dieser Arbeit durchgeführten molekularzytogenetischen Untersuchungen zum Nachweis einer t(2;3)(q13;p25) bzw. des Fusionsgens *PAX8/PPARγ* in benignen wie auch malignen follikulären Schilddrüsenneoplasien zeigen einerseits, dass diese Veränderung mit einer geringen Häufigkeit innerhalb follikulärer Adenome vorkommt, anderseits fanden sich Diskrepanzen bezüglich des Anteils dieser Veränderung im Vergleich zwischen FISH und RT-PCR u.a. in follikulären Schilddrüsenkarzinomen. Die Ergebnisse sprechen zum Teil für eine unterschiedliche Sensitivität der beiden Methoden, es können aber auch variierende Bruchpunkte ursächlich sein. Eine molekularzytogenetische Charakterisierung der Bruchpunktregion 3p25 ergab diesbezüglich, dass Rearrangierungen der Region 3p25 unabhängig einer Beteiligung des in 2q13 lokalisiertem *PAX8* auftreten können und dass diese Region als Hot Spot-Region in Schilddrüsenneoplasien follikulären Ursprungs angesehen werden kann.

Weiterhin erfolgte eigens zum Nachweis von *HMGA1*- und *HMGA2*-Rearrangierungen in uterinen Leiomyomen die Etablierung von FISH-Sonden zur Detektion dieser Veränderungen im Rahmen von quantitativen *HMGA1*- bzw. *HMGA2*-Expressionsstudien. Hierbei konnte gezeigt werden, dass die verwendeten Sonden Translokationen der beteiligten Gene mit variierenden Bruchpunkten sowie auch zytogenetisch nicht nachgewiesene Rearrangierungen erfassen können. Zudem konnte die Beteiligung von *RAD51L1* in chondroiden Hamartomen mit einer t(6;14)(p21;q24) nachgewiesen werden.

Zusammenfassend verdeutlichen die in der vorliegenden Arbeit erzielten Ergebnisse die besondere Stellung der molekularen Zytogenetik hinsichtlich der Analyse tumorspezifischer chromosomaler Aberrationen im allgemeinen sowie, im speziellen, in Bezug auf die Einordnung dieser Aberrationen hinsichtlich ihrer pathogenetischen Relevanz für benigne follikuläre Schilddrüsenläsionen und mesenchymale Tumoren.

6 Summary

Molecular cytogenetics and fluorescence in situ hybridization (FISH), respectively, enables the detection and characterization of specific, recurrent chromosomal aberrations in human neoplasias. In comparison to conventional cytogenetics FISH is characterized by a higher sensitivity as well as resolution making it possible to identify and describe the genes involved in chromosomal aberrations.

The focus of the present study was on the molecular-cytogenetic analysis of the main cytogenetic subgroups in follicular lesions of the thyroid. By quantitative molecular-cytogenetic analysis of 161 benign thyroid lesions it was possible to show that much greater importance is attached to the main cytogenetic subgroups, i.e. trisomy 7 and rearrangements of 2p21 or 19q13.4, than by conventional cytogenetic analysis alone.

To understand the molecular background of both main structural aberrations in benign follicular thyroid lesions with respect to the pathogenesis of these entities molecular-cytogenetic characterization of the breakpoint regions as well as molecular-genetic analysis of the involved genes was done. By these analyses it was possible to identify and to further characterize the target gene, *THADA*, involved in 2p21 rearrangements. Further analyses suggest that functional important structures are located within THADA allowing the assumption that the truncation of THADA is in correlation with the proliferation of epithelial cells und the genesis of benign thyroid lesions.

For 19q13.4 rearrangements the breakpoints were narrowed down to a breakpoint cluster region of about 150 kb. This region is in close proximity to two miRNA clusters, C19MC and mir-371-3, which both are activated as a result of the rearrangements. At least for lesions with the translocation t(1;19)(p35.2;q13.4) the activation of both clusters is most likely caused by a Pol-II driven transcript consisting of both clusters and the *PUM1* gene located within 1p35.2.

The molecular-cytogenetic analysis of benign as well as malign follicular thyroid neoplasias with respect to the translocation t(2;3)(q13;p25) and the *PAX8/PPARγ* fusion gene, respectively, revealed that this aberration occurs only in a small fraction of follicular adenomas. Furthermore, comparing the results of FISH and RT-PCR analysis there were discrepancies in detection of this aberration between both methods. This could be caused

either by a different sensitivity of these methods or by a different localization of breakpoints. With respect to the latter thesis molecular-cytogenetic characterization of the 3p25 breakpoint region reveals that rearrangements of the 3p25 region occur independently of the 2q13 region and the *PAX8* gene, respectively. Thus this region is considered as a hot spot region in thyroid neoplasias with follicular origin.

Specific FISH assays were established making it possible to detect rearrangements of *HMGA1* and *HMGA2* as part of either *HMGA1* or *HMGA2* expression studies in uterine leiomyomas. Both FISH assays were able to discover translocations with different breakpoint localizations as well as rearrangements which were not detectable by conventional cytogenetic analysis. Furthermore, it was shown that *RAD51L1* is also involved in the translocation t(6;14)(p21;q24) in chondroid hamartomas of the lung.

In conclusion the results of the present study point out the status of molecular cytogenetics with respect to the analysis of tumor-specific chromosomal aberrations in general and in particular to the relevance of these aberrations to the pathogenesis of benign follicular thyroid lesions and mesenchymal tumors.

7 Literatur

Algeciras-Schimnich, A., Milosevic, D., McIver, B., Flynn, H., Reddi, H. V., Eberhardt, N. L. and Grebe, S. K. (2010). "Evaluation of the PAX8/PPARG translocation in follicular thyroid cancer with a 4-color reverse-transcription PCR assay and automated high-resolution fragment analysis." Clin Chem **56**(3): 391-398.

Altschul, S. F., Madden, T. L., Schaffer, A. A., Zhang, J., Zhang, Z., Miller, W. and Lipman, D. J. (1997). "Gapped BLAST and PSI-BLAST: a new generation of protein database search programs." Nucleic Acids Res **25**(17): 3389-3402.

Antonini, P., Levy, N., Caillou, B., Venuat, A. M., Schlumberger, M., Parmentier, C. and Bernheim, A. (1993). "Numerical aberrations, including trisomy 22 as the sole anomaly, are recurrent in follicular thyroid adenomas." Genes Chromosomes Cancer **8**(1): 63-66.

Antonini, P., Venuat, A. M., Linares, G., Caillou, B., Schlumberger, M., Travagli, J. P., Berger, R. and Parmentier, C. (1991). "Cytogenetic abnormalities in thyroid adenomas." Cancer Genet Cytogenet **52**(2): 157-164.

Arturi, F., Russo, D., Schlumberger, M., du Villard, J. A., Caillou, B., Vigneri, P., Wicker, R., Chiefari, E., Suarez, H. G. and Filetti, S. (1998). "Iodide symporter gene expression in human thyroid tumors." J Clin Endocrinol Metab **83**(7): 2493-2496.

Ashar, H. R., Fejzo, M. S., Tkachenko, A., Zhou, X., Fletcher, J. A., Weremowicz, S., Morton, C. C. and Chada, K. (1995). "Disruption of the architectural factor HMGI-C: DNA-binding AT hook motifs fused in lipomas to distinct transcriptional regulatory domains." Cell **82**(1): 57-65.

Ashkenazi, A. (2002). "Targeting death and decoy receptors of the tumour-necrosis factor superfamily." Nat Rev Cancer **2**(6): 420-430.

Ashkenazi, A. and Dixit, V. M. (1998). "Death receptors: signaling and modulation." Science **281**(5381): 1305-1308.

Atkin, N. B. and Baker, M. C. (1965). "Chromosome abnormalities, neoplasia, and autoimmune disease." Lancet **1**(7389): 820-821.

Barril, N., Carvalho-Sales, A. B. and Tajara, E. H. (2000). "Detection of numerical chromosome anomalies in interphase cells of benign and malignant thyroid lesions using fluorescence in situ hybridization." Cancer Genet Cytogenet **117**(1): 50-56.

Bartnitzke, S., Herrmann, M. E., Lobeck, H., Zuschneid, W., Neuhaus, P. and Bullerdiek, J. (1989). "Cytogenetic findings on eight follicular thyroid adenomas including one with a t(10;19)." Cancer Genet Cytogenet **39**(1): 65-68.

Beierwaltes, W. H. and al-Saadi, A. A. (1966). "Chromosome abnormalities in human thyroid disease." J Clin Endocrinol Metab **26**(7): 729-734.

Belge, G., Garcia, E., de Jong, P., Bartnitzke, S. and Bullerdiek, J. (1995). "FISH analyses of a newly established thyroid tumor cell line showing a t(1;19)(p35 or p36.1;q13) reveal that the breakpoint lies between 19q13.3-13.4 and 19q13.4." Cytogenet Cell Genet **69**(3-4): 220-222.

Belge, G., Garcia, E., Rippe, V., Fusco, A., Bartnitzke, S. and Bullerdiek, J. (1997). "Breakpoints of 19q13 translocations of benign thyroid tumors map within a 400 kilobase region." Genes Chromosomes Cancer **20**(2): 201-203.

Belge, G., Kazmierczak, B., Meyer-Bolte, K., Bartnitzke, S. and Bullerdiek, J. (1992a). "Expression of SV40 T-antigen in lipoma cells with a chromosomal translocation T(3;12) is not sufficient for direct immortalization." Cell Biol Int Rep **16**(4): 339-347.

Belge, G., Meyer, A., Klemke, M., Burchardt, K., Stern, C., Wosniok, W., Loeschke, S. and Bullerdiek, J. (2008). "Upregulation of HMGA2 in thyroid carcinomas: a novel molecular marker to distinguish between benign and malignant follicular neoplasias." Genes Chromosomes Cancer **47**(1): 56-63.

Belge, G., Rippe, V., Meiboom, M., Drieschner, N., Garcia, E. and Bullerdiek, J. (2001). "Delineation of a 150-kb breakpoint cluster in benign thyroid tumors with 19q13.4 aberrations." Cytogenet Cell Genet **93**(1-2): 48-51.

Belge, G., Roque, L., Soares, J., Bruckmann, S., Thode, B., Fonseca, E., Clode, A., Bartnitzke, S., Castedo, S. and Bullerdiek, J. (1998). "Cytogenetic investigations of 340 thyroid hyperplasias and adenomas revealing correlations between cytogenetic findings and histology." Cancer Genet Cytogenet **101**(1): 42-48.

Belge, G., Thode, B., Bullerdiek, J. and Bartnitzke, S. (1992b). "Aberrations of chromosome 19. Do they characterize a subtype of benign thyroid adenomas?" Cancer Genet Cytogenet **60**(1): 23-26.

Belge, G., Thode, B., Rippe, V., Bartnitzke, S. and Bullerdiek, J. (1994). "A characteristic sequence of trisomies starting with trisomy 7 in benign thyroid tumors." Hum Genet **94**(2): 198-202.

Bentwich, I., Avniel, A., Karov, Y., Aharonov, R., Gilad, S., Barad, O., Barzilai, A., Einat, P., Einav, U., Meiri, E., Sharon, E., Spector, Y. and Bentwich, Z. (2005). "Identification of hundreds of conserved and nonconserved human microRNAs." Nat Genet **37**(7): 766-770.

Blank, C., Schoenmakers, E. F., Rogalla, P., Huys, E. H., Van Rijk, A. A., Drieschner, N. and Bullerdiek, J. (2001). "Intragenic breakpoint within RAD51L1 in a t(6;14)(p21.3;q24) of a pulmonary chondroid hamartoma." Cytogenet Cell Genet **95**(1-2): 17-19.

Boesgaard, T. W., Gjesing, A. P., Grarup, N., Rutanen, J., Jansson, P. A., Hribal, M. L., Sesti, G., Fritsche, A., Stefan, N., Staiger, H., Haring, H., Smith, U., Laakso, M., Pedersen, O. and Hansen, T. (2009). "Variant near ADAMTS9 known to associate with type 2 diabetes is related to insulin resistance in offspring of type 2 diabetes patients--EUGENE2 study." PLoS ONE **4**(9): e7236.

Bol, S., Belge, G., Rippe, V. and Bullerdiek, J. (2001). "Molecular cytogenetic investigations define a subgroup of thyroid adenomas with 2p21 breakpoints clustered to a region of less than 450 kb." Cytogenet Cell Genet **95**(3-4): 189-191.

Bol, S., Belge, G., Thode, B., Bartnitzke, S. and Bullerdiek, J. (1999). "Structural abnormalities of chromosome 2 in benign thyroid tumors. Three new cases and review of the literature." Cancer Genet Cytogenet **114**(1): 75-77.

Bondeson, L., Bengtsson, A., Bondeson, A. G., Dahlenfors, R., Grimelius, L., Wedell, B. and Mark, J. (1989). "Chromosome studies in thyroid neoplasia." Cancer **64**(3): 680-685.

Bortolin-Cavaille, M. L., Dance, M., Weber, M. and Cavaille, J. (2009). "C19MC microRNAs are processed from introns of large Pol-II, non-protein-coding transcripts." Nucleic Acids Res **37**(10): 3464-3473.

Braun, J. and Huttelmaier, S. (2011). "Pathogenic mechanisms of deregulated microRNA expression in thyroid carcinomas of follicular origin." Thyroid Res **4 Suppl 1**: S1.

Cairo, S., Wang, Y., de Reynies, A., Duroure, K., Dahan, J., Redon, M. J., Fabre, M., McClelland, M., Wang, X. W., Croce, C. M. and Buendia, M. A. (2010). "Stem cell-like micro-RNA signature driven by Myc in aggressive liver cancer." Proc Natl Acad Sci U S A **107**(47): 20471-20476.

Carney, S. A., Tahara, H., Swartz, C. D., Risinger, J. I., He, H., Moore, A. B., Haseman, J. K., Barrett, J. C. and Dixon, D. (2002). "Immortalization of human uterine leiomyoma

and myometrial cell lines after induction of telomerase activity: molecular and phenotypic characteristics." Lab Invest **82**(6): 719-728.

Castro, P., Rebocho, A. P., Soares, R. J., Magalhaes, J., Roque, L., Trovisco, V., Vieira de Castro, I., Cardoso-de-Oliveira, M., Fonseca, E., Soares, P. and Sobrinho-Simoes, M. (2006). "PAX8-PPARgamma rearrangement is frequently detected in the follicular variant of papillary thyroid carcinoma." J Clin Endocrinol Metab **91**(1): 213-220.

Chen, Z. J., Zhao, H., He, L., Shi, Y., Qin, Y., Li, Z., You, L., Zhao, J., Liu, J., Liang, X., Zhao, X., Sun, Y., Zhang, B., Jiang, H., Zhao, D., Bian, Y., Gao, X., Geng, L., Li, Y., Zhu, D., Sun, X., Xu, J. E., Hao, C., Ren, C. E., Zhang, Y., Chen, S., Zhang, W., Yang, A., Yan, J., Ma, J. and Zhao, Y. (2011). "Genome-wide association study identifies susceptibility loci for polycystic ovary syndrome on chromosome 2p16.3, 2p21 and 9q33.3." Nat Genet **43**(1): 55-59.

Cheung, L., Messina, M., Gill, A., Clarkson, A., Learoyd, D., Delbridge, L., Wentworth, J., Philips, J., Clifton-Bligh, R. and Robinson, B. G. (2003). "Detection of the PAX8-PPARgamma Fusion Oncogene in Both Follicular Thyroid Carcinomas and Adenomas." J Clin Endocrinol Metab **88**(1): 354-357.

Chia, W. K., Sharifah, N. A., Reena, R. M., Zubaidah, Z., Clarence-Ko, C. H., Rohaizak, M., Naqiyah, I., Srijit, D., Hisham, A. N., Asmiati, A. and Rafie, M. K. (2010). "Fluorescence in situ hybridization analysis using PAX8- and PPARG-specific probes reveals the presence of PAX8-PPARG translocation and 3p25 aneusomy in follicular thyroid neoplasms." Cancer Genet Cytogenet **196**(1): 7-13.

Chiappetta, G., Avantaggiato, V., Visconti, R., Fedele, M., Battista, S., Trapasso, F., Merciai, B. M., Fidanza, V., Giancotti, V., Santoro, M., Simeone, A. and Fusco, A. (1996). "High level expression of the HMGI (Y) gene during embryonic development." Oncogene **13**(11): 2439-2446.

Chiappetta, G., Ferraro, A., Vuttariello, E., Monaco, M., Galdiero, F., De Simone, V., Califano, D., Pallante, P., Botti, G., Pezzullo, L., Pierantoni, G. M., Santoro, M. and Fusco, A. (2008). "HMGA2 mRNA expression correlates with the malignant phenotype in human thyroid neoplasias." Eur J Cancer.

Cigudosa, J. C., Pedrosa Guerra, A., Otero Gomez, A., Carrasco Juan, J. L., Perez Gomez, J. A., Ferrer Roca, O. F. and Garcia Miranda, J. L. (1995). "Translocation (5;19)(q13;q13) in a multinodular thyroid goiter." Cancer Genet Cytogenet **82**(1): 67-69.

Coates, J. C. (2003). "Armadillo repeat proteins: beyond the animal kingdom." Trends Cell Biol **13**(9): 463-471.

Dal Cin, P., Sneyers, W., Aly, M. S., Segers, A., Ostijn, F., Van Damme, B. and Van Den Berghe, H. (1992). "Involvement of 19q13 in follicular thyroid adenoma." Cancer Genet Cytogenet **60**(1): 99-101.

Delellis, R. A. (2006). "Pathology and genetics of thyroid carcinoma." J Surg Oncol **94**(8): 662-669.

DeLellis, R. A., Lloyd, R. V., Heitz, P. U. and Eng, C., Eds. (2004). Tumours of the Thyroid and Parathyroid. Pathology and genetics of tumours of endocrine organs. Lyon, IARC Press.

Dixon, D., Flake, G. P., Moore, A. B., He, H., Haseman, J. K., Risinger, J. I., Lancaster, J. M., Berchuck, A., Barrett, J. C. and Robboy, S. J. (2002). "Cell proliferation and apoptosis in human uterine leiomyomas and myometria." Virchows Arch **441**(1): 53-62.

Drieschner, N., Belge, G., Rippe, V., Meiboom, M., Loeschke, S. and Bullerdiek, J. (2006). "Evidence for a 3p25 breakpoint hot spot region in thyroid tumors of follicular origin." Thyroid **16**(11): 1091-1096.

Drieschner, N., Kerschling, S., Soller, J. T., Rippe, V., Belge, G., Bullerdiek, J. and Nimzyk, R. (2007). "A domain of the thyroid adenoma associated gene (THADA) conserved in vertebrates becomes destroyed by chromosomal rearrangements observed in thyroid adenomas." Gene **403**(1-2): 110-117.

Drieschner, N., Rippe, V., Laabs, A., Dittberner, L., Nimzyk, R., Junker, K., Rommel, B., Kiefer, Y., Belge, G., Bullerdiek, J. and Sendt, W. (2011). "Interphase fluorescence in situ hybridization analysis detects a much higher rate of thyroid tumors with clonal cytogenetic deviations of the main cytogenetic subgroups than conventional cytogenetics." Cancer Genet **204**(7): 366-374.

Dwight, T., Thoppe, S. R., Foukakis, T., Lui, W. O., Wallin, G., Hoog, A., Frisk, T., Larsson, C. and Zedenius, J. (2003). "Involvement of the PAX8/peroxisome proliferator-activated receptor gamma rearrangement in follicular thyroid tumors." J Clin Endocrinol Metab **88**(9): 4440-4445.

Fagin, J. A. (1992). "Genetic basis of endocrine disease 3: Molecular defects in thyroid gland neoplasia." J Clin Endocrinol Metab **75**(6): 1398-1400.

Fejzo, M. S., Yoon, S. J., Montgomery, K. T., Rein, M. S., Weremowicz, S., Krauter, K. S., Dorman, T. E., Fletcher, J. A., Mao, J. I., Moir, D. T. and et al. (1995). "Identification of a YAC spanning the translocation breakpoints in uterine leiomyomata, pulmonary chondroid hamartoma, and lipoma: physical mapping of the 12q14-q15 breakpoint region in uterine leiomyomata." Genomics **26**(2): 265-271.

Filetti, S., Bidart, J. M., Arturi, F., Caillou, B., Russo, D. and Schlumberger, M. (1999). "Sodium/iodide symporter: a key transport system in thyroid cancer cell metabolism." Eur J Endocrinol **141**(5): 443-457.

Fornari, F., Milazzo, M., Chieco, P., Negrini, M., Marasco, E., Capranico, G., Mantovani, V., Marinello, J., Sabbioni, S., Callegari, E., Cescon, M., Ravaioli, M., Croce, C. M., Bolondi, L. and Gramantieri, L. (2012). "In hepatocellular carcinoma miR-519d is upregulated by p53 and DNA hypomethylation and targets CDKN1A/p21, PTEN, AKT3 and TIMP2." J Pathol.

French, C. A., Alexander, E. K., Cibas, E. S., Nose, V., Laguette, J., Faquin, W., Garber, J., Moore, F., Jr., Fletcher, J. A., Larsen, P. R. and Kroll, T. G. (2003). "Genetic and biological subgroups of low-stage follicular thyroid cancer." Am J Pathol **162**(4): 1053-1060.

Gama, N. B., Gama, R., Thome, J. A. and Tajara, E. H. (1991). "Cytogenetic analysis of a multinodular thyroid goiter." Cancer Genet Cytogenet **55**(1): 73-77.

Goodarzi, M. O., Jones, M. R., Li, X., Chua, A. K., Garcia, O. A., YD, I. C., Krauss, R. M., Rotter, J. I., Ankener, W., Legro, R. S., Azziz, R., Strauss, J. F., 3rd, Dunaif, A. and Urbanek, M. (2011). "Replication of association of DENND1A and THADA variants with polycystic ovary syndrome in European cohorts." J Med Genet.

Grarup, N., Andersen, G., Krarup, N. T., Albrechtsen, A., Schmitz, O., Jorgensen, T., Borch-Johnsen, K., Hansen, T. and Pedersen, O. (2008). "Association testing of novel type 2 diabetes risk alleles in the JAZF1, CDC123/CAMK1D, TSPAN8, THADA, ADAMTS9, and NOTCH2 loci with insulin release, insulin sensitivity, and obesity in a population-based sample of 4,516 glucose-tolerant middle-aged Danes." Diabetes **57**(9): 2534-2540.

Gray, J. W. and Pinkel, D. (1992). "Molecular cytogenetics in human cancer diagnosis." Cancer **69**(6 Suppl): 1536-1542.

Gregory, R. I. and Shiekhattar, R. (2005). "MicroRNA biogenesis and cancer." Cancer Res **65**(9): 3509-3512.

Grieco, M., Santoro, M., Berlingieri, M. T., Melillo, R. M., Donghi, R., Bongarzone, I., Pierotti, M. A., Della Porta, G., Fusco, A. and Vecchio, G. (1990). "PTC is a novel rearranged form of the ret proto-oncogene and is frequently detected in vivo in human thyroid papillary carcinomas." Cell **60**(4): 557-563.

Gupta, V., Vinay, D. G., Rafiq, S., Kranthikumar, M. V., Janipalli, C. S., Giambartolomei, C., Evans, D. M., Mani, K. R., Sandeep, M. N., Taylor, A. E., Kinra, S., Sullivan, R. M., Bowen, L., Timpson, N. J., Smith, G. D., Dudbridge, F., Prabhakaran, D., Ben-Shlomo, Y., Reddy, K. S., Ebrahim, S. and Chandak, G. R. (2011). "Association analysis of 31 common polymorphisms with type 2 diabetes and its related traits in Indian sib pairs." Diabetologia.

Heim, S. and Mitelman, F., Eds. (2009). Cancer Cytogenetics, John Wiley and Sons.

Heim, S., Nilbert, M., Vanni, R., Floderus, U. M., Mandahl, N., Liedgren, S., Lecca, U. and Mitelman, F. (1988). "A specific translocation, t(12;14)(q14-15;q23-24), characterizes a subgroup of uterine leiomyomas." Cancer Genet Cytogenet **32**(1): 13-17.

Hennig, Y., Deichert, U., Bonk, U., Thode, B., Bartnitzke, S. and Bullerdiek, J. (1999). "Chromosomal translocations affecting 12q14-15 but not deletions of the long arm of chromosome 7 associated with a growth advantage of uterine smooth muscle cells." Mol Hum Reprod **5**(12): 1150-1154.

Hennig, Y., Deichert, U., Stern, C., Ghassemi, A., Thode, B., Bonk, U., Meister, P., Bartnitzke, S. and Bullerdiek, J. (1996). "Structural aberrations of chromosome 6 in three uterine smooth muscle tumors." Cancer Genet Cytogenet **87**(2): 148-151.

Hirning-Folz, U., Wilda, M., Rippe, V., Bullerdiek, J. and Hameister, H. (1998). "The expression pattern of the Hmgic gene during development." Genes Chromosomes Cancer **23**(4): 350-357.

Hopman, A. H. and Ramaekers, F. C. (2001). "Processing and staining of cell and tissue material for interphase cytogenetics." Curr Protoc Cytom **Chapter 8**: Unit 8 5.

Hu, C., Zhang, R., Wang, C., Wang, J., Ma, X., Lu, J., Qin, W., Hou, X., Bao, Y., Xiang, K. and Jia, W. (2009). "PPARG, KCNJ11, CDKAL1, CDKN2A-CDKN2B, IDE-KIF11-HHEX, IGF2BP2 and SLC30A8 are associated with type 2 diabetes in a Chinese population." PLoS ONE **4**(10): e7643.

Huang, Q., Gumireddy, K., Schrier, M., le Sage, C., Nagel, R., Nair, S., Egan, D. A., Li, A., Huang, G., Klein-Szanto, A. J., Gimotty, P. A., Katsaros, D., Coukos, G., Zhang, L., Pure, E. and Agami, R. (2008). "The microRNAs miR-373 and miR-520c promote tumour invasion and metastasis." Nat Cell Biol **10**(2): 202-210.

Husmann, G. and Berlin, R.-K.-I. (2010). Krebs in Deutschland: 2005/2006 ; Häufigkeiten und Trends ; eine gemeinsame Veröffentlichung des Robert Koch-Instituts und der Gesellschaft der Epidemiologischen Krebsregister in Deutschland e.V, Robert Koch-Inst.

Kang, E. S., Kim, M. S., Kim, C. H., Nam, C. M., Han, S. J., Hur, K. Y., Ahn, C. W., Cha, B. S., Kim, S. I., Lee, H. C. and Kim, Y. S. (2009). "Association of common type 2 diabetes risk gene variants and posttransplantation diabetes mellitus in renal allograft recipients in Korea." Transplantation **88**(5): 693-698.

Kazmierczak, B., Bartnitzke, S., Hartl, M. and Bullerdiek, J. (1990). "In vitro transformation by the SV40 'early region' of cells from a human benign salivary gland tumor with a 12q13----q15 rearrangement." Cytogenet Cell Genet **53**(1): 37-39.

Kazmierczak, B., Bol, S., Wanschura, S., Bartnitzke, S. and Bullerdiek, J. (1996a). "PAC clone containing the HMGI(Y) gene spans the breakpoint of a 6p21 translocation in a uterine leiomyoma cell line." Genes Chromosomes Cancer **17**(3): 191-193.

Kazmierczak, B., Dal Cin, P., Wanschura, S., Borrmann, L., Fusco, A., Van den Berghe, H. and Bullerdiek, J. (1998). "HMGIY is the target of 6p21.3 rearrangements in various benign mesenchymal tumors." Genes Chromosomes Cancer **23**(4): 279-285.

Kazmierczak, B., Meyer-Bolte, K., Tran, K. H., Wockel, W., Breightman, I., Rosigkeit, J., Bartnitzke, S. and Bullerdiek, J. (1999). "A high frequency of tumors with rearrangements of genes of the HMGI(Y) family in a series of 191 pulmonary chondroid hamartomas." Genes Chromosomes Cancer **26**(2): 125-133.

Kazmierczak, B., Rosigkeit, J., Wanschura, S., Meyer-Bolte, K., Van de Ven, W. J., Kayser, K., Krieghoff, B., Kastendiek, H., Bartnitzke, S. and Bullerdiek, J. (1996b). "HMGI-C rearrangements as the molecular basis for the majority of pulmonary chondroid hamartomas: a survey of 30 tumors." Oncogene **12**(3): 515-521.

Kazmierczak, B., Wanschura, S., Rommel, B., Bartnitzke, S. and Bullerdiek, J. (1996c). "Ten pulmonary chondroid hamartomas with chromosome 6p21 breakpoints within the HMG-I(Y) gene or its immediate surroundings." J Natl Cancer Inst **88**(17): 1234-1236.

Khanna, C., Lindblad-Toh, K., Vail, D., London, C., Bergman, P., Barber, L., Breen, M., Kitchell, B., McNeil, E., Modiano, J. F., Niemi, S., Comstock, K. E., Ostrander, E., Westmoreland, S. and Withrow, S. (2006). "The dog as a cancer model." Nat Biotechnol **24**(9): 1065-1066.

Kiechle-Schwarz, M., Sreekantaiah, C., Berger, C. S., Pedron, S., Medchill, M. T., Surti, U. and Sandberg, A. A. (1991). "Nonrandom cytogenetic changes in leiomyomas of the female genitourinary tract. A report of 35 cases." Cancer Genet Cytogenet **53**(1): 125-136.

Kievits, T., Dauwerse, J. G., Wiegant, J., Devilee, P., Breuning, M. H., Cornelisse, C. J., van Ommen, G. J. and Pearson, P. L. (1990). "Rapid subchromosomal localization of cosmids by nonradioactive in situ hybridization." Cytogenet Cell Genet **53**(2-3): 134-136.

Klemke, M., Drieschner, N., Belge, G., Burchardt, K., Junker, K. and Bullerdiek, J. (2011a). "Detection of PAX8-PPARG fusion transcripts in archival thyroid carcinoma samples by conventional RT-PCR." Genes Chromosomes Cancer.

Klemke, M., Drieschner, N., Belge, G., Burchardt, K., Junker, K. and Bullerdiek, J. (2012). "Detection of PAX8-PPARG fusion transcripts in archival thyroid carcinoma samples by conventional RT-PCR." Genes Chromosomes Cancer **51**(4): 402-408.

Klemke, M., Drieschner, N., Laabs, A., Rippe, V., Belge, G., Bullerdiek, J. and Sendt, W. (2011b). "On the prevalence of the PAX8-PPARG fusion resulting from the chromosomal translocation t(2;3)(q13;p25) in adenomas of the thyroid." Cancer Genet **204**(6): 334-339.

Klemke, M., Meyer, A., Nezhad, M. H., Bartnitzke, S., Drieschner, N., Frantzen, C., Schmidt, E. H., Belge, G. and Bullerdiek, J. (2009). "Overexpression of HMGA2 in uterine leiomyomas points to its general role for the pathogenesis of the disease." Genes Chromosomes Cancer **48**(2): 171-178.

Kloth, L., Belge, G., Burchardt, K., Loeschke, S., Wosniok, W., Fu, X., Nimzyk, R., Mohamed, S. A., Drieschner, N., Rippe, V. and Bullerdiek, J. (2011). "Decrease in thyroid adenoma associated (THADA) expression is a marker of dedifferentiation of thyroid tissue." BMC Clin Pathol **11**: 13.

Kondo, T., Ezzat, S. and Asa, S. L. (2006). "Pathogenetic mechanisms in thyroid follicular-cell neoplasia." Nat Rev Cancer **6**(4): 292-306.

Korenberg, J. R., Chen, X. N., Adams, M. D. and Venter, J. C. (1995). "Toward a cDNA map of the human genome." Genomics **29**(2): 364-370.

Kroll, T. G., Sarraf, P., Pecciarini, L., Chen, C. J., Mueller, E., Spiegelman, B. M. and Fletcher, J. A. (2000). "PAX8-PPARgamma1 fusion oncogene in human thyroid carcinoma [corrected]." Science **289**(5483): 1357-1360.

Lappinga, P. J., Kip, N. S., Jin, L., Lloyd, R. V., Henry, M. R., Zhang, J. and Nassar, A. (2010). "HMGA2 gene expression analysis performed on cytologic smears to distinguish benign from malignant thyroid nodules." Cancer Cytopathol **118**(5): 287-297.

Lazar, V., Bidart, J. M., Caillou, B., Mahe, C., Lacroix, L., Filetti, S. and Schlumberger, M. (1999). "Expression of the Na+/I- symporter gene in human thyroid tumors: a comparison study with other thyroid-specific genes." J Clin Endocrinol Metab **84**(9): 3228-3234.

Lee, Y. S. and Dutta, A. (2009). "MicroRNAs in cancer." Annu Rev Pathol **4**: 199-227.

Li, M., Lee, K. F., Lu, Y., Clarke, I., Shih, D., Eberhart, C., Collins, V. P., Van Meter, T., Picard, D., Zhou, L., Boutros, P. C., Modena, P., Liang, M. L., Scherer, S. W., Bouffet, E., Rutka, J. T., Pomeroy, S. L., Lau, C. C., Taylor, M. D., Gajjar, A., Dirks, P. B., Hawkins, C. E. and Huang, A. (2009a). "Frequent amplification of a chr19q13.41 microRNA polycistron in aggressive primitive neuroectodermal brain tumors." Cancer Cell **16**(6): 533-546.

Li, S. S., Yu, S. L., Kao, L. P., Tsai, Z. Y., Singh, S., Chen, B. Z., Ho, B. C., Liu, Y. H. and Yang, P. C. (2009b). "Target identification of microRNAs expressed highly in human embryonic stem cells." J Cell Biochem **106**(6): 1020-1030.

Ligon, A. H. and Morton, C. C. (2001). "Leiomyomata: heritability and cytogenetic studies." Hum Reprod Update **7**(1): 8-14.

Loy, C. J., Evelyn, S., Lim, F. K., Liu, M. H. and Yong, E. L. (2005). "Growth dynamics of human leiomyoma cells and inhibitory effects of the peroxisome proliferator-activated receptor-gamma ligand, pioglitazone." Mol Hum Reprod **11**(8): 561-566.

Markowski, D. N., Bartnitzke, S., Belge, G., Drieschner, N., Helmke, B. M. and Bullerdiek, J. (2010a). "Cell culture and senescence in uterine fibroids." Cancer Genet Cytogenet **202**(1): 53-57.

Markowski, D. N., von Ahsen, I., Nezhad, M. H., Wosniok, W., Helmke, B. M. and Bullerdiek, J. (2010b). "HMGA2 and the p19Arf-TP53-CDKN1A axis: a delicate balance in the growth of uterine leiomyomas." Genes Chromosomes Cancer **49**(8): 661-668.

Marques, A. R., Espadinha, C., Catarino, A. L., Moniz, S., Pereira, T., Sobrinho, L. G. and Leite, V. (2002). "Expression of PAX8-PPAR gamma 1 rearrangements in both follicular thyroid carcinomas and adenomas." J Clin Endocrinol Metab **87**(8): 3947-3952.

Mayr, B., Schleger, W., Loupal, G. and Burtscher, H. (1991). "Characterisation of complex karyotype changes in a canine thyroid adenoma." Res Vet Sci **50**(3): 298-300.

Meiboom, M., Murua Escobar, H., Pentimalli, F., Fusco, A., Belge, G. and Bullerdiek, J. (2003). "A 3.4-kbp transcript of ZNF331 is solely expressed in follicular thyroid adenomas." Cytogenet Genome Res **101**(2): 113-117.

Meloni, A. M., Surti, U., Contento, A. M., Davare, J. and Sandberg, A. A. (1992). "Uterine leiomyomas: cytogenetic and histologic profile." Obstet Gynecol **80**(2): 209-217.

Mitelman, F. (2000). "Recurrent chromosome aberrations in cancer." Mutat Res **462**(2-3): 247-253.

Mitelman, F., Johansson, B. and Mertens, F. (2007). "The impact of translocations and gene fusions on cancer causation." Nat Rev Cancer **7**(4): 233-245.

Mitelman, F., Johansson, B. and Mertens, F. E. (2011). "Mitelman Database of Chromosome Aberrations and Gene Fusions in Cancer (2011)." http://cgap.nci.nih.gov/Chromosomes/Mitelman.

Nezhad, M. H., Drieschner, N., Helms, S., Meyer, A., Tadayyon, M., Klemke, M., Belge, G., Bartnitzke, S., Burchardt, K., Frantzen, C., Schmidt, E. H. and Bullerdiek, J. (2010). "6p21 rearrangements in uterine leiomyomas targeting HMGA1." Cancer Genet Cytogenet **203**(2): 247-252.

Nikiforova, M. N., Biddinger, P. W., Caudill, C. M., Kroll, T. G. and Nikiforov, Y. E. (2002). "PAX8-PPARgamma rearrangement in thyroid tumors: RT-PCR and immunohistochemical analyses." Am J Surg Pathol **26**(8): 1016-1023.

Nilbert, M. and Heim, S. (1990). "Uterine leiomyoma cytogenetics." Genes Chromosomes Cancer **2**(1): 3-13.

Ogilvie, G. K. (1996). Tumors of the Endocrine System. Small animal clinical oncology. S. J. Withrow and E. G. MacEwan. Philadelphia, W. B. Saunders**:** 316 -

Ozisik, Y. Y., Meloni, A. M., Altungoz, O., Surti, U. and Sandberg, A. A. (1995). "Translocation (6;10)(p21;q22) in uterine leiomyomas." Cancer Genet Cytogenet **79**(2): 136-138.

Ozisik, Y. Y., Meloni, A. M., Surti, U. and Sandberg, A. A. (1993). "Deletion 7q22 in uterine leiomyoma. A cytogenetic review." Cancer Genet Cytogenet **71**(1): 1-6.

Pandis, N., Heim, S., Bardi, G., Floderus, U. M., Willen, H., Mandahl, N. and Mitelman, F. (1991). "Chromosome analysis of 96 uterine leiomyomas." Cancer Genet Cytogenet **55**(1): 11-18.

Paoloni, M. C. and Khanna, C. (2007). "Comparative oncology today." Vet Clin North Am Small Anim Pract **37**(6): 1023-1032; v.

Parameswaran, R., Brooks, S. and Sadler, G. P. (2010). "Molecular pathogenesis of follicular cell derived thyroid cancers." Int J Surg **8**(3): 186-193.

Parikh, H., Lyssenko, V. and Groop, L. C. (2009). "Prioritizing genes for follow-up from genome wide association studies using information on gene expression in tissues relevant for type 2 diabetes mellitus." BMC Med Genomics **2**: 72.

Perren, A., Komminoth, P. and Kloppel, G. (2008). Pathologie. Pathologie. W. Böcker, H. Denk, P. U. Heitz and H. Moch. München, Urban und Fischer Verlag**:** 391-407.

Poitras, J. L., Costa, D., Kluk, M. J., Amrein, P. C., Stone, R. M., Lee, C., Dal Cin, P. and Morton, C. C. (2011). "Genomic alterations in myeloid neoplasms with novel, apparently balanced translocations." Cancer Genet **204**(2): 68-76.

Prasad, N. B., Somervell, H., Tufano, R. P., Dackiw, A. P., Marohn, M. R., Califano, J. A., Wang, Y., Westra, W. H., Clark, D. P., Umbricht, C. B., Libutti, S. K. and Zeiger, M. A. (2008). "Identification of genes differentially expressed in benign versus malignant thyroid tumors." Clin Cancer Res **14**(11): 3327-3337.

Reimann, N., Nolte, I., Bonk, U., Werner, M., Bullerdiek, J. and Bartnitzke, S. (1996). "Trisomy 18 in a canine thyroid adenoma." Cancer Genet Cytogenet **90**(2): 154-156.

Rein, M. S., Friedman, A. J., Barbieri, R. L., Pavelka, K., Fletcher, J. A. and Morton, C. C. (1991). "Cytogenetic abnormalities in uterine leiomyomata." Obstet Gynecol **77**(6): 923-926.

Ren, J., Jin, P., Wang, E., Marincola, F. M. and Stroncek, D. F. (2009). "MicroRNA and gene expression patterns in the differentiation of human embryonic stem cells." J Transl Med **7**: 20.

Rijnberk, A., Kooistra, H. S. and Mol, J. A. (2003). "Endocrine diseases in dogs and cats: similarities and differences with endocrine diseases in humans." Growth Horm IGF Res **13 Suppl A**: S158-164.

Rippe, V., Belge, G., Meiboom, M., Kazmierczak, B., Fusco, A. and Bullerdiek, J. (1999). "A KRAB zinc finger protein gene is the potential target of 19q13 translocation in benign thyroid tumors." Genes Chromosomes Cancer **26**(3): 229-236.

Rippe, V., Dittberner, L., Lorenz, V. N., Drieschner, N., Nimzyk, R., Sendt, W., Junker, K., Belge, G. and Bullerdiek, J. (2010). "The two stem cell microRNA gene clusters C19MC and miR-371-3 are activated by specific chromosomal rearrangements in a subgroup of thyroid adenomas." PLoS ONE **5**(3): e9485.

Rippe, V., Drieschner, N., Meiboom, M., Escobar, H. M., Bonk, U., Belge, G. and Bullerdiek, J. (2003). "Identification of a gene rearranged by 2p21 aberrations in thyroid adenomas." Oncogene **22**(38): 6111-6114.

Rogalla, P., Drechsler, K., Frey, G., Hennig, Y., Helmke, B., Bonk, U. and Bullerdiek, J. (1996). "HMGI-C expression patterns in human tissues. Implications for the genesis of frequent mesenchymal tumors." Am J Pathol **149**(3): 775-779.

Roque, L., Castedo, S., Clode, A. and Soares, J. (1992). "Translocation t(5;19): a recurrent change in thyroid follicular adenoma." Genes Chromosomes Cancer **4**(4): 346-347.

Roque, L., Castedo, S., Clode, A. and Soares, J. (1993a). "Deletion of 3p25-->pter in a primary follicular thyroid carcinoma and its metastasis." Genes Chromosomes Cancer **8**(3): 199-203.

Roque, L., Castedo, S., Gomes, P., Soares, P., Clode, A. and Soares, J. (1993b). "Cytogenetic findings in 18 follicular thyroid adenomas." Cancer Genet Cytogenet **67**(1): 1-6.

Roque, L., Nunes, V. M., Ribeiro, C., Martins, C. and Soares, J. (2001). "Karyotypic characterization of papillary thyroid carcinomas." Cancer **92**(10): 2529-2538.

Roque, L., Rodrigues, R., Pinto, A., Moura-Nunes, V. and Soares, J. (2003). "Chromosome imbalances in thyroid follicular neoplasms: a comparison between follicular adenomas and carcinomas." Genes Chromosomes Cancer **36**(3): 292-302.

Roque, L., Serpa, A., Clode, A., Castedo, S. and Soares, J. (1999). "Significance of trisomy 7 and 12 in thyroid lesions with follicular differentiation: a cytogenetic and in situ hybridization study." Lab Invest **79**(4): 369-378.

Sandberg, A. A. (2005). "Updates on the cytogenetics and molecular genetics of bone and soft tissue tumors: leiomyoma." Cancer Genet Cytogenet **158**(1): 1-26.

Sandberg, A. A. and Meloni-Ehrig, A. M. (2010). "Cytogenetics and genetics of human cancer: methods and accomplishments." Cancer Genet Cytogenet **203**(2): 102-126.

Sanghera, D. K., Been, L., Ortega, L., Wander, G. S., Mehra, N. K., Aston, C. E., Mulvihill, J. J. and Ralhan, S. (2009). "Testing the association of novel meta-analysis-derived diabetes risk genes with type II diabetes and related metabolic traits in Asian Indian Sikhs." J Hum Genet.

Sargent, M. S., Weremowicz, S., Rein, M. S. and Morton, C. C. (1994). "Translocations in 7q22 define a critical region in uterine leiomyomata." Cancer Genet Cytogenet **77**(1): 65-68.

Schmid, K. W., Sheu, S. Y., Gorges, R., Ensinger, C. and Totsch, M. (2003). "[Thyroid tumors]." Pathologe **24**(5): 357-372.

Schoenberg Fejzo, M., Ashar, H. R., Krauter, K. S., Powell, W. L., Rein, M. S., Weremowicz, S., Yoon, S. J., Kucherlapati, R. S., Chada, K. and Morton, C. C. (1996). "Translocation breakpoints upstream of the HMGIC gene in uterine leiomyomata suggest dysregulation of this gene by a mechanism different from that in lipomas." Genes Chromosomes Cancer **17**(1): 1-6.

Schoenmakers, E. F., Huysmans, C. and Van de Ven, W. J. (1999). "Allelic knockout of novel splice variants of human recombination repair gene RAD51B in t(12;14) uterine leiomyomas." Cancer Res **59**(1): 19-23.

Schoenmakers, E. F., Wanschura, S., Mols, R., Bullerdiek, J., Van den Berghe, H. and Van de Ven, W. J. (1995). "Recurrent rearrangements in the high mobility group protein gene, HMGI-C, in benign mesenchymal tumours." Nat Genet **10**(4): 436-444.

Seabright, M. (1971). "A rapid banding technique for human chromosomes." Lancet **2**(7731): 971-972.

Sheu, S. Y., Gorges, R. and Schmid, K. W. (2003). "[Hyperplasia of the thyroid gland]." Pathologe **24**(5): 348-356.

Simonis-Bik, A. M., Nijpels, G., van Haeften, T. W., Houwing-Duistermaat, J. J., Boomsma, D. I., Reiling, E., van Hove, E. C., Diamant, M., Kramer, M. H., Heine, R. J., Maassen, J. A., Slagboom, P. E., Willemsen, G., Dekker, J. M., Eekhoff, E. M., de Geus, E. J. and t Hart, L. M. (2010). "Gene variants in the novel type 2 diabetes loci

CDC123/CAMK1D, THADA, ADAMTS9, BCL11A, and MTNR1B affect different aspects of pancreatic beta-cell function." Diabetes **59**(1): 293-301.

Socolow, E. L., Engel, E., Mantooth, L. and Stanbury, J. B. (1964). "Chromosomes of Human Thyroid Tumors." Cytogenetics **10**: 394-413.

Soller, J. T., Beuing, C., Murua Escobar, H., Winkler, S., Reimann-Berg, N., Drieschner, N., Dolf, G., Schelling, C., Nolte, I. and Bullerdiek, J. (2008). "Chromosomal assignment of canine THADA gene to CFA 10q25." Mol Cytogenet **1**(1): 11.

Sornberger, K. S., Weremowicz, S., Williams, A. J., Quade, B. J., Ligon, A. H., Pedeutour, F., Vanni, R. and Morton, C. C. (1999). "Expression of HMGIY in three uterine leiomyomata with complex rearrangements of chromosome 6." Cancer Genet Cytogenet **114**(1): 9-16.

Sozzi, G., Bongarzone, I., Miozzo, M., Borrello, M. G., Blutti, M. G., Pilotti, S., Della Porta, G. and Pierotti, M. A. (1994). "A t(10;17) translocation creates the RET/PTC2 chimeric transforming sequence in papillary thyroid carcinoma." Genes Chromosomes Cancer **9**(4): 244-250.

Sozzi, G., Miozzo, M., Cariani, T. C., Bongarzone, I., Pilotti, S., Pierotti, M. A. and Della Porta, G. (1992). "A t(2;3)(q12-13;p24-25) in follicular thyroid adenomas." Cancer Genet Cytogenet **64**(1): 38-41.

Spassov, D. S. and Jurecic, R. (2002). "Cloning and comparative sequence analysis of PUM1 and PUM2 genes, human members of the Pumilio family of RNA-binding proteins." Gene **299**(1-2): 195-204.

Staiger, H., Machicao, F., Kantartzis, K., Schafer, S. A., Kirchhoff, K., Guthoff, M., Silbernagel, G., Stefan, N., Fritsche, A. and Haring, H. U. (2008). "Novel meta-analysis-derived type 2 diabetes risk loci do not determine prediabetic phenotypes." PLoS ONE **3**(8): e3019.

Stancakova, A., Kuulasmaa, T., Paananen, J., Jackson, A. U., Bonnycastle, L. L., Collins, F. S., Boehnke, M., Kuusisto, J. and Laakso, M. (2009). "Association of 18 confirmed susceptibility loci for type 2 diabetes with indices of insulin release, proinsulin conversion, and insulin sensitivity in 5,327 nondiabetic Finnish men." Diabetes **58**(9): 2129-2136.

Suh, M. R., Lee, Y., Kim, J. Y., Kim, S. K., Moon, S. H., Lee, J. Y., Cha, K. Y., Chung, H. M., Yoon, H. S., Moon, S. Y., Kim, V. N. and Kim, K. S. (2004). "Human embryonic stem cells express a unique set of microRNAs." Dev Biol **270**(2): 488-498.

Takahashi, T., Nagai, N., Oda, H., Ohama, K., Kamada, N. and Miyagawa, K. (2001). "Evidence for RAD51L1/HMGIC fusion in the pathogenesis of uterine leiomyoma." Genes Chromosomes Cancer **30**(2): 196-201.

Tallini, G. (2002). "Molecular pathobiology of thyroid neoplasms." Endocr Pathol **13**(4): 271-288.

Tanaka, T., Arai, M., Wu, S., Kanda, T., Miyauchi, H., Imazeki, F., Matsubara, H. and Yokosuka, O. (2011). "Epigenetic silencing of microRNA-373 plays an important role in regulating cell proliferation in colon cancer." Oncol Rep **26**(5): 1329-1335.

Teyssier, J. R. and Ferre, D. (1989). "Frequent clonal chromosomal changes in human non-malignant tumors." Int J Cancer **44**(5): 828-832.

Teyssier, J. R., Liautaud-Roger, F., Ferre, D., Patey, M. and Dufer, J. (1990). "Chromosomal changes in thyroid tumors. Relation with DNA content, karyotypic features, and clinical data." Cancer Genet Cytogenet **50**(2): 249-263.

Tonnies, H. (2002). "Modern molecular cytogenetic techniques in genetic diagnostics." Trends Mol Med **8**(6): 246-250.

Trask, B. J. (2002). "Human cytogenetics: 46 chromosomes, 46 years and counting." Nat Rev Genet **3**(10): 769-778.

Trubia, M., Albano, F., Cavazzini, F., Cambrin, G. R., Quarta, G., Fabbiano, F., Ciambelli, F., Magro, D., Hernandezo, J. M., Mancini, M., Diverio, D., Pelicci, P. G., Coco, F. L., Mecucci, C., Specchia, G., Rocchi, M., Liso, V., Castoldi, G. and Cuneo, A. (2006). "Characterization of a recurrent translocation t(2;3)(p15-22;q26) occurring in acute myeloid leukaemia." Leukemia **20**(1): 48-54.

Tsai, K. W., Kao, H. W., Chen, H. C., Chen, S. J. and Lin, W. C. (2009). "Epigenetic control of the expression of a primate-specific microRNA cluster in human cancer cells." Epigenetics **4**(8): 587-592.

van den Berg, E., Oosterhuis, J. W., de Jong, B., Buist, J., Vos, A., Dam, A. and Vermeij, B. (1990). "Cytogenetics of thyroid follicular adenomas." Cancer Genet Cytogenet **44**(2): 217-222.

Vangipurapu, J., Stancakova, A., Pihlajamaki, J., Kuulasmaa, T. M., Kuulasmaa, T., Paananen, J., Kuusisto, J., Ferrannini, E. and Laakso, M. (2011). "Association of indices of liver and adipocyte insulin resistance with 19 confirmed susceptibility loci for type 2 diabetes in 6,733 non-diabetic Finnish men." Diabetologia **54**(3): 563-571.

Wanschura, S., Dal Cin, P., Kazmierczak, B., Bartnitzke, S., Van den Berghe, H. and Bullerdiek, J. (1997). "Hidden paracentric inversions of chromosome arm 12q affecting the HMGIC gene." Genes Chromosomes Cancer **18**(4): 322-323.

Wanschura, S., Kazmierczak, B., Pohnke, Y., Meyer-Bolte, K., Bartnitzke, S., Van de Ven, W. J. and Bullerdiek, J. (1996). "Transcriptional activation of HMGI-C in three pulmonary hamartomas each with a der(14)t(12;14) as the sole cytogenetic abnormality." Cancer Lett **102**(1-2): 17-21.

Werner, M., Wilkens, L., Aubele, M., Nolte, M., Zitzelsberger, H. and Komminoth, P. (1997). "Interphase cytogenetics in pathology: principles, methods, and applications of fluorescence in situ hybridization (FISH)." Histochem Cell Biol **108**(4-5): 381-390.

Williams, D. (2002). "Cancer after nuclear fallout: lessons from the Chernobyl accident." Nat Rev Cancer **2**(7): 543-549.

Wu, N., Liu, X., Xu, X., Fan, X., Liu, M., Li, X., Zhong, Q. and Tang, H. (2011). "MicroRNA-373, a new regulator of protein phosphatase 6, functions as an oncogene in hepatocellular carcinoma." FEBS J.

Xiao, S., Renshaw, A., Cibas, E. S., Hudson, T. J. and Fletcher, J. A. (1995). "Novel fluorescence in situ hybridization approaches in solid tumors. Characterization of frozen specimens, touch preparations, and cytological preparations." Am J Pathol **147**(4): 896-904.

Yang, K., Handorean, A. M. and Iczkowski, K. A. (2009). "MicroRNAs 373 and 520c are downregulated in prostate cancer, suppress CD44 translation and enhance invasion of prostate cancer cells in vitro." Int J Clin Exp Pathol **2**(4): 361-369.

Zeggini, E., Scott, L. J., Saxena, R., Voight, B. F., Marchini, J. L., Hu, T., de Bakker, P. I., Abecasis, G. R., Almgren, P., Andersen, G., Ardlie, K., Bostrom, K. B., Bergman, R. N., Bonnycastle, L. L., Borch-Johnsen, K., Burtt, N. P., Chen, H., Chines, P. S., Daly, M. J., Deodhar, P., Ding, C. J., Doney, A. S., Duren, W. L., Elliott, K. S., Erdos, M. R., Frayling, T. M., Freathy, R. M., Gianniny, L., Grallert, H., Grarup, N., Groves, C. J., Guiducci, C., Hansen, T., Herder, C., Hitman, G. A., Hughes, T. E., Isomaa, B.,

Jackson, A. U., Jorgensen, T., Kong, A., Kubalanza, K., Kuruvilla, F. G., Kuusisto, J., Langenberg, C., Lango, H., Lauritzen, T., Li, Y., Lindgren, C. M., Lyssenko, V., Marvelle, A. F., Meisinger, C., Midthjell, K., Mohlke, K. L., Morken, M. A., Morris, A. D., Narisu, N., Nilsson, P., Owen, K. R., Palmer, C. N., Payne, F., Perry, J. R., Pettersen, E., Platou, C., Prokopenko, I., Qi, L., Qin, L., Rayner, N. W., Rees, M., Roix, J. J., Sandbaek, A., Shields, B., Sjogren, M., Steinthorsdottir, V., Stringham, H. M., Swift, A. J., Thorleifsson, G., Thorsteinsdottir, U., Timpson, N. J., Tuomi, T., Tuomilehto, J., Walker, M., Watanabe, R. M., Weedon, M. N., Willer, C. J., Illig, T., Hveem, K., Hu, F. B., Laakso, M., Stefansson, K., Pedersen, O., Wareham, N. J., Barroso, I., Hattersley, A. T., Collins, F. S., Groop, L., McCarthy, M. I., Boehnke, M. and Altshuler, D. (2008). "Meta-analysis of genome-wide association data and large-scale replication identifies additional susceptibility loci for type 2 diabetes." Nat Genet.

Zhao, H., Xu, X., Xing, X., Wang, J., He, L., Shi, Y., Zhao, Y. and Chen, Z. J. (2012). "Family-based analysis of susceptibility loci for polycystic ovary syndrome on chromosome 2p16.3, 2p21 and 9q33.3." Hum Reprod **27**(1): 294-298.

8 Danksagung

Für die Überlassung des Themas sowie die Betreuung dieser Arbeit geht mein Dank an Herrn Prof. Dr. Jörn Bullerdiek.

Herrn PD Dr. Wolfgang Sendt möchte ich für die Bereitstellung von Probenmaterial und insbesondere für die Übernahme des Koreferates danken.

Herrn Prof. Dr. Ludger Rensing danke ich für seine Bereitschaft, am Prüfungsausschuss teilzunehmen und auch für die oft spannenden Spiele beim Tischtennis.

Herrn Dr. Volkhard Rippe gilt mein Dank für die vielen anregenden (manchmal, aber selten, anstrengenden) Gespräche, teils zu später Stunde, in denen wir uns über diese Arbeit, die Wissenschaft, die Politik, die Gesellschaft und im Besonderen die Musik ausgetauscht haben.

Den Kollegen und Kolleginnen aus dem ZHG (auch den ehemaligen) sage ich danke für ihre Unterstützung und Hilfe in all den Jahren. Insbesondere seien hier genannt: PD Dr. Gazanfer Belge, der mich einst die FISH lehrte. Dr. Rolf Nimzyk für die Hilfe in statistischen und sequenzanalytischen Fragen und allem, was darüber hinaus ging („Wie immer, gut."). Dr. Siegfried Löschke (nicht nur) wegen seiner molekular-pathologischen Expertise. Dr. Nicola Reimann-Berg, über die ich das ZHG erstmalig von „Innen" (lang ist's her) kennenlernte und die mich einmal ganz schön in die Enge trieb (aber es ging ja gut aus, wie du weißt). Angelika Schneider-Uhlhorn für ihre Bemühungen und ihre Hilfsbereitschaft! Andrea Gottlieb und Ute Hitzbleck danke ich für ihr „offenes Ohr" und die angenehmen Gespräche.

Nicht unerwähnt bleiben sollten: Lars Kloth, Dr. Maren Meiboom, PD Dr. Hugo Murua Escobar, Dr. Jan Soller, Dr. Anke Meyer. Sowie all' die (ehemaligen) DiplomandInnen, Bachelor- und MasterstudentInnen: Jessica Hommes, Dr. Karen Grigo, Tim Focken, Dr. Holger Heyn, Dagmar Preusse, Sebastian Bönte, Kerstin Waden, Melanie Spyra, Daniela Begandt, Dr. Stefanie Klede, Marta Leider, Bianca Busch, Inga Dietz, Lea Dittberner, Anne Laabs, Verena Lorenz, Sebastian Kirchner, Johannes Debler und Valentina Adam. Svenja Kerschling danke ich für die immer netten Gespräche, auch wenn wir uns nur selten sehen, und vor allem für die Ente!

Danke auch dem Team aus der Diagnostik: Dr. Yvonne Kiefer, Manuela Grund, Kim Hue Tran, Denis Schaap (trotz, vielleicht auch wegen all der Fragen zu Software, Computern und

Mikroskopen, aber auf jeden Fall für den Spaß und den Tee). Dr. Sabine Bartnitzke und Dr. Birgit Rommel – Danke für die zytogenetische Hilfe. Und – last but not least – HenriEke (sic!) Förster, die es stets versucht, doch es nie geschafft hat, aber nah dran war, mich manches Mal „auf die Palme“ zu bringen. Und auch wenn ich mir alle Mühe gegeben habe, Henny, ich glaub‘ ich hab’s bei dir auch nicht geschafft. Einigen wir uns bis hierhin auf Unentschieden? (to be continued…) ;-)

Ein großer Dank für die enorme Hilfe in der FISH geht an Merle Skischus, Sabrina Poltermann (Dorschner!) und Tais Sommerfeldt, deren Beitrag nicht hoch genug einzuschätzen war und ist. Tais, du hast mit aller Ruhe und Gelassenheit nicht nur meine Launen ertragen, ich war mir immer sicher, mich auf dich verlassen zu können (ja, wirklich!). Darüber hinaus danke an alle (ehemaligen) Auszubildenden, die in der FISH oder einfach nur hilfreich waren und sind (in der Reihenfolge ihres Erscheinens, soweit rekonstruierbar): Birgit Burchardt, Julia Twardy, Karmela Sobczyk, Julia Korwitz, Tanja Schwarze, Melissa Dohmel, Frauke Meyer, Nadine Korzeniowsky, Stefanie Wolgast, Josefine Papprott, Alexander Pajung, Aneta Bogaczewicz, Alisa Ivanov, Laura Rogge, Lisa Imbiel, Iris Verena Reinhardt, Caroline Zeiser und Nadine Wahle.

Ganz besonders aber möchte ich Euch danken für den gemeinsamen Weg, den wir gegangen sind und noch gehen, mitsamt all seinen Leiden aber auch Freuden:

Die Titelträger zuerst (Ehre wem Ehre gebührt): Dr. André Fehr (Tack kompis!), Dr. Susanne Winkler (thanks for proofreading and everything else), Dr. Andreas Richter (als ich mit meinem Computerlatein am Ende war, schlug stets deine Stunde). Und natürlich auch: Marietta Müller (für deine Hilfe und Unterstützung vor allem in den letzten Monaten auf dem Weg zur Fertigstellung dieser Arbeit), Nina Winter (es war ein Kopf-an-Kopf-Rennen) und Markus Klemke (auf dass der HSV endlich absteigt).

Nun aber:

Mein besonderer Dank von ganzem Herzen und meine tiefste Zuneigung, die kaum in Worte zu fassen ist, gelten folgenden Freunden:

Martina Lübbing, Julia Ebers, Alexandra (Alex) Geib, Wiebke Krolik, Angela Uhlig van Buhren und Sabine Weyand

Eurer Unterstützung konnte ich in allen Belangen immer sicher sein, wenn ihr mich zuweilen auch daran erinnern musstet. Ihr habt euch die Zeit genommen, wenn es nötig war, und die Worte gefunden – ehrlich, offen und treffend – die mir, auch wenn mir dies manches Mal erst später klar wurde, oft den richtigen Weg wiesen. Bleibt so!

Das gilt auch vor euch: Melli Gaidies, Stefan Siegert, Silke Hubrig, Helen Liebig, Nicola Kemper, Kathrin Schröder und Karen Prager. Sowie die „Stadthäger“ Stephan und Steffi Kittel, Michael Kreft, Ulla Thülig, Mario John Lewetzki, Silke Nagel, Kathrin Haupt-Möller und Udo Schosland. Und natürlich Erika und Karl-Heinz Lübbing, die immer einen besonderen Platz einnehmen werden.

Frei nach Loriot: diese Arbeit ohne euch wäre möglich, aber die Zeit irgendwie sinnlos gewesen.

Meinen Eltern Renate und Günter Drieschner danke ich für die unerschütterliche Unterstützung in den vergangenen 40 Jahren. Danke meinen Geschwistern Michael Drieschner und Rosi Klement, einfach dafür, dass ihr es seid. Und danke auch an Diana Drieschner, Sarah Drieschner, Karl-Heinz Klement, Jessica Klement, Mathias Klement und der kleinen Mara, der die ganzen Abenteuer und Wunder noch bevorstehen.

Und zu guter Letzt danke ich Peter und Paul. Unmissverständlich und unnachgiebig haben sie mir vor Augen geführt, dass ein Platz zum Schlafen, sich kraulen lassen, ein voller Futternapf und eine saubere Katzentoilette die vier Säulen der Zufriedenheit und des Wohlbefindens sind. Wenn es daran nicht fehlt, kann alles andere gar nicht so schlimm sein.

„So Long, and Thanks for All the Fish“

- Douglas Adams -